LA-5883-PR
Progress Report

UC-48
Issued: February 1975

Annual Report of the
Biomedical and Environmental Research Program
of the
LASL Health Division
January through December 1974

Compiled by

E. C. Anderson
E. M. Sullivan

Contributions from the staff are indicated by group.

los alamos
scientific laboratory
of the University of California
LOS ALAMOS, NEW MEXICO 87544

An Affirmative Action/Equal Opportunity Employer

MASTER

UNITED STATES
ENERGY RESEARCH AND DEVELOPMENT ADMINISTRATION
CONTRACT W-7405-ENG. 36

This report presents the status of the Biomedical and Environmental Research Program at LASL. The four most recent reports in this series, unclassified, are:

LA-3848-MS	LA-5227-PR
LA-4923-PR	LA-5633-PR

In the interest of prompt distribution, this progress report was not edited by the Technical Information staff.

The LASL Biomedical and Environmental Research Program was supported by the USERDA Division of Biomedical and Environmental Research.

Experimental animals used in work presented in this report were maintained in animal care facilities that are fully accredited by the American Association for Accreditation of Laboratory Animal Care.

Printed in the United States of America. Available from
National Technical Information Service
U.S. Department of Commerce
5285 Port Royal Road
Springfield, VA 22151
Price: Printed Copy $7.60 Microfiche $2.25

TABLE OF CONTENTS

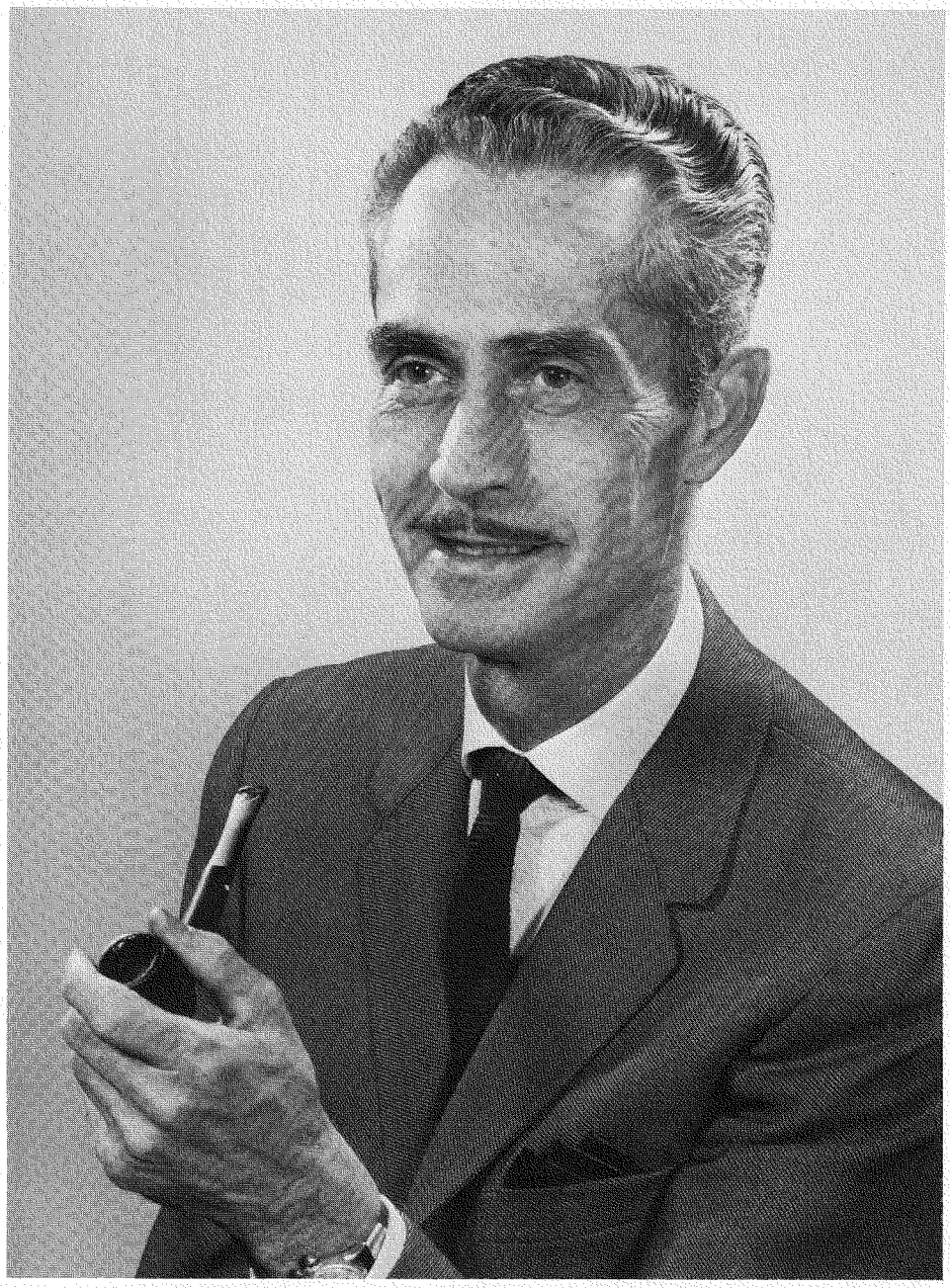

DEDICATION

The year of 1975 will see the abolition of the U. S. Atomic Energy Commission and the transfer of its research responsibilities to the new Energy Research and Development Administration. It seems appropriate, therefore, to dedicate our last annual report under the old system to the man who was most responsible for the initiation and development of the LASL Health Division's Biomedical and Environmental Research Program, Dr. Wright H. Langham, who directed the program from its inception in 1944 until his untimely death in 1972.

ABSTRACT

This report summarizes research and development activities of LASL's Biomedical and Environmental Research Program for calendar year 1974. This program is carried on by several groups within the Laboratory's Health Division with funding from the USAEC Division of Biomedical and Environmental Research. Previous annual reports in this series are LA-4923-PR (1971), LA-5227-PR (1972), and LA-5633-PR (1973).

The primary objective of this document is to convey technical information about the current status and the results obtained in the major areas of research conducted by each group. Enough detail is given to permit a specialist in the field to evaluate the scope, quality, and significance of the work, but the target is closer to an abstract than to a fully developed paper. A list of publications for 1974 is given in the appendix, and the interested reader should consult these for further information.

OUTLINE OF THE PROGRAM

This report summarizes the research and development activities carried out in the Health Division of the Los Alamos Scientific Laboratory with funding from the USAEC Division of Biomedical and Environmental Research (DBER). Four of the five major funding areas of the DBER RX Program are represented: Health Studies, Environmental Studies, Biological Studies, and Physical and Analytical Research Studies. The reports in this document, as in our previous annual reports, are organized according to groups primarily responsible for the research: Mammalian Radiobiology (H-4); Industrial Hygiene (H-5); Environmental Studies (H-8); Cellular and Molecular Radiobiology (H-9); Biophysics and Instrumentation (H-10); and Organic and Biochemical Synthesis (H-11). [Additional DBER RX programs in other LASL Divisions (CNC, CMB, and MP) are not covered here.]

A table of organization of that portion of the Health Division involved in the RX programs is given below. The position of Alternate Division Leader was vacant from 1 September 1974 with the departure of Dr. Chester R. Richmond. Dr. Richmond was in charge of the programs reported here and deserves much of the credit for their organization, direction, and encouragement. As of 1 January 1975, Dr. Donald F. Petersen became Alternate Division Leader, and Dr. Arthur G. Saponara became H-9 Group Leader.

CURRENT EFFORTS

In the Health Studies category are included four projects related to plutonium and other transuranium elements and to the development of radiation protection guides. These projects have developed in response to the needs of the AEC and other agencies for information on the fate and potential biological effects of these elements.

1. The study of high specific-activity particles ("hot particles") in the lung is part of an integrated AEC program involving biological studies at several laboratories and addresses the general question of the relative effects of localized vs diffuse irradiation. Although begun sometime ago in recognition of this important problem, this program has recently assumed greater prominence as a result of challenges of current radiation protection standards.

TABLE OF ORGANIZATION OF LASL HEALTH DIVISION[a]

George L. Voelz, M.D., Division Leader

(open), Alternate Division Leader

John W. Healy, Assistant Division Leader for Radiological Health

Harry S. Jordan, Assistant Division Leader for Environmental Control

Ernest C. Anderson, Scientific Advisor

H-4	H-5	H-8	H-9	H-10	H-11	
Mammalian Radiobiology	Industrial Hygiene	Environmental Studies	Cellular and Molecular Radiobiology	Biophysics and Instrumentation	Organic and Biochemical Synthesis	Other Groups not involved in the RX programs
R. G. Thomas	H. J. Ettinger	L. J. Johnson	D. F. Petersen	P. F. Mullaney	D. G. Ott	

[a] As of December 1974.

2. The development of metabolic information on radioactive isotopes is for use in radiation protection guides (that is, the establishment of permissible concentrations in air and water).

The above two projects will be found in the Mammalian Radiobiology section.

3. The determination of plutonium and environmental metals in man has thus far addressed primarily plutonium, but the autopsy material can be used for assay of other hazardous materials in both workers and the general population. This report is in the Industrial Hygiene section.

4. Clinical follow-up studies on personnel exposed to significant body burdens of plutonium during wartime operations utilize the unique opportunity to search for biological effects in humans exposed as long as 30 years ago. A discussion of this project will also be found in the Industrial Hygiene section.

In the Environmental Studies category are included four projects developed in response to environmental considerations at LASL and to national energy production problems.

1. Ecological studies in radioactive waste disposal areas have been in progress at both Los Alamos and at Trinity Site in southern New Mexico for about two years.

2. The study of Alaskan North Slope ecosystems is new at LASL but represents a continuation of a 14-year study elsewhere.

3. Radiation ecology of northern Alaska is a related investigation which is likewise new here but continues ongoing studies in collaboration with other laboratories.

4. A study of low-level meteorological transport is also new and will attempt to develop computer models of the complex atmospheric dispersal mechanisms operating in the Los Alamos area for application both to LASL problems and to pollutant transport in larger areas such as the Four Corners power generation complex.

The above four projects are discussed in the Environmental Studies section.

Biological Studies comprise a major fraction of our efforts, and results are reported in four of the group sections of this report. Research on the effects of external radiation on living organisms is directed primarily toward the study of whole-body dose protraction and the nature of the long-term lesion in dogs and monkeys and is discussed in the Mammalian Radiobiology section. Studies discussed in the Molecular and Cellular Radiobiology section center on growth, regulation, and synthesis in macromolecular, microbial, and eukaryotic systems. This program includes projects on the synthesis and radiosensitivity of model DNA, radiation effects on genetic information transfer, response of histone metabolism to x-irradiation, biological effects of radiation on cells, and chromosome structure and function. A parallel and closely related effort, discussed in the Biophysics and Instrumentation section, covers electronic sensing and sorting of biological cells. This project reflects an interdisciplinary approach using laser systems, high-speed electronics, and digital data processing to obtain solutions of both basic and mission-oriented biomedical problems. There is a strong emphasis on biological problems rather than on the physical instrumentation.

Another research area under the Biological Studies category is the biological, agricultural, and environmental application of stable isotopic tracers. Not only can new elements be traced (e.g., oxygen and nitrogen), but others (e.g., carbon and sulfur) can be followed to greater dilutions and longer times and, most importantly, without potential health hazards from radioactivity. Current efforts are centered on the synthesis of useful labeled compounds from the enriched isotopes produced by the Chemistry-Nuclear Chemistry Division (this production is also funded by DBER but is not covered in this report) and on the demonstration of their utility by specific applications in collaboration with other laboratories and agencies. The establishment of a proposed national center for stable isotopes at Los Alamos would greatly accelerate the rate of application for this very promising technology to a wide variety of current national problems including energy-related pollutants, fertilizers (both in terms of agricultural efficiency and environmental pollution), clinical medicine, and biochemical studies. This research is discussed in the Organic and Biochemical Synthesis section of this report.

Under Physical and Analytical Research Studies are included important studies directly related to

AEC health and safety requirements. A number of applied studies on aerosol properties and filter performance are found in the Industrial Hygiene section. New studies of the analysis and assessment of plutonium hazards, while performed by Health Division office personnel, are also reported in the Industrial Hygiene section because of their close relation to other projects reported there. Studies on the biological properties of negative pions are given in the Biophysics and Instrumentation section. (Other DBER-funded research on pions conducted by the Medium Energy Physics Division is not covered in this report.)

FUTURE CONSIDERATIONS

Major changes are expected in our programs as a result of the forthcoming transition from AEC to ERDA with the broadening of interest and responsibility implied. Many of our projects fortunately are concerned with underlying mechanisms and with test systems and end points of wide applicability. These range from the studies of fundamental biochemistry to measurement of the properties of aerosols, and they can be rapidly and efficiently extended and redirected to include non-nuclear hazards. The coming of ERDA will provide a useful stimulus and incentive for thorough reexamination of the organization and execution (strategy and tactics) of our programs, both here and in Washington. We expect that the wider range of practical problems will result in strengthening the fundamental basis on which solutions must rest. One of the most productive aspects of the scientific method has been the refinement of understanding which results from the testing of theories and predictions against a wider range of experimental conditions and the greater credibility of working hypotheses and extrapolations that results from the broader viewpoint.

We feel strongly that, in addition to the pursuit of targeted research, it is essential to have investigators working on the cutting edge of their disciplines to recognize findings not only of this Laboratory but of the scientific community at large and to translate these findings into profitable applications in programmatic areas. A failure of early recognition of relevant developments in many other disciplines could be serious in "normal" times; in a time when ERDA must rapidly assume the broad responsibility for health aspects of multiple energy technologies, such failure could be disastrous.

E. C. Anderson
Scientific Advisor
Health Division

MAMMALIAN RADIOBIOLOGY GROUP (H-4)

R. G. Thomas, Ph.D., Group Leader
B. J. Bailey, Secretary

Staff Members

M. R. Brooks, B.Ch.E.
S. G. Carpenter, B.A.
G. A. Drake, B.S.
J. E. Furchner, Ph.D.
L. S. Gomez, Ph.D.
L. M. Holland, D.V.M.
O. S. Johnson, B.S.
P. M. LaBauve, B.A.
J. E. London, B.S.
J. R. Prine, D.V.M.
D. M. Smith, D.V.M., Ph.D.
J. F. Spalding, Ph.D.
J. S. Wilson, B.S.

Animal Colony Assistant Manager

E. A. Vigil

Biology Technicians

R. F. Archuleta
E. C. Rivera[b]
C. A. Thomas[b]

Histopathology Technician

R. H. Wood

Animal Technicians

J. E. Atencio
F. J. Benavidez
J. Cordova[a]
J. E. D. Esquibel
C. N. Gomez
W. F. Johnson[a]
J. S. Martinez
R. Martinez
J. Salazar
J. B. Sanchez
F. Valdez

Visiting Staff Member (Short-Term)

E. L. Gillette, D.V.M.
Colorado State University
Fort Collins, Colorado

Consultants

R. S. Stone, M.D.
Bethesda, Maryland

L. S. Rosenblatt, Ph.D.
Geneticon
Berkeley, California

STEP Program

J. G. Farr
C. A. Trusty

[a] Casual.

[b] Part-time.

INTRODUCTION

The activities of the Mammalian Radiobiology Group (H-4) consist primarily of programmatic research, with major emphasis on the effects of radiation from both external and internal sources on mammals. Through use of various species, the goal is extrapolation of data from experimental animals to man. The external radiation studies are primarily concerned with the effects of total dose and dose rate on the persistent biological lesions that ultimately lead to subtle changes in normal life expectancy. Rodents, dogs, and monkeys have been the major source of data in this area of research, with future long-range plans calling for more emphasis on the mouse. Studies on the effects of internally deposited radioactive materials include interspecies correlations (rodents, dogs, monkeys, and extrapolations to man) of uptake, deposition, and excretion of radionuclides. Data have been obtained that may be used to assess the present standards of both the stable and radioactive forms of the trace metals studied. Research on the effects of particulate material of long residence time in lung tissue has continued to be interesting and challenging. High-specific-activity ceramic spheres, primarily containing $^{239}PuO_2$, have been utilized in an attempt to relate the degree of localized tissue irradiation to the incidence of lung tumors. The obvious ultimate objective of much of this work in mammalian radiobiology is the establishment of radiation protection guides for man, either through extrapolation of metabolic pathways or determination of biological dose-effect relationships. Other research efforts are related to animal radiobiology studies of negative pions for preclinical therapy work conducted at the biomedical facility at the Clinton P. Anderson Meson Physics Facility (LAMPF). To date, limited mouse tumor and cell culture studies have been performed.

Education and Training

During the past year, several seminar-lecture type presentations of an educational nature have been made by members of the Group H-4 staff. These have been to other groups within the Laboratory and to audiences outside of LASL, primarily university-associated.

One involvement within the Laboratory was a joint effort between Dr. J. R. Prine and Group H-1 (Health Physics) personnel, in which he assembled a selected package of histopathology slides from radiation exposures to dogs and monkeys. In the training of health physics monitors, these have been used to demonstrate the lesions that can arise from an overdose of whole-body external gamma rays. The radiation doses involved are interpreted in terms of meter readings to help convey real meaning to the monitoring procedure.

Two STEP (Skills Training Employment Program) personnel have been assigned to the group for most of this calendar year. This program allows a person with an undergraduate degree to observe and participate in various segments of the ongoing research effort. Its intention is to instill a desire in the individual to return to school and to pursue work toward an advanced (graduate) degree. Such participation in the experimental effort is not only advantageous for the STEP employee but also represents a teaching experience for the permanent staff.

A future effort is on the drawing board in which essentially untrained full-time technical employees will be able to learn laboratory procedures pertinent to their work. Such a course, when formulated, will be initially oriented toward work in many aspects of radiobiology, with emphasis on the understanding and use of instrumentation and specialized techniques, plus an appreciation for

EFFECTS OF INTERNAL RADIATION ON LIVING ORGANISMS

(HOT PARTICLE PROGRAM)

[E. C. Anderson, S. G. Carpenter, G. A. Drake, L. M. Holland, J. E. London, J. D. Perrings (H-10), J. R. Prine, D. M. Smith, J. S. Wilson, and R. H. Wood]

Introduction

These studies are designed to provide data on the relative hazard of diffuse vs localized lung irradiation in laboratory animals. To date, the primary emphasis has been on the Syrian hamster which has been widely used in pulmonary carcinogenesis studies and which has been shown by Little *et al.*[1,2] to yield many tumors with short induction times when exposed intratracheally to ^{210}Po. We believe that our experiments provide a very critical test of the Geesaman-Tamplin hypothesis[3] that the lung is very susceptible to tumor induction by isolated particles.

While the concept of a simple ratio between the effectiveness of local vs diffuse energy deposition is an attractive one, it must be determined whether in actual fact such a simplistic parameter is realistic and useful. Tumorigenesis is a very subtle and complicated process even in the context of biological complexities, and without some understanding of the mechanisms, a premature attempt at simplification may be highly erroneous. Therefore, it is essential that studies be made in sufficient depth to provide an adequate experimental basis for the choice of a minimal set of parameters to describe the exposure conditions. For example, it is not yet clear whether humoral and cellular defense systems against transformed cells are crucially involved in such a way as to introduce a strong dependence of tumor probability on the number and distribution of the cells irradiated. Such a dependence would make hazard calculations based solely on local radiation doses meaningless unless adequate account were taken of the complex population dynamics involved. Only biological measurements can, at this stage, identify the parameters which are necessary and sufficient to determine the outcome and which must be included in a minimal model.

Microsphere Experiments

Previous publications[4-7] have described the techniques and some of the results of these experiments. Briefly, the methodology uses jugular vein

injection of ceramic microspheres with a very uniform diameter of 10 μm. This size is chosen to give quantitative and permanent lodgment in the capillary bed of the lung for the lifetime of the animal. The resultant radiation fields can be precisely controlled, and detailed microdosimetry is possible. The radioactivity of the sphere is determined by the kind and amount of radionuclide added in the production process. To date, ^{238}Pu, ^{239}Pu, ^{147}Pm, and ^{57}Co have been used, the last being a gamma-emitting tracer which permits simple determination of sphere numbers both *in vivo* and *in vitro*. The oxide of the radioactive element forms a solid solution in the high-fired ZrO_2 ceramic matrix of the spheres which are very insoluble and physiologically inert. By varying the number and radioactivity of the microspheres administered, a wide range of exposure conditions can be achieved. Among the differences between this method of exposure and aerosol inhalation are the restriction of the radiation exposure to parts of the lung with no translocation to other organs, immobility of the spheres, and greatly reduced incidence of foreign body reactions.

Table I records experiments in which hamsters were given plutonia-zirconia microspheres intravenously. The alpha specific activity is given in column 4 and ranges from 0.016 to 59 pCi/sphere. The actual isotope used was ^{239}Pu in all cases except those noted by footnote b of the table, for which ^{238}Pu was used. These two nuclides are expected to behave similarly in these experiments. For the more energetic alpha rays from ^{238}Pu, the radiation dose rate will be lower close to the sphere (since the LET is somewhat less), but the increased range will result in the exposure of more tissue. Because the volume irradiated increases with the cube of the range, which in turn increases by about 14% for the 6% energy increase between the two isotopos, ^{238}Pu may irradiate about 50% more tissue than ^{239}Pu, but the dose rate averaged over all cells at risk would be 30% less. Exact account must be taken of these factors when accurate dosimetry is required. It should be noted that, in the microspheres used in the present experiments, both plutonium isotopes are heavily diluted with ZrO_2, the maximum PuO_2 concentration being about 1%. Therefore, the effects resulting from the very high specific-activity of pure $^{238}PuO_2$ (such as an apparently greater biological "solubility") are not expected.

These levels cover (on a more or less logarithmic scale) an activity range corresponding to that of pure PuO_2 spheres with diameters from 0.058 to 0.90 μm for ^{238}Pu and from 0.38 to 5.8 μm for ^{239}Pu. A number of criteria governed the choice of activity including respirability, results of other experiments, and predictions of several theoretical models of tumorigenesis.

The number of microspheres per animal varied from 2 000 to 1 600 000, as shown in column 3 (Table I). For randomly distributed particles, the fraction of hamster lung calculated to fall within alpha range varied from about 1 to 99%; the calculation depends on the lung model assumed, as well as on the actual sphere distribution. Various combinations of sphere number and activity were used to give total lung burdens ranging from 0.14 to 710 nCi, as shown in column 5. In some cases, additional insults were used as indicated in the last column.

Mean survival time is given in column 6, as determined from a smoothed curve on a probit plot of fractional survival vs time. For recent experiments in which more than half the animals are still alive, the number given is derived from a linear extrapolation of the available data.

Table II summarizes similar exposures in which the ZrO_2 spheres contained ^{147}Pm (2.6-yr half-life, 225 KeV β^- activity) to provide a more uniform lung irradiation with a radiation of lower LET. Note that the units of specific activity and lung burden are 1000-fold higher than for the alpha exposures.

Table III summarizes the control experiments; as noted in column 3, some of these involve no spheres, while in others spheres tagged with ^{57}Co (as were all the plutonium and promethium spheres) were used. The ^{57}Co activity (of the order of 1 pCi per sphere, in most cases) delivers a radiation dose to the whole hamster which is much less than the natural background dose.

Mean Survival Times

Interpretation of the effect of the microspheres on hamster survival is complicated by changes which have occurred during the course of these experiments. As shown in Fig. 1, there has been a reduction in hamster longevity (or more precisely, an increase in

TABLE I

SUMMARY OF EXPOSURES OF HAMSTERS TO INTRAVENOUS PLUTONIUM MICROSPHERES

Date of Exposure		Number of Animals	Spheres per Animal	Specific Activity (pCi per sphere)	Lung Burden (nCi)	Mean Survival Time (days of age[a])	Other Insults
1971	May	69	2000	0.07	0.14	630	
	May	71	2000	0.22	0.44	795	
	May	74	2000	0.91	1.82	765	
	June	71	2000	0.42	0.84	670	
	June	71	2000	4.30[b]	8.60	635	
	June	71	2000	13.30[b]	26.00	620	
	June	72	2000	59.00[b]	118.00	650	
	August	71	2000	2.10[b]	4.20	720	
	August	47	10 000	0.22	2.20	830	
	November	154	6000	4.30[b]	26.00	720	
	December	148	6000	59.00[b]	354.00	615	
1972	February	142	6000	0.22	1.30	695	
	July	20	1 600 000	0.07	112.00	715	
	July	34	300 000	0.42	126.00	655	
	December	30	6000	8.90[b]	53.00	(350)	Cytoxin
1973	April	109	60 000	0.91	55.00	490	
	April	107	80 000	8.90[b]	710.00	395	
	April	102	80 000	2.10[b]	168.00	515	
	May	104	80 000	0.22	18.00	680	
	June	37	400 000	0.42	170.00	505	
	June	109	150 000	0.06	9.00	455	
	July	97	500 000	0.03	15.00	470	
	July	44	50 000	0.91	45.00	440[c]	
	October	26	900 000	0.016	14.00	480	
	October	15	500 000	0.016	8.00	395	
	November	53	40 000	0.06	2.40	385	
	November	52	20 000	0.06	1.20	450	
1974	January	52	20 000	0.19	3.80	390	
	January	51	40 000	0.19	7.60	385	
	January	60	60 000	1.60	96.00	455	$C_2F_2Cl_4$
	May	76	60 000	2.10[b]	126.00	d	Zymosan
	May	71	30 000	0.19	11.00	d	Zymosan

[a] Animals exposed at age 100 days.

[b] Plutonium-238; all others contain ^{239}Pu.

[c] Weanlings exposed at age 30 days.

[d] No data yet available.

TABLE I

SUMMARY OF EXPOSURES OF HAMSTERS TO INTRAVENOUS PLUTONIUM MICROSPHERES

Date of Exposure		Number of Animals	Spheres per Animal	Specific Activity (pCi per sphere)	Lung Burden (nCi)	Mean Survival Time (days of age[a])	Other Insults
1971	May	69	2000	0.07	0.14	630	
	May	71	2000	0.22	0.44	795	
	May	74	2000	0.91	1.82	765	
	June	71	2000	0.42	0.84	670	
	June	71	2000	4.30[b]	8.60	635	
	June	71	2000	13.30[b]	26.00	620	
	June	72	2000	59.00[b]	118.00	650	
	August	71	2000	2.10[b]	4.20	720	
	August	47	10 000	0.22	2.20	830	
	November	154	6000	4.30[b]	26.00	720	
	December	148	6000	59.00[b]	354.00	615	
1972	February	142	6000	0.22	1.30	695	
	July	20	1 600 000	0.07	112.00	715	
	July	34	300 000	0.42	126.00	655	
	December	30	6000	8.90[b]	53.00	(350)	Cytoxin
1973	April	109	60 000	0.91	55.00	490	
	April	107	80 000	8.90[b]	710.00	395	
	April	102	80 000	2.10[b]	168.00	515	
	May	104	80 000	0.22	18.00	680	
	June	37	400 000	0.42	170.00	505	
	June	109	150 000	0.06	9.00	455	
	July	97	500 000	0.03	15.00	470	
	July	44	50 000	0.91	45.00	440[c]	
	October	26	900 000	0.016	14.00	480	
	October	15	500 000	0.016	8.00	395	
	November	53	40 000	0.06	2.40	385	
	November	52	20 000	0.06	1.20	450	
1974	January	52	20 000	0.19	3.80	390	
	January	51	40 000	0.19	7.60	385	
	January	60	60 000	1.60	96.00	455	$C_2F_2Cl_4$
	May	76	60 000	2.10[b]	126.00	d	Zymosan
	May	71	30 000	0.19	11.00	d	Zymosan

[a] Animals exposed at age 100 days.

[b] Plutonium-238; all others contain ^{239}Pu.

[c] Weanlings exposed at age 30 days.

[d] No data yet available.

TABLE II

SUMMARY OF PROMETHIUM-147 EXPOSURES

Date of Exposure		Number of Animals	Spheres per Animal	Specific Activity (nCi per sphere)	Lung Burden (μCi)	Mean Survival Time (days of age[a])
1973	February	62	6000	0.07	0.42	560
	February	52	300 000	0.07	21.00	560
	March	61	50 000	0.07	3.50	690
	April	64	10 000	0.45	4.50	560
	April	62	50 000	0.45	22.00	610
	May	22	10 000	0.45	4.50	(320)[b]

[a]Animals exposed at age 100 days.

[b]$C_2H_2Cl_4$ infarcts.

TABLE III

SUMMARY OF CONTROLS

Date of Exposure		Number of Animals	Spheres per Animal	Mean Survival Time (days of age[a])
1971	May	70	2000	615
	July	72	None	740
	September	82	10 000	690
1972	April	96	None	615
	May	133	4000	655
	June	24	500 000	380
1973	November	69	None	380
1974	June	70	Variable	b
	June	75	100 000	b

[a]Animals exposed at age 100 days.

[b]No data yet available.

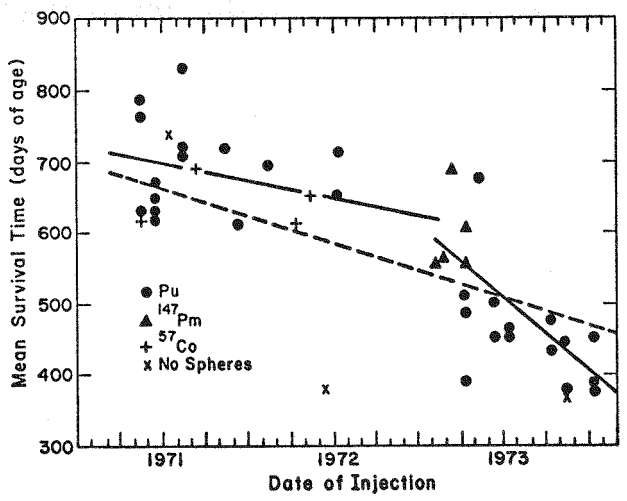

Fig. 1. Mean survival times for experimental hamsters as a function of the date of injection.

the early death rate) when expressed as mean survival time as a function of date of injection with the microspheres. The lines are least-squares fits to the data for three groupings: (1) the period prior to February 1973 (including one of the ^{147}Pm points at 560 days survival and rejecting the very low ^{57}Co point from June 1972); (2) the period subsequent to February 1973 (including all the remaining ^{147}Pm points and the plutonium point in May 1973 at 680 days survival); and (3) the composite of all data (again excepting the low point in June 1972). February 1973 corresponds to the time at which the supplier of hamsters was changed. It is clear that the composite line, which assumes a steady decline in mean survival time, is a poor fit to the data and probably does not correspond to reality. Another

TABLE II

SUMMARY OF PROMETHIUM-147 EXPOSURES

Date of Exposure	Number of Animals	Spheres per Animal	Specific Activity (nCi per sphere)	Lung Burden (μCi)	Mean Survival Time (days of age[a])
1973 February	62	6000	0.07	0.42	560
February	52	300 000	0.07	21.00	560
March	61	50 000	0.07	3.50	690
April	64	10 000	0.45	4.50	560
April	62	50 000	0.45	22.00	610
May	22	10 000	0.45	4.50	(320)[b]

[a]Animals exposed at age 100 days.

[b]$C_2H_2Cl_4$ infarcts.

TABLE III

SUMMARY OF CONTROLS

Date of Exposure	Number of Animals	Spheres per Animal	Mean Survival Time (days of age[a])
1971 May	70	2000	615
July	72	None	740
September	82	10 000	690
1972 April	96	None	615
May	133	4000	655
June	24	500 000	380
1973 November	69	None	380
1974 June	70	Variable	b
June	75	100 000	b

[a]Animals exposed at age 100 days.

[b]No data yet available.

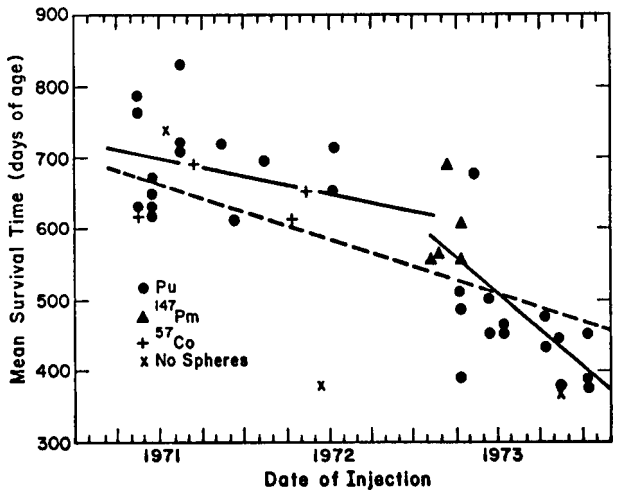

Fig. 1. Mean survival times for experimental hamsters as a function of the date of injection.

the early death rate) when expressed as mean survival time as a function of date of injection with the microspheres. The lines are least-squares fits to the data for three groupings: (1) the period prior to February 1973 (including one of the ^{147}Pm points at 560 days survival and rejecting the very low ^{57}Co point from June 1972); (2) the period subsequent to February 1973 (including all the remaining ^{147}Pm points and the plutonium point in May 1973 at 680 days survival); and (3) the composite of all data (again excepting the low point in June 1972). February 1973 corresponds to the time at which the supplier of hamsters was changed. It is clear that the composite line, which assumes a steady decline in mean survival time, is a poor fit to the data and probably does not correspond to reality. Another

alternative is perhaps most likely: that is, more or less constant survival times of about 700 and 460 days, with a transition period during the first 4 months of 1973. During this period, hamsters from the second supplier appeared to show survival times spanning the entire range, indicating that the problem is not primarily due to the change in supplier.

The only clue to the nature of the difficulty is the predominance of bimodal survival curves in 1973, with an abnormally high death rate at early times. The data presented here have been expressed as a single value for the mean survival time without regard for the slopes or fractions of population for the two components. In addition, it should be noted that much of the 1973 data is based on populations for which a major fraction still survives. The extrapolated survival time, therefore, is subject to revision as more data accumulate. Detailed pathological studies are underway to try to identify the cause of death and thus clarify the situation.

Since the early animals are dying at later times post-exposure, we have investigated the possibility that the cohorts share a single calendar period of increased mortality. No evidence of this possibility has been found, and it is rendered improbable by the fact that the maximum death rate in the early animals occurred in early 1973, while the 1973 groups have not yet reached the expected time of maximum mortality rate.

Because of the wide range of exposures within each of the two periods, it is possible to demonstrate the absence of significant life shortening by the radiation insult in spite of the temporal change in survival. The data are shown in Fig. 2 in which the mean survival time is plotted against lung burden in nCi of plutonium. The numbers beside each point give the number of spheres administered (specific activity can be calculated by dividing this number into the lung burden). The upper curve, containing the 1971-1972 exposures, shows a possible slight decline in survival time with increasing dose, but the effect is not statistically significant. The highest dose of 360 nCi was obtained by exposure to 6000 microspheres of specific activity 59 pCi per sphere. It is estimated that about 2% of the total lung mass was irradiated in this experiment. The median dose to the cells at risk is calculated to be 650 krads per yr; averaging the dose over the entire

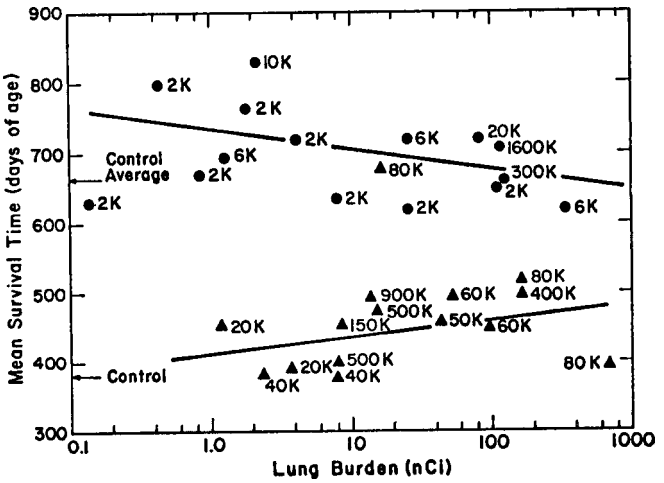

Fig. 2. Mean survival times for experimental hamsters as a function of lung burden (in nCi of plutonium). The two subgroups correspond to different suppliers. The number beside each point is the number of microspheres administered: (-●-) first supplier and (-▲-) second supplier.

lung mass gives a yearly dose of about 36 krads. The cluster of four exposures near 100 nCi was obtained by a variety of conditions, ranging from 2000 to 1 600 000 spheres of specific activities 0.07 to 59 pCi per sphere. The fraction of lung irradiated varied from about 1% to nearly 100%, with no detectable effect on survival.

Absence of radiation-induced life shortening is also suggested by the 1973-1974 exposures, but the shorter and extrapolated mean survival time, greater scatter, and incomplete status of the experiments (the great majority of the animals are still alive) make the data less conclusive. The apparent increase of survival with dose is not statistically significant. The highest of all exposures, 720 nCi from 80 000 spheres (about 20% of lung irradiated) of activity 8.8 pCi per sphere, may show a significant life shortening. This experiment was begun in April 1973, and only 40% of the animals remain alive. The survival curve is bimodal, with a break at 200 days post-exposure (80% survival), but the death rate remains abnormally high. Thus, although the mean survival time of 395 days (295 days post-exposure) is not unusual, the shape of the curve is, and the fraction of the population showing normal death rates -- which has been detected in other short-lived groups -- appears to be absent here. This group will be followed with special interest during the duration of the experiment.

Not shown is the point representing hamsters whose lungs were instilled weekly with 50 nCi of ^{210}Po. The mean survival time is 275 days (175 days after beginning of the exposure). The survival data suggest a possible decline in the death rate, with 60% of the animals dead. It is probable that this life shortening is real (see more detailed discussion of this experiment below).

The acute lethality of the microspheres can be compared with that of inhaled $^{238}PuO_2$ aerosol reported by Hobbs *et al.*[8] They have reported a reduced survival at 100 days post-exposure when the initial lung burden exceeds 200 nCi. In contrast, our hamsters exposed to static microspheres show no such effect at lung burdens up to 720 nCi. The relevant data are summarized in Table IV.

Pathology

We have thus far observed 3 deaths from neoplastic disease originating in the lungs of hamsters exposed to microspheres (Table V). Two have been described previously,[5] a hemangiosarcoma and an undifferentiated sarcoma, which occurred after 41 and 52 wk of exposure, respectively. Both were in the group of 71 animals exposed to 2000 microspheres of specific activity 0.42 pCi/sphere, with a resultant lung burden of 0.84 nCi. An additional lung tumor, a mucinous adenocarcinoma, was found in December 1973 in one of 148 animals exposed to 6000 microspheres of 59 pCi/sphere activity, 354 nCi lung burden. The hemangiosarcoma replaced the left lung almost entirely and severely compressed the adjacent normal lung tissue with no evidence of metastases. In the case of the undifferentiated sarcoma, multiple nodules were found in both lungs. The third tumor involved one lobe of the right lung and was locally invasive.

All hamsters from the initial experiments begun in 1971 and many from the expanded experiments of 1973 have now died. At necropsy, all animals are carefully scanned for gross tumor development, and much of the histological material has been screened for any pathological damage. In addition, intensive search has been made in special groups, such as 254 hamsters with lung burdens of 110 to 360 nCi exposed in 1971 and 1972.

As reported last year,[6] epithelial changes (metaplasia) have been observed at late times (1 to 2 yr) with specific activities above 4 pCi/sphere and lung burdens above 8 nCi. There was an indication that a similar effect might occur after 6 months exposure to a lung burden of 55 nCi from 0.9 pCi per sphere particles. Continued observation of hamsters from these and similar groups have failed to identify any development of this lesion into a tumor.

TABLE IV

COMPARISON OF ACUTE LETHALITY

	Lung Burden (nCi)	Survival at 100 Days (%)
$^{238}PuO_2$ Aerosol[8]		
	720	27 ± 7
	260	81 ± 6
	220	72 ± 6
	100	95 ± 3
ZrO_2 Microspheres		
	720	96 ± 2
	354	96 ± 2
	170	91 ± 4
	126	100 ± 3

Radiation Standards for "Hot Particles"

Tamplin and Cochran predict on page 43,[3] on the

TABLE V

GROSS TUMORS OBSERVED

Number of Microspheres	Specific Activity (pCi per sphere)	Animals in Group	Lung Burden (nCi)	Exposure Time (wk)	Type of Tumor
2000	0.42	71	0.84	41	Hemangiosarcoma
				52	Undifferentiated sarcoma
6000	59.00	148	354.00	104	Mucinous adenocarcinoma

basis of the "Geesaman hypothesis,"[9] that a single microscopic particle with an alpha activity higher than 0.07 pCi will produce lung tumors with a probability of 5×10^{-4} independent of particle activity. The model on which this number rests is rat skin. Therefore, the lung of the hamster, another rodent, would appear to offer a reasonable test, especially since Little *et al.*[1,2] have demonstrated a high frequency of lung tumors in hamsters exposed to 10 to 200 nCi ^{210}Po after induction times of 37 to 53 wk. The majority of the plutonium exposures presented here, therefore, have been of sufficient intensity and duration for the development of any tumors induced.

We summarize our experiments in Table VI to display the total number of spheres used. The groups are formed primarily on the basis of time elapsed since injection (column 1) and also on the basis of number of spheres per animal (column 3) and specific activity (column 6). Column 5 (predicted tumors) is calculated by multiplying the total number of spheres by the Tamplin-Cochran prediction of 1/2000. For 2 of the groups, the sphere specific activity was below that arbitrarily chosen as defining "hot particles." For the remaining set of experiments involving 1565 hamsters and 88 000 000 spheres, the prediction is 44 000 tumors compared with 3 observed.

A more compact grouping of some of the same experiments is given in Table VII. Here the additional constraint has been added that the lung burden be between 50 and 200 nCi, a range in which Little *et al.* have reported high tumorigenicity for ^{210}Po. The 302 hamsters in this table have been observed for 65 to 117 wk (mean survival times were 56 to 89 wk after exposure) and were exposed to 71 000 000 spheres. The Tamplin-Cochran model predicts 35 000 tumors, but none have been observed in these groups.

The enormous discrepancy between prediction and experimental result appears to render the Tamplin-Cochran model and the Geesaman hypothesis completely untenable.

TABLE VI

TUMORS PREDICTED BY TAMPLIN-COCHRAN "HOT PARTICLE" MODEL

Duration of Experiment (wk)	Number of Animals	Spheres per Animal	Total Spheres	Predicted Tumors[a]	Specific Activity (pCi per sphere)
178	570	2000	1 140 000	580	0.07 to 59.00
173	54	300 000 to 1 600 000	42 000 000	21 000	0.07 to 0.42
95 to 169	527	6000 to 20 000	3 900 000	1950	0.22 to 59.00
87	146	150 000 to 400 000	31 000 000	15 500	0.06 to 0.42
87	97	500 000	48 000 000	(24 000)	0.03[b]
52	41	500 000 to 900 000	30 000 000	(15 000)	0.016[b]
39 to 48	268	20 000 to 60 000	10 000 000	5000	0.06 to 1.60

[a]By the Tamplin-Cochran model.

[b]Not "hot particles" by the Tamplin-Cochran definition.

TABLE VII

SUMMARY OF "HOT PARTICLE" EXPOSURES

Date of Exposure	Number of Animals	Spheres per Animal	Specific Activity (pCi per sphere)	Lung Burden (nCi)	Mean Survival Time (days of age[a])	Total Spheres
July 1972	20	1 600 000	0.07	112	715	32 000 000
July 1972	34	300 000	0.42	126	655	10 000 000
April 1973	109	60 000	0.90	55	490	6 500 000
April 1973	102	80 000	2.10	168	515	8 200 000
June 1973	37	400 000	0.42	170	505	14 800 000

[a]Animals exposed at age 100 days.

Other Microsphere Experiments

A group of 100 rats were exposed in January 1972 by jugular injection to 6000 microspheres of 4.3 pCi per sphere activity. These animals showed a mean survival time of 830 days of age, and the last animal died 33 months post-exposure. No pulmonary tumors were observed in this group, and most of the animals died of afflictions common to aging rats. Pulmonary changes typical of chronic respiratory disease were never observed.

In January 1974, a group of 60 hamsters were injected intravenously with 60 000 spheres of activity 1.6 pCi/sphere, followed 2 wk later by an intravenous injection of sym-difluorotetrachloroethane at a dose of either 1 µliter or 5 µliters. This treatment created multiple small infarcts in the peripheral lung. The affected tissue undergoes eschemia, necrosis, and repair, with eventual scar formation. As part of the repair mechanism, there is considerable neo-epithelization in the marginal areas around the infarcts. In many cases, these new epithelial cells are well within alpha range of the microspheres and show no apparent radiation damage. To date, no tumors have occurred in this group.

Polonium-210 Experiments

A collaborative study with Professor John Little and his colleagues at the Harvard University School of Public Health has begun to determine whether the striking difference in tumor incidence between hamsters exposed to intratracheal instillation of ^{210}Po solutions and those given intravenous injection of plutonium microspheres can be associated with differences between our laboratories such as source of the hamsters, local environment, etc. We have supplied microspheres for experiments in Boston and are performing polonium experiments in Los Alamos.

Instillation under Brevital anesthesia was performed according to the Harvard procedure, administering 0.2 ml per animal of freshly prepared solutions (10 µliters of 1 M HNO_3 polonium solution in 10 ml of physiological saline). A dose of 54 ± 3 nCi ^{210}Po was given weekly for 15 wk, as determined by liquid scintillation counting of "dummy dose" aliquots.

Measurements of ^{210}Po in the lungs of 2 hamsters sacrificed at 1.5 h after instillation accounted for 95 and 102% of the instilled dose, respectively (assay by liquid scintillation counting after solution in Protosol*). Measurements of lung, blood, spleen, kidney, and liver from pairs of animals sacrificed at 1, 2, and 4 days post-instillation showed total retention in these organs, declining with an apparent half-time of about 5 days. Retention in the lung alone followed a similar time-course, accounting for 85 to 92% of total recovery independent of time. Six parts of the lungs were assayed separately: upper and lower right, upper and lower left, cardiac, and intermediate lobe. Concentrations in pCi/mg of wet tissue were highly variable, with factors of 10 to 40 between extreme values. No consistent pattern was noted; the distributions were apparently random, depending on the uncontrolled details of the instillation process. As might be expected, animals sacrificed after 4 weekly instillations and 1 week after the last of 15 weekly instillations showed much less variability within the lungs, extremes spanning only factors of 2 to 3 in these cases. These animals showed average lung burdens of 1.14 and 1.37 times the weekly dose at 4 and 16 weeks, respectively, corresponding to an elimination half-time of about 8 days, or slightly longer than the 5 days estimated from the single instillation study.

Autoradiographs of histologic sections have indicated wide distribution and good dispersion of the polonium at the microscopic level. Alpha tracks were seen in primary bronchi, secondary and tertiary bronchioles, and alveoli (Fig. 3). Tracks were also demonstrated in foci of bronchial hyperplasia and squamous metaplasia (Fig. 4). Although some multiple track stars were observed, intense localization of tracks that would indicate agglomeration of activity was rare.

At about 30 wk after the first instillation, it is still too early to determine the extent of our agreement with the Harvard results. Consideration of our exposure of 54 nCi x 15 wk and theirs of 200 nCi x 7 wk shows that the initial rates of death have been comparable: we have lost 13 out of 20 animals for 35% survival, compared with 16 out of 37 for 57% survival at Harvard. At this time, they

*A proprietary quaternary ammonium base tissue solvent from New England Nuclear Corporation.

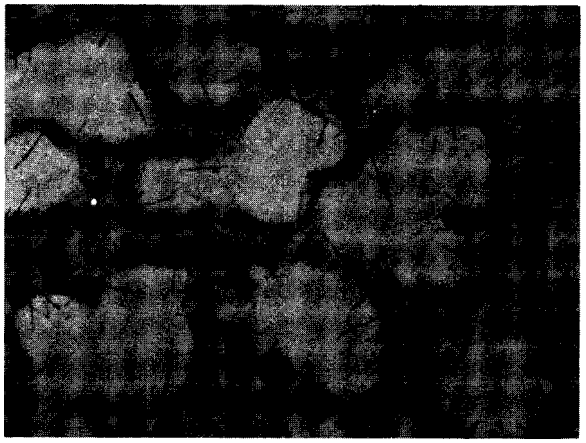

Fig. 3. Autoradiograph of peripheral lung with ^{210}210 alpha tracks.

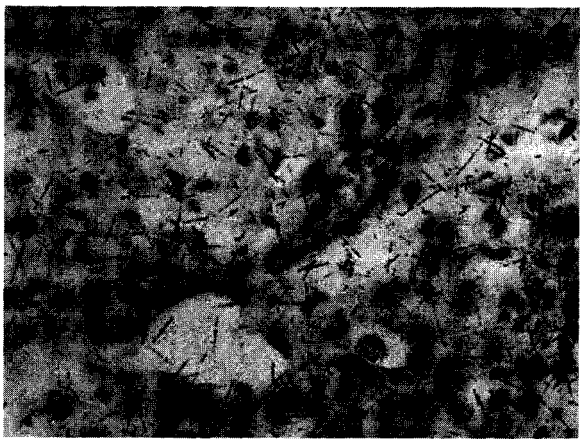

Fig. 4. Autoradiograph of lung with ^{210}Po alpha tracks. Note thickening of alveolar walls and bronchiolar hyperplasia into alveoli.

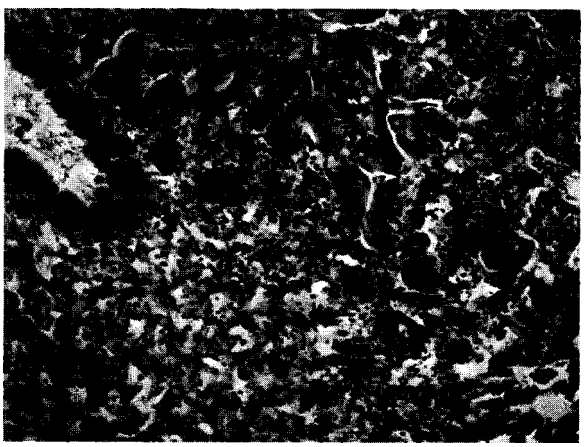

Fig. 5. Prominent squamous metaplasia of lung, accompanied by inflammatory cells (hematoxylin and eosin stain).

reported 8 tumors (50% of deaths), while our result is 1 gross tumor (8% of deaths). The difference is not statistically significant. Detailed study of our animals shows squamous metaplasia and bronchiolar hyperplasia (which may be pre-neoplastic lesions, Fig. 5) in animals sacrificed as early as 2 wk after the last polonium instillation. All of the animals surviving the last instillation that have died thus far (11 out of 18, 7 still alive) had thickened alveolar walls, squamous metaplasia, and hyperplasia of bronchial epithelium. These changes were accompanied by focal areas of acute and/or chronic pneumonia. Animals with longer survival times had more pronounced and more extensive pre-neoplastic lesions. One animal that was sacrificed when moribund 20 wk after the last instillation had a large adenoma of bronchial origin in the left lung. The tumor contained a prominent secretory component (Fig. 6) and non-secretory foci characterized by densely packed cells in acinar configurations (Fig. 7).

Fig. 6. Adenoma of bronchial origin. Note the amorphous secretory product in dilated glands (hematoxylin and eosin stain).

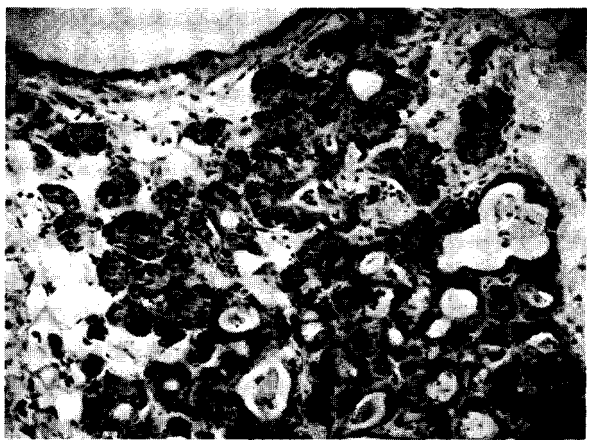

Fig. 7. Adenoma of bronchial origin (hematoxylin and eosin stain).

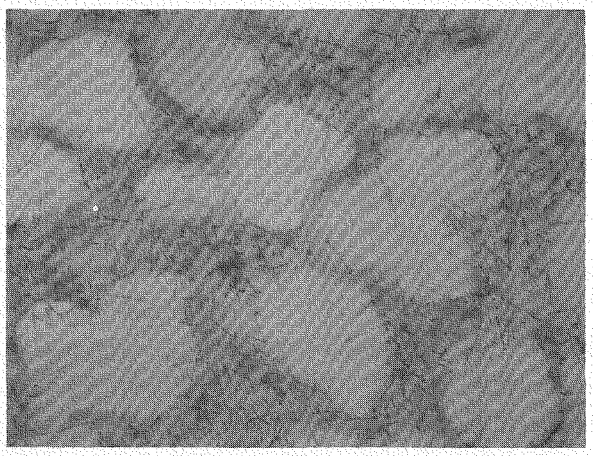

Fig. 3. Autoradiograph of peripheral lung with ^{210}210 alpha tracks.

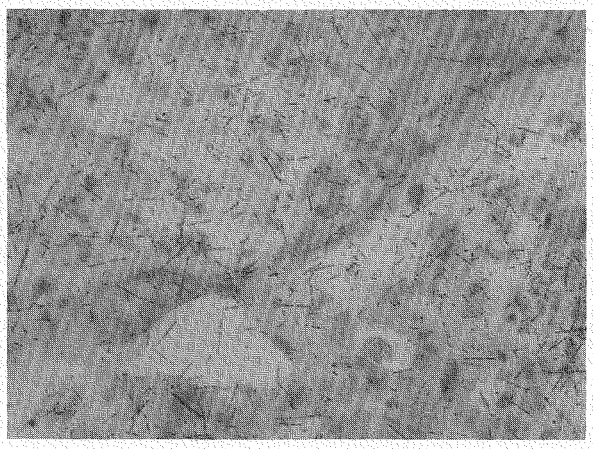

Fig. 4. Autoradiograph of lung with ^{210}Po alpha tracks. Note thickening of alveolar walls and bronchiolar hyperplasia into alveoli.

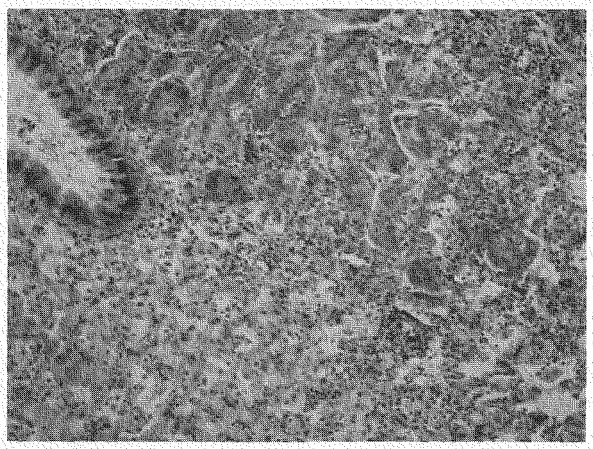

Fig. 5. Prominent squamous metaplasia of lung, accompanied by inflammatory cells (hematoxylin and eosin stain).

reported 8 tumors (50% of deaths), while our result is 1 gross tumor (8% of deaths). The difference is not statistically significant. Detailed study of our animals shows squamous metaplasia and bronchiolar hyperplasia (which may be pre-neoplastic lesions, Fig. 5) in animals sacrificed as early as 2 wk after the last polonium instillation. All of the animals surviving the last instillation that have died thus far (11 out of 18, 7 still alive) had thickened alveolar walls, squamous metaplasia, and hyperplasia of bronchial epithelium. These changes were accompanied by focal areas of acute and/or chronic pneumonia. Animals with longer survival times had more pronounced and more extensive pre-neoplastic lesions. One animal that was sacrificed when moribund 20 wk after the last instillation had a large adenoma of bronchial origin in the left lung. The tumor contained a prominent secretory component (Fig. 6) and non-secretory foci characterized by densely packed cells in acinar configurations (Fig. 7).

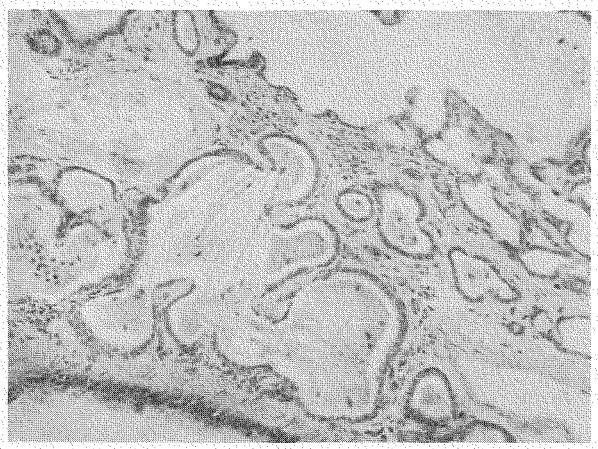

Fig. 6. Adenoma of bronchial origin. Note the amorphous secretory product in dilated glands (hematoxylin and eosin stain).

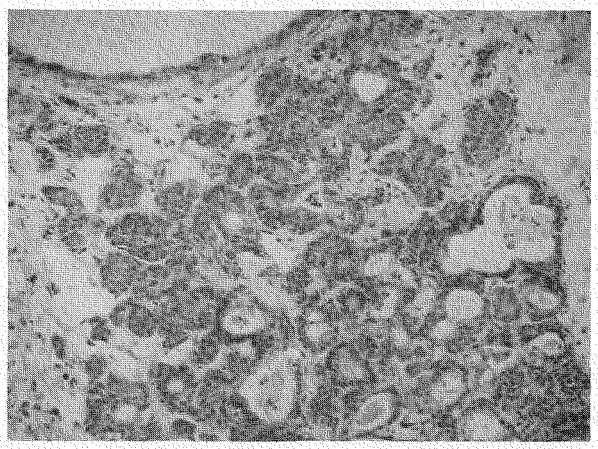

Fig. 7. Adenoma of bronchial origin (hematoxylin and eosin stain).

These polonium effects are compatible with the Harvard findings, but further investigation is necessary before a meaningful quantitative comparison can be made between the polonium results at the two institutions. Even at this early stage, however, the polonium/plutonium dichotomy is confirmed by the striking differences in the pathology of hamsters receiving comparable lung burdens of the two nuclides. The two types of exposure, of course, differ in many ways in addition to the spatial and temporal distribution of energy deposition. These include possible physical and chemical trauma to the lungs during administration and the exposure of additional organs during translocation and excretion of the polonium. We plan additional studies to identify the parameters and mechanisms responsible for the differences in response.

REFERENCES

1. J. B. Little, B. N. Grossman, and W. F. O'Toole, "Respiratory Carcinogenesis in Hamsters Induced by Po-210 Alpha Radiation and Benzo(a)pyrene," in Morphology of Experimental Respiratory Carcinogenesis (P. Nettesheim, M. G. Hanna, Jr., and J. W. Deatherage, Jr., eds.), USAEC Division of Technical Information, Oak Ridge, Tennessee (1970), pp. 383-394.

2. J. B. Little, B. N. Grossman, and W. F. O'Toole, "Factors Influencing the Induction of Lung Cancer in Hamsters by Intratracheal Administration of Po-210," in Radionuclide Carcinogenesis (C. L. Sanders, R. H. Busch, J. E. Ballou, and D. D. Mahlum, eds.), USAEC Division of Technical Information, Oak Ridge, Tennessee (1973), pp. 119-137.

3. A. R. Tamplin and T. B. Cochran, "Radiation Standards for Hot Particles, A Report on the Inadequacy of Existing Radiation Protection Standards Related to Internal Exposure of Man to Insoluble Particles of Plutonium and Other Alpha-Emitting Hot Particles," Natural Resources Defense Council report (February 14, 1974).

4. C. R. Richmond and G. L. Voelz, eds., "Annual Report of the Biological and Medical Research Group (H-4) of the LASL Health Division, January through December 1971," Los Alamos Scientific Laboratory report LA-4923-PR (April 1972), pp. 18-34.

5. C. R. Richmond and G. L. Voelz, eds., "Annual Report of the Biological and Medical Research Group (H-4) of the LASL Health Division, January through December 1972," Los Alamos Scientific Laboratory report LA-5227-PR (March 1973), pp. 1-11.

6. C. R. Richmond and E. M. Sullivan, eds., "Annual Report of the Biomedical and Environmental Research Program of the LASL Health Division, January through December 1973," Los Alamos Scientific Laboratory report LA-5633-PR (May 1974), pp. 1-9.

7. E. C. Anderson, L. M. Holland, J. R. Prine, and C. R. Richmond, "Lung Irradiation with Static Microspheres," in Experimental Lung Cancer, Carcinogenesis and Bioassays, Springer-Verlag, Heidelberg (1974), in press, CONF-740648-1.

8. C. H. Hobbs, J. A. Mewhinney, R. O. McClellan, D. O. Slauson, and J. J. Miglio, "Toxicity of Inhaled $^{238}PuO_2$ in Syrian Hamsters. I," in Inhalation Toxicology Research Institute Annual Report 1972-1973, Lovelace Foundation for Medical Education and Research, Albuquerque, New Mexico, report LF-46 (1974), pp. 146-147.

9. D. P. Geesaman, "An Analysis of the Carcinogenic Risk from an Insoluble Alpha-Emitting Aerosol Deposited in Deep Respiratory Tissue: Addendum," Lawrence Radiation Laboratory report UCRL-50387 (October 9, 1968).

EFFECTS OF IONIZING RADIATION FROM EXTERNAL SOURCES ON LIVING ORGANISMS

(J. F. Spalding, L. M. Holland, P. M. LaBauve, J. E. London, J. R. Prine, O. S. Johnson, and M. R. Brooks)

Introduction

The persistent biological effects of relatively large doses of ionizing radiation, delivered acutely or chronically to man, are not well known. Reasonable estimates of the magnitude of the persistent radiation injury component, referred to as the "irreparable" or long-term residual lesion, are difficult to make because there are few experimental data on large animals and reports based on investigations with rodents are frequently conflicting. Thus, guidelines and recommendations for human exposure to ionizing radiation have a tenuous basis.

Research projects in progress and reported here are programmatically designed to meet the objectives of the whole-body exposure (from external sources) program. These objectives are to recognize and react to problems of the Division of Biomedical and Environmental Research and, thus, to obtain knowledge about the nature and magnitude of the persistent lesion induced by exposure to radiation under different total-dose and dose-rate conditions.

It is well known that dose rate influences the nature of the immediate and persistent biological response to radiation injury. However, the comparative biological effects of dose protraction by continuous exposure at different dose rates and by the acute fractionation method in a given mammalian

species and among different species are not well known. Earlier investigations have clearly demonstrated that the method used to protract a given dose of radiation may significantly influence the nature and magnitude of the biological effect.[1,2]

Investigations in the Mammalian Radiobiology Group (H-4) are designed to obtain needed acute and low dose-rate data in species with different radiation response characteristics. Because the primate (monkey) is a relatively long-lived animal that has not been used widely in low dose-rate investigations, it is of considerable interest as a research species. The dog and monkey differ widely in their response to single high dose-rate exposure and to low dose-rate continuous exposure; therefore, comparative dose-rate studies of the two species under the same exposure conditions should yield data that would be helpful in better understanding the kinetics of radiation injury and recovery. Radiation effects data from these two species should also help to make extrapolations of the prompt and long-term effects from animals to man more meaningful. In addition, rodents have been used extensively to further the interspecies dose-effect comparisons.

Future studies will emphasize the effects of total dose, dose rate, and age at exposure on mice in an attempt to study these variables at the same time under the same laboratory conditions. Such a study has been needed for a long time to help define the radiobiological damage inflicted under minimal exposure conditions. Work with dogs and monkeys will continue but perhaps at a somewhat lower level of effort.

REFERENCES

1. J. F. Spalding, N. J. Basmann, R. F. Archuleta, and O. S. Johnson, "Comparative Effects of Dose Protraction by Fractionation and by Continuous Exposure," Radiation Res. 51, 608 (1972).

2. J. F. Spalding, R. F. Archuleta, O. S. Johnson, and J. E. London, "Comparative Effects of Exposure of the Mouse to Radiation at Constant and Changing Dose Rates," Health Phys. 25, 381 (1973).

Comparative Response of Monkeys and Dogs to Dose Protraction by Fractionation and Continuous Low Dose-Rate Exposure

The monkey (*Macaca mulatta*) is known to be more resistant to acute radiation in the LD_{50}^{30} dose range than is the dog (beagle) by a factor of approximately 2. Dose protraction by low dose-rate continuous exposure has been shown to increase the dose required to cause 50% lethality in both dogs[1,2] and monkeys.[2,3] With continuous exposure at 24 rad/day, the difference in radiation sensitivity between dogs and monkeys (in terms of hematological response and mean survival time) is not significant.[2] We have completed a study to determine the comparative effects of dose protraction by fractionation and continuous low dose-rate exposure in beagles and monkeys (*Macaca mulatta*).

Dogs (12) and monkeys (12) were exposed to 100 rad of ^{60}Co gamma rays, at approximately 18 rad/h, at 28-day intervals until they had accumulated a total dose of 1300 rad. Beginning 84 days after the last (13th) exposure, they were exposed continuously to gamma rays at 35 rad/day. Twelve additional dogs and monkeys with no previous conditioning exposures were also exposed continuously at 35 rad/day to determine possible residual injury in conditioned animals as reflected by a reduction in mean survival time in the radiation field. Blood samples were taken at 7-day intervals throughout the fractionation regime, the 84-day recovery period, and until the animals succumbed to the stress of continuous exposure.

One monkey and 4 dogs died during the fractionation regime, and 2 dogs died shortly thereafter. The 6 deaths out of the original 12 dogs may be considered as representative of a mean survival time. Thirteen 100-rad doses delivered within a period of 336 days is equivalent to a continuous dose rate of 3.87 rad/day. Dogs exposed to gamma rays continuously at a slightly higher dose rate (5 rad/day) were able to tolerate about 7000 rad before reaching their mean survival time, which was at least twice that observed here.[1] This is further indication that continuous irradiation is much less effective biologically than a similar dose given by fractionation. This difference in response of the dog supports earlier studies with mice which showed that equal doses of gamma rays given over an equal span by continuous low dose-rate exposure or by fractionation produced significantly different amounts of injury.[4,5] The seemingly greater sensitivity of dogs over monkeys when exposed to protracted irradiation by the acute fractionation method is

similar to the relative radiation sensitivities observed from single acute exposure in the LD^{30}_{50} dose range.

The mean survival times for the 11 monkeys and 6 dogs that survived the 1300-rad fractionation regime were 54 ± 17 days and 85 ± 46 days, respectively; the difference between the two species is not significant because of the small number of animals involved. Mean survival times for the non-conditioned dogs and monkeys were 58 ± 11 days and 60 ± 9 days, respectively. Thus, non-conditioned dogs and monkeys react similarly with regard to survival during continuous irradiation at this dose rate (35 rad/day).

Mean values of neutrophils, lymphocytes, and packed cell volumes during the 1300-rad fractionation regime and subsequent 84-day recovery period are shown for dogs and monkeys in Fig. 1. Hematopoietic response in terms of the above cellular components of peripheral blood was similar for both species through the 7th 100-rad exposure, but dogs showed less resistance to continued fractionation. Mean values for these hematologic parameters for conditioned dogs and monkeys during continuous gamma-ray challenge at 35 rad/day are shown in Fig. 2. As shown in the figure and the above mean survival time data, non-conditioned dogs and monkeys responded to dose protraction by continuous exposure at 35 rad/day in an almost identical manner. In contrast to the comparative species response to acute sublethal

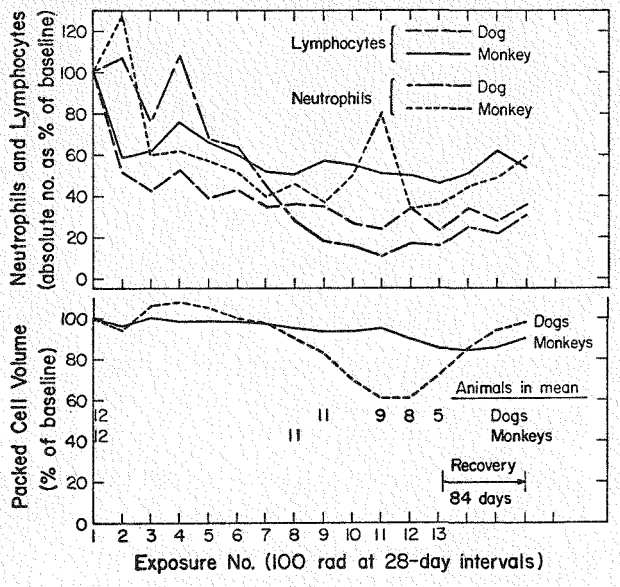

Fig. 1. Hematologic parameters as a function of individual exposure.

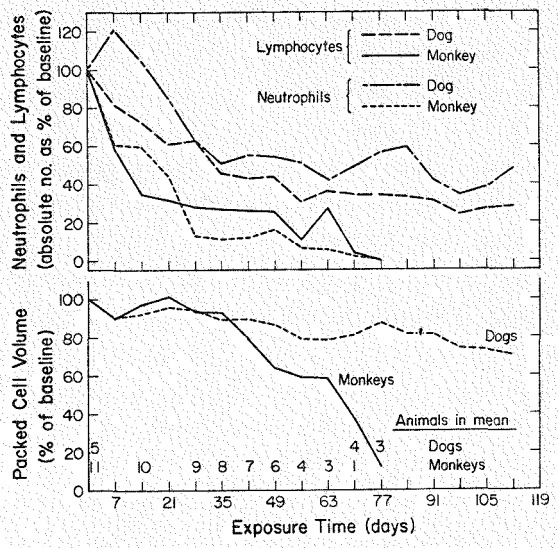

Fig. 2. Hematologic parameters as a function of exposure time.

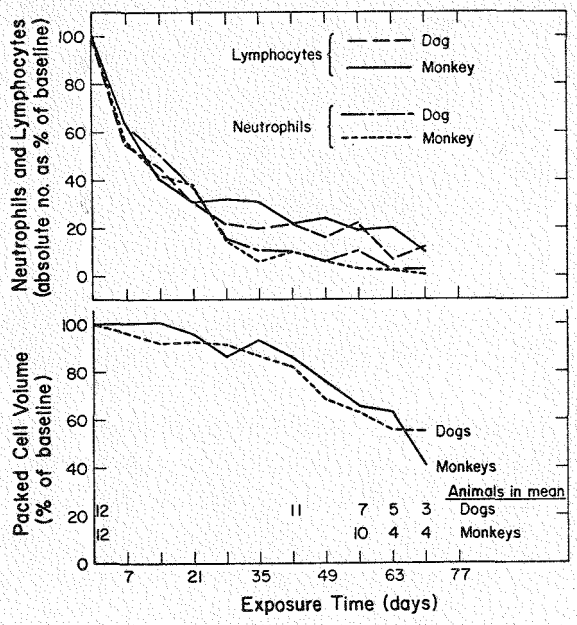

Fig. 3. Hematologic parameters as a function of exposure time.

fractions (shown in Fig. 1), the conditioned dogs responded to the ameliorating effects of dose protraction as well as or better than monkeys (see Fig. 2). The same peripheral blood characteristics for the non-conditioned dogs and monkeys are shown in Fig. 3. The similarities in response of dogs and monkeys to continuous gamma-ray exposure at 35 rad per day are even more striking in the non-conditioned animals.

In conclusion, the attempt to measure residual injury from a 1300-rad conditioning dose as a reduction in mean survival time in a continuous gamma-ray environment at 35 rad/day was unsuccessful. The possibly superior resistance of conditioned dogs to the challenging dose may be due to a selection of radioresistant animals by the high death rate during challenge.

REFERENCES

1. W. P. Norris, T. E. Fritz, and C. M. Pool, in: Argonne National Laboratory report ANL-8070 (1973), p. 31.

2. J. F. Spalding, L. M. Holland, J. R. Prine, P. M. LaBauve, and J. E. London, "Comparative Effects of Dose Protraction and Residual Injury in Dogs and Monkeys," Radiation Res. 54, 453-462 (1973).

3. J. F. Spalding, L. M. Holland, O. S. Johnson, J. R. Prine, J. E. London, and P. M. LaBauve, "Recovery and Residual Injury in Monkeys Exposed to Large Doses of Radiation by Fractionation," Los Alamos Scientific Laboratory report LA-5724-MS (September 1974).

4. J. F. Spalding, N. J. Basmann, R. F. Archuleta, and O. S. Johnson, "Comparative Effects of Dose Protraction by Fractionation and by Continuous Exposure," Radiation Res. 51, 608 (1972).

5. J. F. Spalding, R. F. Archuleta, O. S. Johnson, and J. E. London, "Comparative Effects of Exposure of the Mouse to Radiation at Constant and Changing Dose Rates," Health Phys. 25, 381 (1973).

Recovery Rate and Life Reduction in Mice Exposed to Gamma-Ray Fractionation at Different Dose Levels

Models to describe the kinetics of radiation-induced biological injury and repair with reasonable accuracy have been sought for over a decade. Although most investigators and theorists introduce slightly different concepts into their various models,[1-8] two factors (namely, short-term reparable and irreparable or long-term injury) and the uncertainties revolving around them are basic to all models. This study was done to investigate the two-component concept of radiation injury by observing the comparative effects of three levels of gamma-ray exposure administered by the fractionation method.

Two hundred RF strain virgin female mice 90 ± 7 days of age were randomly assigned to 4 groups of 50 mice each and given discrete, fractionated exposures to gamma radiation from ^{60}Co. For group I, the total integrated dose reached 1, 2, and 3 multiples of the acute LD_{50}^{90} dose (800 rad) at 35, 92, and 145 days, respectively. Group II reached 810 and 1600 rad at 65 and 145 days, and Group III reached 800 rad at 145 days. Group IV was the control group. Exposures were made at time intervals varying from 3 to 14 days in a random pattern, all three groups being exposed at the same times. Each dose was calculated to give the desired cumulative total at the time of delivery.

The dose rate for all exposures was approximately 0.5 rad/min; the time for each discrete exposure during the total fractionation period (i.e., 145 days) was varied to meet the total dose requirements. Mice were housed on wood shavings in box-type (13 by 20 by 30 cm) stainless steel cages between exposures and were checked daily. Blood samples were obtained from a few animals in each group prior to each exposure. Body weight and voluntary activity were observed through 400 days of age in each group.

Red blood cell (RBC) counts and mean cell volume (MCV) values through 190 days of the exposure regime are shown in Fig. 1. The stress of gamma-ray exposure caused general depression of RBC counts in the peripheral blood in all dose levels, and there was some tendency for the degree of depression to correlate with radiation dose. The MCV values of exposed groups were generally larger than were control group values and, in most instances, were greater for animals in the higher dose regimes. None of the differences observed were remarkable, but the deviations from control values do indicate a

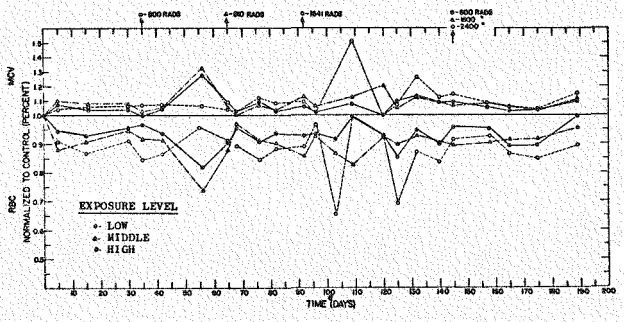

Fig. 1. Total RBC and MCV of control and 3 groups of mice receiving different gamma-ray exposures by dose fractionation. In this radiation regime, the high exposure level had accumulated gamma-ray doses equal to 1, 2, and 3 acute LD_{50}^{90}s for this strain by the 35th, 92nd, and 145th days. The middle exposure level had accumulated 1 and 2 LD_{50}^{90}s by the 65th and 145th days, and the low exposure level had accumulated 1 LD_{50}^{90} by the 145th day.

degree of bone marrow damage. If the apparent correlation with dose is real, one would be tempted to imply a progressive marrow lesion, but this must be accompanied by a non-impaired recovery process (RBC repopulation of peripheral blood) to yield the data shown in Fig. 1. Such a bone marrow resilience would not be unique to the mouse. We have reported similar responses in dogs and monkeys following gamma-ray exposure by fractionation.[9,10]

Voluntary activity (wheel revolutions per 24-h test period in activity chambers) was observed at 241, 305, and 403 days of age to test for a possible reduction in vigor associated with the residual radiation-induced injury. These observations are shown in Table I. At 241 days of age, less than 10% of the mice in any of the 4 groups had died, and Groups I, II, and III had accumulated gamma-ray doses of 824, 1648, and 2472 rad, respectively. Activity in the exposed groups was significantly less than in the control group, but there were no significant differences among the 3 exposed groups; the activity picture was the same at 305 days of age. A change in general vigor with increased age from 305 to 403 days was observed in control animals (an observation consistent with earlier studies[11]) and in Groups I and III. However, only Group III showed significantly less activity at this age than that of control animals (Table I). Voluntary activity did not appear to be a sensitive enough end point to measure dose-dependent residual

TABLE I

VOLUNTARY ACTIVITY AS MEASURED IN ACTIVITY WHEEL REVOLUTIONS PER 24-H PERIOD (AVERAGE PER GROUP TESTED)

	Voluntary Activity[a] and Accumulated Gamma-Ray Dose							
	Control		Group I		Group II		Group III	
Age (days)	Dose (rad)	Activity	Dose (rad)	Activity	Dose (rad)	Activity	Dose (rad)	Activity
241	0	11 506 ± 573	824	8756 ± 451	1648	7329 ± 679	2472	8803 ± 538
305	0	11 510 ± 573	1043	8591 ± 684	2080	7722 ± 648	3120	8822 ± 685
403	0	8310 ± 893	1301	6845 ± 796	2596	7481 ± 537	3894	5778 ± 822

[a]Mean of activity (wheel revolutions per 24-h period) ± standard error.

TABLE II

BODY WEIGHTS (GROUP AVERAGES) FOR CONTROL AND IRRADIATED GROUPS FROM AGES 186 THROUGH 400 DAYS

	Accumulated Gamma-Ray Dose[a]							
	Control		Group I		Group II		Group III	
Age (days)	Dose (rad)	Mean Weight	Dose (rad)	Mean Weight	Dose (rad)	Mean Weight	Dose (rad)	Mean Weight
186	0	33.0 ± 0.32	593	33.6 ± 0.49	1186	33.4 ± 0.40	1779	33.0 ± 0.42
200	0	32.2 ± 0.29	665	33.7 ± 0.45	1331	33.3 ± 0.40	1997	32.0 ± 0.45
213	0	33.3 ± 0.26	710	34.7 ± 0.39	1420	33.7 ± 0.31	2130	32.5 ± 0.42
224	0	33.1 ± 0.26	766	34.6 ± 0.45	1534	35.0 ± 0.40	2300	33.8 ± 0.41
238	0	34.2 ± 0.36	824	35.9 ± 0.44	1648	35.0 ± 0.42	2472	34.0 ± 0.45
251	0	34.4 ± 0.35	867	36.1 ± 0.46	1733	34.8 ± 0.48	2600	33.9 ± 0.45
258	0	35.0 ± 0.34	895	36.6 ± 0.46	1790	35.3 ± 0.53	2685	34.6 ± 0.51
272	0	35.0 ± 0.45	930	37.2 ± 0.48	1859	35.7 ± 0.52	2789	34.9 ± 0.43
294	0	35.0 ± 0.46	1018	37.8 ± 0.57	2031	36.2 ± 0.57	3046	35.1 ± 0.50
341	0	37.9 ± 0.55	1148	40.3 ± 0.93	2294	38.3 ± 0.85	3440	37.4 ± 0.68
400	0	40.5 ± 0.55	1289	43.4 ± 0.95	2572	39.6 ± 1.46	3859	38.2 ± 1.27

[a]Column entries represent mean values ± their standard error.

radiation injury with these dose differences.

Body weights from 186 through 400 days of age are tabulated in Table II. Weights among the 4 groups were not different at 186 days of age. From age 200 days, significant differences in body weights among the 4 groups were observed; however, Group III, with the highest exposure level, did not differ significantly from controls at any age tested. At 238 days of age and above, Group I had mean body weights greater than all other groups, including the control. The shape of the weight vs age curve for all groups was consistent with that obtained earlier in a lifetime body-weight study done on the same strain of mice.[12]

Necropsies revealed that thymic lymphomas, tumors, etc., as described by Cosgrove,[13] were the cause of most early mortality; the mean body weight seemed to be associated with tumor incidence (i.e., groups with high incidence of tumors weighed more).

Survival data for the control and irradiated groups are plotted as percent survival vs time (in days) at 25-day intervals in Fig. 2. Mean survival times $\pm$ the standard error of the mean were 581 $\pm$ 24, 420 $\pm$ 18, 374 $\pm$ 16, and 402 $\pm$ 15 days, respectively, for controls and Groups I, II, and III; the irradiated group survival times were less than that of the control but were not different from each other. Thus, fractionated exposure regimes with total doses differing in magnitude by a factor of 3 did not result in a significant dose-dependent life shortening.

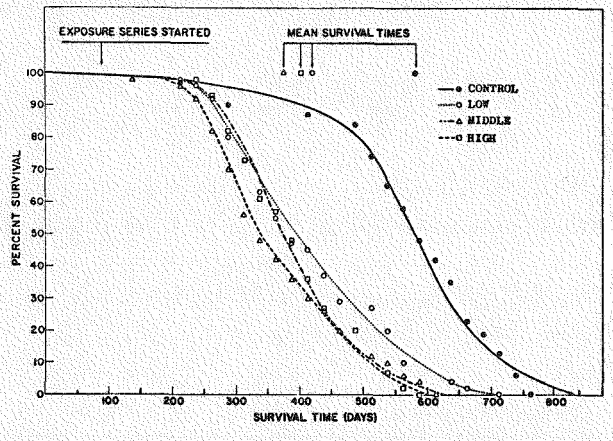

Fig. 2. Survival data for control and 3 groups of mice receiving different gamma-ray exposures by dose fractionation.

REFERENCES

1. G. A. Sacher, "Lethal Effects of Whole-Body Irradiation in Mice," Radiol. Clin. North Amer. 3, 227-241 (1965).

2. J. S. Krebs and R. W. Brauer, "Comparative Accumulation of Injury from X-, Gamma and Neutron Irradiation -- The Position of Theory and Experiment," in Biological Effects of Neutron and Proton Irradiations, Vol. II (International Atomic Energy Agency, Vienna, 1964).

3. R. H. Mole, "Quantitative Observation on Recovery from Whole Body Irradiation in Mice. II. Recovery during and after Daily Irradiation," Brit. J. Radiol. 30, 40-46 (1957).

4. J. B. Storer, "Recovery from Radiation Injury in Mammals," Ann. N. Y. Acad. Sci. 114, 126-137 (1964).

5. G. J. Dienes, "A Kinetic Model of Biological Radiation Response," Radiation Res. 28, 183-202 (1966).

6. H. A. Blair, "A Formulation of the Injury, Life Span, Dose Relations for Ionizing Radiations. I. Application to the Mouse," University of Rochester report UR-206 (1952).

7. H. A. Blair, "The Constancy of Repair Rate and of Irreparability during Protracted Exposure to Ionizing Radiation," University of Rochester report UR-621 (1963).

8. A. R. Vincent and J. W. Cable, "A Prediction of Early Radiation Lethality Using an Effective Dose," USAEC Technical Analysis Branch report TAB-R (1964).

9. J. F. Spalding, L. M. Holland, J. R. Prine, P. M. LaBauve, and J. E. London, "Comparative Effects of Dose Protraction and Residual Injury in Dogs and Monkeys," Radiation Res. 54, 453-462 (1973).

10. L. M. Holland, J. F. Spalding, J. R. Prine, and O. S. Johnson, "Comparative Immediate and Long-Term Effects of Gamma-Ray Dose Protraction by Fractionation and Continuous Low-Dose-Rate Exposure in Dogs and Monkeys," in Proceedings of the 6th International Congress of Radiation Research, Seattle, Washington (July 14-20, 1974), p. 144, Abstract No. B-37-1.

11. J. F. Spalding, "Lifetime Activity Studies in Mice from Ten to Thirty Generations of X-Irradiated Progenitors," Proc. Soc. Exp. Biol. Med. 124, 833-836 (1967).

12. J. F. Spalding, M. R. Brooks, and G. L. Tietjen, "Lifetime Body Weights and Mortality Distributions of Mice with 10 to 35 Generations of Ancestral X-Ray Exposure," Genetics 63, 897-906 (1969).

13. G. E. Cosgrove, "Late Effects of Radiation Exposure in Laboratory Mice," J. Amer. Vet. Radiol. Soc. VI, 95-102 (1965).

The General Site of Origin of the Persistent Radiation Lesion

It is a well established fact that whole-body exposure of the mouse to ionizing radiation from external sources causes a persistent lesion that can be measured both as a reduction in life span[1,2] and as a reduction in mean survival time during continuous gamma-ray stress.[3] The general site of origin of this radiation-induced lesion is not known, but it would be quite useful for partial-body shielding against radiation exposure under emergency conditions to know what portion of the body (if any) might be primarily responsible for the long-term radiation lesion.

Techniques have been developed to make selective body area and *in situ* organ shielding (or exposure) to x-rays possible. Studies in progress are to estimate the magnitude of the persistent radiation lesion in whole-body exposed, gut exposed, and bone exposed mice. Eleven experimental groups, with 24 mice per group, are treated as described in Table I.

The conditioning doses are given in 200-rad fractions at 7-day intervals so that the last fraction in each conditioned group is given on the same day. Twenty-eight days after the last conditioning exposure, all groups are challenged to death in a ^{60}Co gamma-ray field with a dose rate of 50 rad/24-h day. Mice are bled and weighed prior to the first conditioning exposure, the day after the last exposure, prior to the challenge exposure, and at 1- to 3-wk intervals during the challenge exposure. Mice that succumb to the challenge exposure are necropsied to determine the cause of death. The experimental protocol described is being carried out with 2 strains of mice (RF and C_{57}Black). In addition, a double replication study using the same 2 strains of mice and conditioning exposures are to be saved for life-shortening studies. Using 2 mouse strains and 2 methods of measuring the persistent lesion should provide meaningful data on the nature, magnitude, and general site of origin of the lesion.

TABLE I

CONDITIONING EXPOSURE TREATMENT FOR 11 GROUPS ON GENERAL SITE OF ORIGIN OF PERSISTENT LESION INVESTIGATION

Group	Treatment
1	No conditioning dose; no anesthesia
2	No conditioning dose; with anesthesia
3	1200-rad whole-body conditioning dose during anesthesia
4	800-rad whole-body conditioning dose during anesthesia
5	400-rad whole-body conditioning dose during anesthesia
6	1200 rad to gut tissue during anesthesia
7	800 rad to gut tissue during anesthesia
8	400 rad to gut tissue during anesthesia
9	1200 rad to bone tissue during anesthesia
10	800 rad to bone tissue during anesthesia
11	400 rad to bone tissue during anesthesia

Preliminary studies using only the RF strain have been completed, and these data do indicate that this experimental method is a feasible approach to the problems in question. Data from preliminary studies show a persistent lesion equivalent to a reduction in mean after-survival time of 1.3, 0.8, and 0.0 days/100 rad, respectively, for whole-body, gut, and bone conditioned mice. Data now coming in from the first replication of the formal studies indicate that bone-exposed mice will show a dose-related persistent lesion. This was not observed in the preliminary studies.

REFERENCES

1. J. F. Spalding, O. S. Johnson, R. F. Archuleta, and G. L. Tietjen, "Dose-Rate Effect on Life Shortening in Mice," Los Alamos Scientific Laboratory report LA-5722-MS (September 1974).

2. J. F. Spalding, O. S. Johnson, and P. C. McWilliams, "Dose Rate-Total Dose Effect from Single Short-Duration Gamma-Ray Exposures on Survival Time in Mice," Radiation Res. 32, 21-26 (1967).

3. J. F. Spalding, V. G. Strang, and F. C. V. Worman, "Effect of Graded Acute Exposures of Gamma Rays or Fission Neutrons on Survival in Subsequent Protracted Gamma-Ray Exposures," Radiation Res. 13, 415-423 (1960).

A Population Monitor on the Possible Genetic Impact of Whole-Body Exposure to X-Irradiation to Successive Generations of Mammals

There is a continuing concern by scientists and the general public for the possible genetic consequences to future generations of man from increased environmental levels of ionizing radiation. Predictions of the genetic impact of population exposures

to a few rad of ionizing radiation range from the genetic death of a population to inconsequential effects.

Four populations of mice (2 sublines and 2 treatment groups) are being used to monitor for some of the more obvious possible genetic effects of whole-body exposure to acute doses of x-rays each generation. This study is the residual from a much larger scale program that was begun many years ago. The continued experimentation is at a minimal level but will extract significantly more information from the large investment of time and effort in the full-scale program which was terminated after 45 generations of exposure.[1] Because of the limited effort involved, genotypic changes that may be influenced by ionizing radiation are not observed unless these changes are expressed phenotypically or in one of the litter characteristics which is being recorded.

The mammals used in this study were obtained from populations produced from lines propagated from 2 sibling pairs of RFM strain mice. Male mice in each of 70 generations in the experimental line were sibling-mated after being exposed to 200 rad of whole-body x-irradiation at the age of 26 $\pm$ 2 days. Control line mice were sibling-mated for the same number of generations but received no x-ray exposure. Serotype tests of 40th generation mice in both lines showed that two H-2 genotypes ($H\text{-}2^f$ and $H\text{-}2^k$) were segregating in both lines. Thus, mice used in this study were obtained from these 4 populations. One-year observations were made on approximately 40 mated pairs from each of the 4 populations. Experimental mice were progeny of 70 generations of x-irradiated males and were either subline $H\text{-}2^f$ or subline $H\text{-}2^k$. Control mice were progeny of 70 generations of non-irradiated sibling matings. Both groups received identical treatment except for radiation exposure in the experimental line.

Animals in this investigation were used exclusively for comparative reproduction observations. Each pair was housed on wood shavings in stainless steel (13 by 20 by 30 cm) box-type cages. Fresh bedding and water were provided weekly, and Rockland-Teklad rodent food was provided *ad libitum*. Daily observations were made for proper animal husbandry and for recording litter data. The radiation conditions for the experimental lines were 250 kVp, 30 mA, Thoraeus II filter, 2.55 mm copper HVL, 60 cm target-to-specimen distance, 45 to 50 rad/min dose rate, and 200 rad total midbody air dose.

Characteristics observed were those that should indicate possible trends detrimental to the genetic well-being of the population in question. These characteristics are listed and compared for significant differences in Table I.

One pair of mice in the control line and 2 pairs in the irradiated line were non-productive. No significant differences were seen in the age of the dam at first litter or in the sex ratio of the offspring at weaning. Irradiated sublines had fewer conceptions per dam and longer litter intervals than did their control counterparts. However, irradiated sublines weaned a significantly greater number of offspring than did their control counterparts.

No visible phenotypic mutations were observed in control or irradiated lines. The characteristics observed have shown that inbreeding *per se* may have a more significant impact on future generations than

TABLE I

CHARACTERISTICS OF REPRODUCTIVE FITNESS OF MICE WITH 70 GENERATIONS OF WHOLE-BODY X-IRRADIATION

	Control Population		Irradiated Population		
Characteristic	$H\text{-}2^f$	$H\text{-}2^k$	$H\text{-}2^f$	$H\text{-}2^k$	Significant at 0.05 Level
Number of Pairs	37	37	39	34	--
Age at First Litter (days)	76	81	80	77	No
Number of Conceptions (per dam)	6.9	7.7	5.0	6.6	Yes
Conception Interval (days)	36.9	32.8	43.0	36.9	Yes
Number of Mice Born per Litter	4.6	4.4	5.0	4.2	Yes
Number of Mice Weaned per Litter (0 included)	1.6	1.0	2.5	1.9	Yes
Sex Ratio at Weaning	0.57	0.56	0.55	0.52	No
Sterile Pairs	1	0	1	1	--

inbreeding combined with x-irradiation to each of 70 generations of male mice. It is possible that viable mutations are induced in animals subjected to x-rays generation after generation, but if this is true, these radiation-induced mutations appear to introduce a degree of useful heterogeneity not seen in non-irradiated but inbred mice.

REFERENCE

1. J. F. Spalding and M. R. Brooks, "Comparative Litter and Reproduction Characteristics of Mouse Populations with X-Ray Exposure, Including 45 Generations of Male Progenitors," Proc. Soc. Exp. Biol. Med. 141, 445-447 (1972).

MAMMALIAN METABOLISM

Introduction

This programmatic effort continues in extrapolation of results from animal experimentation on the metabolism of radionuclides to man for establishment of maximum permissible working and population levels. The studies utilize various species of laboratory animals, primarily the mouse, rat, dog, and monkey, administered the radioactive materials by a variety of routes. In addition, a normal New Mexico human population continues to be whole-body counted for determination of their individual ^{137}Cs contents. These data are of interest as a measure of residual radioactive fallout and also as a guide in the study of other pollutants of the atmosphere.

Estimate of Radiation Protection Guides for Selenium-75

(J. E. Furchner, J. E. London, and J. S. Wilson)

Selenium is an element that is considered to be both necessary for normal growth and development of, and toxic to, many domesticated animals. Interest in radiation protection guides (RPGs) for selenium derives chiefly from the use of 120-day ^{75}Se in diagnostic scanning of the pancreas and parathyroids. The following data were collected to estimate RPGs for humans from the retention parameters found in smaller mammals.

Within 30 min of the delivery of oral doses (IG) of ^{75}Se-selenite in the range of 0.6 to 2.2 μCi, the animals (mice, rats, monkeys, and dogs) were counted in large-volume liquid scintillation detectors to determine the initial activity. The animals were counted subsequently at intervals of more than a day to determine the time-course of ^{75}Se retention. These data were analyzed by a computer programmed to fit multiple exponential functions to the data. The results (Table I) are given as percent effective retention (no correction for radioactive decay) of initial body burden.

The time-integral of the retention functions (last column, Table I) gives a value for the equilibrium body burden during chronic exposure to an unchanging daily dose. A power function relating body-weight and the time-integral of the retention functions for the four species is used to estimate the equilibrium body burden in man by extrapolation to 70 kg (Fig. 1). The calculated best fit function is $EF = 13.7\ BW^{0.182}$, where EF is the time-integral and BW is the body-weight in kg. At 70 kg, the EF value is 30 (that is, under conditions of chronic ingestion of constant amounts of ^{75}Se, a 70-kg mammal would attain an equilibrium body burden of 30 times the daily dose).

TABLE I

EFFECTIVE RETENTION PARAMETERS FOR SELENIUM-75 GIVEN ORALLY TO MICE, RATS, MONKEYS, AND DOGS

Species	Weight (kg)	a_1[a]	k_1[a]	T_e[b]	a_2	k_2	T_e	a_3	k_3	T_e	EF[c]
Mice	0.026	41.7	2.0	0.35	43.0	0.15	4.6	15.3	0.041	16.7	6.7
Rats	0.130	37.0	0.7	1.00	34.1	0.07	9.9	28.9	0.027	25.3	16.0
Monkeys	5.400	73.7	1.3	0.55	12.5	0.07	9.6	13.8	0.015	46.3	11.5
Dogs	15.600	34.1	0.7	1.00	47.3	0.05	14.0	18.7	0.012	59.6	26.2

[a] Percent retention $= R_t = \sum_{i=1}^{n} a_i e^{-k_i t}$, where a_i and k_i are constants given in this table, e is the base of natural logs, and t is the time in days.

[b] T_e is the effective half-time in days.

[c] Time-integral $= EF = \int_0^\infty R_t\, dt/100$.

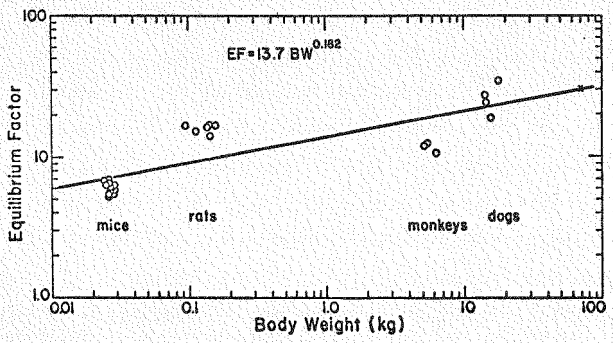

Fig. 1. Equilibrium factor (time-integral of retention function) for IG animals as a function of body-weight. Extrapolation to 70 kg (X) gives a value of 30.

The maximum permissible body burden for ^{75}Se is given by the International Commission on Radiation Protection[1] as 100 μCi when the total body is the organ of interest. If the equilibrium body burden is 30 times the daily intake, then a daily intake of 100 μCi/30 = 3.3 μCi will bring the body burden up to 100 μCi. If the sole source of contamination is water and if the daily water intake is 2.2 liters, then the MPC_w is 3.3/2.2 = 1.5 μCi/liters or 1.5 nCi/cm^3. This number is just half of the value given by the ICRP for continuous occupational exposure to ^{75}Se.

REFERENCE

1. International Commission on Radiation Protection, "Report of Committee II on Permissible Dose for Internal Radiation," Health Phys. 3 (1960).

Cesium-137 Activity in a Normal New Mexico Population

(J. E. Furchner and J. S. Wilson)

A group of about 40 normal resident New Mexicans have been assayed for low-level gamma-ray activity. Results have been reported periodically for more than 15 yr.[1] These data may be utilized to assess radiation exposures following future biospheric contamination.

Data collection and analysis methods have been reported.[2] The ^{137}Cs body burdens in nanocuries for January 1974 to October 1974 are given in Fig. 1, as is the concentration in picocuries/g of body potassium. The data are separated into weekly (lines) and monthly (closed circles) values. The fluctuations appear to follow no readily discernible

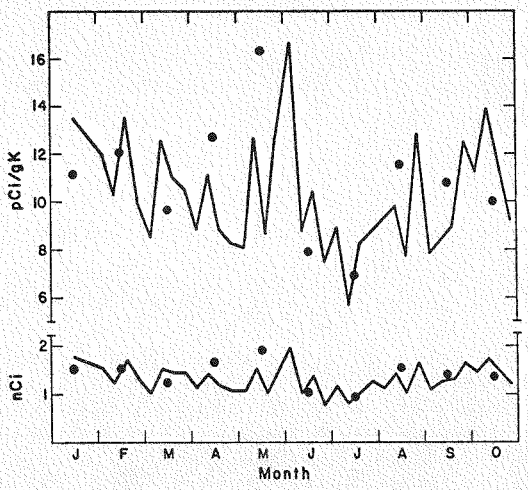

Fig. 1. Fallout ^{137}Cs body burdens in resident New Mexicans. The burden is expressed in nanocuries and the concentration in picocuries/g potassium. Lines give weekly average values for a group of 10, and the closed circles give monthly average values for about 30 people.

pattern. Monthly and weekly average values do not diverge widely. Whole-body ^{137}Cs burdens are more than an order of magnitude smaller than ^{40}K burdens.

REFERENCES

1. J. S. Wilson and J. E. Furchner, "Cesium-137 Activity in a Normal New Mexico Population," in: Los Alamos Scientific Laboratory report LA-5633-PR (1973), pp. 17-18.

2. C. R. Richmond, J. E. London, and J. S. Wilson, "Cesium-137 Content of New Mexico Control Subjects," in: Los Alamos Scientific Laboratory report LA-3610 (1966), pp. 170-176.

Cesium-137 Body Burden in Potassium-Depleted Rats

(J. E. Furchner and G. A. Drake)

A continuing low-level contamination of a human population with fallout ^{137}Cs suggests a long-lived compartment possibly in bone or in some slowly released external source of contamination. An attempt to increase body burdens, and thus bone burdens, was made by exposing rats to drinking water with low levels of ^{137}Cs. To enhance the uptake and retention of ^{137}Cs, some rats were maintained on a synthetic low potassium diet.[1]

After exposure for 5 months to contaminated drinking water, the whole-body ^{137}Cs burden of the potassium-deficient rats was more than a factor of 7 greater than that of rats maintained on a normal

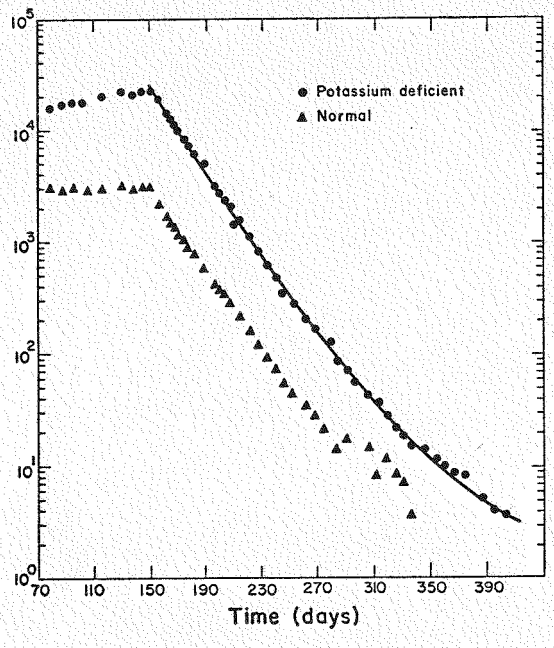

Fig. 1. Body burdens in rats during access to ^{137}Cs-contaminated drinking water and after cessation of such exposure at day 150. A potassium-deficient diet increased the ^{137}Cs burden by a factor of 7.

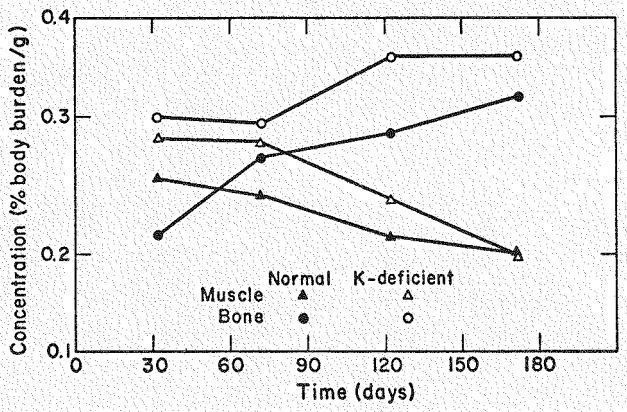

Fig. 2. Relative concentration (percent body burden/g) of ^{137}Cs during (days 32, 72, and 122) and after exposure to ^{137}Cs-contaminated drinking water. The relative concentration in muscle decreases, while that in bone increases.

diet. At this time, the 150th day after the beginning of exposure (Fig. 1), the rats were supplied with normal tap water. It appears that the rats receiving a normal diet were at or near equilibrium (i.e., the excretion of ^{137}Cs was equal to the intake), whereas the animals receiving the low potassium diet were excreting less than they were taking in. There was an immediate exponential decrease in the ^{137}Cs body burden when uncontaminated tap water was given to the animals. The body burden of the potassium-depleted rats decreased by 4 orders of magnitude. The data were fit by the sum of two exponentials with about 14- and 30-day half-times. In contrast, the data of Thomas and Thomas[2] showed body burdens, after a single intraperitoneal injection, decreasing by 5 orders of magnitude during a 450-day period. Their data were described by the sum of four exponentials with half-times of 2, 10, 19, and 157 days. Their doses were in the 1.5- to 2.0-mCi range. The maximum doses in the present study were about an order of magnitude smaller and were apparently inadequate to demonstrate longer components unequivocally.

Figure 2 shows the change in relative concentration (percent of body burden/g tissue) for muscle and bone during and after chronic exposure. The relative concentration in muscle decreases, while that in bone increases, thus lending support to the thesis that bone may be a reservoir for low levels of cesium.

REFERENCES

1. J. E. Furchner and G. A. Drake, "Disposition of Cesium-137 during Potassium Depletion in Rats," in: Los Alamos Scientific Laboratory report LA-5633-PR (May 1973), pp. 14-15.

2. R. G. Thomas and R. L. Thomas, "Long-Term Retention of ^{137}Cs in the Rat," Health Phys. 15, 83 (1968).

Modification of the Oral Absorption of Barium

(J. E. Furchner and G. A. Drake)

Cuddihy and Griffith[1] mistakenly reported a factor of 7 difference in the gastrointestinal absorption of barium by beagles at their laboratory, compared with similarly exposed beagles at this Laboratory.[2] They gave the barium by gavage, whereas at this Laboratory the barium solution was in a gelatin capsule that was digitally thrust into the esophagus of the dogs. Neither report stated whether the animals were fasted. The difference is actually about 3-fold rather than 7-fold. Moreover, the absorption value reported by Cuddihy and Griffith is based on 2 dogs which differ by about a factor of 3.

Five groups of rats (4 per group) and 5 groups of mice (6 per group) were given $^{133}BaCl_3$ by intravenous (IV), intraperitoneal (IP), and intragastric (IG) routes. The IV and IG animals were lightly anesthetized with ether. Of the three IG groups of

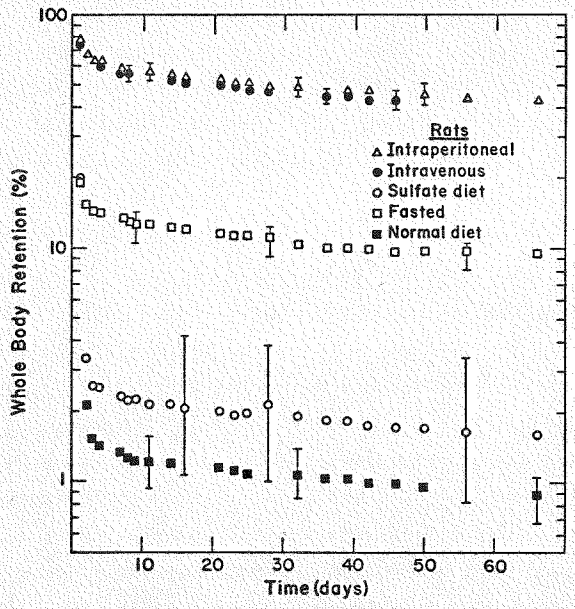

Fig. 1. Retention of ^{133}Ba after IV, IP, and IG administration to rats. The symbols represent the average values for 4 rats at each point. The vertical bars indicate the range of values at a few points.

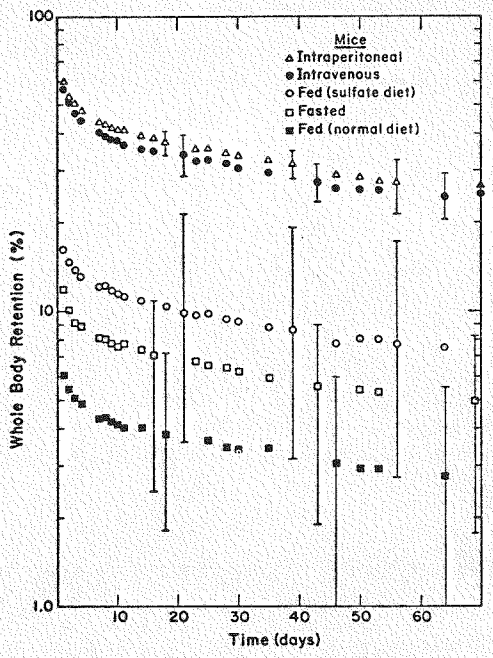

Fig. 2. Retention of ^{133}Ba after IV, IP, and IG administration to mice. The symbols represent the average values for 6 mice. High and low values are indicated at a few points by vertical bars.

rats and three IG groups of mice, one was fasted for 24 h before dosage by gavage; a second group, maintained on a normal diet, was not fasted before gavage, and a third group, also not fasted, was given a diet with 0.006 g of $MgSO_4 \cdot 7\ H_2O$/kg of normal diet starting the day of administration. Within 30 min after injection, the animals were assayed for barium activity.

Figure 1 shows the retention in rats for a period of about 2 months after injection. The vertical bars on a few of the data points indicate the range of values. Similar data for mice are given in Fig. 2. It is apparent that parenteral administration results in more nearly uniform retention and excretion patterns, that the range of retention values in mice was greater than in rats after oral administration, and that mice and rats responded to fasting by absorbing more of the ingested barium than did the unfasted animals. Sulfate in the diet resulted in about a 2-fold increase in the average retention in both rats and mice. The effects of fasting, of course, were produced during the first few hours after injection, as were the effects of the added sulfate. The supplemental sulfate in the diet produced no further change, although it was continued for more than a month after ^{133}Ba injection.

Some of the factors governing gastrointestinal absorption of barium appear to be readily modified by external manipulation. Other unknown factors produce wide variations in retention among homogeneous groups of animals receiving grossly similar treatment. Further treatment of individually caged animals receiving carefully controlled diets may delineate more clearly some of these factors.

REFERENCES

1. R. G. Cuddihy and W. C. Griffith, "A Biological Model Describing Tissue Distribution and Whole-Body Retention of Barium and Lanthanum in Beagle Dogs after Inhalation and Gavage," Health Phys. 23, 621 (1972).

2. C. R. Richmond and J. E. Furchner, "Radionuclide Metabolism," in: The Beagle as an Experimental Dog (A. C. Andersen and L. S. Good, eds.), University Press, Ames, Iowa (1970), pp. 479-488.

INDUSTRIAL HYGIENE GROUP[a] (H-5)

H. J. Ettinger, M.C.E., Group Leader
E. E. Campbell, M.S., Assistant Group Leader for Industrial Hygiene Services
B. J. Held, M.P.H. (I.H.), Assistant Group Leader for Research and Development Studies

Staff Members

H. A. Boyd, Ph.D.
B. C. Eutsler, B.S.
C. I. Fairchild, M.S.
M. Gonzales, M.S.
J. F. McInroy, Ph.D.
M. I. Tillery, M.S.

Electron Microscopist

B. L. Isom

Mechanical Technicians

G. W. Royer
D. R. Redmond

Tissue Study Technicians

O. C. Ramsey
A. J. Sanchez

AWU Graduate Student

E. L. McGuire
University of Arkansas
Little Rock, Arkansas

Consultants

Professor M. Corn
University of Pittsburgh
Graduate School of Public Health
Pittsburgh, Pennsylvania

Professor T. T. Mercer
University of Rochester
Rochester, New York

Professor J. Pierce
University of Missouri
Columbia, Missouri

Michael W. Stewart, M.D.
Pathology Department
Los Alamos Medical Center
Los Alamos, New Mexico

[a]Personnel assigned part- or full-time to AEC/DBER-funded programs.

INTRODUCTION

The Division of Biomedical and Environmental Research funds several projects in the Industrial Hygiene Group (H-5) related to health hazards associated with the working environment. These include studies on the sampling, characterization, and control of aerosols and analyses of tissues from autopsies of persons in the general public and those exposed to materials associated with AEC operations.

Specific aerosol studies include a computer assessment of air cleaner performance in terms of mass, number concentration, haze formation potential, and respirable mass; assessment of inhalation hazards from glovebox leaks; resuspension of particulates; cyclic flow filtration; and generation of insoluble aerosols for inhalation studies. A study of the filtration of ultrafine (< 0.1 μm) particles is starting during FY 1975.

Evaluation of data collected since 1959 from the chemical analyses of human tissues for plutonium has continued. Emphasis has been placed on the interpretation of data from deceased former LASL employees having had occupational exposures to plutonium. It is from this group that knowledge of plutonium metabolism and kinetics is most likely to be obtained. Tissues from the general population, collected from several geographic locations throughout the United States, having only environmental exposures to fallout plutonium, have also been examined in a continuing effort to establish baseline concentrations of plutonium in non-occupationally exposed persons, and potential trends in changing baselines are being monitored. The analyses of nonradioactive trace metals associated with industry have been made on a few selected tissues.

AEROSOL STUDIES

[C. I. Fairchild, J. Farr (Group H-4), M. Gonzales, E. L. McGuire, and M. I. Tillery]

Computer Assessment of Air Cleaner Performance in Terms of Mass, Number Concentration, Haze Formation Potential, and Respirable Mass

Regulations for control of particulate emissions are usually defined in terms of weight per unit volume of gas. The magnitude of many environmental and health effects of airborne particulates is dependent on particle size; however, this parameter is

seldom considered in emission control and ambient monitoring regulations. In an effort to determine the relationships between efficiency in terms of mass collection and other aerosol parameters, a computer analysis of several typical industrial air cleaners has been carried out. This analysis was done with respect to emission control of mass, respirable mass, light-scattering cross section, total surface area, and number of particles. Seven typical industrial air cleaners have been analyzed: a low-efficiency cyclone, spray tower, venturi scrubber, dry electrostatic precipitator, small-diameter tubular cyclone, medium-efficiency high-throughput cyclone, and high-efficiency long cyclone. The analysis was carried out by computer generation of aerosols having different log-normal size distributions, then characterization of the challenge aerosol with respect to the parameters noted above. The aerosol was then passed through each cleaner, decreasing the number of particles in each size interval on the basis of the efficiency curve for the cleaner given as a function of particle size.[1] Penetrating aerosol size was characterized and compared to the challenge aerosol to determine the efficiency with respect to parameters of interest. Each cleaner has been challenged by 150 size distributions having volume median aerodynamic diameters (VMAD) ranging from 0.05 to 70 μm and geometric standard deviations (σ_g) ranging from 2.5 to 4.2.

Size distributions were generated by approximate integration of the log-normal distribution function for small intervals of particle size. All aerosol parameters of interest were calculated for each interval and summed. Respirable mass was determined from the lung deposition curve of the American Conference of Governmental Industrial Hygienists.[2] This curve defines as respirable a particle that penetrates to the deep lung with a fraction of this material having long-term retention. This definition would not be valid for particles that are toxic to upper airways or to the gastrointestinal tract nor for very soluble particles. The light-scattering cross section was calculated from the equation:[3]

$$b = \sum_{i=1}^{n} N_i K_i \pi r_i^2,$$

where b is the scattering coefficient, N_i is the number of particles having radius r_i, and K_i is the scattering area ratio for a particle of radius r_i. K is determined from approximate values given by Van de Hulst,[4] assuming illumination light of wavelength 0.524 μm, and non-adsorbing spherical particles with an index of refraction of 1.5. The parameters volume, surface area, and particle number are calculated from geometrical considerations of the volume associated with each size interval.

The results of this analysis for one type of cleaner (small-diameter tubular cyclone) are given in Figs. 1 and 2 for aerosols having σ_g values of 2.5 and 4.2. For aerosols having σ_g = 2.5 and a VMAD = 10 μm, the mass collection efficiency is 80%; number collection efficiency 24%; respirable mass removal efficiency 52%; and removal of potential

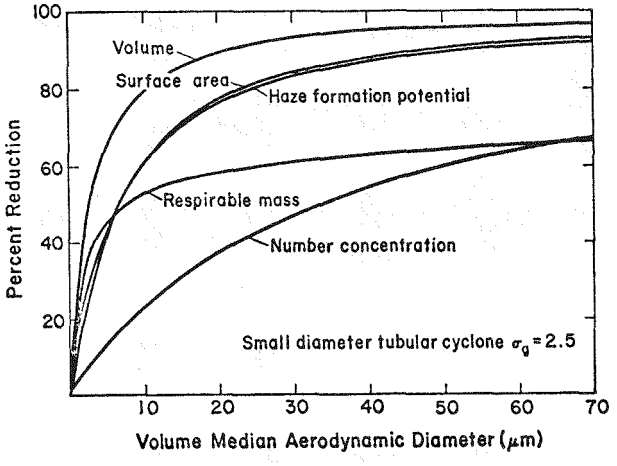

Fig. 1. Collection efficiency of small-diameter tubular cyclone for aerosols having a geometric standard deviation (σ_g) of 2.5.

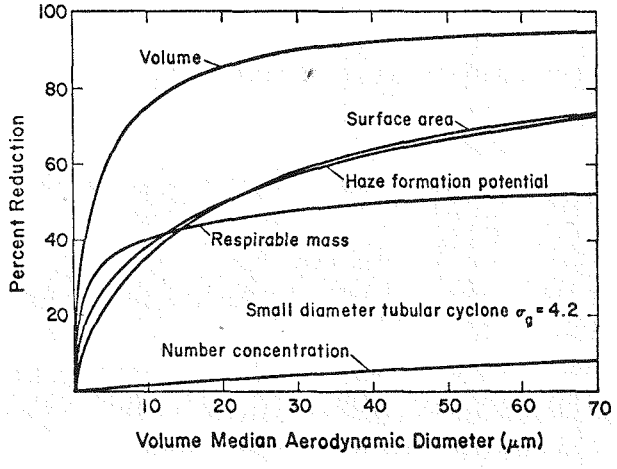

Fig. 2. Collection efficiency of small-diameter tubular cyclone for aerosols having a geometric standard deviation (σ_g) of 4.2.

for haze formation 60%. For an aerosol having this same VMAD and σ_g = 4.2, mass collection efficiency is approximately 75%; number collection efficiency only 1.4%; respirable mass removal 40%; and removal of haze formation potential 38%. These calculations show that mass collection efficiency can be a misleading index of performance with respect to other parameters of the same aerosol. For different aerosols having similar mass collection efficiencies, the performance of the cleaner can vary significantly with respect to other parameters.

In general, results of the analysis indicate that, for efficient cleaners (i.e., electrostatic precipitators) and for challenge aerosols having narrow size distributions, mass collection efficiency is a reasonable index of air cleaner performance with respect to other parameters. For air cleaners having moderate to good mass collection efficiencies and for challenge aerosols having a wide size distribution, the mass reduction efficiency is a poor index of performance with respect to other parameters. These results emphasize the importance of size information in characterizing the performance of air cleaners. Mass collection efficiencies provide little information on overall performance if particle size data are not included. If mass collection efficiencies are used to characterize performance, then particle size of the challenge aerosol should be given or performance should be measured against standard test aerosols, including a significant small particle size component.

REFERENCES

1. C. J. Stairmand, "Removal of Dusts from Gases," in Processes for Air Pollution Control, Chap. 12 (G. Nonhebel, ed.), CRC Press (1972).

2. American Conference of Governmental Industrial Hygienists, "Threshold Limit Values of Airborne Contaminants for 1973" (1973).

3. E. Robinson, "Effects of Air Pollution on Visibility," in Air Pollution, Vol. 1, Chap. 7B (A. C. Stern, ed.), Academic Press, Inc., New York (1962).

4. H. C. Van de Hulst, "Light Scattering by Small Particles," John Wiley & Sons, Inc., New York (1957).

Assessment of Inhalation Hazard from Glovebox Leaks

The use of air sampling data for estimating the probable hazard from airborne radionuclides requires correlation between breathing zone concentrations and concentrations at the sampler location. While there are a great many possible variations of ventilation air-flow patterns, sampler locations, and leaks, the more important situations can be covered by a small number of experimental measurements. In glovebox operations, most leaks result from tears or holes in gloves and the pressure fluctuations that arise from glove movement, with exposure potential being highest for the glovebox operator. In this situation, air samples are frequently taken with fixed samplers located on top of and close to the glovebox, with low flow-rate lapel samplers on the operator, by portable "giraffe" samplers located close to the operator, or by an area monitor (with an alarm) located near the exhaust duct.

To determine the relationship between breathing zone concentration and concentration indicated by these monitors, a mockup of a drybox system was constructed.[1] The mockup consisted of a room 6.1 x 6.1 x 2.43 m (20 x 20 x 8 ft). Two opposite walls of the room were covered with pegboard having 0.634-cm (0.25-in.) diameter holes located 2.54 cm apart on a horizontal and vertical grid. A plenum located behind each of these walls was connected to air blowers and HEPA filters. Various air-flow patterns could be established by covering portions of each wall. A glovebox was mounted on a movable table to permit various orientations of the glovebox leak with respect to air flow. A dummy placed in front of the glovebox was instrumented to provide breathing zone and lapel air samples. The dummy also redirected the ventilation air as a worker would.

Measurements were made with three different ventilation systems. In the first system (VS1), air flowed evenly across the room as both pegboard walls were unobstructed. In the second (VS2), air entered at the top center of one wall through a 1.2-m (4-ft) wide by 0.3-m (1-ft) high opening and was exhausted through a similar opening at the bottom center of the opposite wall. Similar openings were used for the third (VS3) arrangement, with air entering the room in the upper left-hand corner of one wall and exiting through the lower right-hand corner of the

opposite wall. A flow rate of 9 air changes/h was used for all measurements. Successive air concentration measurements were made with the air flow directed from the rear (0°), front (180°), and side (90°) of the glovebox. For 0° flow direction, the glovebox operator faced the air inlet.

Dioctyl phthalate (DOP) aerosol was generated inside the glovebox using a Naval Research Laboratory Model III compressed air nebulizer.[2] The leak was simulated by a small orifice mounted in one glove port, with the flow controlled by regulating the pressure in the glovebox. Andersen cascade impactor[3] samples were taken during all runs to ensure a consistent particle size. Aerosol mean mass median aerodynamic diameter (MMAD) for 32 samples was 0.8 ± 0.075 μm, with a geometric standard deviation of 1.80 ± 0.27. Concentration measurements were made using a forward light-scattering photometer.[4] The samples were taken throughout the room in the horizontal plane containing the leak and in horizontal planes 0.3 m (1 ft) above and below the leak. Specific samples were also taken at the top left-hand corner of the glovebox, 1.83 m (6 ft) and 2.13 m (7 ft) above the floor. These locations are similar to typical permanently mounted samplers. Samples were also collected from the breathing zone of the worker and from the region where a lapel sampler would be located. With the two ventilation systems having simulated exhaust ducts, a sample was also taken from the center of the simulated exhaust duct for each ventilation system. These samples are referred to as the +6, +7, BZ, lapel, and outlet samples, respectively.

Figure 1 shows isoconcentration areas near the glovebox for the breathing zone plane, 0° orientation, and VS2 ventilation flow pattern. The leak (100%) concentration was measured 2.54 cm (1 in.) in front of the leak orifice. In almost all cases, the breathing zone concentrations were 1 to 2% of the leak concentrations. In the remaining cases, the concentration was 2 to 4%.

Ratios of concentrations at specific points are given in Table I for all orientations and ventilation systems. The lapel samples overestimated the breathing zone concentrations by a factor of approximately 2.5. Samplers located above the drybox underestimated the breathing zone concentrations by a factor of 8, with a coefficient of variation

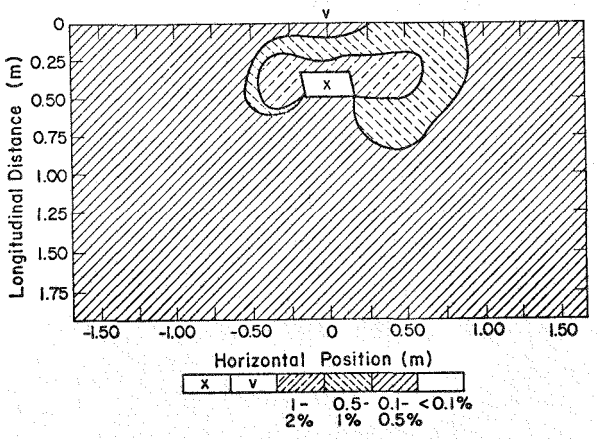

Fig. 1. Isoconcentration curves at the horizontal plane 0.30 m above leak level, 9 air changes/h, 0° air direction for VS2 sampler.

TABLE I

CONCENTRATION RATIOS EXPRESSED AS (BREATHING ZONE CONCENTRATIONS/SAMPLING LOCATION CONCENTRATIONS)

Ventilation System	Sampler Location	Orientation 0°	90°	180°
VS1	Lapel	0.43	0.39	0.45
VS1	+6	5.9	3.8	8.5
VS1	+7	6.2	4.2	6.7
VS2	Lapel	0.36	0.39	0.25
VS2	+6	4.0	9.6	6.3
VS2	+7	9.6	12.2	8.6
VS2	Outlet	19.2	9.6	12.0
VS3	Lapel	0.42	0.32	0.49
VS3	+6	7.5	7.9	12.2
VS3	+7	7.8	11.5	11.3
VS3	Outlet	21.0	12.5	12.0

of ~34%. Samplers located at the exhaust duct underestimated the breathing zone concentration by a factor of 14.4, with a coefficient of variation of ~32%. These results indicate that lapel samplers provide the best estimate of breathing zone concentration. The overestimate of the breathing zone concentration resulted from the sampler location between leak and breathing zone. A sampler located in the center of the room exhaust duct provided a better estimate of breathing zone concentration than the other area samplers. This offers a considerable advantage, as a single sampler will detect a leak at any drybox in a room with this type of ventilation system. The sampler will not pinpoint

leaks within the room; therefore, samples should also be taken at each operational glovebox. However, these samples need be counted only when the outlet sample indicates a leak. Samples collected in this manner will provide as much reliable information as several area samplers and with lower operational costs.

In operational conditions, leaks may be of short duration. To determine the validity of these sampling procedures for short-term leaks, measurements were made with leaks of 1, 5, 10, and 20 min. In all cases, the integral exposure at each point was compared. The forward light-scattering photometer indicated instantaneous concentration and, since all samples were taken at the same flow rate, the integrated exposure was taken as the product of concentration and time. For the 1-min release, dilution was so great that only the breathing zone and lapel samplers had concentrations high enough to read. The ratios were similar to the ratios observed with steady-state conditions for all samples. Filter samples measure the integrated concentrations and will not be greatly affected by dilution; therefore, all conclusions reached with respect to steady-flow should apply for short-term releases.

REFERENCES

1. E. L. McGuire, "A Study of Aerosol Dispersion from a Simulated Glove Box Leak to Assess Methods of Air Sampling," M.S. Thesis, University of Arkansas (1974).

2. W. H. Echols and J. A. Young, "Studies of Portable Air-Operated Aerosol Generators," Naval Research Laboratory report 5929 (1963).

3. A. A. Andersen, "New Sampler for the Collection, Sizing and Enumeration of Viable Airborne Particles," J. Bacteriol. 76, 471 (1958).

4. R. D. Hiebert, L. L. Pollat, and R. G. Stafford, "Improved Light Scattering Photometer for Air Filtration System Studies," Los Alamos Scientific Laboratory report LA-4627-MS (1971).

Resuspension of Particulates

Resuspension studies are being conducted to gain information that will aid in the prediction of probable spread or migration of surface contaminants. Initial studies are using spherical particles and smooth surfaces in a wind tunnel. The tunnel (see Fig. 1), constructed of metal tubing (diameter 20.3 cm), is approximately 7.0 m long. A flat removable floor (width approximately 18 cm) results in a D-shaped cross section. Instrumentation on the tunnel includes a hot-wire anemometer and pitot tubes for velocity measurements, humidity and temperature indicators, isokinetic probes for collecting airborne particles at known distances above the floor, and an aerosol particle size monitor.

Characterization of the velocity profiles in the tunnel indicates sufficient length for fully developed turbulent flow in the experimental region. Maximum center-line velocities of 32.5 m/sec are obtainable.

Surface roughness of the floor being used in the tunnel was determined from the relationship:[1]

$$U/U_* = 1/K \ln (Z/Z_0),$$

where K is von Karman's constant, U the velocity at height Z above the floor, U_* the friction velocity, and Z_0 the roughness height. By measuring the velocity profiles at several flow rates, it is possible to plot ln Z as a function of velocity U, which has a slope K/U_* and an intercept ln Z_0. The average value obtained for roughness height was 0.9 μm for a polished stainless steel floor.

Initial resuspension studies were conducted with single glass spheres. These studies showed that the resuspension velocity varies inversely with particle size. Resuspension velocities for particles of the same size varied over an order of magnitude, indicating a wide range of adhesive forces between the surface and particles of the same size. A cumulative plot of the fraction of particles resuspended as a function of velocity gave a non-linear curve. A similar relationship was obtained when the fraction resuspended of a dispersion of monodisperse particles was plotted against mean center-line velocity. Prolonged exposure to air flow did not seem to affect the movement of the particles. Increasing the velocity would immediately result in an additional fraction of the particles being resuspended. However, maintaining the velocity for a prolonged period did not markedly increase the resuspended fraction. When particles of different sizes were mixed to give volume median diameters (VMD) similar to the diameters of monodisperse particles, it was found that lower velocities were required to resuspend the same fraction of particles.

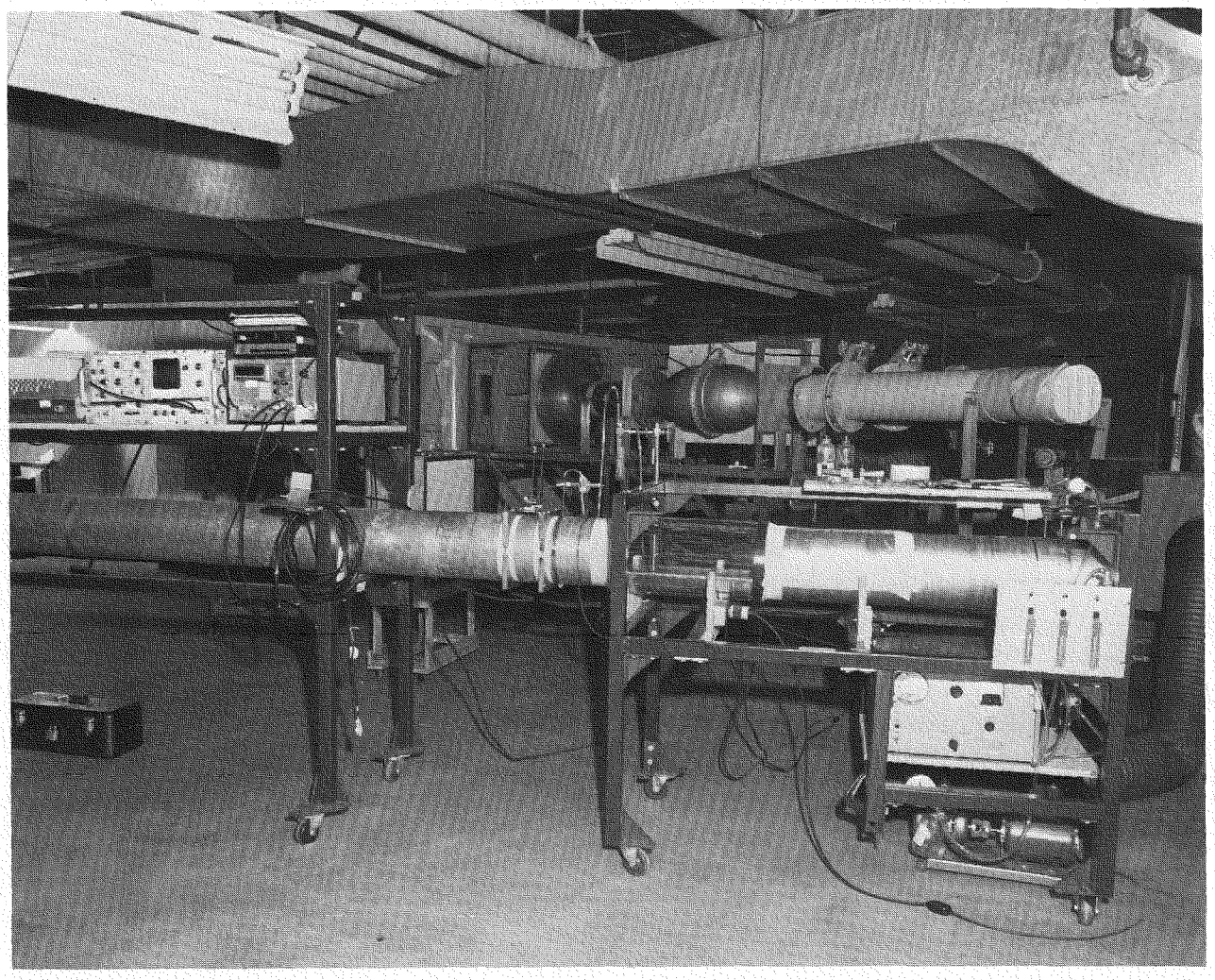

Fig. 1. Wind tunnel used in determining the resuspension of surface contaminants.

These results indicate that mechanical impact between particles, in addition to flow field distortions, is an important mechanism in resuspension. Moreover, collisions between particles of different sizes seem to be more effective than collisions between particles of similar sizes. This effect is apparent in Fig. 2, where the threshold resuspension velocity (mean center-line velocity necessary to resuspend 1% of the particles) is plotted for several values of geometric standard deviation (σ_g). For the same VMD the threshold velocity is smaller for larger values of σ_g.

Measurements of mass transport by resuspension have been made by installing isokinetic probes at 1, 4, and 7 cm above the floor, to measure the vertical mass concentrations, and a creep collector across the floor of the tunnel, to measure the mass movement along the tunnel floor. Gravimetric samples were obtained from each of these samplers after each velocity increment by stopping the air flow to remove the collected sample. Figure 3 gives the fraction of mass flux resuspended per unit width of the

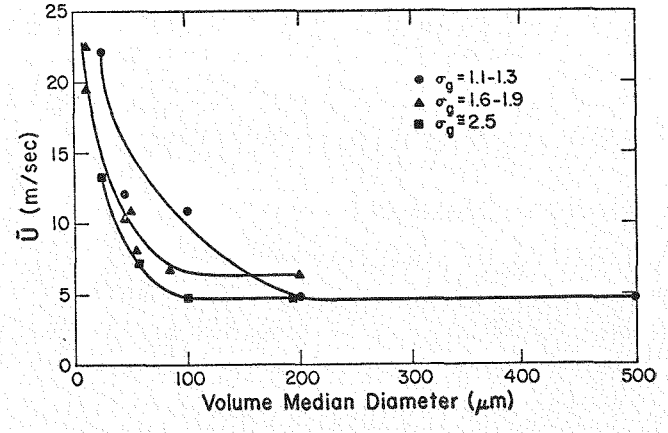

Fig. 2. Resuspension of spheres as a function of wind velocity.

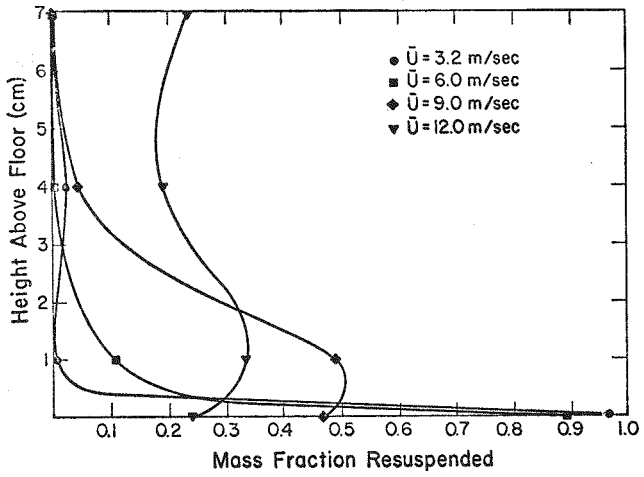

Fig. 3. Vertical mass flux (horizontal) distribution of B2b glass spheres (~ 100 μm VMD, $\sigma_g \sim 2.5$).

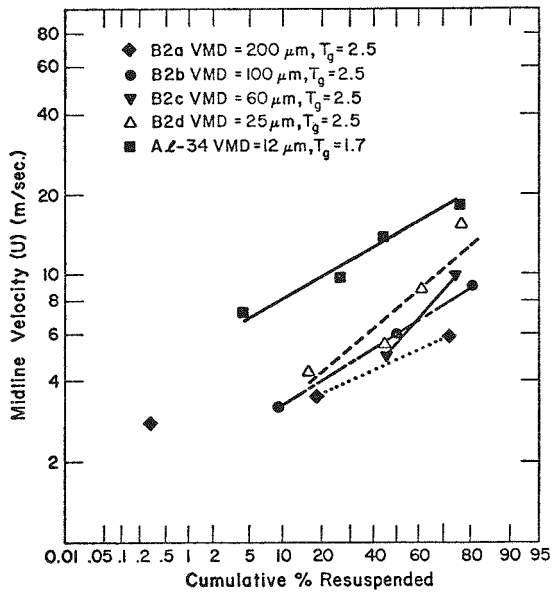

Fig. 4. Resuspension distribution (mass) of spherical particles as a function of wind velocity.

resuspension surface for one size of glass spheres and for mean center-line velocities. The intercept (Z = 0) is the fraction of resuspended mass that moves by creep along the floor of the tunnel. It is apparent from these data that most mass transport takes place very close to the surface for particles of 100 μm VMD. The fraction of material present on the plate at the beginning of that velocity increment, which is collected as creep, is plotted (Fig. 4) as cumulative percent of the material moved by creep as a function of mean center-line velocity. These data indicate that the fraction of material moved or resuspended by creep is normally distributed with respect to the natural logarithm of mean center-line velocity.

The largest fraction of mass transport occurs as creep flow or saltation close to the surface. Interactions that occur between particles in this region may also be responsible for generation and resuspension of small particles having significant lifetimes in air. Because of the importance of resuspension in the transport of material and the spread of surface contamination, the movement and interactions involved in creep flow and saltation will be investigated more thoroughly. A more thorough understanding of the resuspension mechanism will aid in the design of recirculating air systems for energy conservation and in development of control methods for limiting the spread of surface contamination.

REFERENCE

1. G. A. Sehmel, "Particle Deposition from Turbulent Air Flow," J. Geophys. Res. 75(9), 1766-1781 (1970).

Cyclic Flow Filtration Efficiency

Test criteria for evaluation of filters to be used on respirators require testing with steady flow of 32 liters/min for filters from single-filter masks and 16 liters/min for filters from double-filter masks. In use, flow through the filter will be cyclic, matching the inhalation portion of the wearer's breathing cycle if the mask has an exhalation valve. To determine the relationship between steady flow test performance and performance with cyclic flow, a series of experimental measurements have been made using both types of flow and media commonly used for respirator filters. An empirical model has also been applied to both types of flow to determine any probable areas of difference.

The model used to investigate possible differences in steady and cyclic flow efficiencies was proposed by Davies.[1] In this model, empirical and theoretical relationships are combined to predict the total mat efficiency based on packing fraction, approach velocity, pressure drop as a function of velocity, filter thickness, and air viscosity. Several of these terms are combined with an empirical relationship to determine an effective fiber radius.

This radius is then used with particle parameters for diffusion and inertial collection mechanisms to estimate the total mat collection efficiency. This model was used to estimate the efficiency of glass fiber filter mat having a packing fraction of 0.025. Figure 1 shows the efficiencies predicted by the model. Data used for the cyclic flow model were collected during measurements of cyclic flow efficiency in which a respirator pump was used to simulate the air flow patterns. When the model is used to predict mat efficiencies, the effective fiber diameter is adjusted so that the efficiency curve matches the experimental data at some point. However, for our purposes, we sought only points of major differences in performance with steady and cyclic flow. These results required only a consistent use of the model for each method of flow. Steady flow at 12 cm/sec is compared to cyclic flow for a work rate of 830 kg-m/min, as the average velocity through this filter during inhalation is 13.8 cm/sec. The curves clearly indicate no significant differences in performance between the two flow methods.

Efficiencies of several filtration media were determined using a method that measures total mass efficiency. The results of these measurements for one filtration medium are given in Fig. 2. The results have the same characteristics as the model for particles larger than 0.6 μm. However, for smaller particles, there is a considerable difference between steady and cyclic flow efficiencies, as contrasted at no difference seen in the model. A measurement made on a somewhat more efficient medium (Fig. 3) shows good agreement except for the smallest particles (0.126 μm).

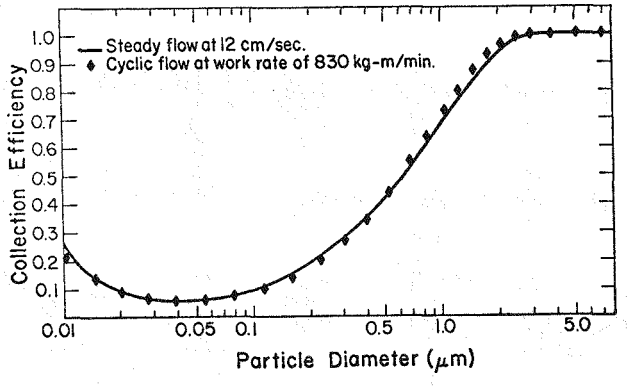

Fig. 1. Calculated filtration efficiency of glass fiber filter mat with steady and cyclic flow.

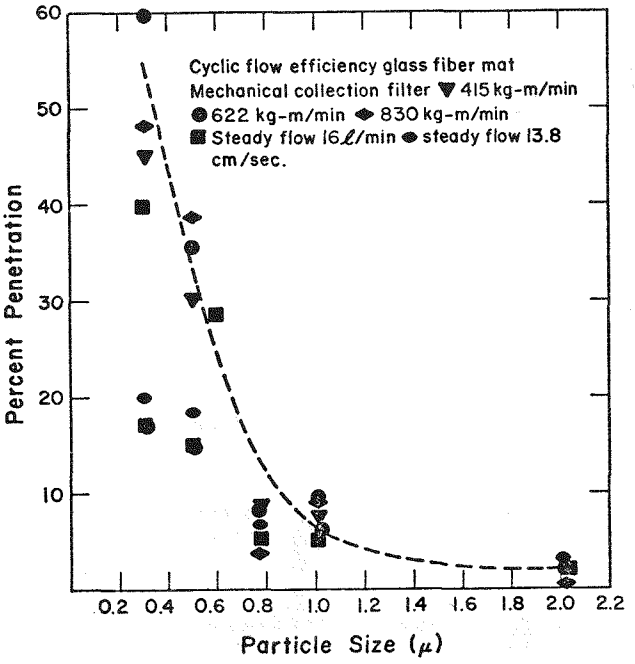

Fig. 2. Cyclic flow efficiency glass fiber mat mechanical collection filter: (-▼-) 415 kg-m/min; (-●-) 622 kg-m/min; (-◆-) 830 kg-m/min; (-■-) steady flow at 16 liters/min; and (-●-) steady flow at 13.8 cm/sec.

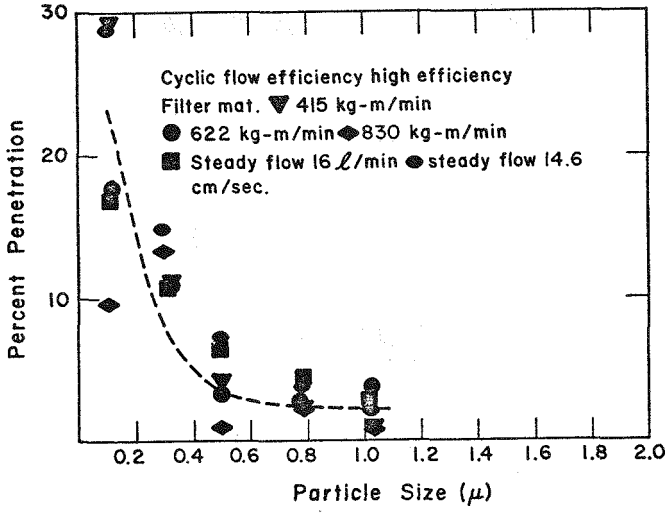

Fig. 3. Cyclic flow efficiency for the high-efficiency filter mat: (-▼-) 415 kg-m/min; (-●-) 622 kg-m/min; (-◆-) 830 kg-m/min; (-■-) steady flow at 16 liters/min; and (-●-) steady flow at 14.6 cm/sec.

The results of this study indicate that performance measured with steady flow equal to the average flow during the inhalation cycle provides a good estimate of filter performance under operational conditions for particles larger than 0.5 μm. In most cases, particles in this size range will contribute the significant fraction of the inhaled

mass. With respect to very small particles, the steady flow efficiency measurements may not be a good estimate of performance. Considerable difficulty has been encountered in measuring the efficiencies for small particles (diameter $\leq$ 0.31 μm). The aerosol monitoring system used is not as sensitive for small particles, and it is difficult to generate high concentrations of singlets. In an effort to resolve the problem, all efficiencies for small particles have recently been remeasured. The data analysis for these runs is not yet completed.

REFERENCE

1. C. N. Davies, "The Separation of Airborne Dust and Particles," in Institute of Mechanical Engineering Proceedings, Vol. B (1952-1953), p. 185.

Generation of an Insoluble Aerosol for Inhalation Studies

The feasibility of generating an aerosol of respirable particles similar to those used in the "hot particle" program was investigated to initiate inhalation experiments which will permit a comparison of the biological effects for different intake routes.

To provide aerosol particles with chemical characteristics similar to those used in the "hot particle" programs,[1] a generation procedure was devised that provided similar treatment. Aerosol particles are much smaller than the microspheres used in the injection studies; therefore, less treatment is required for drying and solidification. Because the particles are radioactive, the generation procedure must be contained and capable of operation with minimal exposure to the operators.

The generation procedure developed involves nebulization of an aqueous solution of colloidal hydrated zirconium oxide, followed by heat treatment to provide a dry solid aerosol. Nebulization is with a modified Wright generator[2] developed at the Lovelace Foundation.[3] Operation of this generator at a pressure of 1.38×10^5 Pa (20 psig) nebulizes approximately 25 liters of solution per liter of jet air. The droplets are dried by mixing the aerosol (~ 1 liter/min) with dry filtered air (~ 7 liters/min) in a small chamber. The aerosol is heated to 860°C by passage through a quartz glass tube of approximately 30 mm diameter and 460 mm long. The tube is wound with nichrome heating wire and covered with asbestos cement insulation. The aerosol then passes through a delay tank for cooling to approximately room temperature.

The characteristics of the aerosol were checked initially by sampling the aerosol at the cooling chamber with the LASL Spiral Centrifuge Aerosol Spectrometer.[4] This instrument separates particles according to aerodynamic diameter, making density determination possible for spherical particles. The density measured at the cooling chamber was $4.61 \pm 0.40/cm^3$, which is similar to the measured densities of "hot particles."[1] This aerosol was collected on membrane filters, then resuspended in water by ultrasonic agitation and renebulized. The renebulized aerosol was collected with the Spiral Centrifuge Aerosol Spectrometer to confirm that there is no change in density resulting from suspension in water.

To measure *in vivo* solubility of material encapsulated in these particles, an aerosol will be generated with a ^{57}Co tag added to the nebulizer solution. This material will be aerosolized, heat-treated, collected on a membrane filter, and resuspended in water by ultrasonic agitation. The material will then be injected intramuscularly in hamsters to measure the clearance rate. If the ^{57}Co is relatively insoluble, this procedure will be used to produce aerosols with ^{238}Pu encapsulated in ZrO_2 particles.

A small-animal exposure chamber has been acquired.[5] A containment glovebox for the chamber and aerosol generation equipment have been designed and are currently being fabricated.

REFERENCES

1. C. R. Richmond and E. M. Sullivan, eds., "Annual Report of the Biomedical and Environmental Research Program of the LASL Health Division, January through December 1973," Los Alamos Scientific Laboratory report LA-5633-PR (May 1974), p. 1.

2. B. M. Wright, "A New Nebulizer," Lancet, p. 24 (July 5, 1958).

3. T. T. Mercer, M. I. Tillery, and H. Y. Chow, "Operating Characteristics of Some Compressed Air Nebulizers," Amer. Ind. Hyg. Assoc. 29, 66 (1968).

4. W. R. Moss, H. J. Ettinger, and J. R. Coulter, "Aerosol Density Measurements Using a Modified

Spiral Centrifuge Aerosol Spectrometer," Envir. Sci. Tech. 6, 614 (1972).

5. O. G. Raabe, J. E. Bennick, M. E. Light, C. H. Hobbs, R. L. Thomas, and M. I. Tillery, "An Improved Apparatus for Acute Inhalation Exposure of Rodents to Radioactive Aerosols," Tox. Appl. Pharm. 26, 264 (1973).

Filtration Efficiency for Particles Smaller than 0.1 μm

Initial development of procedures for evaluating air cleaner performance against challenge aerosols having aerodynamic diameters less than or equal to 0.1 μm is being directed at aerosol generation, sampling, and characterization. Generation procedures are being developed in conjunction with the measurement of HEPA filter performance against challenge aerosols of PuO_2. The Chemistry and Metallurgical Division at LASL is preparing a colloidal suspension of PuO_2 having sizes ranging from 0.005 to 0.01 μm. The procedure is a standard reactor fuel processing method involving controlled growth of particles. A diluted suspension of the hydrosol will be nebulized to produce an aerosol of small particles.

Several systems are being investigated for characterization of these aerosols. These include diffusion batteries, low pressure cascade impactors, and electron microscopy. Diffusion batteries seem to be the preferred method, as they directly measure the particle parameter that controls filtration for this particle size. Design requirements for the size range of interest and a detection method for upstream and downstream concentration measurements are being developed currently.

Filtration, as the result of impaction, is a function of the inertial parameter P_i, where

$$P_i \propto \rho a^2 u/\eta R.$$

ρ is the particle density, a is the particle diameter, u is the particle velocity, η is the gas viscosity, and R is the diameter of the fiber. Collection by diffusion is proportional to the diffusion parameter P_d, where

$$P_d \propto 1/a^2 qR.$$

Thus, efficiency measurements for small particles will be required with at least two aerosols of widely separated densities to separate the filtration mechanisms of impaction and diffusion.

PLUTONIUM AND ENVIRONMENTAL METALS IN MAN

[J. F. McInroy, H. A. Boyd, M. W. Stewart (Consultant), B. C. Eutsler, W. D. Moss, and G. L. Tietjen (Group C-5)]

Minimum Detection Limits and Confidence Intervals

The measurement of environmental concentrations of many radioactive elements, including plutonium, is very difficult when the instrument background counts contribute significantly to the total count observed. This has been a continuous problem in our environmental monitoring of plutonium in human tissues due to the extremely small concentrations of plutonium inhaled or ingested by humans not having had occupational exposures to plutonium or because of the small tissue specimens available for analyses (i.e., thyroid, spleen, gonads, etc.). The measured activities have sometimes been suspect as to whether they were truly different from zero. In our own work, there are at least two basic parameters to be identified with all measurements: (1) the minimum detection limit (or the lower limit of detection) as determined by the maximum capabilities of the detection instrumentation being utilized and (2) the uncertainties associated with a given measurement related to counting statistics, chemical recovery, background variation, and detector efficiency. We have attempted to identify and define these parameters.

In dealing with samples with low counts, it is important to define carefully a minimum detection limit (i.e., a count below which results are not very meaningful due to the difficulty of distinguishing sample count from background). The point we have chosen to call the minimum detection limit (L_c) is what Currie[1] has called the critical level and Altschuler and Pasternak[2] have called the minimum significant measured activity. If a net sample count falls above this point, we can say that something was detected and give a point estimate and an interval estimate of the activity. If a net sample count falls below L_c, we shall say that nothing was detected.

L_c is a function only of the background and the

type I error α (the risk of claiming there is activity present in the sample when, in fact, there is none). We have taken $\alpha = 0.01$ so that the point L_c is the 99th percentile of the background distribution. Since L_c is expressed as a net count, the mean background is subtracted from it. Hence, L_c is not a function of the chemical recovery or of the sample count. For low counts, the background count has more nearly a Poisson distribution than a normal distribution; hence, we have defined $(L_c + B)$ as the 99th percentile of a Poisson distribution with a parameter equal to the average background (B) of a particular counter. This yields slightly different values of L_c for different counters, as detailed in Table I for one set of alpha pulse-height detectors.

Another number called by Currie[1] the minimum detectable true activity (L_D) may be calculated which has the following interpretation. If we let β be the risk of making a type II error (claiming that nothing is present in the sample when, in fact, some activity is present), then L_D is the mean net count which would have to be present in a sample in order to be detected [greater than $(L_c + B)$ "most" of the time or $(1 - \beta)$ 100% of the time]. If we take $\beta = 0.10$, our values of $(L_D + B)$ are given in Table I. The figure L_c is used with every sample count, but L_D is merely a figure which is a measure of the capability of the counting equipment (i.e., of what activity could be detected most of the time *if it were present*).

Estimating Confidence Intervals for Plutonium Analyses in Autopsy Tissue Samples. A point estimate of the dis/min (D) of ^{239}Pu in autopsy tissue is made by calculating

$$D(S/t_1 - B/t_2)/RE,$$

where E is the efficiency of the ^{239}Pu counter, R is the fraction of ^{239}Pu recovered chemically, S is the gross count on the sample (counted for t_1 min), and B is the gross background count (counted for t_2 min). R is calculated as

$$R = (S'/t_1 - B'/t_2)/AE',$$

where S', B', and E' are sample count, background count, and efficiency for the ^{242}Pu spike added to the solution. A is the amount of spike added. Simplifying, we obtain:

$$D = (S - \rho B)A/(S' - \rho B'),$$

where $\rho = t_1/t_2$. Propagating the error on D, we obtain:

$$\hat{\alpha}_D^2 = \left(\frac{\partial D}{\partial S}\right)^2 \alpha_S^2 + \left(\frac{\partial D}{\partial B}\right)^2 \alpha_B^2 + \left(\frac{\partial D}{\partial S'}\right)^2 \alpha_{S'}^2 + \left(\frac{\partial D}{\partial B'}\right)^2 \alpha_{B'}^2$$

$$= \left[(S + \rho^2 B)\, A^2 + D^2\, (S' + \rho^2 B')\right] / (S' - \rho B')^2$$

Since we would like to use $\hat{\alpha}_D^2$ to place a confidence interval on δ (the true dis/min in the sample), we thought it best to investigate the distribution of D. This was done by means of a Monte Carlo study. One thousand Poisson-distributed random variables were generated on the computer with mean S (with S close to the number of counts in the autopsy tissue samples). This process was repeated for variables with mean B, S', and B'. From this information, 1000 values of D were calculated, holding A and ρ fixed. It was then shown (by means of a chi-square, goodness-of-fit test) that D was normally distributed. This fact gives adequate justification for using $D \pm 2\hat{\alpha}_D$ as a good approximation for a 95% confidence interval on δ.

Since a confidence interval can be used as a test of hypothesis, it can be said that, if the confidence interval includes zero, then δ is not significantly different from zero at the 5% level of significance. Confidence limits are being placed on

TABLE I

IDENTIFICATION OF MINIMUM DETECTION LIMITS FOR A SET OF ALPHA PULSE-HEIGHT DETECTORS

Detector	Average B (dis/min)	$(L_c + B)$ (dis/min)	L_c (dis/min)	$(L_D + B)$ (dis/min)
1	0.0107	0.018	0.007	0.025
2	0.0134	0.022	0.009	0.030
3	0.0111	0.018	0.007	0.025
4	0.0096	0.017	0.007	0.024
5	0.0051	0.011	0.006	0.017
6	0.0023	0.006	0.004	0.011
7	0.0034	0.008	0.005	0.013
8	0.0167	0.027	0.010	0.031

all samples, regardless of whether the sample count is "detectable" or not. This gives quantitative, rather than merely qualitative, limits on δ. The confidence limits take into account recovery and variation in the preparation of the sample, as well as the capability of the counting equipment; hence, they may vary somewhat from a judgment based on L_c alone (i.e., on the counting equipment alone).

REFERENCES

1. L. A. Currie, "Limits for Qualitative Detection and Quantitative Determination," Anal. Chem. 40, 586-592 (1968).
2. B. Altschuler and B. Pasternak, "Statistical Measures of the Lower Limit of Detection of Radioactivity Counters," Health Phys. 9, 293-298 (1963).

Plutonium Concentration in Urine Samples Collected from Early Plutonium Workers

Twenty-five former male employees at LASL who worked with plutonium during World War II have been requested to submit urine samples for plutonium

TABLE I

PLUTONIUM CONCENTRATION IN URINE SAMPLES COLLECTED FROM EARLY PLUTONIUM WORKERS

	Year Samples were Collected					
	1946 (dis/min/sample collected)	1957-1958	1971 (dis/min/24-h sample)			1974
Employee Identification	Termination Single Sample	Single Sample	Multiple Analysis of Several Samples (n)	(mean)	(± 1 σ)	Single Sample
3	5.1	0.46	7	5.06	1.08	4.54
4[a]	8.2[b]	1.28	10	2.61	0.30	2.54
1	8.5 (1945)	1.00	5	1.99	0.34	1.76
7	7.5	1.03	6	1.57	0.88	1.89
9	11.7	0.46	6	1.53	0.47	1.03
5	1.4	0.71	3	1.53	0.70	--
18	4.9	1.14	3	1.09	0.53	0.82
8	4.6	0.13	6	1.04	0.10	1.10
17	4.6	--	2	0.92	0.17	0.78
6	10.2	0.63	4	0.91	0.18	0.78
12	3.2	--	2	0.63	0.77	--
10[a]	14.6 (1945)	0.35	4	0.57	0.26	0.50
16	0.0	0.20	6	0.54	0.18	--
2	--	--	4	0.52	0.14	0.10
20	2.0	0.34	2	0.49	0.07	0.45
22	5.4	0.08	4	0.44	0.24	0.18
23	9.3	0.22	2	0.35	0.01	0.21
28[a]	3.1[b]	0.23	8	0.26	0.03	0.24
27[a]	12.0	0.17	7	0.30	0.13	0.09
24	0.5	0.70	2	0.22	0.08	0.44
21	2.2	0.14	2	0.22	0.05	--
25[a]	2.1[b]	0.08	5	0.12	0.02	0.09
13	6.1	0.08	4	0.11	0.08	0.07
26	0.8	0.00	6	0.08	0.08	0.07
19	2.0	0.27	-	--	--	0.49

[a] Presently employed at LASL.

[b] Mean of 1946 results.

analysis. This was the third such effort to review the plutonium excretion rate per 24-h period in these early plutonium workers. Table I shows the plutonium results of samples collected upon termination from LASL in 1946, results from a 1957 and 1958 sampling, results from a 1971 collection, and the 1974 data. These data were arranged in order of high-to-low based on the 1971 results. The 1971 samples were collected by the subjects while they were in Los Alamos for a complete medical study. Several 24-h urine samples were collected during this visit. Some samples were subdivided to study the analytical error associated with the analysis and sampling. The 1971 data are believed to represent the best estimate of each man's 24-h plutonium excretion rate. The 1946 and 1957 data were requested to be 24-h samples, but no effort was made to confirm the collection of a true 24-h urine sample. The 1971 and 1974 data were corrected to 24-h voiding, based on urinary creatinine measurements, and were confirmed by the subject's own records of collection times.

Five of the 20 subjects have been in continuous employment at LASL since 1944 and are indicated in Table I. These 5 men have been sampled at regular periods to study their plutonium excretion rates. These data suggest that the plutonium excretion rate is constant with time after the early, rapid drop during the first 2 yr following exposure.

Plutonium in Occupationally Exposed Workers

Analyses of autopsy tissues from 17 former LASL employees have been completed this calendar year. This brings the total number of occupationally exposed cases analyzed by this Laboratory to 77. The number of organs and tissues collected at autopsy have been increased from the routine lung, liver, tracheobronchial lymph nodes, kidneys, and bone specimens to include the spleen, thyroid, and gonads. The guidelines suggested by the U. S. Transuranium Registry[1] have been utilized to divide the cases into a high potential exposure group (33 cases of transuranium workers) and a low potential exposure group (44 cases). Estimates of whole-body contents of plutonium extrapolated from tissue data were compared with PUQFUA[2] body burden estimates based upon urine analysis data and are detailed in Table I. The ratio of urine assay body burdens to the tissue extrapolated systemic body burdens is less than 10 in 70% of the cases having positive results in both urine and tissue analyses, with a range from 0.5 to 155. Eighty-eight percent of the positive ratios are greater than 2, indicating a conservative trend in using the urine bio-assay data for health physics protective measures. The PUQFUA estimates were generally positive when the systemic tissue results indicated the presence of plutonium, with only 4 exceptions. However, in 3 of the 4 exceptions, only a single urine sample was analyzed and was the basis of the PUQFUA calculation. The fourth exception had 5 urine samples analyzed. Since these employees each lived from 4 to 22 yr after their last urine analysis, it is conceivable that a subsequent unrecorded exposure occurred prior to their death. In 3 of the 5 cases where the tissue systemic burdens were zero and the urine estimates were positive, we were unable to estimate the skeletal burden because bone samples were not collected at autopsy or, in one case, the activity measured in the bone specimen was below our minimum detection level.

A comparison of the ponderal method proposed by Durbin[3] for estimating skeletal burdens has been made to the "standard man" skeletal calculations (see Table II). The ponderal method recognizes the nonuniform distribution of plutonium observed in different bones and also the differences in skeletal mass in individuals. Unfortunately, no data are currently available on the fractional concentrations of plutonium in individual bones compared with the entire skeletal burden; therefore, it was assumed that the plutonium kinetics would be similar to that measured in man for ^{226}Ra and ^{90}Sr. The distribution fractions determined for these bone-seeking isotopes were utilized in the ponderal calculations. The standard man calculations assume a uniform distribution of plutonium throughout the skeleton and, for a 70-kg man, a skeletal mass of 10 kg. From Table II it can be seen that there is relatively little difference in the ponderal and standard man extrapolations when the bone analyzed was a vertebral wedge. The standard man uniform distribution estimates were, on the average, 1.2 times higher than the ponderal estimates. However, use of the rib or sternum concentrations with the uniform distribution calculations

TABLE I

COMPARISON OF THE ESTIMATES OF BODY CONTENT FROM TISSUES AND URINE ANALYSES

Case Number	Date of Death	Time from First Exposure to Death (yr)	Last Urine Sample Date	Number of Urine Samples Analyzed	PUQFUA[1] Body Burden (nCi)	Systemic[a] Body Burden (nCi)	Lung and Lymph Node Burden (nCi)	Whole[b] Body Burden (nCi)	Estimated Body Burden (urine/tissue)
1-039	1959	13	1958	71	24.60	18.30	2.60	21.00	1.3
1-094	1960	5	1952	5	0.00	0.02	0.01	0.03	NC[c]
1-128	1961	NA[d]	1957	4	0.06	0.00[e]	0.00	0.00	NC
1-150	1961	4	1961	7	0.10	0.02	0.10	0.12	5.0
2-004	1961	15	1958	49	17.00	2.03[e]	3.31	5.31[e]	8.5
2-014	1961	NA	1961	5	0.33	0.00[e]	0.02	0.02[e]	NC
2-030	1962	15	1961	58	10.00	4.24	4.52	8.76	2.4
2-058	1962	10	1961	26	3.10	0.02[b]	0.03	0.05	155.0
2-064	1962	NA	1958	1	0.00	0.02	0.02	0.05	NC
2-068	1962	14	1954	1	0.00	0.00[e]	0.01	0.01	0/0
2-100	1962	12	1961	13	2.80	0.27	0.01	0.28	10.4
2-126	1962	8	1962	23	2.40	0.00	0.45	0.46	NC
2-130	1962	7	1962	18	3.20	0.95	0.25	1.20	3.4
3-014	1965	22	1955	1	0.00	5.15	0.00	5.15	NC
3-016	1965	19	1965	40	3.40	0.68	0.19	0.87	5.0
3-028	1966	8	1966	7	0.00	0.00[f]	0.00	0.00	0/0
3-088	1968	4	1964	1	0.00	0.00[f]	0.00	0.00	0/0
5-064	1970	10	1969	8	0.23	0.00[f]	0.01	0.01	NC
5-076	1970	17	1964	16	0.22	0.04	0.01	0.05	5.5
5-080	1970	15	1957	4	0.16	0.01	0.01[g]	0.02	16.0
5-114	1970	NA	1948	1	0.00	0.28	0.06	0.35	NC
5-138	Living	30	1971	5	28.40	0.01[f]	6.40	6.50[h]	-
5-150	1971	22	1970	14	2.70	0.00	0.01	0.01	NC
7-006	1971	14	1970	12	0.11	0.01	0.00	0.01	11.0
7-054	1972	NA	1965	14	0.29	0.05	0.12	0.17	5.8
7-066	1972	25	1971	42	30.00	0.64	0.15	0.79	46.9
7-072	1972	NA	1964	5	4.70	0.12	0.04	0.16	39.2
7-074	1972	10	1962	2	0.01	0.02	0.02	0.04	0.5
7-084	1972	NA	1965	16	0.93	0.14	0.23	0.37	6.6

[a] Systemic body burden is extrapolated from the measured plutonium contents in liver, skeleton, kidney, and other soft tissues analyzed, excluding the lung and pulmonary lymph nodes.

[b] Whole body burden is the systemic burden plus lung and pulmonary lymph node burden.

[c] NC = not calculable, since one factor is zero.

[d] NA = not available.

[e] No bone sample available for analysis.

[f] Bone sample analyzed was below the detection level.

[g] Lung tissue unavailable for analysis.

[h] Biopsy samples considered too small for reliable estimate of body burden.

TABLE II

COMPARISON OF EXTRAPOLATION METHODS FOR ESTIMATION OF SKELETAL BURDENS

Case Number	Bone Analyzed	Extrapolated Skeletal Burden: Standard Man (dis/min)	Extrapolated Skeletal Burden: Ponderal (dis/min)	Ratio of Skeletal Estimates (Standard Man/Ponderal)
1-039	Vertebra	23 900	21 280	1.1
1-039	Rib	11 600	6 525	1.8
1-039	Sternum	11 200	9 828	1.1
2-030	Vertebra	6 100	4 510	1.4
2-064	Vertebra	49	33	1.5
2-100	Vertebra	644	591	1.1
2-126	Vertebra	1 070	1 004	1.1
2-130	Vertebra	1 780	1 534	1.2
3-014	Rib	19 040	10 996	1.7
3-016	Vertebra	340	308	1.1
3-058	Vertebra	1 840	1 549	1.2
3-072	Vertebra	86	65	1.3
3-108	Vertebra	15	12	1.2
3-142	Vertebra	27	26	1.0
5-024	Vertebra	32	29	1.1
5-040	Vertebra	102	74	1.4
5-076	Vertebra	118	90	1.3
5-080	Vertebra	12	13	0.9
5-108	Vertebra	7	6	1.2
5-114	Vertebra	899	522	1.7
5-116	Vertebra	22	20	1.1
5-118	Vertebra	203	150	1.4
5-138	Rib	35 500	18 158	2.0
7-004	Vertebra	30	25	1.2
7-006	Rib	33	24	1.4
7-016	Vertebra	48	29	1.7
7-054	Vertebra	119	107	1.1
7-066	Vertebra	660	478	1.4
7-072	Vertebra	62	63	1.0
7-082	Vertebra	40	32	1.2
7-084	Vertebra	244	223	1.1
7-088	Vertebra	40	40	1.0
7-118	Vertebra	13	18	0.7

Mean Ratio (vertebra)	1.2 ± 0.2
Mean Ratio (rib)	1.7 ± 0.2

gave skeletal concentrations that were factors of 2 lower than the vertebral estimates.

It is unknown which method or which bone analyses result in the most accurate estimation of the true skeletal burden, since no data are presently available on plutonium distribution ratios within various bones compared with the entire skeletal content. With the variation observed above in the

skeletal estimates, it seems obvious that very high priorities should be placed upon obtaining several willed bodies, each having measurable plutonium concentrations in the bones, so that knowledge concerning the skeletal distributions may be gained.

In other work with tissues from occupationally exposed cases, it was observed that 33 of the 77 cases analyzed had tracheobronchial lymph node depositions of plutonium ranging from 0.1 to as high as 4000 dis/min/g of tissue (0.05 to 1800 pCi/g). From this group of 33 cases, 14 were of such a nature as to require the pathologist to remove tracheobronchial lymph nodes at the time of autopsy and to subsequently prepare histological slides for examination. Selected information on these 14 cases is shown in Table III. The time elapsed since the first potential exposure is represented by the years from the date of hire at LASL to the death of the individual. It was assumed that the exposure incidents were via inhalation that occurred during the early years of the Laboratory operation (1945 to 1955), before improved industrial hygiene and health physics requirements significantly reduced the air levels of plutonium in the laboratories and the workers were provided with more efficient personal respiratory protection.

Microscopic examination of the stained thin sections of lymph node revealed no abnormalities other than what would be expected from individual disease processes that caused the death of the various persons in this study. Many of the nodes appeared to contain normal activity such as hyperplasia, as in the case of pneumonia, and tumor metastasis, as in the case of cancer. The pulmonary lymph nodes of persons dying from trauma were pathologically unremarkable.[4] It will be noticed that 2 of the 14 cases listed in Table III died of lung cancer. The national incidence of lung cancer has been reported as one case out of every 35 autopsies performed.[5] Since these data represent 77 autopsies, the presence of 2 lung cancers is within the reported national norms and was not surprising.

The tracheobronchial lymph nodes from case 7-138 contained sufficiently high concentrations of plutonium (average 770 pCi/g) to enable the use of the autoradiographic techniques developed by Leary[6] to estimate the particle size distribution within the lymph nodes. The number of alpha tracks in the photographic emulsion (Fig. 1) radiating outward from the particles (assumed to be PuO_2) were counted optically assuming a 50% geometry. It was also assumed in the calculations that the radioactive

TABLE III

CONCENTRATION OF ^{239}Pu IN TRACHEOBRONCHIAL LYMPH NODES OF OCCUPATIONALLY EXPOSED WORKERS

Case Number	Occupation	Cause of Death	Year of Death	Age at Death	Years since First Exposure[a]	Alpha Activity (pCi/g)
7-138	Metal fabrication technician	Crushed chest	1973	47	26	770
5-138	Chemist	Living[b]	1971[b]	50[b]	27	254
2-004	Health physics monitor	Cancer (lung)	1961	68	12	29
5-114	Chemistry technician	Stroke	1970	49	21	6.3
7-084	Pipe fitter	Cancer (lung)	1972	58	23	1.8
7-004	Accountant	Carcinoma (colon)	1971	76	24	0.24
1-150	Plumber	Cardiac arrest	1961	51	8	0.23
5-024	Physicist	Heart attack	1969	43	5	0.21
7-076	Maintenance mechanic	Ruptured aorta	1972	72	24	0.18
3-142	Engineer	Cardiac arrest	1969	48	14	0.11
7-016	Machinist	Heart attack	1971	62	26	0.09
3-108	Technician	Pneumonia	1968	69	26	0.09
3-086	Technician	Diabetes	1968	34	15	0.05
7-028	Design engineer	Heart disease	1971	60	28	0.05

[a] Years from time of hire to death.

[b] Biopsy tissue taken in 1971.

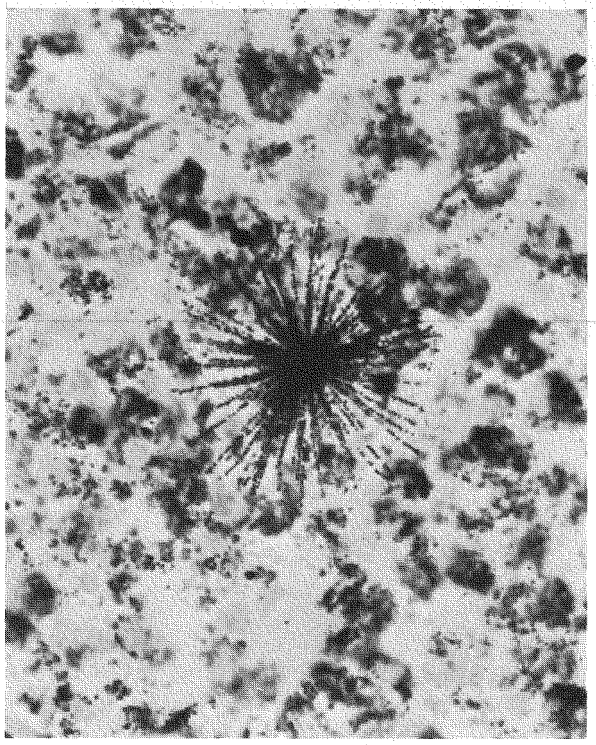

Fig. 1. Tracheobronchial lymph node tissue section showing alpha tracks radiating out from an active particle in a typical "star" pattern.

isotope was essentially all ^{239}Pu. Chemical analyses using alpha pulse-height spectrophotometry indicated < 2% ^{238}Pu and 12% ^{241}Am. The use of the long-lived ^{239}Pu tends to maximize the estimations of the particle sizes in the calculations. By knowing the exposure time for the autoradiograph, the physical half-life of the isotope, and the density of PuO_2, the sizes of the plutonium particles were estimated. The frequency distribution of the particle sizes, determined from 1215 such stars, is shown in Table IV. These data were assumed to be log-normally distributed, and the log-probability plot of these data is shown in Fig. 2. The distribution of $^{239}PuO_2$ particles in one tracheobronchial lymph node was determined to have an activity median diameter of 0.3 μm, with a geometric standard deviation of 1.6. Ninety-five percent of the particles in the node was determined to have a ^{239}Pu concentration of less than 0.22 pCi.

TABLE IV

FREQUENCY DISTRIBUTION OF PLUTONIUM PARTICLES FROM STARS OBSERVED IN TRACHEOBRONCHIAL LYMPH NODE[a]

Plutonium Particle Diameter (μm)	Frequency	Cumulative Percent
0.11	92	7.5
0.14	141	19.2
0.18	146	31.2
0.20	147	43.1
0.22	125	53.6
0.24	206	70.5
0.30	199	86.9
0.38	92	94.5
0.52	52	98.8
0.65	15	100.0

[a]Taken from No. 6, 7-138 (0.66 nCi).

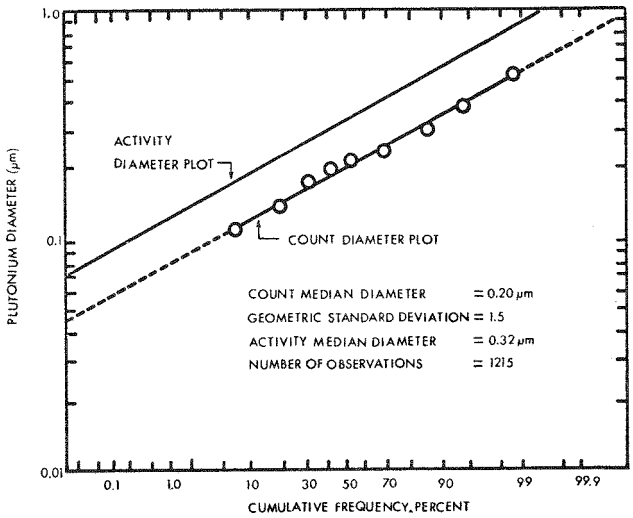

Fig. 2. Log-normal cumulative frequency plot of $^{239}PuO_2$ particles in tracheobronchial lymph node.

REFERENCES

1. W. D. Norwood and C. E. Newton, Jr., "United States Transuranium Registry Summary Report to June 30, 1974, to USAEC Division of Biomedical and Environmental Research," Hanford Environmental Health Foundation, Richland, Washington (June 1974).

2. J. N. P. Lawrence, "PUQFUA: An IBM-704 FORTRAN Code for Determining Plutonium Body Burden from Urine Assays," Los Alamos Scientific Laboratory report LA-2329 (1960).

3. P. W. Durbin, "Plutonium in Man: A New Look at the Old Data," in Radiobiology of Plutonium (W. S. S. Jee and B. J. Stover, eds.), University of Utah Press, Salt Lake City, Utah (1972).

4. J. F. McInroy, M. W. Stewart, and W. D. Moss, "Studies of Plutonium in Human Tracheobronchial Lymph Nodes," in Proceedings of the 14th Annual Hanford Biology Symposium (1974), in press.

5. C. C. Lushbaugh, M.D., Pathology Department, Oak Ridge Associated Universities, Inc., Oak Ridge, Tennessee. Personal communication.

6. J. A. Leary, "Particle-Size Determination in Radioactive Aerosols by Radioautograph," Anal. Chem. 23, 850-853 (1951).

Plutonium in Tissues of the General Population

Additional data are being accumulated to establish baseline concentrations of environmental plutonium in the general population of various geographical regions throughout the United States. This information is essential for the assessment of risk parameters associated with the growth of the nuclear industry. The evaluation of the first 100 autopsy cases from one area is nearing completion. This was the number of cases judged necesssary for analysis to give statistically reliable estimates of baseline concentrations for a given variable. Tissues will be collected from this area on a reduced scale to permit monitoring of the established plutonium baseline levels. Other areas under study are continuing to collect tissues. Two new locations of interest to the AEC have been added to the program. Tissues from the Chicago, Illinois, and from the Erie, Pennsylvania, areas are presently being analyzed for plutonium in addition to the samples collected from Colorado, Georgia, New Mexico, South Carolina, Tennessee, and New York. A summary of the total number of cases collected is shown in Table I.

TABLE I

NUMBER OF AUTOPSY CASES RECEIVED FROM THROUGHOUT THE UNITED STATES

Area	Number of Cases (calendar 1974)	Number of Cases (1959 to 1974)
Colorado	72	241
Georgia-South Carolina	57	62
Illinois	10	11
Pennsylvania	98	98
New York	36	36
New Mexico (includes LASL)	34	351
Tennessee	52	54
Total	359	853

The median concentrations of plutonium in tissues collected and analyzed from the inception of the tissue analysis program in 1959 through 1974 are shown in Table II. The highest concentrations of plutonium, in decreasing order of levels, were found in pulmonary lymph nodes, liver, lung, and vertebra. More than 50% of the kidney and gonadal tissue concentrations were below the minimum detection level (discussed earlier). The largest deposition in a single organ was estimated to be the skeletal burden due to the large mass of the system. The median concentration of plutonium in the lung and liver for all areas was statistically the same as reported in 1973[1] and in 1974.[2] The analyses of more cases have

TABLE II

FIFTIETH PERCENTILE DISTRIBUTION OF PLUTONIUM IN HUMAN TISSUE FOR THE NON-OCCUPATIONALLY EXPOSED (1959-1974)

Location	Lung (pCi/kg)	Liver (pCi/kg)	Lymph Nodes (pCi/kg)	Kidney (pCi/kg)	Vertebra (pCi/kg)	Gonad (pCi/kg)
Los Alamos	0.60 (66)[a]	0.55 (60)	3.94 (60)	0.10 (64)	0.35 (41)	b
New Mexico and United States	0.39 (99)	0.49 (85)	1.07 (93)	< MRL[c] (91)	0.18 (66)	< MRL (9)
Colorado	0.23 (111)	0.77 (95)	0.56 (89)	< MRL (76)	0.19 (45)[d] 0.39 (73)[d]	< MRL (61)
New York	0.30 (35)	0.62 (31)	e	e	0.73 (32)	0.34 (33)
Georgia-South Carolina	0.17 (20)	0.64 (14)	b	< MRL (11)	< MRL (13)	b
All Populations	0.33 (331)	0.61 (285)	1.35 (242)	< MRL (242)	0.23 (197)	< MRL (103)

[a] Number of samples received.

[b] Insufficient number analyzed for statistical significance.

[c] Minimum reporting levels.

[d] Rib specimens (not included in All Populations data).

[e] Samples not requested and/or not received.

resulted in a lowering of estimates of median concentrations of plutonium in the lymph nodes and vertebra of all areas except for the residents of Los Alamos. It is difficult to judge if this difference is real or a result of the extrapolated estimates from the original data. Statistical evaluation of these data is currently being studied.

An interesting observation can be made with the bone data from Colorado. Table II lists the concentration of plutonium in vertebra (45 cases) and in rib (73 cases). The concentration in rib is twice the concentration found in vertebra (0.39 and 0.19 pCi/kg, respectively). This is the reverse effect observed in the occupationally exposed cases but, because of the larger number of cases analyzed, may be of more significance. However, the lower levels of concentration in this population result in greater doubt in the reliability of the analytical measurements. Additional measurements of bone concentrations in various specimens from the occupational exposure cases are necessary to evaluate this apparent contradiction in observations.

The reporting of median values for the kidney and gonad specimens identifies a problem area in data reporting that is currently under study at this Laboratory. For example, the Colorado gonad data had 43 of the 61 analyses for plutonium below the minimum detection limit. The question arises as to whether one should attempt a least-squares fit of a line to the data and to extrapolate to the median concentration value or, alternatively, to simply identify the median as being below the minimum reporting level. We have chosen the latter as the most reasonable approach statistically at this time and are evaluating the problem of handling this as "censored" data. The pooling of samples from similar cases (i.e., similar age, cause of death, sex, residential and occupational histories, etc.) is being evaluated as a possible means of avoiding this problem by increasing the mass of tissue available for analysis.

REFERENCES

1. E. E. Campbell, M. F. Milligan, W. D. Moss, H. F. Schulte, and J. F. McInroy, "Plutonium in Autopsy Tissue," Los Alamos Scientific Laboratory report LA-4875 (1973).

2. C. R. Richmond and E. M. Sullivan, eds., "Annual Report of the Biomedical and Environmental Research Program of the LASL Health Division, January through December 1973," Los Alamos Scientific Laboratory report LA-5633-PR (May 1974).

Other Isotope Screening (Diagnostic)

Each large tissue (i.e., mainly lung and liver) brought into the laboratory for analyses is screened for gamma- and x-ray activities. This is a precautionary measure to alert this Laboratory to the presence of radionuclides in tissues from medical treatment prior to death. The first screening occurs when the frozen tissue is delivered or as soon thereafter as practical. The counting statistics are relatively poor due to geometry parameters, but the presence of medicinal isotopes is readily identified in most cases. The tissues are then ashed and recounted. The small mass of the ash results in a much improved geometry, and the counting results are more quantitative. Cesium-137 and ^{40}K are routinely identified. Indium-130, ^{60}Co, ^{131}I, and ^{134}Cs have been observed. Cesium-134, an activation product of stable ^{133}Cs, is not normally found in nature nor used medicinally; however, more than 30 autopsy cases have been identified containing this isotope. It is suspected that these cases may have received radioisotopes for medical scanning diagnostics. Although ^{134}Cs is not used for this purpose, it does occur as a contaminant on the columns and in eluates of commercial ^{99m}Tc generators. We have received confirmation of ^{99m}Tc administration in 14 of 20 cases (from two locations) having positive ^{134}Cs activity in their tissues. We are waiting the results of further inquiries.

Trace Metal Analyses in Tissue

Interest in determining the exposure of the general population to trace metals resulting from emissions associated with the fossil fuel power production industry has resulted in our evaluation of techniques suitable for the analysis of nanogram quantities of trace metals in human tissue. Frozen tissue specimens retained for this purpose from the plutonium analysis program were utilized for the analyses. The tissues are being analyzed for lead, cadmium, beryllium, mercury, and such additional elements of interest as determined by the investigation.

Anodic stripping voltametry (ASV) permits four samples to be run simultaneously. A precision of

TABLE I

TRACE METALS IN AUTOPSY TISSUE

Case Number	Sample Analyzed	Metal Analyzed	Wet Tissue (μg/g)	Reported Ranges[1] (μg/g)
10-004	Liver	Cadmium	2.04	0.5 to 7.2
		Lead	0.89	0.6 to 6.0
		Copper	1.01	1.4 to 25
13 Los Alamos	Lung	Lead	0.18 (average)	0.22 to 2.5
10 New York	Lung	Lead	0.25	0.22 to 25

± 5 to ± 15% can be obtained for samples containing 100 to 1.0 nanograms, respectively, of mixtures of metal ions. Cadmium, lead, and copper are obtained readily; bismuth, thallium, and zinc may also be analyzed with some changes either in solution composition or electrode coating. At this point, it seems that zinc would be better done by atomic absorption (AA) methods. The manufacturer claims that arsenic analysis is feasible using gold-coated electrodes. Analyses by ASV are not easier than by AA, but the former is more sensitive and offers the advantage of at least three metals simultaneously and at the low levels at which they occur in normal tissue. The usual method of digest of tissue samples by an HNO_3, H_2SO_4, $HClO_4$ acid mixture used for ASV would prepare the samples equally well for AA; the same standards, glassware, etc., can be used for both. However, ASV requires less sample than AA.

One can schedule routine analyses of large numbers of samples (100 to 150) per day by acid digesting a 1- to 2-g sample, analyzing an aliquot for cadmium, lead, and copper by ASV, and using another aliquot for AA analyses of zinc, nickel, magnesium, or some other element for correlation. The limit would be the availability of sample, since AA requires 1 to 2 ml per analysis. Another possibility lies in using the graphite furnace attachment to the AA, which would be feasible for beryllium analysis. This uses small amounts of sample and is highly sensitive; one could use the same sample digest.

The results of analyses for trace quantities of cadmium, lead, and copper, performed on selected lung and liver tissues using ASV and AA spectrometry techniques, are shown in Table I. Although the results are preliminary and the exercise was primarily to develop procedures rather than to obtain data, the ASV methods seem to hold promise for trace metal analyses in tissue.

REFERENCE

1. I. H. Tipton, M. J. Cook, J. M. Foland, J. Rittner, M. Hardwick, and K. K. McDaniel, "Spectrographic Analysis of Normal Human Tissues from Tacoma and Seattle, Washington," Oak Ridge National Laboratory central file report CF-58-10-15 (1958).

Studies on Plutonium Workers

(G. L. Voelz, M.D., and L. H. Hempelmann, M.D.)

The value of following humans exposed to plutonium was recognized early at Los Alamos and led to the establishment of a long-term study at Los Alamos by Dr. L. H. Hempelmann and the late Dr. Wright H. Langham in the early 1950s. During the Manhattan Project days of 1943 to 1945 at Los Alamos, a number of workers were exposed while performing operations in plutonium purification, fluorination, reduction to metal, and plutonium recovery procedures. The exposures occurred primarily through inhalation of airborne aerosols as a result of the crude containment and detection procedures used during this hectic wartime period. Twenty-six of the individuals with the highest exposures, as judged by early urinary excretion values and counts on nose swipes, were selected for the study in 1953. One individual in the group has died of coronary heart disease, while 25 individuals continue to be followed today. The systemic body burdens of these individuals, estimated by urinary excretion, are shown in Table I. Despite the uncertainties of body burden estimates, it appears that this group of individuals have had exposures around the current permissible body burden value for nearly 30 yr.

The medical studies have revealed no abnormalities except for ailments that one would expect in a group of men mostly in their early fifties. One individual (age 38) died of coronary heart disease as mentioned, while another has recovered from a

TABLE I

LASL PLUTONIUM WORKERS STUDY

Fraction of MPBB[a]	Number of Persons in Study: Original Study	Expanded Study	Currently Located
5 to 10	3	3	3
3 to 5	5	6	6
1 to 3	10	19	18
0.1 to 1	7	229	130
Total	25	257	157
Deceased	1	12	

[a]The maximum permissible body burden (MPBB) is 40 n-Ci of ^{239}Pu or ^{238}Pu.

coronary attack. A malignant melanoma has been removed from the chest wall of one of the subjects. Another had a partial gastrectomy for a bleeding ulcer. There are the expected assortment of mild hypertension, ulcers, and obesity. These studies and findings are described by Hempelmann *et al.*[1,2]

As these studies are continued, it should be obvious that the natural incidence of disease will provide interpretation difficulties as to the etiology of disease. The number of workers is so small that to date it has not been considered necessary to establish a control group but, rather, simply to record our observations. Beginning in 1974, these studies are being expanded to include all Los Alamos workers exposed in excess of 10 nCi whole-body burden. This effort involves a search to locate those individuals who have left the employ of the Los Alamos Scientific Laboratory. Table I also lists both the original study group as well as the expanded group. The number of individuals who have been located to date are listed.

Questionnaires have been sent to all persons on whom we have addresses and who are no longer employed at the LASL. Following the return of these questionnaires, the individuals are requested to submit urine samples for plutonium analysis. An updated body burden estimate will be calculated as these new data become available. Medical examinations will be performed by the individual's own physician, while special procedures including plutonium chest counts and chromosome aberration studies will be performed at Los Alamos when we are able to bring these individuals to Los Alamos for study. An expanded medical examination program on the Los Alamos residents in this study is now in progress. The contents of the current studies are listed in Table II.

A general summary of the available knowledge about plutonium from human studies[3] was presented at the Los Alamos Symposium on "Plutonium -- Health Implications for Man" in May 1974. The expanded studies since that time have not progressed to a point where significant new data are available.

These follow-up studies on plutonium workers complement both the LASL tissue program and the U. S. Transuranium Registry (Richland, Washington), since it affords additional opportunities to seek autopsy studies. Autopsy samples will continue to provide the opportunity for specialized studies such as the recent study of plutonium in human tracheobronchial lymph nodes.[4] This program also provides incentive to find new study techniques, including better *in vivo* counting methods. A recent study at Los ALamos demonstrated the feasibility of using a new scintillation detector in the esophagus to count plutonium in the tracheobronchial lymph nodes in humans.[5]

TABLE II

MEDICAL STUDIES ON LASL PLUTONIUM WORKERS

Medical history
Physical examination
Complete blood count
Urinalysis (clinical)
Radiological urinalysis
Body burden estimate (PUQFUA code)
Chest counts for plutonium
Monitoring of old wound sites
Lung cytology
Chromosome analysis
Blood chemistry profile
- Alkaline phosphatase
- Cholesterol
- Total bilirubin
- Total protein
- Albumin, globulin, and albumin/globulin ratio
- Total lipid
- Transaminase (SGOT)
- Lactic dehydrogenase (LDH)
- Creatinine
- Glucose
- Urea nitrogen (BUN)
- Urea

REFERENCES

1. L. H. Hempelmann, W. H. Langham, C. R. Richmond, and G. L. Voelz, "Manhattan Project Plutonium Workers: A Twenty-Seven Year Follow-Up Study of Selected Cases," Health Phys. 25, 461 (1973).

2. L. H. Hempelmann, W. H. Langham, G. L. Voelz, and C. R. Richmond, "Biomedical Follow-Up of the Manhattan Project Plutonium Workers," in Proceedings of the Third Congress of the International Radiation Protection Association, Washington, D. C. (September 9-14, 1973), in press (1974).

3. G. L. Voelz, "What We Have Learned about Plutonium from Human Data," in Proceedings of the Los Alamos Life Sciences Symposium on "Plutonium -- Health Implications for Man," Los Alamos, New Mexico (May 22-24, 1974), Health Phys. (1974), to be published.

4. J. F. McInroy, M. W. Stewart, and W. D. Moss, "Studies of Plutonium in Human Tracheobronchial Lymph Nodes," in Proceedings of the 14th Hanford Biology Symposium, Richland, Washington (September 1974), to be published.

5. K. L. Swinth, J. F. Park, G. L. Voelz, and J. H. Evans, "In-Vivo Detection of Plutonium in the Tracheobronchial Lymph Nodes with a Fiber Optic Coupled Scintillator," in Proceedings of the 14th Hanford Biology Symposium, Richland, Washington (September 1974), to be published.

Analysis and Assessment

(C. R. Richmond, J. W. Healy, and R. L. Thomas)

A small effort on the analysis and assessment of current information on the effects of plutonium on man and the environment was started in 1974. Primary emphasis is to be placed on assessment of the potential effects of the LMFBR and associated fuel cycle. In addition to starting the formulation of an overall appraisal aimed at identifying areas requiring additional study, several specific studies were undertaken.

The petition of the Natural Resources Defense Council[1] requesting a lowering of limits for insoluble, alpha-emitting "hot particles" by a factor of 116 000 was accompanied by a document prepared by Drs. Tamplin and Cochran[2] providing the rationale for the petition. A review of this document was made,[3] with the conclusion that the hypothesis advanced was poorly founded on inappropriate information and was not supported by existing information in the literature on the effects of such alpha-emitting particles. It was concluded, therefore, that the hypothesis did not provide a basis for the proposed change.

Assistance was given to the staff of DBER in studying comments on the plutonium toxicity section of the Draft Environmental Impact Statement of the LMFBR. Proposed answers were prepared for many of the comments, and assistance was given in redrafting the section to adequately reflect the comments.

In response to concerns expressed about the possible genetic effects of plutonium, a review[4] was made of information available on the actinide content of gonads of mammalian species following various routes of administration. The fraction of the administered amount following intravenous administration was about 3×10^{-4}, with little difference apparent between sexes, among species, or as a function of time since administration. The gonadal fraction tends to be smaller following inhalation or subcutaneous implant. Data on other actinides are qualitatively similar to those for plutonium.

The uptake of plutonium in plants has been considered to be a relatively minor pathway to man because the data indicate a low value for the uptake. Preliminary information on other transuranic elements indicates that this may not be true for these materials. A review of the information available, with emphasis on americium because of its ingrowth from ^{241}Pu, has indicated that the experimental data are meager, but a search continues.

The Second Annual Life Sciences Symposium on "Plutonium -- Health Implications for Man" was held on May 22-24, 1974. This symposium provided an excellent review of the current situation, and the papers are currently being edited for publication in Health Physics.

REFERENCES

1. Natural Resources Defense Council, "Petition to Amend Radiation Protection Standards as They Apply to Hot Particles," submitted to the U. S. Atomic Energy Commission and the Environmental Protection Agency (February 14, 1974).

2. A. R. Tamplin and T. B. Cochran, "Radiation Standards for Hot Particles. A Report on the Inadequacy of Existing Radiation Protection Standards Related to Internal Exposure of Man to Insoluble Particles of Plutonium and Other Alpha-Emitting Hot Particles," Natural Resources Defense Council, 1710 North Street, N. W., Washington, D. C. (February 14, 1974).

3. J. W. Healy, C. R. Richmond, and E. C. Anderson, "A Review of the Natural Resources Defense Council Petition Concerning Limits for Insoluble Alpha-Emitters," Los Alamos Scientific Laboratory report LA-5810-MS (November 1974).

4. C. R. Richmond and R. L. Thomas, "Plutonium and Other Actinide Elements in Gonadal Tissue of Man and Animals," Health Phys. (1974), in press.

5. J. W. Healy, ed., "Plutonium -- Health Implications for Man," Health Phys. (1975), to be published.

ENVIRONMENTAL STUDIES GROUP[a] (H-8)

L. J. Johnson, Ph.D., Group Leader
K. J. Schiager, Ph.D., Alternate Group Leader
W. C. Hanson, Ph.D., Associate Group Leader
V. Lee, Technical Writer
M. A. Rosenthal, Group Secretary
D. Lucero, Secretary
P. Baldwin, Secretary

ECOLOGY SECTION

Staff Members

L. E. Eberhardt
T. E. Hakonson
D. F. Knab
F. R. Miera, Jr.
J. W. Nyhan

Technicians

K. V. Bostick
J. L. Martinez
G. M. Romero
R. Romero
E. Trujillo
R. B. Whipple

Visiting Staff Member

M. J. Romine

ENVIRONMENTAL SECTION

Staff Members

S. Barr
W. E. Clements
D. A. Dahl

Technicians

F. R. Craven
J. A. Archuleta
N. Elliott (student)

SOLID WASTE MANAGEMENT SECTION

(13 Staff Members;
4 Technicians)

---

[a]Personnel assigned part- or full-time to AEC/DBER-funded programs.

INTRODUCTION

The Los Alamos Scientific Laboratory's radioecology program began in 1972 to supply information on the environmental implications of the Laboratory's radioactive waste disposal practices, with particular reference to the study of plutonium in the environment. An environmental inventory was recognized as an integral part of the program to define the systems within which the studies were conducted and was emphasized by DBER interest in promoting Environmental Research Parks. These activities were summarized in our 1973 annual report. During 1974, the scope and objectives of the radiation ecology were expanded considerably by new research programs in both nuclear and non-nuclear areas of interest. The new programs began in July 1974 and are, therefore, in their initial stages of development. The summaries that follow will outline briefly current progress in the several areas now investigated by the Health Division's ecology programs.

ENVIRONMENTAL RESOURCES INVENTORY

(T. E. Hakonson and W. C. Hanson)

An initial map of LASL overstory vegetation on a scale of 1:24 000 was completed in 1974 from color infrared aerial photographs supplemented with field observations. Copies are available to interested parties by request. An indication of the diversity of plant communities is indicated by representative vegetation along a 25-km transect on mesa tops from the 1700-m elevation along the Rio Grande River on the eastern LASL boundary to the 3200-m elevation of Pajarito Mountain on the western boundary (see Fig. 1). The variety of habitats created by the

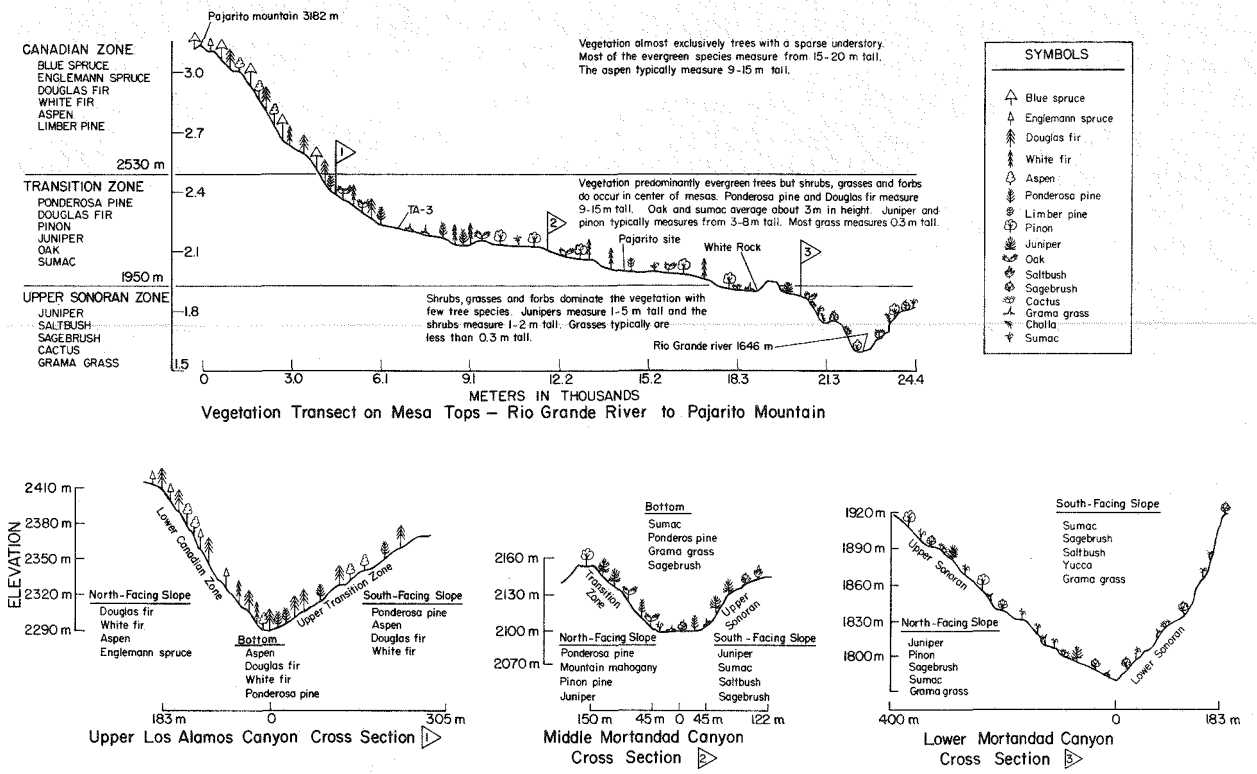

Fig. 1. An elevational profile depicting vegetation on the mesas and selected canyon cross sections on a transect from the Rio Grande River to Pajarito Mountain.

east-west orientation of the mesa/canyon ecosystems is reflected by cross sections of canyons shown; north-facing slopes support biota of the next higher Life Zone; south-facing slopes contain representatives of the next lower Life Zone; and canyon floors are an intergradation of biota representing both Life Zones.

Work was begun on an improved overstory vegetation type map on a scale of 1:6000 to be drawn from color and color infrared photographs obtained through joint efforts with the Waste Management Section. Inclement weather resulted in the cancellation of the color infrared portion of the mission until next year. The color photographs will be analyzed by two techniques to estimate species frequency and relative cover. One technique employs a miniature quadrat which is placed over a film transparency or print and viewed through a calibrated stage microscope. Numbers and diameters of overstory species are then measured directly from the photograph. Replicate measurements provide for statistical comparisons of areas. The second technique measures regions of equal color density on a photographic print or transparency. Vegetation type mapping is accomplished by utilizing the characteristic colors of various species which are electronically integrated to provide an estimate of relative ground cover. The initial map and ground truth data will be used to verify both of these new techniques.

Understory Vegetation Analysis

(M. J. Romine and L. E. Eberhardt)

Analysis of understory vegetation was begun in August 1974 as a part of the integrated ecological study of small mammals, carnivores, and vegetation along a 1500-m elevational gradient from the Rio Grande River to the Jemez Mountains and centered on the main canyons that receive liquid waste effluents that contain plutonium and other radionuclides. Data were completed in 6 of 11 selected study sites within the major vegetation types of the region. One site is within a subalpine meadow at an elevation of 2865 m, two are within each of the fir-aspen-spruce (2865 m) and ponderosa pine-fir (2560 m) vegetation types, and one is within the ponderosa pine/piñon-juniper (2256 m) vegetation type. One additional site will be located at 2256 m and two

within each of the piñon-juniper (1951 m) and juniper (1646 m) vegetation types.

A canopy coverage method of vegetation analysis was used in which two 20 x 50-m plots were located and permanently marked within small mammal trapping plots for integrated study purposes. Canopy coverage, frequency, and density of understory plant species were determined in forty 20 x 50-cm subplots located at 1-m intervals along one 50-m side of each major plot. Elevational differences in species numbers and community composition were also noted.

The results showed only a slight variation in species numbers at different elevations. There were 28 species at 2865 m in the fir-aspen-spruce vegetation type and 24 species in the subalpine meadow. The number decreased to 23 species at 2560 m in the ponderosa pine-fir vegetation type and to 21 species at 2256 m in the ponderosa pine/piñon-juniper vegetation type. However, considerable differences in species composition were noted, with 48% of the species at 2560 m not found at 2865 m and 86% of the species at 2256 m not found at 2560 m. The number of families represented decreased from 2865 m (17 families) to 2560 m (8 families) and 2256 m (9 families).

Values for canopy-coverage, frequency, and density were highest for species in the *Compositae* and *Graminae* families for all sites studied. These species are also of prime interest as vectors of radionuclides to herbivorous animals.

To supplement previous environmental resource data on the dominant overstory species for a 310-km^2 portion of Los Alamos County, including the 120 km^2 occupied by the LASL, vegetation collections of understory species within the five major vegetation types of the region (juniper, piñon-juniper, ponderosa pine-fir, and fir-aspen-spruce) and a subalpine meadow have been made. These data will be used to develop a map of understory species for the area. The collections include representatives of 36 families with 164 species. Examples of each species have been placed in the herbarium at LASL.

Species Diversity and Composition of Small Mammal Communities

(F. R. Miera, Jr., and L. E. Eberhardt)

An integrated ecological evaluation of small mammals, carnivores, and vegetation along a 1500-m elevational gradient from the Rio Grande River to the Jemez Mountains was begun to supplement the previous studies of LASL overstory vegetation and the ongoing intensive studies within the three major canyon ecosystems that contain varying amounts of plutonium and other radionuclides. Eleven sites were selected: 2 within each of the 5 major vegetation types of this region (juniper, piñon-juniper, ponderosa pine/fir, and fir-aspen-spruce) and 1 within a subalpine meadow.

The major objectives of this small-mammals study will be to determine species composition, diversity and preliminary indications of densities, movement patterns, and food habits in populations exposed to several radionuclides of interest. It is anticipated that these objectives can be obtained through the use of modified North American Census of Small Mammals (NACSM) trapping lines as proposed by Calhoun. This procedure consists of two parallel trap lines 80 m apart, with 20 stations per line and 10-m intervals between stations. Three Sherman live traps are placed at each station within a 3-m radius of the line. Traps are prebaited for 1 day, followed by 3 consecutive days of trap-mark-release procedures.

Small-mammal trapping in 5 of the 11 selected study sites has been completed. Trapping success ranged from 48% in the subalpine meadow to 32 and 34% at the two sites located in the fir-aspen-spruce vegetation zone and 28% in each of the two sites located in the ponderosa pine-fir vegetation zone. In 1800 trap nights for these 5 sites, a total of 609 captures were made, with 385 individual animals marked. Species composition for these sites included the least chipmunk (*Eutamias minimus*), deer mouse (*Peromyscus maniculatus*), montane vole (*Microtus montanus*), Gapper's red-backed mouse (vole) (*Clethrionomys gapperi*), Mexican woodrat (*Neotoma mexicana*), dwarf shrew (*Sorex nanus*), and immature cottontail rabbits (*Sylvilagus* spp). Numerous observations were also noted of the red squirrel (*Tamiasciurus hudsonicus*) in both vegetative zones.

The predominant species in the subalpine meadow was *M. montanus* which comprised 93.2% of all captured individuals. The only other species captured in the meadow site was *P. maniculatus*. Species composition for the fir-aspen-spruce vegetation zone consisted of *M. montanus* comprising 55% of the

captures, *P. maniculatus* (26.9%), *E. minimus* (9.9%), *C. gapperi* (4.7%), *N. mexicanus* (3.5%), and *S. nanus* (1.2%). An approximate 300-m decrease in elevation to the two sites located in the ponderosa pine-fir vegetation type resulted in *P. maniculatus* becoming the dominant species (72.3% of the individuals captured). Other species and their capture rate were *N. mexicanus* (13%), *E. minimus* (7.5%), *M. montanus* (3.2%), and *C. gapperi* (1.1%).

Specimens of each species trapped were collected for preparation as study skins and for food habits analysis. A more definitive study of data will be undertaken when trapping at all sites has been completed.

Radiotelemetry Study of Mammalian Predators

(L. E. Eberhardt)

Primary emphasis during the predator studies will be placed on their activities in low-level radioactive liquid waste disposal areas. However, considerable effort will be devoted to obtaining other basic biological information on the species involved.

Investigations into the feasibility of using radiotelemetry for studying the activities of predators such as coyotes (*Canis latrans*) and foxes (*Vulpes fulva* and *Urocyon cinereoargentatus*) residing within LASL boundaries were begun during August 1974. Field tests utilizing equipment and personnel provided by the Cedar Creek Biotelementry Laboratory of the University of Minnesota indicated that attenuation of radio signals by terrain features was considerably less than expected and that the reception ranges were entirely satisfactory.

Soils of the Los Alamos Scientific Laboratory

(J. W. Nyhan)

The physical and chemical characteristics of the alluvial soils in the canyon study areas were listed in our 1973 annual report. A formal soil survey of Los Alamos County was initiated in June 1974 by the U. S. Department of Agriculture Soil Conservation Service, the Forest Service, and LASL scientists. The final field identification of soils in the county was completed in November, and laboratory work is now in progress to characterize the physical, chemical, and hydrologic properties of over 300 soil samples. Final soil maps are being prepared, and about 60 newly characterized soil series with proposed names will be subjected to national review (via computer searches of national soil data banks) to ensure their unique identities. The results of this survey will provide a detailed data base for future radiation ecology studies, for engineering and waste management operations, for LASL environmental impact statements, and for urban planning in Los Alamos County.

National Environmental Research Park Proposal

(W. C. Hanson)

A National Environmental Research Park (NERP) is a protected outdoor laboratory where research may be carried out to achieve national environmental goals that were clearly expressed by the National Environmental Policy Act of 1969. Such a park would provide sites to develop ecological knowledge and to construct examples of manipulation so that the public can be informed as to the range of environmental options or land use practices available to them. Each of the 10 proposed or potential NERPs at USAEC installations is planned to develop into a regional environmental reference center which can serve its particular region of the United States. This coordination of AEC environmental efforts with other state and federal agencies is confirmed by Section 110 of the Energy Reorganization Act of 1974 (H. R. 11510). A proposal to designate LASL properties as a NERP received the approval of the LASL Director on 13 December 1973 and has subsequently been under consideration by AEC officials.

RADIATION ECOLOGY STUDIES

Honeybees as Biological Indicators of Radionuclide Contamination

(T. E. Hakonson and K. V. Bostick)

As an extension of previous studies of honeybees,[1] a study was conducted to assess the utility of honeybees as indicators of tritium (as HTO) released to the environment from a single source. Technical Area 33 (TA-33), which is located in the southeast corner of the Laboratory property, was chosen as the study area because relatively large amounts of tritium (~ 3500 Ci/yr) are released from a single stack to the atmosphere surrounding the facility. In addition, there were no other significant sources of tritium to the environment, either

gaseous, liquid, or solid, within at least 10 km of the stack at TA-33.

Samples of stack air, environmental air, vegetation, and soils were collected each week to relate the tritium concentrations in each sample type to corresponding data for bee and honey samples. Twelve sampling locations were established at various distances and directions from the stack based on wind speed and direction from TA-33, and 3 locations at distances of 0.46, 1.2, and 2.1 km from the stack were chosen for placement of honeybee colonies. Some tentative conclusions can be drawn from the limited amount of data which is available at this time. First, the rapid initial increase in tritium concentrations in bees which was observed in this experiment and in a previous study[1] demonstrated the ability of the insect to respond rapidly to changes in environmental tritium concentrations. A tritium elimination half-time of about 1 day, as measured previously, at least partly accounts for this ability. Second, there appears to be an inverse relationship between tritium levels in bees and the distance from the stack source. Defining this relationship has not been attempted as yet because factors such as atmospheric dilution of the effluent as a function of distance, tritium levels as probable sources of the radionuclide to bees (i.e., vegetation) and in soils as a function of distance, and worker bee foraging distances have yet to be considered. Finally, there appears to be little relationship between air concentrations of tritium and levels measured in honeybees, a finding which also was observed previously. If further analysis of the data substantiates this observation, then it would appear that air monitoring data would have little use in predicting tritium concentrations in nectivorous and perhaps herbivorous species.

REFERENCE

1. T. E. Hakonson and K. V. Bostick, Los Alamos Scientific Laboratory, unpublished data, 1974.

Radiation Ecology Studies of Canyon Liquid Waste Disposal Areas

(T. E. Hakonson, F. R. Miera, Jr., and J. W. Nyhan)

Radionuclide concentrations, particularly the isotopes of plutonium, were further studied at the 39 stations located in Acid-Pueblo, DP-Los Alamos, and Mortandad Canyons as previously described.[1] The maximum concentrations of plutonium in alluvial sediments occurred within 320 m of the respective effluent outfalls. Over 300 pCi ^{238}Pu/g (dry) was measured in Mortandad Canyon sediments, whereas 82 pCi ^{239}Pu/g and 54 pCi ^{239}Pu/g were the maxima for Acid-Pueblo and DP-Los Alamos Canyons, respectively (Table I).

There was an inverse relationship between the log transforms of plutonium concentration (pCi/g) and distance (m) post-outfall. Regression correlation coefficients (r) of -0.67 (n = 11), -0.74 (n = 9), and -0.90 (n = 9) for Acid-Pueblo, DP-Los Alamos, and Mortandad Canyons were all significant (α = 0.05). The data for Acid-Pueblo and DP-Los Alamos Canyons, along with environmental monitoring measurements,[1] demonstrated that plutonium has moved down the canyons during snow melt or rainfall runoff events.

A pronounced vertical migration of plutonium to sampling depths of 30 cm into the soils has occurred in all the canyons where seasonal or permanent surface water flows. The rate of plutonium migration into the soils under the semiaquatic conditions that exist in the canyons may be rapid, as evidenced by the complete mixing of ^{238}Pu to a 30-cm depth in Mortandad Canyon soils over a 4-year period. Additions of ^{238}Pu to this canyon began in 1968.

Considerable differences in plutonium concentrations between replicate sediment samples were indicated by the data. The coefficient of variation (CV = standard deviation/mean x 100) among triplicate samples was typically about 80%.

There appeared to be a distributional relationship between the ^{137}Cs and plutonium concentrations in post-outfall stream channel sediments from Mortandad and DP-Los Alamos Canyons. A least squares regression on the log transformed ^{137}Cs and plutonium concentration data from Mortandad Canyon yielded a correlation coefficient (r) of 0.91 for a sample size of 33. The ^{137}Cs vs plutonium regressions for DP-Los Alamos and Acid-Pueblo Canyons yielded an r of 0.74 (n = 25) and 0.31 (n = 26), respectively. Acid-Pueblo Canyon soils contained very little ^{137}Cs that can be attributed directly to Laboratory activities.[2]

Gamma exposure rates were measured with several types of survey instruments to investigate the

TABLE I

PLUTONIUM IN SEDIMENTS IN LIQUID WASTE RECEIVING CANYONS

Distance from Waste Outfall	Plutonium Concentrations (pCi/g dry) Acid-Pueblo Canyon Minimum	Maximum	Average	DP-Los Alamos Canyon Minimum	Maximum	Average	Mortandad Canyon Minimum	Maximum	Average
0	0.7	5.7	2.5 ± 2.8	22	54	38 ± 23	140	290	220 ± 70
20 m	1.0	3.0	2.0 ± 1.0	4	47	9.4 ± 24	3	310	180 ± 160
40 m	0.4	14.0	6.9 ± 6.8	0.2	2	0.6 ± 0.8	18	190	91 ± 90
80 m	0.4	82.0	50 ± 43	0.3	6	3.0 ± 3.0	19	77	48 ± 28
160 m	10.0	15.0	13 ± 3.5	0.4	1	0.8 ± 0.3	22	250	120 ± 120
320 m	9.0	13.0	12 ± 2.7	0.3	54	19 ± 31	5	47	24 ± 21
640 m	7.0	13.0	10 ± 3.0	0.5	1	1 ± 0.5	19	24	21 ± 2
1.28 km	2.0	3.0	2 ± 1.0	-	-	-	5	13	9 ± 4
2.56 km	0.03	0.6	0.4 ± 0.3	0.04	0.3	0.2 ± 0.1	3	26	11 ± 13
5.12 km	0.6	2.0	1 ± 0.7	0.1	0.8	0.4 ± 0.3	0.1	0.2	0.1 ± 0.1
10.24 km	0.1	0.3	0.2 ± 0.02	-	-	-	0.01	0.1	0.03 ± 0.02

TABLE II

PLUTONIUM VEGETATION IN LIQUID WASTE RECEIVING CANYONS

Distance from Waste Outfall	Plutonium Concentrations (fCi/g wet) Acid-Pueblo Canyon Minimum	Maximum	Average	DP-Los Alamos Canyon Minimum	Maximum	Average	Mortandad Canyon Minimum	Maximum	Average
0	-	-	-	5	6300	2100 ± 3600	26	2100	1000 ± 1100
20 m	230	3900	2100 ± 1800	0	44	22 ± 31	27	5200	1100 ± 2200
40 m	-	-	-	3	59	26 ± 29	7	150	57 ± 64
80 m	20	2600	1000 ± 1400	24	151	80 ± 65	37	2300	710 ± 1100
160 m	13	150	96 ± 74	8	65	28 ± 27	19	11 000	5400 ± 7700
320 m	50	130	91 ± 58	3	149	47 ± 69	-	-	-
640 m	24	500	200 ± 270	7	26	13 ± 8	9	170	52 ± 80
1.28 km	3	96	18 ± 34	-	-	-	2	24	9 ± 10
2.56 km	0	3	2 ± 2	2	17	7 ± 6	7	2	4 ± 2
5.12 km	1	200	38 ± 83	1	134	26 ± 48	5	20	10 ± 9
10.24 km	1	9	5 ± 4	-	-	-	0	4	2 ± 1

possibility of utilizing a field survey instrument for measuring ^{137}Cs and indirectly plutonium in stream channel soils. Exposure rates, which measured about 1 mr/h near the Mortandad and DP-Los Alamos Canyon effluent outfalls, were well correlated with the corresponding ^{137}Cs concentrations in soils from the two canyons. Correlation coefficients of 0.81 and 0.80 ($n = 11$) for DP-Los Alamos and Mortandad Canyons were significant at $\alpha = 0.01$. The external exposure rates in Acid-Pueblo Canyon were not correlated with soil ^{137}Cs concentrations due to the low levels of this radionuclide in the soil. Further studies relating to this finding are in progress. A positive relationship between ^{137}Cs and plutonium may provide information on the mechanisms of radionuclide movement in each of the canyons.

Plutonium and Americium in Vegetation. Plutonium concentrations in post-outfall vegetation samples measured 100 to 1000 times fallout plutonium levels in northern New Mexico vegetation and were about 1 to 0.001 times the concentrations/g of stream channel sediments (Table II). The vegetation-to-soil concentration ratios were somewhat higher

than values of 10^{-4} to 10^{-6} which are commonly reported for experimental plutonium plant uptake studies. However, the association of plutonium with canyon vegetation has not been defined and may represent a condition where root absorption and external deposition have both occurred.

Maximum plutonium concentrations in terrestrial vegetation were consistently measured in mosses, lichens, and grass species downstream from the outfall areas. Grass samples also contained the highest concentrations of ^{241}Am. The decline in plutonium and ^{241}Am concentrations in vegetation with distance post-outfall was similar to the pattern observed for plutonium in the alluvial soils. The lowest growth forms (i.e., grasses, lichens, and mosses) contained the highest plutonium concentrations. This observation was also noted for plutonium concentrations in Trinity Site vegetation and may be related to plant-surface area and mass or other physiological features.

Preliminary data on algae from the Mortandad Canyon stream channel indicated that concentrations of plutonium in this aquatic species can exceed 1 nCi/g.

Plutonium and Americium-241 in Rodent Tissues. The plutonium and ^{241}Am concentrations in rodent tissues were generally low, although individual tissues contained up to 8 pCi/g. Maximum concentrations in most tissues were found at the effluent outfall sampling locations and generally decreased with distance post-outfall (Table III). The pelt and lungs contained the highest average plutonium and ^{241}Am concentrations, indicating that resuspension is probably a major pathway for plutonium and ^{241}Am movement into canyon rodents.

The plutonium concentrations in various other animal species were extremely low or undetectable. Levels of plutonium in some or all of 9 mule deer (*Odocoileus hemionus*) averaged 0.36 ± 0.48 fCi/g muscle, 2.0 ± 1.9 fCi/g hide, 0.22 ± 0.12 fCi/g lung, 1.3 ± 0.76 fCi/g bone, and 2.1 ± 3.4 fCi/g kidney. Concentrations of plutonium were also very low in coyotes (*Canis latrans*), ravens (*Corvus corax*), and Steller's jays (*Cyanocitta stelleri*).

Plutonium Activity Ratios in Canyon Samples. The ^{238}Pu/^{239}Pu activity ratios in the various sample types were, in most cases, indicative of the canyons from which the samples were obtained. The activity ratios in Mortandad Canyon sediments, vegetation, and rodent samples were 3.6 ± 1.8, 3.0 ± 3.5, and 4.6 ± 4.3, respectively. Ratios for Acid-Pueblo Canyon samples averaged 0.06 ± 1.6, 0.32 ± 0.55, and 2.0 ± 3.0; DP-Los Alamos Canyon ratios averaged 0.19 ± 0.12, 0.77 ± 1.5, and 0.58 ± 1.2. The waste disposal histories of the three canyons have been quite different. Acid-Pueblo Canyon during a 20-yr period from 1943 to 1964 received primarily ^{239}Pu contaminated effluent, while DP-Los Alamos Canyon during a

TABLE III

PLUTONIUM IN RODENTS IN LIQUID WASTE RECEIVING CANYONS

Canyon and Distance from Waste Outfall	Total Plutonium Concentration in Soft Tissues (fCi/g wet)											
	Liver			Lungs			Hide			Carcass		
	Min.	Max.	Average	Min.	Max.	Average	Min.	Max.	Average	Min.	Max.	Average
Acid-Pueblo												
0	4	91	27 ± 43	0	41	25 ± 18	67	226	144 ± 80	0.4	55	20 ± 24
2.6 km	0	200	24 ± 47	0	619	67 ± 150	11	215	32 ± 50	0	14	4 ± 4
10.2 km	1	16	4 ± 5	3	38	25 ± 18	4	82	32 ± 29	0.4	3	1 ± 1
DP-Los Alamos												
0	2	110	27 ± 32	0	110	24 ± 27	72	680	310 ± 200	0	310	51 ± 75
2.6 km	0	20	9 ± 10	0	86	30 ± 38	2	44	19 ± 16	0	15	6 ± 7
Mortandad												
0	9	66	33 ± 24	19	1500	460 ± 710	66	1500	790 ± 520	0.2	100	39 ± 44
2.6 km	0	26	10 ± 9	18	6000	840 ± 2100	4	710	100 ± 240	0	15	3 ± 5
10.2 km	0	210	33 ± 68	0	7800	1100 ± 2500	4	6300	500 ± 1700	0.1	92	10 ± 25

20-yr period (1952 to present) received a combination of $^{238}Pu/^{239}Pu$ contaminated effluents which currently averages about 50% ^{239}Pu of total activity. Mortandad Canyon during a 10-yr period (1963 to present) also received a mixture of $^{238}Pu/^{239}Pu$ which for 1973 averaged 92% ^{238}Pu.

Information relating to the physical transport of radionuclides down Mortandad Canyon was obtained on September 15 following a rainfall of 3.8 cm on the upper Mortandad Canyon watershed that resulted in a total estimated discharge of 3530 m^3 (3.53 x 10^6 liters) of water. Samples of water were collected through the subsequent 4.5 h runoff event to relate the radioactivity transported by the event to the aqueous and suspended particulate fractions. In addition, measurements on stream velocity and channel cross-sectional area in conjunction with the radionuclide data provided sufficient data to estimate the total radioactivity transported by the runoff event.

The ^{137}Cs concentrations in water and suspended sediment fraction for samples collected within 10 cm of the stream surface are presented in Fig. 1 along with suspended sediment concentrations in water (g/liter). The remaining curve in Fig. 1 was obtained by multiplying the suspended sediment concentration (g/liter) by the ^{137}Cs concentration in the sediment (pCi/g) to provide a means of comparing the fractional distribution of the ^{137}Cs between the aqueous and particulate phases. Concentrations of ^{137}Cs in the suspended sediments were relatively high and uniform throughout the entire runoff event. The concentrations ranged from about 200 pCi/g to 600 pCi/g. Concentrations of ^{137}Cs in soils at 8 sampling locations upstream from the water collection site ranged from about 100 pCi/g to 3000 pCi/g during 1972. An estimated transport of about 7 mCi ^{137}Cs occurred during the runoff event. A ^{137}Cs inventory of about 200 mCi was estimated from 39 soil cores from Mortandad Canyon collected in 1972. Assuming that the inventory estimate was realistic, the runoff event resulted in the redistribution of about 3% of the total ^{137}Cs inventory. Observations on the leading edge of the runoff stream verified that the runoff and its associated radioactivity were not leaving site boundaries.

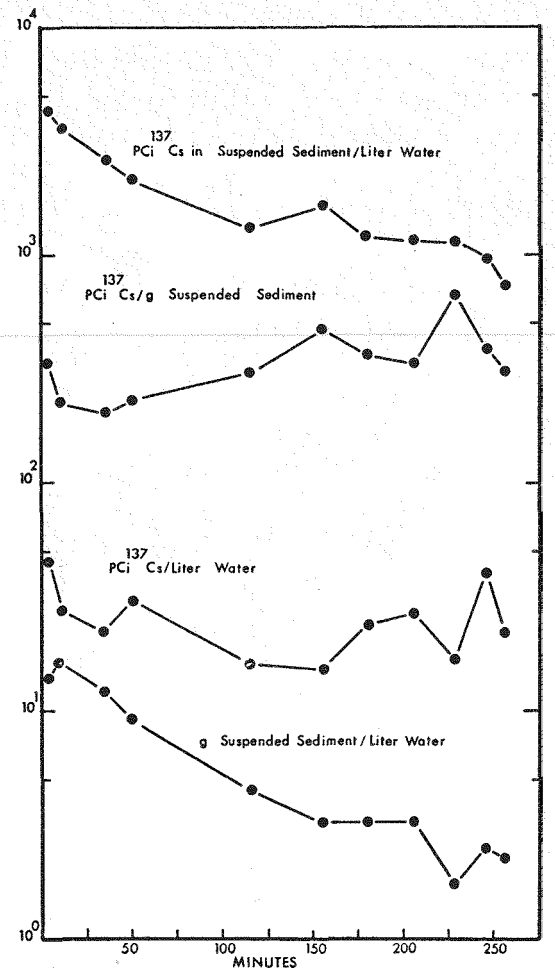

Fig. 1. Cesium-137 concentrations in water and suspended sediment fractions of Mortandad Canyon runoff stream water following a 3.8-cm rainfall event on September 15, 1974.

REFERENCES

1. T. E. Hakonson, J. W. Nyhan, L. J. Johnson, and K. V. Bostick, "Ecological Investigations of Radioactive Materials in Waste Discharge Areas at Los Alamos for the Period July 1, 1972, through March 31, 1973," Los Alamos Scientific Laboratory report LA-5282-MS (1972).

2. K. J. Schiager and K. E. Apt, "Environmental Surveillance at Los Alamos during 1973," Los Alamos Scientific Laboratory report LA-5586 (1974).

Small-Mammal Studies in Los Alamos Liquid Waste Disposal Areas

(F. R. Miera, Jr.)

Density estimates of small mammals are essential to understanding annual cycles and fluctuations, abundance, distribution in relation to vegetation and soil types found within the various life zones, food habits, reproduction and sex ratios, and the

presence of ectoparasites. These topics are fundamentally related to animal population performance within the liquid waste disposal areas. Trapping results will ultimately be combined with the plant and soil surveys now in progress to better define the biotic associations found in contaminated and uncontaminated areas of the LASL environs.

Results for this report were completed from 11 intensive small-mammal study sites during May and June 1974 in Mortandad (M), DP-Los Alamos (DP), and Acid-Pueblo (AP) Canyons. Eight of the sites were selected on the basis of relative radionuclide (especially $^{238,239,240}Pu$) concentrations, and 3 sites, one in each canyon system, were controls (BKG).

Due to terrain, habitat, and the fact that most concentrations of radionuclides are confined primarily to the stream channels, a modified grid with dimensions of 25 m perpendicular to the stream channel by 100 m parallel to the stream channel was employed and permanently marked. Two stations were located on both banks of the stream channel approximately 5 m apart and one station 10 m from the bank on each side. Stations parallel to the stream channel were separated by a distance of 10 m, giving a trapping grid of 4 by 11 stations. Two Sherman live traps were placed at each station, giving a total of 88 traps per site. Small-mammal trapping was conducted through the entire series on a schedule of 2 days of prebaiting (traps closed), followed by 5 consecutive days of trap-mark-release procedures. The animals were marked by a standard system of toe amputation.[1] Data recorded on all captures included station number where caught, genus and species, sex, age class, reproductive condition, and weight.

A total of 5544 trap nights for all sites yielded 886 total captures of 432 different animals (Table I), of which approximately 200 were collected for radionuclide and food habit analyses. Because the animals were collected on almost all trapping days in an attempt to ensure a sufficient number of samples for analysis, an accurate estimate of trapping success (number of animals caught/number of traps open) cannot be calculated at this time.

In all, 10 species of mammals were captured with the predominant species at most sites being the piñon mouse (*Peromyscus truei*) (37.9% of total individuals captured), deer mouse (*P. maniculatus*) (14.7%), *Peromyscus* spp. juveniles (6.8%), western harvest mouse (*Reithrodontomys megalotis*) (6.3%), least chipmunk (*Eutamis minimus*) (30.4%), and the meadow vole (*Microtus pennsylvanicus*) (2.3%). Other species trapped included the Mexican woodrat (*Neotoma mexicana*), dwarf shrew (*Sorex nanus*), valley pocket gopher (*Thomomys bottae*), rock squirrel (*Spermophilus variegatus*), and one immature cottontail rabbit (*Sylvilagus* spp.). Several tassel-eared or Abert squirrels (*Sciurus aberti*) were noted through field observations.

TABLE I

TRAPPING EFFORT (RESULTS AND TOTAL BIOMASS ESTIMATES) AT SMALL-MAMMAL STUDY SITES DURING MAY AND JUNE 1974

Location	Trap Nights	Total Individuals Captured	Total Biomass (g/m^2)[a]
M-BKG	528	72	0.55
M-I	440	49	0.32
M-II	528	65	0.54
M-III	440	25	0.10
DP-BKG	616	36	0.37
DP-I	704	26	0.14
DP-II	440	43	0.34
AP-BKG	528	23	0.19
AP-I	352	34	0.35
AP-II	528	30	0.20
AP-DP-III	440	29	0.29
Total	5544	432	

[a]Total biomass calculated for all individuals captured at the site.

Approximately 70% of *P. truei* were captured more than once, while *P. maniculatus*, *E. minimus*, and *R. megalotis* were recaptured at frequencies of 56, 48, and 37%, respectively. *Peromyscus truei* and *E. minimus* were caught at all sites but one and *P. maniculatus* at all but four sites. *Reithrodontomys megalotis* were caught at only 4 of the 11 sites.

With the exception of *E. minimus*, of which an equal number of males and females were caught, the sex ratios of *P. truei* and *P. maniculatus* were in favor of females (Table II). This was considered unusual for *Peromyscus* spp. when compared to other reported studies. The standard error for the mean

TABLE II

SEX RATIOS, WEIGHTS, AND MOVEMENTS BETWEEN CAPTURES AND BIOMASS ESTIMATES FOR FOUR SPECIES AT SMALL-MAMMAL STUDY SITES DURING MAY AND JUNE 1974

Location	Sex Ratio M:F[a]	$\bar{x}$ Ad. Weight (g) M	$\bar{x}$ Ad. Weight (g) F	$\bar{x}$ Distance between Captures (m)	Biomass (g/m^2)
Peromyscus truei					
M-BKG	11:16	20.2 (0.65)[b]	20.6 (0.55)	18.3 (2.7)[b]	0.14[c]
M-I	20:19	21.7 (0.39)	22.0 (0.83)	14.4 (3.4)	0.22
M-II	13:19	22.4 (0.6)	24.0 (0.68)	11.6 (2.29)	0.19
M-III	-	--	--	--	--
DP-BKG	7:7	22.9 (0.33)	23.1 (1.53)	10.3 (1.93)	0.08
DP-I	1:1	--	--	--	0.01
DP-II	5:4	21.7 (0.78)	22.6 (1.47)	--	0.05
AP-BKG	5:4	21.1 (0.92)	26.6 (0.83)	--	0.07
AP-I	5:5	22.1 (0.82)	23.3 (1.29)	--	0.07
AP-II	5:6	22.4 (0.17)	22.6 (0.78)	--	0.08
AP-DP-III	3:5	25.6 (1.15)	25.8 (0.86)	21.0 (6.3)	0.06
Peromyscus maniculatus					
M-BKG	11:6	17.7 (0.51)	16.7 (1.33)	17.0 (3.14)	0.08
M-I	2:2	--	--	--	0.02
M-II	5:7	18.6 (0.35)	24.6 (0.74)	--	0.07
M-III	10:10	17.3 (0.45)	16.3 (0.52)	--	0.09
DP-BKG	-	--	--	--	--
DP-I	1:4	--	16.2 (0.16)	--	0.02
DP-II	1:2	--	--	--	0.01
AP-BKG	0:1	--	--	--	0.01
AP-I	-	--	--	--	--
AP-II	-	--	--	--	--
AP-DP-III	-	--	--	--	--
Eutamis minimus					
M-BKG	13:5	57.4 (1.26)	59.2 (2.49)	32.5 (4.08)	0.27
M-I	2:3	--	--	--	0.07
M-II	5:6	55.2 (2.36)	57.6 (3.19)	--	0.16
M-III	-	--	--	--	--
DP-BKG	14:6	59.1 (1.07)	65.5 (4.84)	--	0.28
DP-I	0:2	--	--	--	0.03
DP-II	8:12	58.2 (1.33)	64.2 (1.83)	25.0 (6.14)	0.24
AP-BKG	3:5	--	60.9 (4.06)	--	0.12
AP-I	1:10	53.5 (0.86)	66.9 (3.58)	--	0.28
AP-II	1:5	--	60.5 (2.9)	--	0.10
AP-DP-III	8:11	56.3 (3.06)	61.2 (3.85)	--	0.23
Reithrodontomys megalotis[d]					
M-BKG	-	--	--	--	--
M-I	-	--	--	--	--
M-II	-	--	--	--	--
M-III	3:2	10.7 (0.85)	9.9 (1.85)	--	0.01
DP-BKG	-	--	--	--	--
DP-I	7:4	11.4 (0.33)	11.1 (0.83)	--	0.03
DP-II	2:1	--	--	--	0.01
AP-BKG	-	--	--	--	--
AP-I	-	--	--	--	--
AP-II	5:2	12.4 (0.45)	--	--	0.02
AP-DP-III	-	--	--	--	--

[a] Sex ratio includes all age individuals captured.

[b] Standard error of the mean values in parentheses: S.E. = standard deviation/$\sqrt{n}$.

[c] Biomass calculated for all individuals of that species captured.

[d] Insufficient data were available for computing $\bar{x}$ distances between captures.

weights of adult *Peromyscus* was much larger for females than males and was attributed to the presence of pregnant females and varying sample sizes. Approximately 43% of *P. truei* females and 22% of *P. maniculatus* females were judged to be pregnant at the time of capture. Additionally for *E. minimus*, the presence of yearlings in the populations also contributed to a larger standard error of the mean adult weights.

Table II also lists minimal biomass estimates, all based on live weights of individuals captured for each of the 4 major species, and total estimate for each site is given in Table I. The data indicate that the highest rodent densities and mass were generally associated with the ponderosa pine/piñon-juniper woodland and were lowest in the piñon-juniper woodland. This was the reverse of previous snap-trapping data obtained during 1972.[2] In Mortandad Canyon, an approximate 120-m decrease in elevation over a 4000-m horizontal distance corresponded to more than a 5-fold decrease in combined rodent mass. However, such dramatic decreases were not as evident in the other two canyon systems. Low densities recorded at site locations DP-1 and AP-BKG can be attributed, in part, to the large number of traps sprung by predators.

Movement patterns were calculated, where data were available, as mean distances between captures for at least 3 adult individuals of each species captured a minimum of 4 times. Data for both males and females were combined for all species. At site M-BKG, data from 8 *P. truei* were used in the calculation, with 6, 12, 4, and 4 individuals used at M-I, M-II, DP-BKG, and AP-DP-III sites, respectively. Data for only 3 individuals of *P. maniculatus* were obtained from M-BKG site. Data for 5 individuals at site M-BKG and 3 individuals from site DP-II were used in the calculations for *E. minimus*. Because of the manner in which the grid was established, mean distance movements represent a measure of movement parallel to the stream channel and cannot be interpreted as movement perpendicular to the stream channel. More trapping data are needed along with employment of trapping techniques[1,3] designed specifically for measuring movement patterns before we can judge the present data as being accurate.

Both *P. truei* and *E. minimus* were captured at all sites but one, indicating that they are distributed through most canyon systems. *Peromyscus maniculatus* and *R. megalotis* were generally associated with habitats having dense stands of grasses and forbs as was also concluded from the 1972 trapping data.

REFERENCES

1. D. H. Brant, "Measures of the Movements and Population Densities of Small Rodents," Univ. Calif. Publ. Zool. 62, 105-184 (1962).

2. T. E. Hakonson, J. W. Nyhan, L. J. Johnson, and K. V. Bostick, "Ecological Investigation of Radioactive Materials in Waste Discharge Areas at Los Alamos for the Period July 1, 1972, through March 31, 1973," Los Alamos Scientific Laboratory report LA-5282-MS (1972).

3. M. H. Smith, R. Blessing, J. C. Chelton, J. B. Gentry, F. B. Golley, and J. T. McGinnis, "Determining Density for Small Mammal Populations Using a Grid and Assessment Lines," ACTA Theriologica 16(B), 105-125 (1971).

Small-Mammal Population Densities and Composition at Trinity Site

(F. R. Miera, Jr., and T. E. Hakonson)

In October 1974, trapping grid networks were permanently marked at the four sites which had previously been selected in September 1973 at Trinity Site.[1] A combined total of 1560 trap nights for all sites yielded 6 species and 32 animals captured. Only a single Ord kangaroo rat (*Dipodomys ordii*) was collected at the control site. Species caught at the remaining 3 sites, along with *D. ordii*, included the Merriam kangaroo rat (*D. merriami*), bannertail kangaroo rat (*D. spectabilis*), northern grasshopper mouse (*Onychomys leucogaster*), silky pocket mouse (*Perognathus flavus*), piñon mouse (*Peromyscus truei*), and spotted ground squirrel (*Spermophilus spilosoma*). *Perognathus flavus* (9.3% of the total individuals captured) and *D. merriami* (3.1%) were captured solely at GZ site and *S. spilosoma* (12.5%) only at the site 16 km northeast of ground zero. *Peromyscus truei* (6.6%) were captured at GZ site and the 50-km site. *Dipodomys spectabilis* (9.3%) were captured at the 16- and 50-km sites. *Dipodomys ordii* (28.1%) and *O. leucogaster* (31.3%) were captured at the 3 sites.

Biomass estimates based on live weights ranged from 0.02 g/m^2 at GZ site to 0.07 g/m^2 at the 16-km site and 0.04 g/m^2 at the 50-km site. Data were insufficient at the control site to estimate biomass.

Rodent biomass differences between the sites will be correlated in future reports with data on vegetation densities, frequencies and biomass, soil types, and the more obvious factors attributable to elevational differences between sites. Specimens collected are awaiting radionuclide analysis.

REFERENCE

1. C. R. Richmond and E. M. Sullivan, eds., "Annual Report of the Biomedical and Environmental Research Program of the LASL Health Division, January through December 1973," Los Alamos Scientific Laboratory report LA-5633-PR (May 1974).

Distribution of Plutonium in Trinity Soils

(J. W. Nyhan and F. R. Miera, Jr.)

In October 1973, 4 permanent study sites were established in the Trinity Site environs, as described in our 1973 annual report. On the basis of the results of plutonium analyses on the 1972 transect samples, a set of 12-60 cm soil cores were obtained from each site and cut up into 0-2.5, 2.5-5.0, 5.0-10, 10-15, 15-20, 20-25, 25-32.5, 32.5-40, and 40-60 cm segments. Two soil cores were taken at each corner of these hectare plots, and the 4 soil cores taken in the center of the plot were composited by depth and 6 soil separates obtained for each composite soil sample (resulting in samples with particle diameter ranges of < 53 μm, 53-105 μm, 105-500 μm, 500-1000 μm, 1-2 mm, and 2-23 mm).

Although the plutonium analyses on this set of 1973 samples are currently incomplete, several observations can be made about the distribution of plutonium at the intensive sites. The plutonium in Trinity soils was initially deposited on the soil surface and was found to be almost exclusively confined to the top 2.5 cm of soil 21 yr ago. The 1973 plutonium data show that 76 and 53% of the ^{239}Pu inventory at G2 and 21 sites, respectively, occurred at the 5-25 cm depth. This represents a substantial redistribution of the plutonium with increased exposure to the environment and under conditions where only one detonation occurred 28 yr ago. A one-way analysis of variance of the plutonium data from the four corners of the sites showed no significant differences in plutonium concentrations between corner locations within these sites per soil depth. However, a similar statistical analysis of the plutonium concentrations per soil depth indicated significant decreases in ^{239}Pu concentrations at 21 site at the 0-2.5, 2.5-5.0, and 5.0-10 cm depths (2.0, 1.0, and 0.2 pCi/g, respectively). Except for these differences, plutonium concentrations at all other soil depths were found to be statistically similar. This was mainly due to the large natural variation of plutonium in these samples, which exhibited coefficients of variation 0.5 to 1.0 in the surface horizons and of 1.4-1.8 with increased soil depth.

In 1974, Raymond Neher of the USDA Soil Conservation Service identified the soils of the background and G2 site as being the Dona Ana sandy loam and the soils at the 10 and 21 sites as being LaLande sandy loam and the Rance loam, respectively. In addition, a second set of samples were taken to 30 cm, similar to those taken in 1973, and a water-leaching experiment was carried out in the field to determine the extent of plutonium leaching with the application of water in amounts equal to 1 yr of precipitation.

Waste Disposal Canyon Intensive Site Studies

(T. E. Hakonson, J. W. Nyhan, and K. V. Bostick)

The data obtained from the 1972 and 1973 soil and vegetation samples were used as a basis for selecting 9 intensive study sites in the three canyons. The establishment of these sites represented a shift in the emphasis of the canyon studies from the previous transuranic inventory-type annual samplings to experimental designs involving fewer, more intensively sampled field locations. The objectives were to determine plutonium variability in ecosystem components and to observe seasonal changes in radionuclide concentrations in the soils and biota at each site.

Each site consists of a 100 x 20-m plot bisected longitudinally by a waste disposal stream. Ten randomly selected sampling locations were chosen at each site in May, and 0.25-m^2 vegetation plots were harvested at each location. Stems and leaf sheaths were clipped to within 3 cm of the soil surface, and the litter layer was also harvested; these 90 samples were frozen and sorted in the laboratory into 3 subsamples: green grasses, green forbs and shrubs, and non-green plants. Four soil cores (30 cm in length by 2.5 cm in diameter) were then collected within the clipped vegetation plot on the stream bank, and one soil core was taken in the center of the stream

channel in front of each vegetation plot. The sets of 4 soil cores taken in the vegetation plots were composited later, and the stream channel cores were cut up into 0-7.5 and 7.5-30 cm segments in preparation for radionuclide analysis. In addition, FIDLER measurements were taken at each site in the stream channel sampling locations. Radionuclide determinations were initiated on these samples, and a second set of samples was taken in December similar to those obtained in May.

An additional set of soil and vegetation samples was collected in May at the intensive sites to determine concentration gradients of radionuclides across the canyon sites (i.e., from mesa top to mesa top). These data will allow us to develop improved sampling procedures, to document what proportion of the radionuclide inventory is contained in the stream channel and nearby soils and biota, and to determine regional levels of fallout in the ecosystem components. Thus, one set of 60-cm soil cores was obtained from each half of the intensive site at locations of 0.02, 0.1, 0.2, 0.5, and 10 m from the stream channel, as well as on the adjacent mesa tops. These 12 cores were frozen and cut up into 0-10, 10-20, 20-40, and 40-60 cm segments for each site. Vegetation plots were harvested, as described previously, at locations of 0-0.25, 0.25-0.5, and 10.0-10.25 m from the stream channel on each side of the intensive study site.

Rio Grande River Studies

(T. E. Hakonson and W. C. Hanson)

A third series of fish and sediment samples were collected at each of the major canyons draining the Los Alamos area as part of a continuing effort to document radionuclide levels in the Rio Grande River below the LASL. A sediment core sampling technique was employed to provide a more quantitative basis for comparing future samples. The fish collected included 5 species of herbivores and 2 species of carnivores. In 1973, catfish, northern pike, and largemouth bass were introduced into the Cochiti Reservoir about 32 km downstream from the LASL; this indicates an intended use of the area by fishermen and increased food-chain considerations.

Concentrations of plutonium in sediments collected in September 1973 were near the analytical detection limits (0.05 pCi/sample). The levels of plutonium in 13 samples ranged from non-detectable to 0.009 pCi/g, which compares to concentrations of 0.001 to 0.1 pCi/g for several background radioactivity sediments.

Cesium-137 was undetectable in 23 pooled samples of fish. The analytical detection limit was 160 pCi ^{137}Cs/kg wet weight for a 50-g sample during an 83-min count time. The samples are being recounted for a longer time to better estimate the ^{137}Cs concentrations.

ALASKAN ARCTIC ECOSYSTEM STUDIES

Ecological Investigations of Alaskan North Slope Oil Field Development

(W. C. Hanson and L. E. Eberhardt)

Investigations are being conducted in 3 areas related to Alaskan petroleum development: (1) the cultural implications of oil field development on the natives of northern Alaska, especially the people of Anaktuvuk Pass; (2) continuation of ecological studies conducted during the summers of 1971, 1972, and 1973 on the birds and mammals of the Gas Arctic-Northwest Project Prudhoe Bay Test Site; and (3) the ecology of the Arctic and red fox populations along the North Slope oil pipeline route. These studies are a natural extension of the long-term interest of the USAEC in northern Alaska that began with the 1959 initiation of Project Chariot.

Work on the current project was begun in July 1974. Because of the shortness of the northern Alaskan field season, the late date of funding, and the difficulties involved in arranging for suitable field quarters, little actual field work was accomplished. Major effort was made in contacting the several private, state, and federal agencies that have responsibility for oil-related activities in northern Alaksa.

Cultural Implications of Oil Development on Alaskan Natives. These studies will center on the inland Eskimos of Anaktuvuk Pass, where cultural information has been recorded continuously since 1962 in connection with radiation ecology studies.[1] Earlier periods of cultural change occurred in connection with major contact with white man prior to 1950 and were considered slow and gradual changes until 1964, when the snowmobile was introduced into the culture. Since then, an accelerating rate of cultural change has continued to modern times.

The recent Alaskan Native Land Claims Settlement Act and the prospect of revenue to be derived from the North Slope oil development have escalated social change within the *nunamiut* society and will be the subject of this research. Contact has been re-established with the Eskimos in the new context of these studies, and related radiation ecology studies will be centered at Anaktuvuk Pass.

Ecological Studies of Birds and Mammals of the Gas Arctic-Northwest Project Prodhoe Bay Test Site. An intensive ecological study of birds and mammals in the vicinity of Prudhoe Bay, Alaska, was conducted during the summers of 1971, 1972, and 1973 and is summarized elsewhere.[1,2] These studies described the resident bird and mammal populations of the local area and investigated the beneficial and detrimental effects of the construction and operation of a natural gas pipeline test loop in permafrost environments.

Because of the wealth of information generated by the above studies, additional investigations are planned during 1975 to evaluate the long-term ecological effects of the pipeline loop and to obtain additional information on the local populations of birds and mammals, especially the Arctic fox and lemmings. Permission was obtained to use the past data and the test site facilities in conjunction with our future studies, making a substantial contribution to the program.

Ecology of the Arctic and Red Fox along the North Slope Oil Pipeline Route. Foxes were selected for intensive study along the North Slope oil pipeline route because (1) they are an important and relatively abundant carnivore of the region transversed by the pipeline and are closely dependent upon small mammals and birds that may be affected by oil development activities; (2) there is a widespread but unsubstantiated opinion that red foxes are displacing the more commercially valuable Arctic foxes in certain areas of the North Slope and that alternation of the habitat by pipeline activities may have substantial effects upon the relationships of these species; (3) foxes have important relationships with human activities from the standpoints of their being a fur resource, their destruction of equipment related to petroleum exploration and development, the functioning of the fox population as a reservoir of rabies, and the attraction of foxes to human habitation, which will be particularly important once the pipeline haul-road is opened to the public; and (4) there is little information presently available on the ecology of the two species in northern Alaska.

A portion of the study has been subcontracted to the University of Alaska Wildlife Research Unit. Responsibility has been divided into two broad categories: (1) the basic biology of the two fox species will be investigated by the University of Alaska; and (2) the LASL personnel will determine and monitor population densities and movements of both species along the pipeline route. Both groups of investigators will examine the interrelationships between oil development activities and fox populations.

Limited observations made by University of Alaska investigators indicate that the fox populations along the North Slope oil pipeline route are at or near a cyclic low. In addition, it appears that the removal of gravel from river beds for the construction of roads and other pipeline-related facilities may adversely affect some denning sites of the red fox; seven dens were located in the Sagwon-Franklin Bluffs study area during the period of August 8 to September 3, 1974. Information was obtained from construction personnel on the relative abundance of foxes in several areas to optimize future field operations.

REFERENCES

1. W. C. Hanson, "Fallout Strontium-90 and Cesium-137 in Northern Alaskan Ecosystems during 1959-1970," Colorado State University report COO-2122-12 (May 1973).

2. W. C. Hanson, "Ecological Studies of Birds and Mammals of the Gas Arctic/Northwest Project Prudhoe Bay Test Site, Summers 1971 and 1972," Consultant report (October 1972).

3. W. C. Hanson, "Ecological Studies of Birds and Mammals of the Gas Arctic/Northwest Project Prudhoe Bay Test Site, Summer 1973," consultant report (October 1973).

Radiation Ecology Studies of Northern Alaska

(W. C. Hanson)

Funding for this program began in July 1974 and was originally planned to be conducted in cooperation with Battelle Memorial Institute's Pacific Northwest Laboratory. However, the entire program

was transferred to LASL following the 1974 summer season. All samples collected in northern Alaska and Greenland during the period 1962 to 1974 were transferred via truck, and the remaining samples and data will be gradually transferred over the next 6 months.

Calibration counts of lichen samples were made with standard samples measured at Battelle-Northwest, Colorado State University, and LASL to assure data compatibility. A limited number of lichen samples were collected during September 1974 at long-term study sites at Anaktuvuk Pass. These are now being meticulously sorted into the populations (lichen species, litter, and vascular plants) that compose the lichen community that is typified by the dominant lichen species.

Initial plutonium analyses were performed on selected samples of 1971, 1972, and 1973 lichens collected at Anaktuvuk Pass, Prudhoe Bay, and Cape Thompson sites. Average concentrations of 0.3 pCi ^{239}Pu/g dry weight were found in *Cladonia* and *Cetraria* species, with a ^{238}Pu/^{239}Pu ratio nearly constant at 0.06. Considerable variation occurred in the values obtained in other species and in other community components, suggesting that substantial analyses remain to be done to clarify the plutonium fractionation phenomena in arctic lichen communities.

About 40 lichen community samples of the Thule, Greenland, environments were obtained during participation in a Danish scientific resurvey of that area in August 1974. These community samples are now being separated into their population components for comparison between species, locations, and with similar 1968 samples.[1] These samples provide a broad spectrum of comparisons of transuranic element behavior in ecosystems varying from the hot desert environments of the Trinity Site to the cold deserts of the Arctic Zone.

A cooperative study with Battelle-Northwest to evaluate various sources of radiation exposure to Alaskan Eskimos was continued to finalize the observations of chromosomal aberrations noted in Anaktuvuk Pass residents during February and August 1969. Battelle scientists are calculating the radiation doses received from natural and worldwide fallout radionuclides by the study subjects, while LASL cooperators evaluate medical x-ray exposures received by the people during treatment for tuberculosis and other complaints. Medical records were examined at the Alaska Native Health Service in the Fairbanks and Tanana hospitals, and a relatively few records remain to be evaluated at the Anchorage and Kotzebue hospitals.

REFERENCE

1. W. C. Hanson, "Plutonium in Lichen Communities of the Thule, Greenland Region," Health Phys. 22, 39-42 (1972).

ATMOSPHERIC TRANSPORT STUDIES

Terrain Influence on Low-Level Meteorological Transport

(S. Barr, W. Clements, and D. Dahl)

The early phases of the complex terrain meteorology project have been devoted to organization and fundamental problem identification, scoping, and planning. An important basis of approach into the rather complicated problems of terrain influence is the balance of modeling and field experiments. Personnel were recruited to provide the field experiment capability, as well as augmenting an existing capability in model development.

A considerable amount of effort has been devoted to defining problems which arise from real, practical requirements and which can be fruitfully addressed in the early stages of analysis. Study of the mechanics of canyon flows, including turbulence structure as it affects contaminant transport and dispersal, is the focus of present efforts. The transport within narrow steep-walled canyons is one of the pragmatic problems in safety and environmental considerations at LASL and in all mountainous terrain wind fields. The present program will approach such a building block first, then build on it through canyon-mesa interactions, sub-regional ensembles of canyon-ridge-mesa-valley units, and finally to whole regions ($\sim 10^5$ km^2). With limited equipment, the canyon offers a limited domain and, hence, is an ideal starting place for a few carefully selected measurement locations. In addition to planning, the assembly of useful analytical tools has been a vital part of the early phases of study. These tools include instrument and instrument-array concepts, theoretical models, and computational methods.

The initial problems in transport and dilution in complex terrain center around the fundamental

questions of inhomogeneity of the mean wind and turbulence fields. The terrain plays a dual role as a complicated obstacle in a free-stream flow and as a source of local temperature gradients which give rise to gravity flows. In both cases, the geometric considerations tend to make analytical approaches intractable. Also, particularly in the obstacle flow case, the non-linearity of the governing equations forces the use of numerical models for studies of the mean wind structure.

One of the most promising class of models available for the present applications is the finite difference formulation based on a full set of viscous, non-linear, fluid-flow equations. Updated versions of the marker and cell technique have been tested in a series of numerical experiments aimed at explaining observed wind profile anomalies in cross mesa flow. Figure 1 is an example of the calculations of flow over a series of simplified obstacles including the mesa at the site of the meteorology tower (see Fig. 1d). A detailed description of the

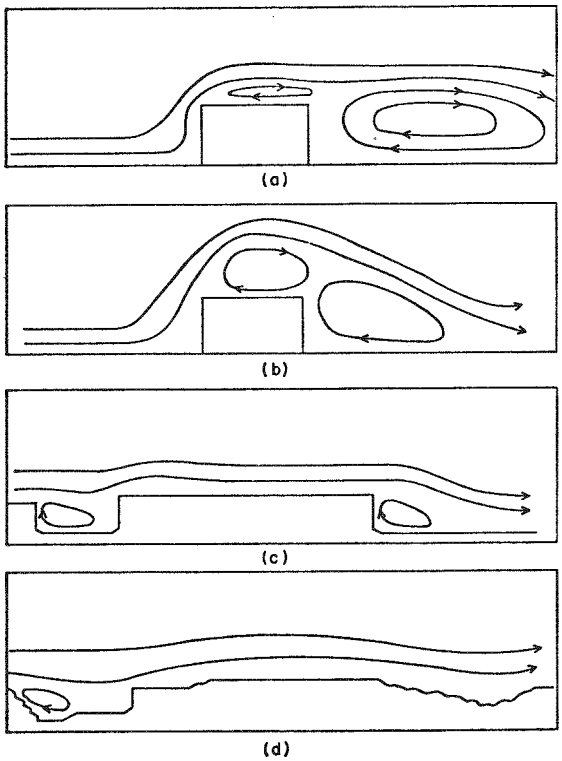

Fig. 1. Sample calculated steady flows for a variety of boundary conditions: (a) flow over a simple rectangle, constrained to be horizontal at the upper boundary; (b) same as (a) except unconstrained upper boundary; (c) flow over terrain with exaggerated sharp edges; and (d) flow over terrain observed at Los Alamos.

study is included in a typical report in progress. An extension of the strictly two-dimensional formulation is the so-called "shallow water theory" which represents the third dimension in an integral sense. This type of model is useful for terrain flows when the vertical direction is taken as the integrated dimension and horizontal velocity fields are calculated explicitly. A version of a code with this capability was recently made available.

The estimates of distribution of hazardous material include, of course, the rates of dilution as well as the net transport. With the complicated, three-dimensional, time-dependent flow fields encountered in regions of complex terrain, it is necessary to have a diffusion model which is not mathematically constrained to simplified mean flows. We have on hand a particle-in-cell code with the diffusion parameterized by a simple random walk about a specified mean transport wind. This is available on a local time-sharing system for rapid turn-around at a convenient terminal. In addition, we have developed a Monte Carlo diffusion code which utilizes the information contained in the entire turbulence spectrum as input. Since the fact of the fundamental dependence of diffusion on turbulence structure is well known, models which incorporate more information on turbulence should be theoretically more successful than those which have less detail. Of course, this focuses the problem on the detail and validity of available turbulence observations. Considerable progress has been made recently in this area.

The wind fields observed in the vicinity of Los Alamos respond to a wide range of scales in the basic forcing functions. The free-stream flow which forces the local obstacle flows depends on the whole range of synoptic to mesoscale atmospheric dynamic fluctuations. In turn, there are many scales of topographic variation which influence the perturbed velocity field. The experimental program logically has begun at the smallest scale which can be treated deterministically. When the properties of this scale are documented, the larger scales may be built up as ensembles of the basic building block plus the influence of the larger scale smoothed topography. Scales of motion smaller than the basic terrain scale must be parameterized as a form of stochastic roughness.

The basic terrain features selected for initial study at Los Alamos are the drainage canyons cut into the Pajarito Plateau. There are approximately 10 major canyons within Los Alamos County, all oriented generally west to east, ranging in width from 100 m to 1 km and in depth from about 30 to 100 m. There are several prevalent flow regimes which affect canyon air flows. Two wind conditions driven by a large-scale pressure gradient are the southerly winds across the mesa-canyon complex and the westerly winds channeled down-canyon. Both are associated with vigorous mixing conditions. A preliminary experiment with the release of neutral density balloons in Los Alamos Canyon demonstrated the existence of a large eddy caused by flow separation from the south rim under southerly winds. The eddy was similar in character to that shown in Fig. 1. Perhaps the most important flow condition, from the point of view of pollutant dispersal, is the gravity-forced drainage wind under stable thermal stratification. Lateral mixing is bounded by canyon walls, and vertical cloud growth may be limited to a thermally defined mixing layer. In a canyon with sloping walls, the pollutant cloud distribution and dilution depend critically on vertical structure of the drainage flow.

A field program systematically designed to study the following properties of canyon flows has been initiated. The properties, in roughly the order of investigation, are (1) magnitude; (2) duration; (3) depth; (4) mean velocity, turbulence, and temperature cross sections; (5) tracer dilution characteristics; and (6) canyon-mesa interactions.

Los Alamos Canyon, a major drainage path from the Jemez Mountains to the Rio Grande River, is spanned by a bridge near the townsite. A cable system from the bridge to the canyon floor for mounting meteorological equipment is currently in design, which will provide the capability of determining the profiles of meteorological quantities on a continuous basis. The instrument platform can serve also as a tracer release or sampling point. We expect that design and fabrication of the cable system will take several months and that it will be in the field by spring 1975.

Preliminary measurements have been made in two canyons to address some features of magnitude and duration and to assess the feasibility of the next stage of experiment. Table I presents a summary of measurements from Pajarito Canyon which originates on the Pajarito Plateau at an altitude about 150 m above the observation site. The measurement site is about 2.4 km from the head of the canyon. The interesting features of Table I are the weakness of the flow (0.14 m sec^{-1}) and the rather long time necessary for onset of the drainage wind.

In sharp contrast are the results from Los Alamos Canyon, near the site of the proposed cable system. This canyon originates 10 km to the west at 2900 m altitude in the Jemez Mountains, about 770 m above the observation point. Although the results have not yet been summarized, several points are clear: a steady downslope flow is established within 1 h after sunset, and the mean flow is about 2.5 m sec^{-1} -- an order of magnitude greater than the smaller canyon.

Finally, in support of both theoretical and experimental studies, a comprehensive literature study is underway on slope winds and canyon flows.

TABLE I

SUMMARY OF PAJARITO CANYON DOWNSLOPE FLOW PROPERTIES

Property	Average Value	Range
Onset time	3.6 h after temperature begins to drop in canyon in the evening	-4 to 7 h after temperature drop
End time	as soon as temperature begins to rise in canyon in the morning	-4 to 1 h after temperature rise
Duration of flow	9 h	5 to 14 h
Mean flow speed	0.14 m sec^{-1}	0.04 to 0.34 m sec^{-1}
Transport distance	4.5 km	0.9 to 16 km

CELLULAR AND MOLECULAR RADIOBIOLOGY GROUP (H-9)

D. F. Petersen, Ph.D., Group Leader
T. M. Williams, Secretary

Staff Members

B. J. Barnhart, Ph.D.
E. W. Campbell, B.S.
S. H. Cox, B.A.
L. L. Deaven, Ph.D.
M. D. Enger, Ph.D.
G. T. Fritz, B.S.[a]
L. R. Gurley, Ph.D.
J. M. Hardin, M.S.
F. N. Hayes, Ph.D.
C. E. Hildebrand, Ph.D.
D. E. Hoard, Ph.D.
P. M. Kraemer, Ph.D.
A. M. Martinez, B.S.
E. L. Martinez, B.S.
R. T. Okinaka, Ph.D.
R. L. Ratliff, Ph.D.
P. C. Sanders, M.S.
A. G. Saponara, Ph.D.[b]
G. R. Shepherd, Ph.D.[b]
D. A. Smith, Ph.D.
R. A. Tobey, Ph.D.
R. A. Walters, Ph.D.
D. L. Williams, M.S.

Visiting Staff Member (Short-Term)

R. T. O'Brien, Ph.D.
New Mexico State University
Las Cruces, New Mexico

Chemistry Technicians

J. L. Hanners
P. Jose[a]
V. E. Mitchell
E. C. Wilmoth

Cell Culture Technician

J. G. Valdez

Consultant

A. G. Atherly, Ph.D.
Iowa State University
Ames, Iowa

[a]Half-time.

[b]Leave of absence through September 1974.

INTRODUCTION

Fundamental features of growth, regulation, and synthesis in biologically important macromolecular, microbial, and eukaryotic systems have been the major focus of the Cellular and Molecular Radiobiology Group for approximately 10 years. Although in the past the principal objective has been description and understanding of responses of progressively more complex systems to electromagnetic radiations, phenomenology in unperturbed systems has received major attention as the basis for comparative description of radiation effects. Without conscious effort beyond recognition that understanding underlying mechanisms is essential to understanding toxic effects, the result of these efforts has emerged as a multidisciplinary collection of assay systems generally applicable to a wide variety of subtle toxicologic problems. A major current effort concerns examination of these probes to determine their utility for assessing effects other than ionizing radiations. Primarily because these systems effectively compress the time frame required to produce specific toxic manifestations, they offer an attractive means of efficiently gathering data crucial for recognition of hazards associated with expanding energy technologies. The following summary describes briefly highlights of observations made during the past year, and the reader is urged to consult the brief accounts and published reports for detail.

Studies at the molecular level have involved synthesis of specific oligodeoxyribonucleotide sequences, their chemical and enzymatic amplification to known sequences of sufficient length to act as templates for DNA polymerase, use of the oligodeoxyribonucleotides as models for studying the radiation chemistry of DNA, for measurement of buoyant density properties related to sequence and fidelity of transcription following x-irradiation, and as probes for identification of radiation-induced, covalently bound adducts. In the past year, the radiation chemistry studies have been extended to polymer systems where it is possible to measure concurrently the effects of individual free radical species in terms of base destruction and strand scission. Of greatest interest has been the demonstration that geometrical

differences in the distribution of dTMP when incorporated into a larger polymer appear to be responsible for reduction of radiolytic yields of chromophore destruction by approximately half. Evidence has also been collected suggesting that the increased number of binding sites for RNA polymerase on irradiated DNA templates are breaks capable of covalent linkage with ribonucleotides rather than products of base damage. A comparison of buoyant density properties of natural and synthetic DNA polymers in cesium chloride and Cs_2SO_4 has shown that accurate interrelations can be established by taking into account second-neighbor influences and that deviation from randomness in base sequences can be detected in polymers where base composition is known.

Studies of the cell cycle have been extended to reveal several additional details of cell-cycle progression. Identification of adjacent modified bases in specific locations of mammalian tRNAs has led to the suggestion that interactions involving modified bases contribute to the L-shaped conformation the molecule assumes. The interrelationships between heterogeneous nuclear, messenger-like, and messenger RNAs examined in synchronized cell populations now show clearly that the cycle-dependent synthetic rates of all three species increase but fail to be coordinated in a way suggesting a precursor product relationship with cytoplasmic messenger-like RNA, a storage form. Histone phosphorylation is involved in the conversion of non-dividing to dividing cells. Using synchronized Chinese hamster cells, different histone phosphorylation events were shown to occur in sequence as cells progressed related to cycle-dependent changes in biological activity. Further evidence for cycle-dependent changes in chromatin structure has been obtained by taking advantage of the specificity with which polyanions bind histones. The natural polyanion heparin disperses early G_1 chromatin more readily than chromatin from cells farther advanced in the cell cycle, with a profound transition preceding S phase by 2 h and coincident with the f1 phosphorylation described above. Because so much effort depends on the precise localization of cohorts within cell populations, either cycling or stationary depending on a specific toxic insult, a method based on the DNA content but independent of precursor uptake has been developed. Mithramycin reacts rapidly and specifically with DNA and fluoresces in the proper region to be suitable for flow microfluorometric analysis. The protocol requires only 20 min and permits convenient multiple analyses of cell population status during the course of an experiment. To properly interpret radiation effects on DNA synthesis, deoxynucleoside triphosphate pools have been examined quantitatively in cultured mammalian cells. Radiation causes expansion and increased specific activity of the deoxycytidine triphosphate pool, which explains the anomalous stimulation of deoxycytidine incorporation into DNA. Whether or not cells are arrested or simply cycle at abnormally slow rates following various stimuli has been studied in confluent diploid fibroblast cultures which, when maintained in 0.5% serum, survive for prolonged periods and retain almost imperceptible but nonetheless real capability to cycle. The bulk of the population exhibits the DNA content typical for cells in G_1, and the similarity to tissues *in situ* suggests that the system may be a useful *in vitro* model for studying regulatory processes in tissues showing similar cycle distributions.

Continued investigation of the paradox related to stability of DNA content and variability of chromosome number within heteroploid cell populations has led to the examination of clones of Chinese hamster cells with sufficient instability to permit observation of the transition from stability to instability numerous times within fairly brief cultivation intervals. The amount of DNA present appears to be closely regulated, and the unstable clones exhibit some bias toward excessive numbers of small chromosomes and minutes.

Ultraviolet-irradiated temperate *Haemophilus* phage exhibit several intriguing dose-dependent features. Heavily irradiated phage show an enhanced probability of entering the lysogenic pathway while, at lower ultraviolet doses, lytic infection predominates. Quantitative properties of the system make it potentially attractive for exploration of the effects of agents other than radiation. Electron micrographs of sectioned ultraviolet-induced lysogens harboring a T_s mutant *Haemophilus* phage show the wild-type phage to be deficient in regulation of its development, while the mutant lysogen appears to be more stable at permissive temperatures. Thus, the mutant will be useful in phage maturation studies

(for example, phage DNA packaging).

Summer workshops and meetings continued to occupy an important place in the summer activities of the group. A joint LASL-TCA workshop was held in July 1974, and a small informal somatic cell genetics conference is planned for May 1975. We find that the small conference is ideally suited to our facilities and expect to continue to organize them whenever appropriate topics arise.

STUDIES WITH MODEL DNA POLYMERS

Chemical Synthesis of Oligodeoxyribonucleotides

(D. L. Williams and E. L. Martinez, Jr.)

As part of our continuing synthesis program, two preparations of oligomers of 5'-thymidylic acid were made for use in radiation studies and other biological investigations. One series of the oligonucleotides ranging from $(pT)_2$ to $(pT)_{13}$ was methyl-labeled with tritium. Following the cleavage of pyrophosphate linkages in the initial reaction mixture, members of each series were separated by anion exchange column chromatography on DEAE-cellulose (bicarbonate form). Each oligomer was then rigorously purified by further column chromatography at pH 2.5 and at pH 7.5. The purity and identity of a product were also verified by enzymatic degradation; for example, $(pT)_2$ gave only TpT when treated with alkaline phosphatase. Degradation of the latter compound with venom diesterase gave pT and thymidine in the ratio 1.00.

As reported previously,[1] in the stepwise chemical synthesis of oligonucleotides, we have adopted the 2-phenylmercaptoethyl group[2] as protective group for 5'-phosphate. Although not retained quantitatively during reactions, the group is readily applied, and complete removal can be effected. This aromatic group imparts to the two phosphate-protected species, the oligonucleotide, and the starting intermediate sufficient affinity for benzoylated DEAE-Sephadex that unreacted mononucleotides and by-products with free phosphate groups can be essentially eluted first from the column. The 5'-phosphate-protected species are then eluted with an alcoholic gradient and further resolved by gel filtration on a G-25 superfine Sephadex column.

As shown in Table I, d-ϕSEtpTpG^{iBu} and d-ϕSEtpTpG^{iBu}pG^{iBu} were synthesized in good yield and isolated as outlined above. However, the separation on

TABLE I

STEPWISE SYNTHESIS OF DEOXYRIBO-OLIGONUCLEOTIDES

Oligonucleotide[a]	Yield (%)
ϕSEtpTpG^{iBu}	64
ϕSEtpTpG^{iBu}pG^{iBu}	59
pTpG^{iBu}pG^{iBu}	42
ϕSEtpC^{BOC}pC^{BOC}	58
ϕSEtpC^{BOC}pC^{BOC}pA^{Ac}	64
pC^{BOC}pC^{BOC}pA^{Ac}	--

[a]Abbreviations and symbols used are: phenylmercaptoethyl, ϕSEt; isobutyryl, iBu; isobutyloxycarbonyl, BOC; and acetyl, Ac.

BD-Sephadex of unreacted d-pG^{iBu} from the product in each step required large volumes (13 to 23 liters) of eluant. In each case, complete removal of the product from the column, as indicated by paper chromatography of fractions, also required large volumes of alcoholic solvent (13 to 18 liters). Further purification of 5'-phosphate protected products by gel filtration on G-25 superfine Sephadex is also time-consuming due to the limited capacity of even large columns (5.5 x 90-cm). After removal of the ϕSEt group, final purification of the product d-pTpG^{iBu}pG^{iBu} to eliminate d-pTpG^{iBu} and d-TpG^{iBu}pG^{iBu} was effected by repeated fractionation on DEAE-cellulose columns as indicated by paper chromatographic monitoring of fractions.

The complementary trinucleotide, d-pC^{BOC}pC^{BOC}pA^{Ac}, was also prepared in good yield (see Table I) using the ϕSEt protective group for phosphate. Since the various protective groups, especially the aromatic ϕSEt group, render the oligonucleotides soluble in chloroform, the d-ϕSEtpC^{BOC}pC^{BOC} and d-ϕSEtpC^{BOC}pC^{BOC}pA^{Ac} were isolated much more rapidly by repetitive $CHCl_3$ extractions from a concentrated aqueous solution. The excess of unreacted d-pA^{Ac} was left largely in the aqueous phase. $CHCl_3$ extracts were then further resolved by gel filtration on G-25 superfine Sephadex (see Table II).

Although the chloroform extraction of product was not complete (84%), the preliminary fractionation made it possible to recover the remainder by applying the aqueous phase to the G-25 superfine

TABLE II

ISOLATION OF ϕSEtpC^{BOC}pC^{BOC}pA^{Ac} BY $CHCl_3$ EXTRACTION

$CHCl_3$ Extractions	Product (% of total)[a]
1 through 22	80.5
22 through 39	3.2
Final H_2O phase	16.2

[a]After resolution on G-25 superfine Sephadex.

TABLE III

VENOM DIESTERASE DEGRADATION OF OLIGONUCLEOTIDES

Compound	Ratios Found	
d-pTpG	d-pG:d-pT	1.03
d-pTpGpG	d-pG:d-pT	2.09
d-pCpCpA	d-pC:d-pA	2.08

Sephadex column in 8 equal fractions. The purity of final products was checked by paper chromatography and degradation to mononucleotides with venom diesterase (as shown in Table III). This pair of pure, complementary trimers will be chemically polymerized to obtain repeating trinucleotide sequences of sufficient length to act as template for DNA polymerase amplification.

REFERENCES

1. C. R. Richmond and E. M. Sullivan, eds., "Annual Report of the Biomedical and Environmental Research Program of the LASL Health Division, January through December 1973," Los Alamos Scientific Laboratory report LA-5633-PR (May 1974), pp. 43-44.

2. S. A. Narang, O. S. Bhanat, J. Goodchild, R. H. Wightman, and S. K. Dheer, "A New General Method for the Synthesis of Phosphate-Protected Deoxyribonucleotides. IV," J. Amer. Chem. Soc. 94, 6183 (1972).

Radiation Chemistry of Models for DNA

(F. N. Hayes, D. E. Hoard, E. C. Wilmoth, and V. E. Mitchell)

In previous work,[1,2] we established that the mononucleotide dTMP is probably superior to the free base thymine as a model for assessing radiation-induced damage to the thymine base residues of DNA. During the past year, we have performed further experiments designed to establish the extent to which the various species generated by radiolysis of water contribute to destruction of the base residue of dTMP in aqueous solution. Sets of experimental conditions have been devised under which attack of a molecule of nucleotide by free radicals is limited to those of one or at most two species of radical (Table I); some of these have been described previously.[1,3] A so-far limited number of experiments have also been performed with poly dT under identical conditions; with the polynucleotide target, it is possible to measure the effectiveness of individual species of free radical for producing both base destruction and strand scission concurrently.

Hand-in-hand with the experimental work, an effort has been made to further develop mathematical models for damage which we hope ultimately will permit quantitative estimates to be made of the interactions between target and radicals of each type which produce biologically significant chemical changes in DNA itself. A reasonably accurate approximation of the interactions between free radicals of each species ($OH\cdot$, $H\cdot$, and e^-_{aq}) and dTMP giving rise to chromophore destruction is shown in Eq. (1):

$$G(-\text{chrom}) = g_{OH} \cdot \frac{\alpha_{OH} k^T_{OH} C_T}{k^T_{OH} C_T + \Sigma k^S_{OH} C_S + \beta_{OH}} + g_H \cdot \frac{\alpha_H k^T_H C_T}{k^T_H C_T + \Sigma k^S_H C_S + \beta_H} + g_E \cdot \frac{\alpha_E k^T_E C_T}{k^T_E C_T + \Sigma k^S_E C_S + \beta_E} \quad \text{(Eq. 1)}$$

G(-chrom) is the yield of molecules of chromophore destroyed per 100 eV of 250-kVP x-irradiation absorbed; the factors g_{OH}, g_H, and g_E represent, respectively, yields of hydroxyl radicals, hydrogen atoms, and hydrated electrons given upon the irradiation of pure water.[4,5] The various quantities k are published second-order reaction rate constants[5-8] for the reactions occurring between radicals of each type and target (T) or radical-scavenging (S) solutes. The three parameters α represent the fractions of radical-target interactions which lead to the measured effect (chromophore destruction); the three parameters β represent rates of disappearance of radicals of the three species due to their interaction with one another and with unsuspected impurities in the solutions. The six parameters are

TABLE I

SUMMARY OF dTMP EXPERIMENTS

Experiment Number	Solution	pH	Atmosphere	Principal Free-Radical Scavengers	Principal Free Radicals Attacking dTMP
1	M tert-C_4H_9OH; 0.014 M phosphate	7.00	Inert (N_2)	tert-C_4H_9OH $H_2PO_4^-$	e^-_{aq}
2	0.025 M nitrate; 0.014 M phosphate	6.99	Inert (Ar)	NO_3^- $H_2PO_4^-$	OH·
3	M tert-C_4H_9OH; 0.200 M phosphate	6.22	Inert (Ar)	tert-C_4H_9OH $H_2PO_4^-$ H_3O^+	H·; e^-_{aq}
4	M tert-C_4H_9OH; (deionized H_2O)	7.00	Inert (Ar)	tert-C_4H_9OH	e^-_{aq}
5	0.025 M nitrate (3x distilled H_2O)	6.98	Inert (Ar)	NO_3^-	OH·
6	0.10 M tert-C_4H_9OH; (acidified 3x distilled H_2O)	2.99	Inert (Ar)	tert-C_4H_9OH H_3O^+	H·; e^-_{aq}
7	0.014 M phosphate	7.00	Air or O_2	O_2[a] $H_2PO_4^-$	OH·
8	3x distilled H_2O	6.63	Air or O_2	O_2[a]	OH·

[a]No difference in result was observed whether atmosphere was air or pure oxygen.

TABLE II

VALUES DETERMINED FOR PARAMETERS α AND β OF EQ. (1)

	Free Radical OH				Free Radical H				Free Radical e^-_{aq}			
Experiment Number	α	Standard Deviation (%)	β (s^{-1})	Standard Deviation (%)	α	Standard Deviation (%)	β (s^{-1})	Standard Deviation (%)	α	Standard Deviation (%)	β (s^{-1})	Standard Deviation (%)
1,2,3	0.636	2.92	1.83×10^5	15.10	0.566	29.95	1.69×10^5	99.47	0.773	7.69	1.20×10^5	35.84
4,5,6	0.730	4.11	3.85×10^5	13.66	0.444	8.33	6.23×10^4	25.24	0.718	4.34	9.48×10^4	13.72
1,3,7	0.629	4.51	8.45×10^4	25.24	0.567	29.95	1.69×10^5	99.42	0.774	7.69	1.20×10^5	35.83
4,6,8	0.566	2.99	1.64×10^4	47.92	0.460	8.40	6.63×10^4	24.87	0.718	4.34	9.48×10^4	13.72

evaluated by a computer program which determines the values giving best least-squares fits between experimental measurements and the equation. A selection of results obtained for x-ray-produced dTMP chromophore destruction is given in Table II.

In experiments 3 and 6 (Table I), irradiation is carried out at a lower pH to partially convert hydrated electrons into hydrogen atoms. In the absence of published data on the variation in rate constant for the reaction between hydrated electrons and dTMP with pH, it has been necessary to derive an equation for such a relationship from theoretical considerations. This relationship requires that the secondary phosphoryl dissociation constant of dTMP be known. A source of uncertainty is probable variation both in the secondary phosphoryl dissociation of dTMP and in the degree of dissociation of the $H_2PO_4^-$ ion in the presence of tertiary-butyl

alcohol; the concentration of the latter ion present under a given set of experimental conditions is important because the $H_2PO_4^-$ ion also converts radiolytically generated hydrated electrons into hydrogen atoms. Trial calculations in which depression of these dissociation constants in proportion to the tert-butyl alcohol concentration was assumed have failed to reconcile the discrepancy between the values for the α- and β- parameters computed from measurements made in the systems containing phosphate buffer and those computed from measurements made in the unbuffered systems.

The major approximation involved in the use of Eq. (1) is the treatment of the target concentration (C_T) as remaining constant with time. In practice, it is necessary to assume an average value for this quantity, such as the geometric mean of the concentration initially present and that measured at the end of irradiation. A more exact mathematical treatment[1] takes into account the continuous decrease in target concentration that takes place as irradiation proceeds.

Radiolysis yields of chromophore destruction observed in poly dT (average length 484 nucleotides) were only 0.4-0.5 as great as the yields for dTMP under the conditions of experiments 1, 2, and 3. This difference is attributable to the different distribution of dTMP throughout a solution when it has been incorporated into polymer chains. Without independently measured rate constants for the reactions between radicals and poly dT, one cannot compute directly values for the α- and β- parameters by fitting Eq. (1) to the polymer data. However, if it is assumed that the values of such parameters for poly dT do not differ from those calculated for dTMP, the experimental data can be employed for the computation of geometry factors which specify the degree by which the rate of reaction of each species of free radical with nucleotide is lowered when the nucleotide is part of a polymeric chain.

From various models which have been proposed[9-12] for the conformation of single-strand polynucleotides in solution, we have made estimates of the frequency of collisions between free radicals and poly dT during irradiation. From these and from the estimates we have made of the probable rate constants for poly dT-radical reactions, it is possible to calculate the fraction of collisions between poly dT molecules and radicals of each species which result in chemical reaction. Estimated efficiencies for chromophore destruction depend on the model chosen for polynucleotide conformation but are of the order of 30% for hydroxyl radicals, 15% for hydrogen atoms, and 8% for hydrated electrons.

REFERENCES

1. C. R. Richmond and E. M. Sullivan, eds., Annual Report of the Biomedical and Enviromental Research Program of the LASL Health Division, January through December 1973, Los Alamos Scientific Laboratory report LA-5633-PR (1974), pp. 46-49.

2. D. E. Hoard, F. N. Hayes, and W. B. Goad, Intern. J. Radiation Biol. 25, 603 (1974).

3. F. N. Hayes, D. E. Hoard, P. N. Dean, and W. B. Goad, Intern. J. Radiation Biol. (1974), in press.

4. I. G. Draganíc and Z. D. Draganíc, The Radiation Chemistry of Water, Academic Press, Inc., New York (1971), p. 140.

5. M. Anbar, M. Bambanek, and A. B. Ross, Selected Specific Rates of Reactions of Transients from Water in Aqueous Solution. I. Hydrated Electron, U. S. Department of Commerce Publication NSRDS-NBS 43, Washington, D. C. (1973), pp. 1, 15, 35.

6. M. Anbar and P. Neta, Intern. J. Radiation Isotopes 18, 493 (1967).

7. G. Grabner, N. Getoff, and F. Schwörer, Intern. J. Radiation Phys. Chem. 5, 405 (1973).

8. L. M. Myers, Jr., In: Radiation Chemistry of Macromolecules (M. Dole, ed.), Vol. II, p. 323, Academic Press, Inc., New York (1973).

9. P. C. Schragge, H. B. Michaels, and J. W. Hunt, Radiation Res. 47, 598 (1971).

10. H. B. Michaels and J. W. Hunt, Radiation Res. 56, 57 (1973).

11. L. D. Inners and G. Felsenfeld, J. Mol. Biol. 50, 373 (1970).

12. E. G. Richards, C. P. Flessel, and J. R. Fresco, Biopolymers 1, 431 (1963).

Effects of X-Irradiation of DNA on Transcription

(D. A. Smith and A. M. Martinez)

Our continuing investigations on the effects of irradiation upon the transcription process and its components[1-3] have focused recently on the influence of x-irradiation of DNA upon the mechanisms of initiation of RNA synthesis. Although there is evidence obtained both *in vitro* and *in vivo* that RNA

synthesis is initiated with a purine nucleoside triphosphate, it has been known for some time that *in vitro* RNA synthesis can be initiated with oligoribonucleotides complementary to a DNA template.[4] We have recently shown that complementary deoxyribonucleotides also serve as initiators for RNA synthesis *in vitro* through their covalent incorporation into the RNA chain.[5] We have shown also, as have others, that breaks in double-stranded DNAs also serve as covalent initiation points for RNA synthesis *in vitro*. This finding leads to the possibility that x-irradiation of DNA would produce new sites for covalent initiation of RNA synthesis, and we have shown this to be the case.[6] Although the total amount of RNA synthesized decreased as a function of the dose given to the DNA template poly d(A-T):d(A-T), its capacity to support covalent initiation of RNA synthesis increases as a function of dose. Thus, some of the breaks in DNA caused by x-irradiation are competent to serve as initiation sites for RNA polymerase.

In the presence of excess enzyme, the amount of RNA initiated by covalent attachment to DNA is a function of the number of 3'-hydroxyl groups available to RNA polymerase. This is shown in the following experiment. Poly d(A-T):d(A-T) was incubated with a low concentration of DNase I for varying periods of time, and the DNase was then denatured with heat, and the other components of the end addition reaction were added. As can be seen in Fig. 1, mild DNase treatment causes first a considerable increase and then a decrease in the amount of RNA synthesis initiated by covalent attachment to the DNA. This is interpreted as due to an increase in number of 3'-hydroxyl groups as digestion proceeds and then a decreased incorporation as the DNA fragments are further degraded. With longer digestion times or higher DNase concentrations, no incorporation of UTP into alkali-stable, acid-insoluble material is seen.

When irradiated poly d(A-T):d(A-T) is assayed for ability to promote initiation of RNA synthesis by covalent attachment, the results depend upon the ratio of enzyme to DNA in the reaction mixture. If there is a large excess of enzyme to 3'-hydroxyl groups in the unirradiated DNA, the incorporation of UTP into alkali-stable, acid-insoluble form increases as a function of dose (Fig. 2). However,

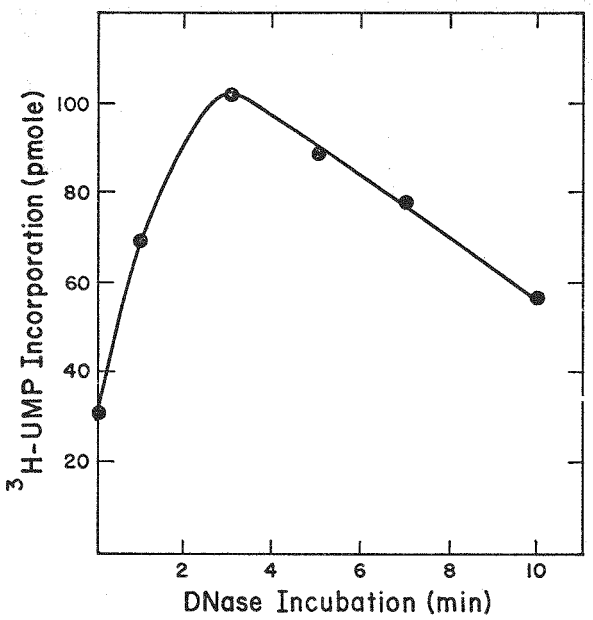

Fig. 1. Effect of DNase I digestion of poly d(A-T):d(A-T) on incorporation of UMP into alkali-stable, acid-insoluble form. Poly d(A-T):d(A-T) was incubated with DNase I, and aliquots were removed at the indicated times, placed in a boiling water bath, and subsequently assayed for UMP incorporation.

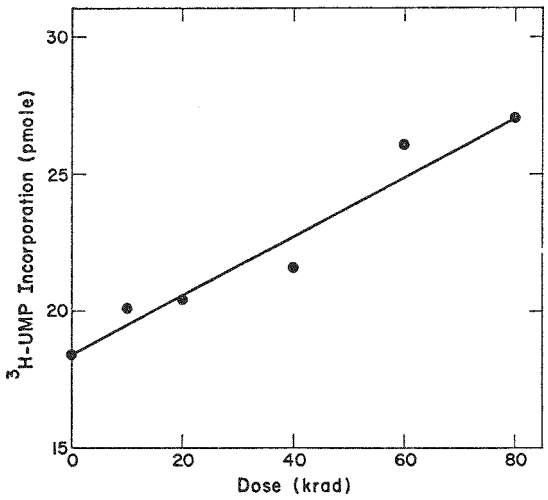

Fig. 2. Effect of x-irradiation on the ability of poly d(A-T):d(A-T) to support UMP incorporation into alkali-stable, acid-insoluble form when assayed under conditions of enzyme excess.

if the experiment is performed under conditions of enzyme limitation, a decrease in the amount of UTP added to DNA is seen as a function of dose (Fig. 3). At intermediate enzyme levels, it is possible to demonstrate first an increase and then a decrease in UTP addition to the DNA at higher doses. These results indicate that x-irradiation produces new

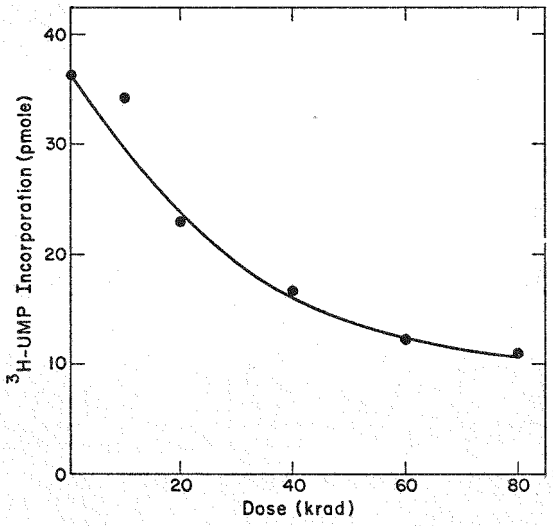

Fig. 3. Effect of x-irradiation on the ability of poly d(A-T):d(A-T) to support UMP incorporation into alkali-stable, acid-insoluble form when assayed under conditions of enzyme limitation.

active sites for initiation by this mechanism as well as new inactive binding sites. As long as there are excess enzyme molecules, any increase in the number of active sites due to irradiation produces more covalent attachment of RNA. However, when the total of active and inactive binding sites is greater than the number of enzyme molecules, then any increase in inactive binding sites due to radiation would cause the end addition reaction to decrease. Previous studies of the effects of x-irradiation of DNA on its ability to serve as a template for RNA synthesis have not taken this mechanism of initiation of RNA synthesis into account. Thus, others have found that irradiation increased the binding sites for RNA polymerase and that some of the new binding sites were active in promoting RNA synthesis.[7] They proposed that the new active sites arose from some type of base damage, but, on the basis of our experiments, we propose that the new sites are that fraction of breaks in the DNA which are capable of covalent linkage with incoming ribonucleotides.

REFERENCES

1. G. F. Strniste, D. A. Smith, and F. N. Hayes, "X-Ray Inactivation of the *Escherichia coli* Deoxyribonucleic Acid-Dependent Ribonucleic Acid Polymerase in Aqueous Solution. I. Studies on Binding and Substrate Concentration Dependence in the Inactivation of Enzymatic Activity," Biochemistry 12, 596 (1973).

2. G. F. Strniste, D. A. Smith, and F. N. Hayes, "X-Ray Inactivation of the *Escherichia coli* Acid-Dependent Ribonucleic Acid Polymerase in Aqueous Solution. II. Studies on Initiation and Fidelity of Transcription," Biochemistry 12, 603 (1973).

3. G. F. Strniste and D. A. Smith, "Induction of Stable Linkage between the Deoxyribonucleic Acid-Dependent Ribonucleic Acid Polymerase and $d(A\text{-}T)_n \cdot d(A\text{-}T)_n$ by Ultraviolet Light," Biochemistry 13, 485 (1974).

4. S. K. Niyogi and A. Stevens, "Studies of the Ribonucleic Acid Polymerase from *Escherichia coli*. IV. Effect of Oligonucleotides on the Ribonucleic Acid Polymerase Reaction with Synthetic Polyribonucleotides as Templates," J. Biol. Chem. 240, 2593 (1965).

5. D. A. Smith and A. M. Martinez, "Initiation of *in vitro* RNA synthesis with Deoxyribosyl Oligomers," Biochim. Biophys. Acta 353, 475 (1974).

6. D. A. Smith and A. M. Martinez, "Initiation of *in vitro* RNA Synthesis by Covalent Attachment to X-Irradiated DNA," Federation Proc. 33, 1417 (1974).

7. J. P. Goddard, J. J. Weiss, and C. M. Wheeler, "Studies on RNA Synthesis Primed by Damaged Templates. I. DNA Templates Damaged by Deoxyribonuclease Treatment and by γ-Radiation," Biochim. Biophys. Acta 199, 126 (1970).

Buoyant Densities Considered as Sequence-Dependent Properties

(R. L. Ratliff and D. A. Smith)

The buoyant densities in CsCl and Cs_2SO_4 are measurements useful in characterizing natural and synthetic DNAs. The buoyant densities in CsCl of natural cellular DNAs have an approximately linear dependence on base composition over the range of 30 to 70% G + C. The buoyant densities in Cs_2SO_4 of natural DNAs of 30 to 70% have at least a quadratic dependence on G + C content. Synthetic DNAs of simple sequence do not have buoyant densities in either CsCl or Cs_2SO_4 that are uniquely related to base composition. For example, the buoyant densities (g/cm^3) in CsCl of poly d(AC)·d(GT) and poly d(AG)·d(CT), each of which contains 50% G + C, are 1.6905 and 1.711, respectively,[1] and the buoyant densities in CsCl of poly d(A)·d(T), poly d(AT)·d(AT), and poly d(AAT)·d(ATT), polymers that contain 100% A + T, are 1.6735, 1.672, and 1.666, respectively.[2] These differences are well outside the measurement error of $\pm$ 0.001 (g/cm^3). It is reasonable to assume that short regions of natural DNAs also have

sequence-dependent buoyant densities; however, for most cellular DNAs of a given base composition, there is a nearly random distribution of bases which averages out this dependence. Exceptions are those fractions of the DNA of higher organisms which appear in density gradients as "satellite" bands separated from the main band of DNA and which often have simple base sequences which are serially repeated. Such satellite DNAs, like synthetic DNAs, have buoyant densities which are not uniquely related to base composition.

We have shown[3] that a previously published approach for interrelating the sequence-dependent values of a property[4] can be applied to the buoyant densities of DNAs and that the buoyant densities of natural and synthetic DNAs can be accurately interrelated if second-neighbor influences are taken into account. We have derived the following expressions based partly on the buoyant densities of six synthetic DNAs for the buoyant densities, ρ (g/cm^3), of DNAs having random sequences:

In CsCl:

$$\rho = 1.659 + 0.099\ H_G - 0.065\ H_G^2 + 0.080\ H_G^3$$

In Cs_2SO_4:

$$\rho = 1.417 + 0.011\ H_G - 0.004\ H_G^2 + 0.035\ H_G^3$$

In these equations, H_G is the mole fraction of G:C base pairs in the DNA, and the buoyant densities are calculated relative to densities for *Escherichia coli* DNA of 1.703 and 1.426 (g/cm^3) on CsCl and Cs_2SO_4, respectively. These equations (solid lines) are graphed in Fig. 1 along with published data for bacterial DNAs. Also graphed (dashed lines) are curves generated taking only first-neighbor influences into account. The second-neighbor curve is clearly superior. The fact that not all bacterial DNAs have buoyant densities which lie on these curves implies that certain bacterial DNAs have significant deviations from random base sequences. These curves can be used to evaluate the randomness of base sequence of DNAs of known base composition.

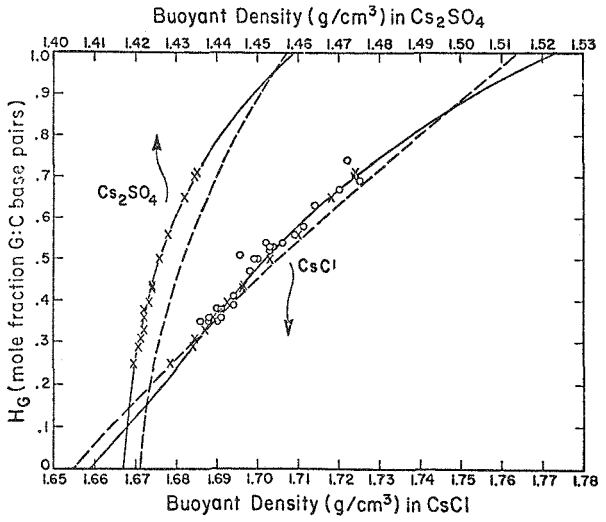

Fig. 1. The buoyant densities of bacterial DNAs in CsCl and Cs_2SO_4, compared with the densities calculated from the equation based wholly or partly on the buoyant densities of synthetic DNAs. The dashed lines are curves generated from the equations which take only first-neighbor influences into account. The solid lines are curves generated from the equations based on second-neighbor influences.

REFERENCES

1. R. D. Wells and J. E. Blair, "Sedimentation and Buoyant Density Studies of Some DNA-Like Polymers with Repeating Nucleotide Sequences," J. Mol. Biol. 27, 273 (1967).

2. R. L. Ratliff, D. L. Williams, F. N. Hayes, E. L. Martinez, Jr., and D. A. Smith, "Preparation and Properties of the Repeating Sequence Polymer $d(A\text{-}A\text{-}T)_n \cdot d(A\text{-}T\text{-}T)_n$," Biochemistry 12, 5005 (1973).

3. D. M. Gray, C. W. Gray, R. L. Ratliff, and D. A. Smith, "Buoyant Densities of Natural and Synthetic DNAs Considered as Sequence-Dependent Properties," Biopolymers 13, 2265 (1974).

4. D. M. Gray and I. Tinoco, Jr., "A New Approach to the Study of Sequence-Dependent Properties of Polynucleotides," Biopolymers 9, 223 (1970).

Circular Dichroism Spectra of Synthetic Polynucleotides

(R. L. Ratliff and D. A. Smith)

It is known that the circular dichroism (CD) spectra of natural DNAs in solution are drastically altered by the presence of ethanol. To test whether or not the effects of ethanol on DNA are consistent with changes in the secondary structure, we have measured the spectra of a synthetic DNA, poly d(AC):d(GT), a synthetic RNA, poly r(AC):r(GU), and the DNA:RNA hybrids, poly d(AC):r(GU) and poly r(AC):d(GT).[1]

The synthetic DNA, poly d(AC):d(GT), was synthesized as previously described.[2] The RNA polymer, poly r(AC):r(GU), was made using the DNA as template

for RNA polymerase from *Escherichia coli*. The DNA was digested with pancreatic DNAse to yield a pure RNA product. Strands of poly d(AC):d(GT) were separated by centrifugation in alkaline CsCl, and the DNA:RNA hybrids were prepared using the separated strands as templates for RNA polymerase. All polymers were characterized as to buoyant density and temperature melting profile.

Ultraviolet CD spectra were obtained in aqueous solutions in the presence and absence of ethanol for the four polymers. In the absence of ethanol, the RNA and DNA spectra are dissimilar, while the spectra of the hybrids show differing degrees of similarity to that of the RNA. In the presence of ethanol, the spectra of the DNA and both hybrids become much closer to that of the RNA which remains relatively unchanged. The results are interpreted as indicating that DNA can undergo a change to an A-like conformation in the presence of ethanol and that the DNA:RNA hybrids are not wholly restricted to an RNA-like conformation in the absence of ethanol. They are consistent with the suggestion that DNA strands may acquire an A-like conformation during transcription in order to pair with RNA strands which are restricted to an A-like conformation.[3] The results also provide the first evidence that hybrids of different base sequences in the ribosyl and deoxyribosyl strands may differ significantly in their abilities to assume RNA-like conformations in solution.

REFERENCES

1. D. M. Gray and R. L. Ratliff, "Circular Dichroism Spectra Show that the Conformations of Poly d(AC):d(GT), Poly r(AC):r(GU), and Hybrids Poly d(AC):r(GU) and Poly r(AC):d(GT) are Similar in the Presence of Ethanol," Biopolymers (1974), in press.

2. F. N. Hayes, E. H. Lilly, R. L. Ratliff, D. A. Smith, and D. L. Williams, "Thermal Transitions in Mixtures of Polydeoxyribodinucleotides," Biopolymers 9, 1105 (1970).

3. S. Arnott, W. Fuller, A. Hodgson, and I. Prutton, "Molecular Conformations and Structure Transitions of RNA Complementary Helices and Their Possible Biological Significance," Nature 220, 561 (1968).

CELLULAR METABOLISM

Modification of Ribonucleic Acids

(A. G. Saponara, M. D. Enger, and J. L. Hanners)

The t-RNA of cell cultures of Chinese hamster cells contains small amounts of a modified uridine which has a γ-linked α-aminobutyrate residue derived from methionine at N-3.[1,2] The presence of the nucleoside is easily assayed, even in unfractionated nucleic acid preparations, since it and a similarly modified pseudouridine (ABA-18) in 18S ribosomal RNA appear to be the sole nucleic acid substituents which are labeled *in vivo* by the 1- or 2-carbons of methionine. These modified nucleosides have a number of distinguishing properties such as resistance to pancreatic RNase and susceptibility to acylation by the esters of N-hydroxysuccinimide. In our previous annual report, we suggested that ABA-4 was equivalent in structure and position to the then unidentified nucleoside X which is present in the variable loop sequence 7mGpXpC of a number of *Escherichia coli* t-RNAs. The proposal has been independently substantiated by the work of Nishimura[3] and Friedman.[4] In this report, we present data on the oligonucleotides obtained by pancreatic RNase digestion of ^{3}H-acetylated *E. coli* and yeast t-RNAs. A large fraction of the acetylated oligonucleotides from *E. coli* contains a labeled nucleoside with similar chromatographic mobility to acetylated ABA-4. Each of these oligonucleotides contains a 7mG, since the mild chemical hydrolytic procedure devised by Zachau and coworkers for the specific cleavage of a nucleic acid at 7mG results in expected changes in chromatographic behavior.[5]

We first determined the extent to which deaminoacylated commercial preparations of *E. coli* t-RNA could be acetylated with acetoxysuccinimide. Yeast t-RNA was similarly treated, since it had been reported to be unreactive toward acetoxysuccinimide.[6] The samples were digested with pancreatic RNase and alkaline phosphomonoesterase, and the oligonucleotides were separated according to their net negative charge at neutral pH by chromatography on DEAE-cellulose in 7 M urea. Figure 1 shows the patterns obtained from *E. coli* B (top), *E. coli* K12 (middle), and yeast t-RNA (bottom). The absorbancy (from left to right) results from mononucleosides (mainly Pyr) with no net charge, dinucleoside monophosphates

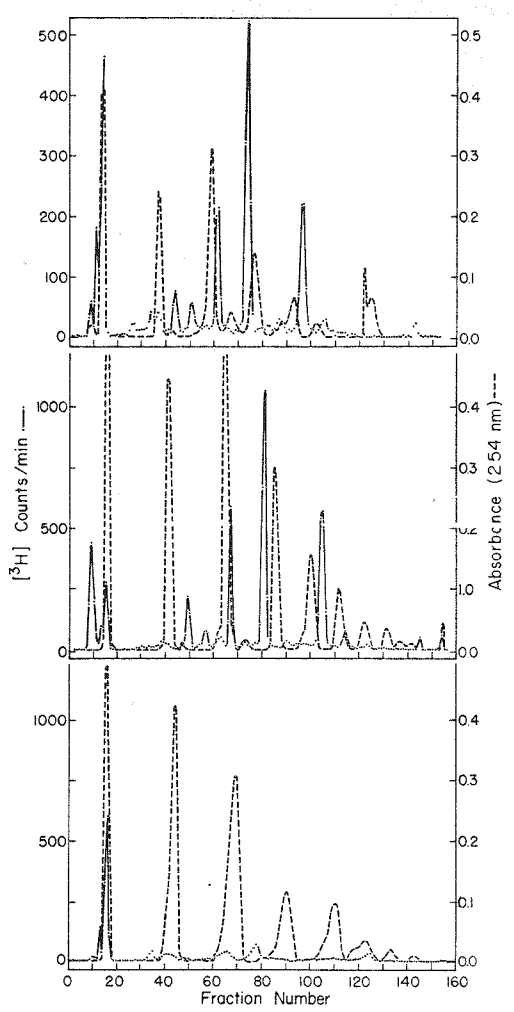

Fig. 1. Oligonucleotides obtained from ^{3}H-acetylated t-RNAs after hydrolysis with pancreatic RNase. The patterns are from 0.5 mg of *E. coli* B (top), 1 mg of *E. coli* K-12 (middle), and 1 mg of yeast (bottom). Each deaminoacylated t-RNA was dissolved in 1 ml of 0.1 M triethylammonium acetate, pH 8.0, containing 0.01 M $MgCl_2$, and was reacted with an equal weight of ^{3}H-acetoxysuccinimide, specific activity 9.77 μCi/μM, dissolved in tetrahydrofuran. The acetoxysuccinimide was added to the t-RNA in 10 equal aliquots over a period of 30 min, during which time the temperature was maintained at 0°C. The t-RNA was precipitated twice from 2.5 volumes of ethanol and digested with one-tenth its weight of pancreatic RNase. The oligonucleotides were separated on DEAE, equilibrated with 0.1 M ammonium acetate, pH 7.0, and 7 M urea. Columns were eluted with a linear gradient of sodium chloride, proceeding to a final concentration of 0.3 M over a total volume of 500 ml. Fractions of approximately 3.5 ml were collected every 15 min. Radioactivity was assayed by counting a 0.5-ml aliquot in a liquid scintillation counter.

(PupPyr) with one negative charge, trinucleoside diphosphates (PupPupPyr) with two negative charges, etc. The patterns for *E. coli* K12 and yeast each result from the processing of 1 mg of t-RNA and are, therefore, directly comparable. Yeast t-RNA is less acetylatable than t-RNA from *E. coli*. Most of the label from yeast elutes with mononucleosides; only relatively small amounts are more strongly adsorbed. We are not sure whether this label represents the acylation of a nucleoside or is of trivial significance (e.g., due to incomplete deaminoacylation, acylation of a non-nucleic acid impurity in the commercial preparations, or incomplete removal of low molecular weight products resulting from side reactions of the highly labeled ^{3}H-acetoxysuccinimide). Because the nucleoside X is not hydrolyzed by pancreatic RNase, the smallest possible oligonucleotide containing it would be XpPyr with a charge of -2. If X exists in our postulated sequence, the smallest possible pancreatic oligonucleotide would be 7mGpXpC, which also has a net charge of -2, since the extra negative charge of the additional 7mGp residue is neutralized by the positive charge associated with that quaternary nucleoside. These arguments allow us, for the time, to defer consideration of the labeled nucleoside-like material. The relative deficiency of higher acetylated oligonucleotides in yeast suggests that X is not present in substantial amounts. In fact, known sequences of yeast t-RNA do not contain a modified pyrimidine with the properties of X. Those yeast t-RNAs which have a 7mG contain sequences such as 7mGpUpC or 7mGpDiHUpC. It is possible that X exists in as yet unsequenced yeast t-RNAs. Should this be the case, our data indicate that the hypothetical X must have a derivatized amino, since it is not chemically acetylatable.

Examination of the *E. coli* patterns reveals three major acetylated oligonucleotides in the theoretically interesting charge range of -2 or greater. These are localized in both strains B and K12 at positions slightly after the absorbancy from PupPupPyr, slightly before the absorbancy due to PupPupPupPyr, and slightly after the absorbancy due to PupPupPupPupPyr. For the purpose of further discussion, we will refer to these oligonucleotides as I, II, and III. In contrast to the less charged

acetylated species, I, II, and III are in a fairly constant ratio. Of the total count in oligonucleotides of charge -2 or greater, I, II, and III represent 21.7, 47.7, and 27.0% in strain B and 16.3, 45.5, and 34.7% in strain K12. Each of these oligonucleotides has been further digested with the nonspecific nuclease T2. A labeled nucleoside with chromatographic mobility similar to that of acetylated ABA-4 from Chinese hamster t-RNA has been obtained in each case.

We next describe a protocol used to further characterize oligonucleotides I, II, and III. The procedure was devised so that it could be extended to mammalian cell culture t-RNA populations which are available in relatively small amounts. The experiments are based on the extreme lability of 7mG toward mild alkali, which causes opening of the imidazole ring with concomitant loss of the positively charged quaternary nitrogen. The glycosidic bond of the resulting open ring is hydrolyzed at pH 3.5, and the phosphodiester chain is ruptured at the free ribose by an amine-catalyzed reaction. Zachau *et al.* have made a thorough study of these reactions and have been able to devise a set of conditions with sufficient specificity to allow cleavage of phenylalanine t-RNA into two fragments at the single 7mG of that polymer.[5] Figure 2 is a scheme for the reactions involved:

(1) Depicting a possible sequence in intact t-RNA containing ABA-4, symbolized by X. A structural diagram of ABA-4 is shown at the bottom of Fig. 2. X is shown with a free amino and carboxyl to emphasize the expected charges, which are listed to the right of the oligonucleotides.

(2) The product formed by acetylation of intact t-RNA. The acetylated amine is no longer ionized at neutral pH, and the base X now has a net negative charge.

(3) The oligonucleotide resulting from complete digestion with pancreatic RNase and alkaline phosphomonoesterase. Pancreatic RNase does not hydrolyze pyrimidines with N-3 substituents and, therefore, does not remove X. Note that the parent structure in step 1 has two purines preceding 7mG. The actual number could be more or less than two; in which case, the pancreatic oligonucleotide would be correspondingly longer or shorter than that shown. Alternatively, the 7mG could be preceded by a Pyr;

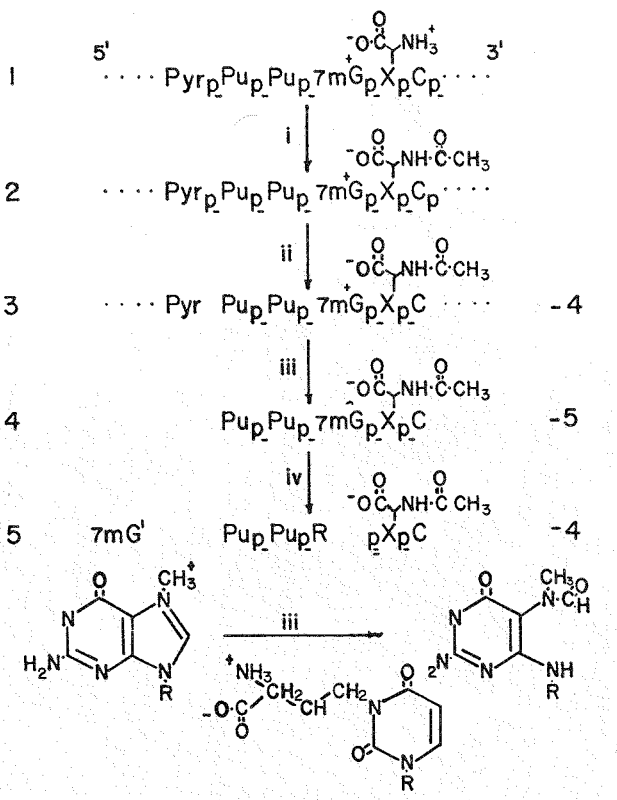

Fig. 2. Schematic representation of an ABA-4 containing oligonucleotide. The steps in the sequence are (i) acetylation; (ii) hydrolysis with pancreatic RNase; (iii) hydrolysis with ammonia; and (iv) cleavage with aniline acetate at pH 3.5. The figure is discussed in more detail in the text.

in which case, the smallest possible oligonucleotide, 7mGpXpC, would be generated.

(4) Elimination of the positive charge of 7mG by treatment with mild alkali. The structural conversion is shown in more detail at the bottom of Fig. 2.

(5) Cleavage of the open ring form of 7mG induced by aniline acetate at pH 3.5. Notice particularly that the phosphate which had linked 7mG to its adjacent 3'-nucleotide in the intact structure is transferred to that neighboring nucleotide. Since this phosphate is terminal, it supplies two negative charges to an associated oligonucleotide.

The scheme predicts that all oligonucleotides containing acetylated X residues which have as immediate neighbors a 5'-7mG and a 3'-pyrimidine, first, should increase by a net negative charge after mild alkaline hydrolysis and, second, undergo transformation to a single oligonucleotide of net charge -4 after aniline acetate treatment. The

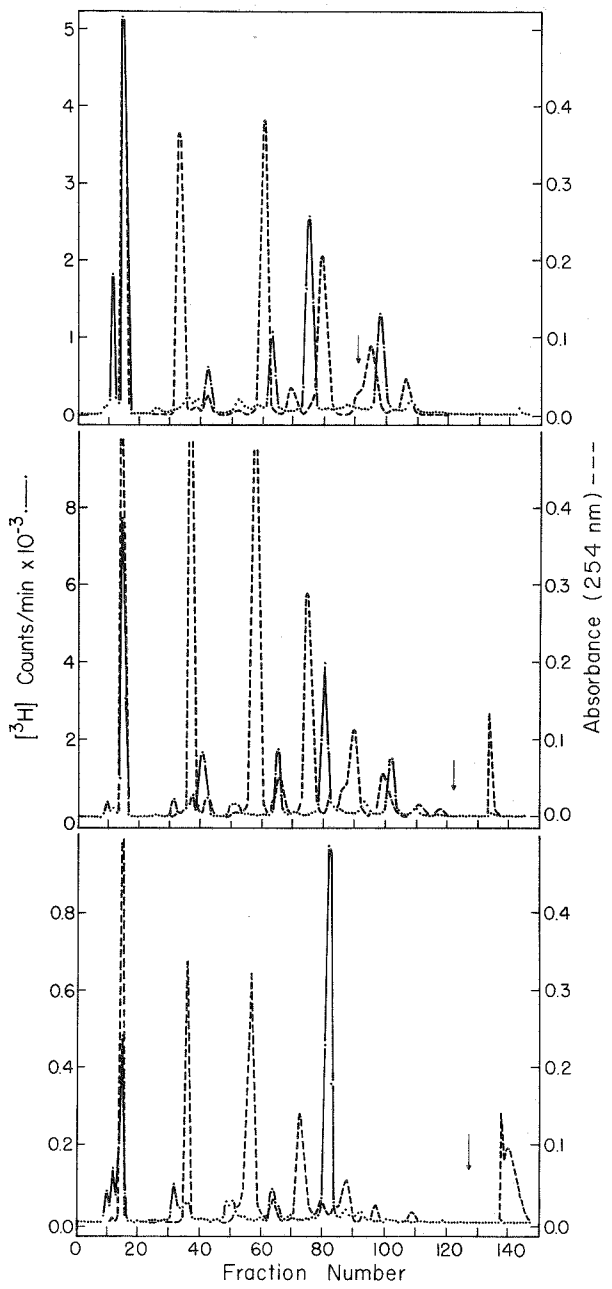

Fig. 3. Effects of Zachau's specific cleavage procedure for 7mG on the ^{3}H-acetylated pancreatic RNase oligonucleotides of *E. coli* B. The panels are patterns obtained after no additional treatment (top), ammonia hydrolysis (middle), and acidic aniline acetate cleavage (bottom).

results of treating ^{3}H-acetylated *E. coli* B by this protocol is shown in Fig. 3. Similar data (not shown) have been obtained with strain K12. The panels of Fig. 3 (from top to bottom) show the experimental results corresponding to steps 3, 4, and 5 of Fig. 2. The three major oligonucleotides I, II, and III give rise to species with a more negative charge after ammonia treatment. Close examination of the control patterns of *E. coli* B and K12 shown in Fig. 1, as well as the control of Fig. 3, shows that there are minor labeled species in positions corresponding to those obtained after ammonia treatment. We interprete these as arising from 7mG ring opening which occurred during the period of hydrolysis with RNase or possibly during preparation of the RNA. The extent of ammonia-induced shift for III (viz. from a position to the right of the pentamer absorbancy to a position to the right of the hexamer absorbancy) is of the expected magnitude for a species which has increased by a net negative charge. Oligonucleotides I and II, although they have clearly shifted in the right direction, have undergone a shift of less than the expected magnitude. This may indicate that these three oligonucleotides have a more complex structural relationship to one another than that envisioned in our theoretical scheme. The chromatographic behavior of the controls is also indicative of complexity, since species I, II, and III do not differ in mobilities by integral charge units as is predicted by a common 7mGpXpC preceded by a variable number of purines. Examination of the ammonia-treated sample shows that these have relative mobilities more like those which are theoretically expected. More work will be required to determine whether this unexpected behavior has to do with the nature of the polypurine sequence, the X base, or some as yet unformulated possibility. The bottom panel of Fig. 3 shows the effects of aniline acetate. A single major peak is formed with an apparent net charge of about -3.5. This major peak accounts for 83.5% of the total label of charge -2 or greater. The percent conversion of I, II, and III to the major product can be calculated to be 51, 95, and 85%, respectively. The aniline cleavage product has not yet been completely characterized. This should be accomplished easily by hydrolysis with the non-specific nuclease T2, which should give a mononucleoside diphosphate and a nucleoside. Demonstration that the acetylated nucleoside X is liberated as a diphosphate would constitute proof that its immediate 3'-neighbor was 7mG. This already seems likely from the data presented. The charge of the acidic aniline product suggests that it is a nucleoside diphosphate. Separation of the

acetylated nucleoside from 7mG by an additional interspersed purine would have given a product of expected charge -5, which is clearly inconsistent with the data. Moreover, the fact that acidic aniline gives rise to a single product with a charge which is greater than two of its precursors, I and II, eliminates the possibility that X is to the 5' of 7mG since, in that case, the product or products would have to be of lower charge. From the specificity of pancreatic RNase, the 3'-member of the dinucleoside diphosphate must be a susceptible pyrimidine, thus requiring that X be the 5'-member and, therefore, adjacent to 7mG.

Our data suggest possible roles which adjacent 7mG and ABA-4 may have in the maintenance of particular conformational states. The pronounced alkaline lability of 7mG has been discussed. As the free nucleoside, quantitative conversion to the open ring form is effected by incubation in 1 N ammonia at 37°C for 1 h. The acetylated oligonucleotides are more stable. Figure 4 shows oligonucleotide II after a 0.5-h incubation at 37°C in 1 N ammonia. Only 40% conversion to the open ring has occurred. It is likely that the carboxyl of ABA-4 interacts with the positively charged 7mG and shields it from nucleophilic attack by hydroxyl ion. Molecular models show that such an ionic bond is sterically possible. Detailed three-dimensional models of

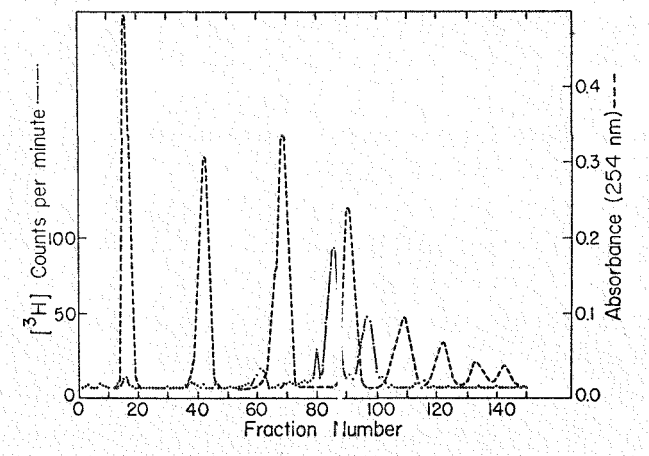

Fig. 4. The effects of ammonia on the ^{3}H-acetylated oligonucleotide II. Oligonucleotide II (see text) from *E. coli* K12 was dissolved in 1 N ammonia and incubated for 1 h at 37°C. After removal of ammonia by lyophilization, a cold pancreatic digest of RNA was added as an absorbancy marker, and the mixture was fractionated by DEAE-urea chromatography.

yeast phenylalanine t-RNA based on crystal X-ray diffraction measurements show that the variable loop contributes significantly to the tertiary structure. The uridine in the variable loop, which is modified to form X in the *E. coli* t-RNAs we have been discussing, is the only nucleoside in that part of the molecule which is freely accessible. In particular, both of its immediate neighbors, 7mG and 7C, are interacting with nucleosides in the dihydrouridine loop and its stem. These interactions are, in part, responsible for the L-shaped conformation which the molecule assumes.[7,8] If the exposed X could undergo reversible modification at its amino or carboxyl, it is possible that the modified X would interact differently with 7mG and allow the molecule to assume alternative three-dimensional conformations. Such altered conformations might expose previously sequestered nucleotides for interaction with ribosomes or other cellular components.

REFERENCES

1. M. D. Enger and A. G. Saponara, "Incorporation of ^{14}C from [2-^{14}C]Methionine into 18S but not 28S RNA of Chinese Hamster Cells," J. Mol. Biol. 33, 319-322 (1968).

2. A. G. Saponara and M. D. Enger, "The Isolation from Ribonucleic Acid of Substituted Uridines Containing α-Aminobutyrate Moieties Derived from Methionine," Biochim. Biophys. Acta 349, 61-77 (1974).

3. Z. Ohashi, M. Maeda, J. A. McCloskey, and S. Nishimura, "3-(3-Amino-3-carboxypropyl)Uridine: A Novel Modified Nucleoside Isolated from *E. coli* Phenylalanine Transfer RNA," Biochemistry 13, 2620-2625 (1974).

4. S. Friedman, H. J. Li, K. Nakanishi, and G. Van Lear, "3-(3-Amino-3-carboxy-n-propyl)Uridine. The Structure of the Nucleoside in *Escherichia coli* Transfer Ribonucleic Acid that Reacts with Phenoxyacetoxysuccinimide," Biochemistry 13, 2932-2937 (1974).

5. W. Wintermeyer and H. G. Zachau, "A Specific Chemical Chain Scission of t-RNA at 7-Methylguanosine," FEBS Letters 11, 160-164 (1970).

6. N. de Groot, Y. Lapidot, A. Panet, and Y. Wolman, "The Synthesis of N-Acetylphenylalanyl-sRNA," Biochem. Biophys. Res. Commun. 25, 17-22 (1966).

7. S. H. Kim, F. L. Suddath, G. J. Quigley, A. McPherson, J. L. Sussman, A. H. J. Wang, N. C. Seeman, and A. Rich, "Three-Dimensional Tertiary Structure of Yeast Phenylalanine Transfer RNA," Science 185, 435-440 (1974).

8. J. D. Robertus, J. E. Ladner, J. T. Finch, D. Rhodes, R. S. Brown, F. B. C. Clark, and A. Klug, "Structure of Yeast Phenylalanine t-RNA at 3 Å Resolution," Nature 250, 546-551 (1974).

Messenger-Related RNA Metabolism in Cultured Chinese Hamster Cells

(M. D. Enger, E. W. Campbell, and J. L. Hanners)

Animal cells contain a number of messenger-related RNA species whose exact relationship to polysomal messenger RNA (mRNA) has not been fully determined. Heterogeneous nuclear RNA (HnRNA), for example, is known to include within its total population a relatively small number of molecules which are precursors to mRNA.[1-7] However, the quantitative and qualitative relationship of the bulk HnRNA population, which is degraded within a short time without leaving the nucleus, to the pre-mRNA population is obscure. A population of messenger-like RNA exists similarly in the cytoplasm unassociated with ribosomes.[8-11] This population is associated with protein to form particles called informosomes.[10] At least one defined messenger RNA has been detected in such a ribosome-free ribonucleoprotein form.[12,13] The relationship of the bulk informosomal mlRNA population to the polysomal mRNA population again is not defined. That is, informosomes may represent intermediates in messenger RNA processing, being products of HnRNA and precursors to mRNA. Such a possibility could obtain for all of the informosome population, giving a simple relationship among the species such that (HnRNA) $K_1 \rightarrow$ (mlRNA) $K_2 \rightarrow$ mRNA. Part or all of the informosome population alternatively could be so constituted as to prevent association with ribosomes and, thus, would represent temporarily or permanently repressed cytoplasmic messenger species. Such a population could be metabolically distinct from ribosome-associable mRNA and could perhaps even derive from a distinguishable fraction of HnRNA. In such instance, the mlRNA population could conceivably be stimulated or repressed independently of mRNA.

Analysis of messenger-related RNA metabolism subsequent to exposure to moderate doses of ionizing radiation indicated that this agent provides just such a differential stimulus: in the later portion of division delay following irradiation, the incorporation of nucleoside precursors into HnRNA or mRNA is stimulated relative to that into mlRNA.[14] On a per aliquot basis, HnRNA and mRNA incorporation increased 23 to 30%, with no increased mlRNA incorporation. This suggests that, unless radiation alters processing constants, there is not a simple precursor-product relationship among the totality of HnRNA, mlRNA, and mRNA populations.

These results raised questions concerning the nature of the radiation-induced stimulation of HnRNA and mRNA incorporation. Since x-irradiation induces division delay and accumulation in G_2,[15] the possibility existed that the effect actually resulted from the fact that RNA metabolism patterns change during the cell cycle. This possibility was advanced when it was found that analysis of irradiated and control populations synchronized in the same portion of the life cycle at time incorporation was measured showed there to be little or no direct radiation effect.[16] These observations predicted that examination of relative synthesis (incorporation) rates for HnRNA, mlRNA, and mRNA would reveal quantitative differences in their rate changes during the cell cycle. Direct analysis of synthetic patterns in synchronized cells tested this prediction.[17] Cultured Chinese hamster ovary cells were synchronized by mitotic selection. Relative synthesis rates for informosomal messenger-like RNA (mlRNA), polysomal messenger RNA (mRNA), and heterogeneous nuclear RNA (HnRNA) were estimated from the amount of labeled adenosine or uridine incorporated into these species in early and late interphase. The amounts of uridine incorporated into HnRNA, mRNA, and mlRNA during a pulse administered 9.75 to 10.75 h post-mistosis were 3.48, 4.64, and 2.82 times the amounts incorporated 1.5 to 2.5 h post-mitosis. Adenosine incorporation values 9.5 to 11 h post-mitosis were 1.64 (HnRNA), 2.49 (mRNA), and 1.18 (mlRNA) times the 1.5- to 3.0-h values. The relative incorporation into mRNA of large polysomes corresponded to incorporation into mRNA of small polysomes. Thus, synthesis rates of mRNA, mlRNA, and HnRNA were found to increase during interphase in a non-coordinate fashion.

An additional fact was made apparent in these studies that was not immediately obvious in the radiation-effects studies: mRNA and HnRNA synthesis (nucleoside incorporation) rates do not increase to the same extent. Interestingly, the increase in HnRNA synthesis is *intermediate* in magnitude,

compared to the cycle-dependent increases in mRNA and mlRNA synthesis. These results suggest the consideration of a non-linear relationship among these species, one involving distinguishable HnRNA populations serving as precursors to mRNA and mlRNA in an independent fashion. Most importantly, the cell-cycle-dependent changes in messenger-related RNA metabolism demonstrated by these investigations suggest that synchronized populations may provide a useful tool for further defining the relationships among these species.

REFERENCES

1. J. D. Darnell, G. N. Pagoulatos, U. Lindberg, and R. Balint, Symposia on Quantitative Biology 35, 555-560 (1970).
2. J. E. Darnell, L. Philipson, R. Wall, and M. Adesnik, Science 174, 505-510 (1971).
3. M. Edmonds, M. H. Vaughan, Jr., and H. Nakazato, Proc. Natl. Acad. Sci. USA 68, 1336-1340 (1971).
4. W. Jelinek, M. Adesnik, M. Sadlitt, D. Sheiness, R. Wall, G. Molloy, L. Philipson, and J. E. Darnell, J. Mol. Biol. 75, 515-532 (1973).
5. R. H. Stevens and A. R. Williamson, Nature 245, 101-104 (1973).
6. T. Imaizumi, H. Diggelmann, and K. Scherrer, Proc. Natl. Acad. Sci. USA 70, 1122-1126 (1973).
7. M. MacNaughton, K. B. Freeman, and J. O. Bishop, Cell 1, 117-125 (1974).
8. R. P. Perry and D. E. Kelley, J. Mol. Biol. 35, 37-59 (1968).
9. E. C. Henshaw and J. Loebenstein, Biochim. Biophys. Acta 199, 405-420 (1970).
10. K. Scherrer, G. Spohr, N. Gran Boulan, C. Morel, J. Grosclaude, and C. Chezzi, Symposia on Quantitative Biology 35, 539-559 (1970).
11. A. S. Spirin, Eur. J. Biochem. 10, 20-35 (1969).
12. G. D. Olsen, P. Gaskill, and D. Kabat, Biochim. Biophys. Acta 272, 297-304 (1972).
13. E. S. Gander, A. G. Stewart, C. M. Morel, and K. Scherrer, Eur. J. Biochem. 38, 443-452 (1973).
14. M. D. Enger, E. W. Campbell, and R. A. Walters, Biochim. Biophys. Acta 324, 120-132 (1973).
15. R. A. Walters, L. R. Gurley, R. A. Tobey, M. D. Enger, and R. L. Ratliff, Radiation Res. 51, 455 (1972).
16. M. D. Enger, R. A. Walters, and E. W. Campbell, Biochim. Biophys. Acta 353, 227-237 (1974).
17. M. D. Enger and E. W. Campbell, "RNA Synthesis in Chinese Hamster Cells. III. Non-Coordinate Increases during Interphase in Synthesis Rates for Informosomal, Polysomal, and Heterogeneous Nuclear RNAs," Biochim. Biophys. Acta (1974), submitted.

The Involvement of Histone Phosphorylation with Cell Proliferation, DNA Replication, and Chromosome Condensation

(L. R. Gurley, R. A. Walters, R. A. Tobey, J. G. Valdez, J. L. Hanners, and P. C. Sanders)

Chromosome formation and mitotic cell division are fundamental to all eukaryote life. In cancer cells, these processes are under less restricted control than in normal cells; therefore, an understanding of the control of these processes is necessary if the mechanisms of carcinogenesis are to be determined.

Recent experiments in this Laboratory have demonstrated that histone phosphorylation is involved in the conversion of nondividing cells into dividing cells.[1-3] Furthermore, results were obtained implicating histone phosphorylation in the mechanism of mitosis.[4-6] The potential importance of the relationship of histone phosphorylation to cell proliferation[3,5,6] has made it necessary to extend our investigations to determine the details of these phosphorylation events.

Using synchronized Chinese hamster cells (line CHO), we have determined that three of the five histones are phosphorylated significantly.[1-9] Histone f2a2 phosphorylation occurs in nonproliferating cells as well as in all the cell-cycle phases of proliferating cells.[1-9] Therefore, the phosphorylation of this particular histone is not correlated with any cell growth parameter.[2] However, the phosphorylations of histones f1 and f3 are correlated with specific cell growth parameters.[3-6] Histone f1 phosphorylation is absent in nonproliferating cells but is activated in the G_1 phase of proliferating cells.[3,5,6] This f1 histone is further superphosphorylated just prior to cell division at mitosis.[5,6] Histone f3 is not phosphorylated in any phase of interphase cells, but it is rapidly phosphorylated at mitosis simultaneously with the f1 superphosphorylation.[5,6]

It has been demonstrated by Kinkade and Cole[10] that histone f1 is composed of several different

subfractions. Also, we have subfractionated histone f3 into two subfractions.[8] Therefore, the question arises: does the phosphorylation of histones f1 and f3 occur on all f1 and f3 subfractions or preferentially on one subfraction? We have observed that the f1 phosphorylation rate accelerates as cells traverse S and G_2.[3,5] Is this accelerated phosphorylation simply the result of an increase in the phosphorylation rate, or is it due to (a) different f1 subfractions being phosphorylated at different times, (b) new sites being phosphorylated in late interphase, or (c) a larger proportion of the f1 molecules being phosphorylated in late interphase? Similarly, what is the nature of the superphosphorylation of f1 at mitosis?

By modifying the ion exchange column chromatography method of Kinkade and Cole,[10] we were able to separate the various f1 subfractions from each other while, at the same time, separating the phosphorylated f1 from its unphosphorylated parent (see Fig. 1a). Alkaline phosphatase treatment of f1 resulted in the loss of the phosphorylated f1 fraction, indicating that incorporated $^{32}PO_4$ existed in f1 as a monoesterified phosphate in interphase cells (see Fig. 1b). CHO f1 was found to consist of five unphosphorylated subfractions, one subfraction existing in great excess (74%) over the others (see Fig. 1b). In exponential cultures, 29% of the f1 was phosphorylated (see Fig. 1a).

To determine the detailed nature of f1 phosphorylation in early interphase, cells were pulse-labeled with $^{32}PO_4$ during G_1 and S following synchronization in early G_1 by isoleucine deficiency.[11] Ion exchange chromatography of histone f1 isolated from these cells demonstrated that two phosphorylated forms of f1 existed in early interphase (Fig. 2). The first phosphorylated form appeared early in the cell cycle (Fig. 2B). The second phosphorylated form appeared later in the cycle as a shoulder on the first phosphorylated form (Figs. 2C and 2D) and had a $^{32}P/^{3}H$ ratio twice that of the first phosphorylated form. Analysis of these chromatographs demonstrated that all f1 subfractions were phosphorylated rather than one particular f1 subfraction and that phosphorylation began in G_1 preceding S phase by 2 h (Fig. 3). From a plot of the relationship of S phase to the two different phosphorylated forms of f1 (Fig. 4), it was clear

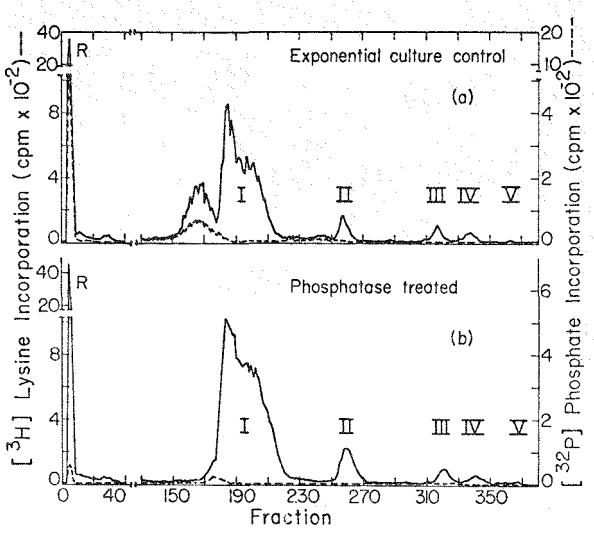

Fig. 1. Separation of CHO histone f1 into subfractions I, II, III, IV, and V and their phosphorylated and nonphosphorylated forms. Histone f1 was isolated from CHO cells as previously described[15] except that 0.05 M sodium bisulfite was present in all extraction solutions. Subfractionation of f1 was performed by a modification of ion exchange column chromatography on Bio-Rex 70.[16] (a) f1 isolated from an exponential culture; and (b) alkaline phosphatase-treated f1 isolated from an exponential culture. The cultures were labeled for five generations with [^{3}H]-lysine (——) and pulse-labeled for 1 h with $^{32}PO_4$ (---).

that two different cell-cycle-dependent phosphorylation events existed in early interphase. The first event began in G_1 and the second event precisely at the time when cells entered S phase.

To determine the nature of f1 phosphorylation in late interphase, cells were pulse-labeled with $^{32}PO_4$ during S and G_2 following synchronization at the G_1/S boundary by a combination of isoleucine-deficiency and hydroxyurea treatments.[12] Ion exchange chromatography of f1 from cells arrested in late G_1 by hydroxyurea confirmed that only the first phosphorylated form of f1 existed in G_1 (Fig. 5A). Analysis indicated that this phosphorylation occurs on only 20% of the "old" presynthesized f1 molecules in G_1 prior to the beginning of S phase. Cells in S and G_2 were found to contain both phosphorylated forms of f1, one form containing twice the $^{32}PO_4$ of the other (Figs. 5B and 5C). The mitotic-rich culture contained two new phosphorylated fractions preceding the first phosphorylated form of f1 (Fig. 5D). The $^{32}P/^{3}H$ ratio of both these new forms was approximately four times that observed in the first phosphorylated form. The pattern of phosphorylation for

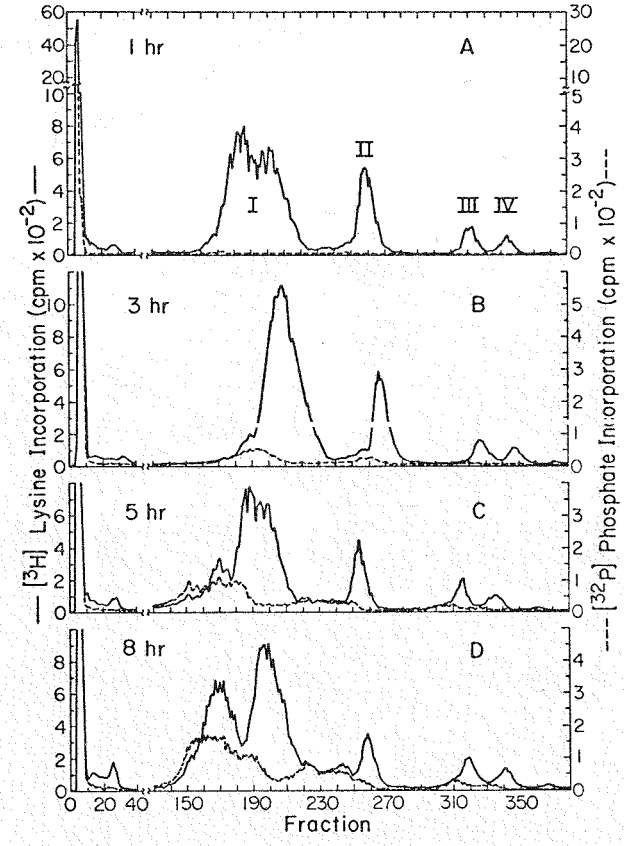

Fig. 2. Column chromatography of f1 isolated from synchronized CHO cells traversing the G_1 and S phases. [^{3}H]Lysine prelabeled cultures were synchronized in early G_1 by isoleucine deficiency and then released by adding isoleucine. The cultures were pulse-labeled with $^{32}P_i$ for 1 h prior to harvest at (A) 1 h; (B) 3 h; (C) 5 h; and (D) 8 h after release. [^{3}H]Lysine incorporation (——) and $^{32}P_i$ incorporation (---).

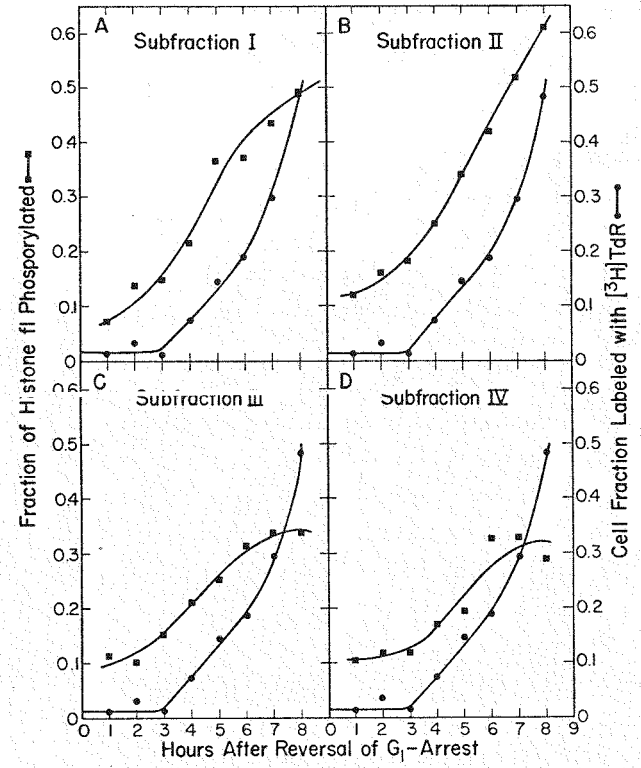

Fig. 3. Relationship between entry of cells into S phase and phosphorylation of the various f1 subfractions shown in Fig. 2: (A) subfraction I; (B) subfraction II; (C) subfraction III; and (D) subfraction IV. Phosphorylation of each f1 subfraction is presented as a function of $^{32}P_i$ incorporation per total [^{3}H]lysine incorporated into the sum of the phosphorylated and non-phosphorylated forms of that subfraction (-●-). Fraction of S-phase cells in the culture after release from isoleucine-deficiency synchronization (-●-).

the small subfractions was the same as that observed for the major subfraction I, indicating that these phosphorylation events are general for all molecular species of f1.

Cell-cycle analysis of the various f1 phosphorylated forms (Fig. 6) indicated that the fraction of unphosphorylated f1 steadily decreased as cells traversed late interphase. The amount of f1 in the first phosphorylated form [i.e., that phosphorylated form which first appeared in G_1 ($f1_{G_1}$)] rises and accumulates through S and G_2. The amount of f1 in the second phosphorylated form [i.e., that phosphorylated form which first appeared in S phase ($f1_S$)] rises in S but does not reach a very large proportion, suggesting that $f1_S$ phosphorylation is a transitory event. The rapid increase in the phosphorylated forms of f1 in metaphase-rich cultures suggests that this third phosphorylation event ($f1_M$) is associated specifically with mitosis.

From calculations of the electrophoretic mobility reduction resulting from the $f1_{G_1}$ phosphorylation event, it is concluded that $f1_{G_1}$ phosphorylation involves one phosphorylation site. It is tentatively concluded from the $^{32}P/^3H$ ratios of the various phosphorylated forms in Figs. 2 and 5 that the $f1_S$ phosphorylation event involves an additional phosphorylation site and that the $f1_M$ phosphorylation event involves three additional phosphorylation sites.

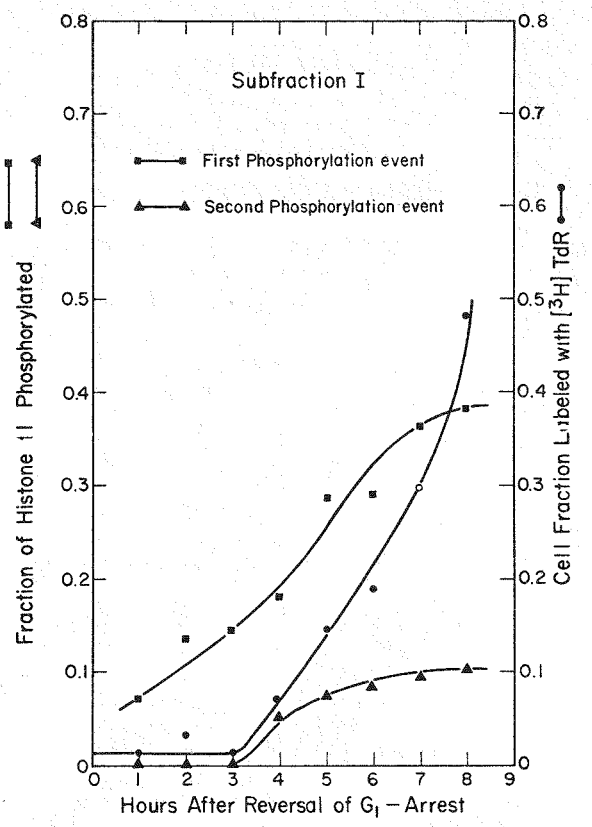

Fig. 4. Fraction of f1 subfraction I existing in different phosphorylated forms after release from G_1-arrest. The fraction of S-phase cells in the culture after release from isoleucine-deficiency synchronization (-●-). The fraction of f1 in the first occurring phosphorylated form (-■-) was estimated from the phosphorylated peak immediately preceding the unphosphorylated form in Fig. 2. The fraction of f1 in the second occurring phosphorylated form (-▲-) was estimated from the greater phosphorylated shoulder on the left side of the phosphorylated peak in Fig. 2.

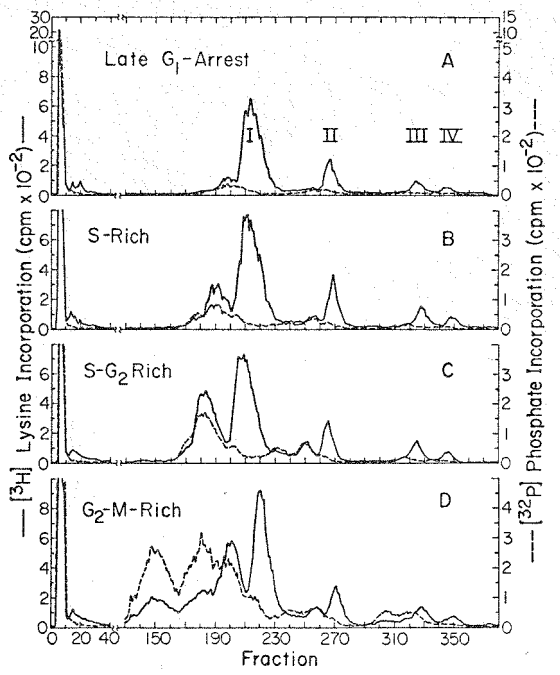

Fig. 5. Column chromatography of histone f1 isolated from synchronized CHO cells traversing the S and G_2 phases. [^{3}H]Lysine prelabeled cultures were synchronized by isoleucine deficiency, resynchronized at the G_1/S boundary with hydroxyurea, and then released to traverse late interphase by resuspending the cells in hydroxyurea-free medium. Cultures were then pulse-labeled for 1 h with $^{32}P_i$ and immediately harvested thereafter at the various times indicated by arrows in Fig. 6A: (A) culture synchronized at the G_1/S boundary by exposure to hydroxyurea for 8 h (98.2% G_1 and 1.8% S cells) and harvested without release into S phase; (B) S-rich culture (17% G_1 and 83% S cells) harvested 3.5 h after release from hydroxyurea blockade; (C) S-G_2-rich culture (17% G_1, 49% S, and 34% G_2 cells) harvested 6 h after release from hydroxyurea blockade; and (D) G_2-M-rich culture (17% G_1, 12% S, 29% G_2, and 42% M cells) harvested 9 h after release from hydroxyurea blockade (Colcemid was added to this culture 4.5 h after release to prevent the cells from passing through mitosis into G_1). [^{3}H]-Lysine incorporation (——) and $^{32}P_i$ incorporation (---).

The phosphorylation of f1 and f3 histones associated with mitosis was investigated using cultures highly synchronized at mitosis by mitotic selection.[13] By ion exchange chromatography of f1, it was observed that all f1 molecules were phosphorylated to the $f1_M$ form in cells undergoing the transition from G_2 to mitosis (Fig. 7A). Cells also exhibited $f1_M$ phosphorylations while being held in metaphase arrest (Fig. 7B). When cells labeled with $^{32}PO_4$ during the G_2 to M transition were allowed to reenter G_1 in the absence of $^{32}PO_4$, the highly phosphorylated $f1_M$ was rapidly converted back to the nonphosphorylated form (Fig. 7C).

Using the same cell cultures, the mitotic phosphorylation of histone f3 was also investigated using Triton X-100 polyacrylamide gel electrophoresis to subfractionate f3 into two subfractions.[8] The high rate of f3 phosphorylation was observed to occur on both f3 subfractions during the transition from G_2 to M (Fig. 8B) and during metaphase arrest (Fig. 8C). As was the case with $f1_M$ phosphorylation, the $^{32}PO_4$ incorporated into f3 during mitosis was rapidly lost when the cells were allowed to reenter G_1 in the absence of $^{32}PO_4$ (Fig. 8D). It is

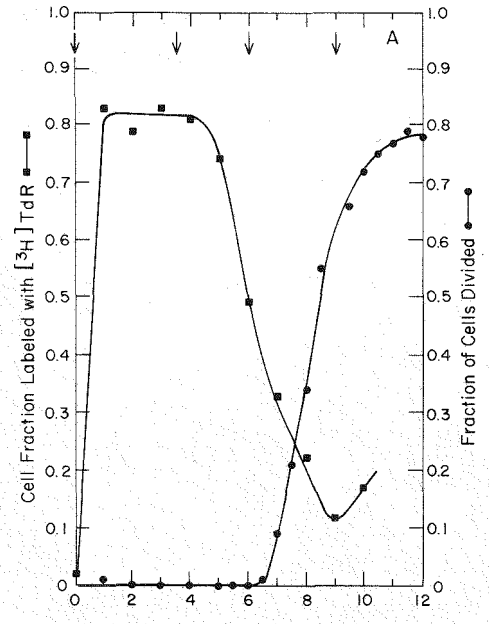

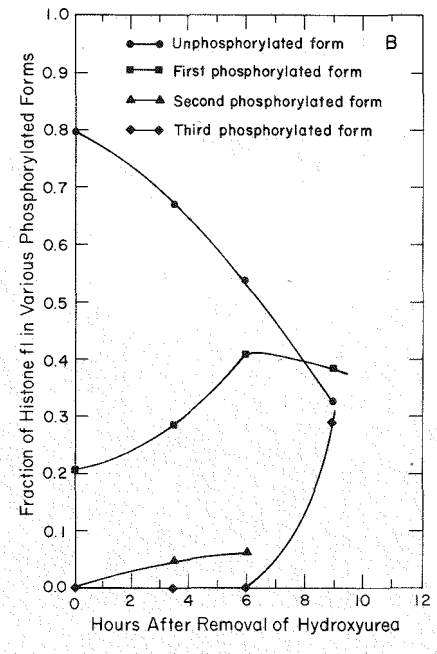

Fig. 6. Fraction of f1 subfraction I existing in the various phosphorylated forms during late interphase: (A) cell-cycle kinetics of CHO cultures released from hydroxyurea resynchronization at the G_1/S boundary. The arrows indicate the time cells were harvested following a 1-h pulse with $^{32}P_i$. Fraction of cells in S phase (-■-) and fraction of cells divided (-●-) were determined from an unlabeled replica culture. (B) The fraction of unphosphorylated f1 (-●-) was estimated from the unphosphorylated peak of subfraction I in Fig. 5. The fraction of f1 in the first phosphorylated form (-■-) was estimated from the phosphorylated peak immediately preceding the unphosphorylated form in Fig. 5. The fraction of f1 in the second phosphorylated form (-▲-) was estimated from the greater phosphorylated shoulder on the left side of the phosphorylated peaks in Figs. 5B and 5C. The fraction of f1 in the third phosphorylated form (-◆-) was estimated from the sum of the two highly phosphorylated peaks (fraction numbers 130-190) having similar $^{32}P/^{3}H$ ratios in Fig. 5D.

concluded that phosphorylation of f3 is a general mitotic event occurring on all f3 subfractions.

From these studies, we have extended our description of the cell-cycle-dependent histone phosphorylation (Fig. 9). By correlating these phosphorylation events with other sequential events of the cell cycle, we hope to get some insight concerning the function of this modification.[5,6] For example, the first cell-cycle-dependent histone phosphorylation event, $f1_{G_1}$, occurs concomitantly with an enhanced association of DNA with lipoprotein in G_1 approximately 2 h prior to entry of CHO cells into S phase.[14] Also, as cells progress through S and G_2, the association of DNA with lipoprotein is enhanced over that observed in late G_1.[14] Similarly, $f1_{G_1}$ phosphorylation was observed to accumulate in chromatin during S and G_2. These observations have led us to speculate that this $f1_{G_1}$ phosphorylation event may trigger chromatin structural changes involving lipoprotein which are necessary for the conversion of nonproliferating cells to proliferating cells. Maintenance of this $f1_{G_1}$ phosphorylation and the DNA-lipoprotein complex through S and G_2 suggests that this chromatin structural change may be necessary for the orderly separation of daughter DNA molecules following genome replication.

The second f1 phosphorylation event ($f1_S$ in Fig. 9) begins exactly when cells enter the S phase, suggesting that this event may be directly involved with DNA synthesis or with the deposit of newly synthesized f1 on the newly synthesized DNA. The transitory existence of phosphorylated $f1_S$ throughout S phase opens for consideration the speculation that $f1_S$ phosphorylation may occur only at the site of the DNA replication fork and that $f1_S$ is then dephosphorylated when the replication fork has passed that part of the chromatin on which that f1 molecule is located.

The high phosphorylation rate of f3 and $f1_M$, beginning at prophase and continuing through metaphase, followed by the rapid dephosphorylation of these histones when cells reenter G_1 (Fig. 9),

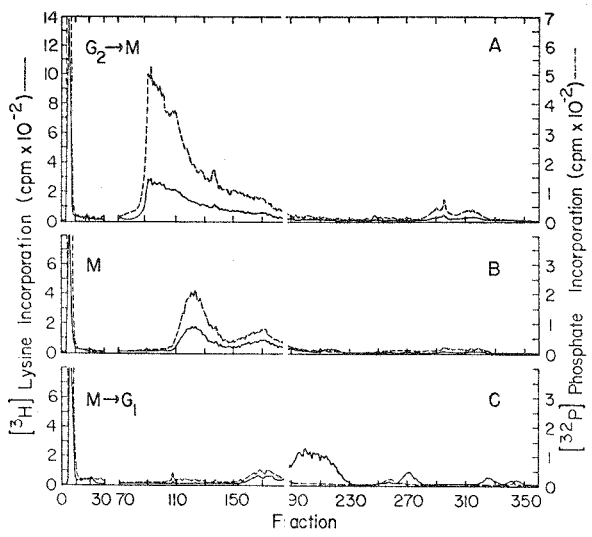

Fig. 7. Column chromatography of histone f1 isolated from mitotic cells. [^{3}H]Lysine prelabeled cells were grown exponentially in monolayer culture: (A) metaphase cells were accumulated in the presence of Colcemid and $^{32}P_i$ for 2 h and removed by mitotic selection to produce a culture labeled with $^{32}P_i$ while traversing from G_2 into metaphase (i.e., $G_2 \rightarrow M$ cells). (B) Metaphase cells were accumulated for 2 h in the presence of Colcemid and removed by mitotic selection. These cells were then labeled for 2 h with $^{32}P_i$ while arrested in metaphase (i.e., M cells). (C) Metaphase cells labeled with $^{32}P_i$ during the $G_2 \rightarrow M$ transition [as in (A) above] were removed by mitotic selection and resuspended in Colcemid-free medium for 2 h before harvest, which allowed 90% of the cells to reenter G_1 (i.e., $M \rightarrow G_1$ cells).

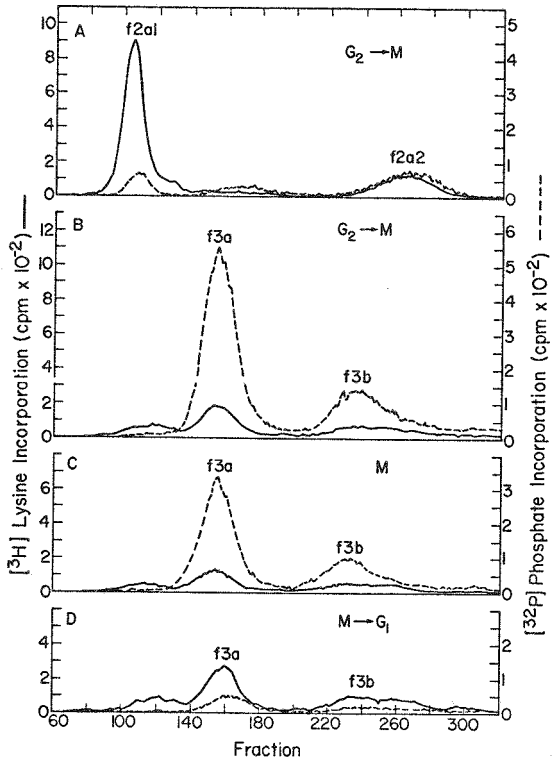

Fig. 8. Preparative Triton X-100 polyacrylamide gel electrophoresis of histones isolated from mitotic cells. Arginine-rich histones were isolated from the same cultures described in Fig. 7: (A) electrophoresis of histones f2a1 and f2a2 obtained from cells incorporating $^{32}P_i$ during the $G_2 \rightarrow M$ transition; (B) electrophoresis of histone f3 obtained from cells incorporating $^{32}P_i$ during the G_2 M transition; (C) electrophoresis of histone f3 obtained from cells incorporating $^{32}P_i$ during metaphase-arrest; and (D) electrophoresis of histone f3 obtained from cells which were labeled with $^{32}P_i$ during the $G_2 \rightarrow M$ transition [as in (B) above] and then allowed to reenter G_1 (i.e., $M \rightarrow G_1$ cells).

coincides with the condensation of chromatin into chromosomes at mitosis, followed by the dispersion of chromosomes following cell division. This fact strongly suggests that f3 and $f1_M$ phosphorylations are involved in some aspect of the formation and maintenance of these condensed chromatin structures.

REFERENCES

1. L. R. Gurley, R. A. Walters, and R. A. Tobey, "The Metabolism of Histone Fractions. VI. Differences in the Phosphorylations of Histones during the Cell Cycle," Arch. Biochem. Biophys. 154, 212 (1973).

2. L. R. Gurley, R. A. Walters, and R. A. Tobey, "The Independence of Histone Phosphorylations from DNA Synthesis," In: Protein Phosphorylation in Control Mechanisms, Miami Winter Symposia (F. Huijing and E. Y. C. Lee, eds.), Vol. 5, p. 297, Academic Press, Inc., New York (1973).

3. L. R. Gurley, R. A. Walters, and R. A. Tobey, "The Metabolism of Histone Fractions. Phosphorylation and Synthesis of Histones in Late G_1-Arrest," Arch. Biochem. Biophys. 164, 469 (1974).

4. L. R. Gurley, R. A. Walters, and R. A. Tobey, "Histone Phosphorylation in Late Interphase and Mitosis," Biochem. Biophys. Res. Commun. 50, 744 (1973).

5. L. R. Gurley, R. A. Walters, and R. A. Tobey, "Cell-Cycle-Specific Changes in Histone Phosphorylation Associated with Cell Proliferation and Chromosome Condensation," J. Cell Biol. 60, 356 (1974).

6. R. A. Tobey, L. R. Gurley, C. E. Hildebrand, R. L. Ratliff, and R. A. Walters, "Sequential Biochemical Events in Preparation for DNA Replication and Mitosis," In: Control of Proliferation in Animal Cells (B. Clarkson and

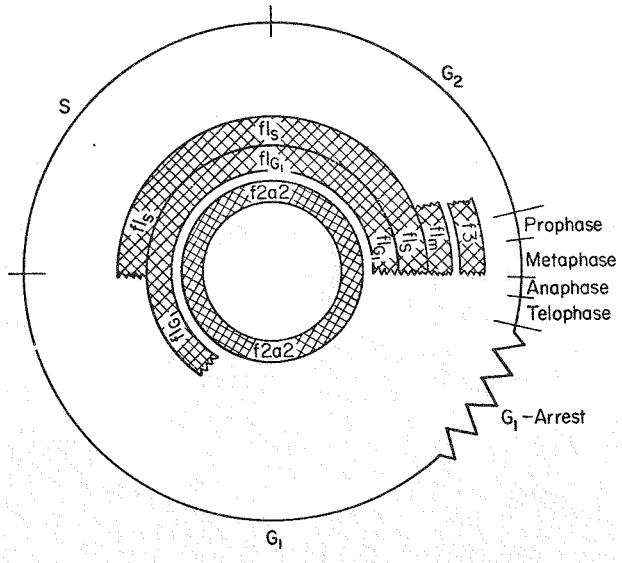

Fig. 9. Relationship of histone phosphorylation to the cell cycle of line CHO Chinese hamster cells. The 16.5-h generation time of these cells in F-10 medium may be divided into 9 h G_1, 4 h S, 3 h G_2, and 0.5 h M.[17] The periods in which histones f1, f2a2, and f3 are phosphorylated are indicated by the shaded bands. $F1_{G_1}$ denotes f1 phosphorylation which begins in the G_1 phase. $F1_S$ denotes f1 phosphorylation which begins in the S phase. $F1_M$ denotes f1 phosphorylation which occurs in mitosis.

R. Baserga, eds.), Vol. 1, p. 665, Cold Spring Harbor Laboratory Press, New York (1974).

7. L. R. Gurley and R. A. Walters, "Response of Histone Turnover and Phosphorylation to X Irradiation," Biochemistry 10, 1588 (1971).

8. L. R. Gurley and R. A. Walters, "Evidence from Triton X-100 Polyacrylamide Gel Electrophoresis that Histone f2a2, not f2b, is Phosphorylated in Chinese Hamster Cells," Biochem. Biophys. Res. Commun. 55, 697 (1973).

9. R. A. Walters, L. R. Gurley, and R. A. Tobey, "Effects of Caffeine on Radiation-Induced Phenomena Associated with Cell-Cycle Traverse of Mammalian Cells," Biophys. J. 14, 99 (1974).

10. J. M. Kinkade and R. D. Cole, "The Resolution of Four Lysine-Rich Histones Derived from Calf Thymus," J. Biol. Chem. 241, 5790 (1966).

11. R. A. Tobey and K. D. Ley, "Isoleucine-Mediated Regulation of Genome Replication in Various Mammalian Cell Lines," Cancer Res. 31, 46 (1971).

12. R. A. Tobey and H. A. Crissman, "Preparation of Large Quantities of Synchronized Mammalian Cells in Late G_1 in the pre-DNA Replicative Phase of the Cell Cycle," Exp. Cell Res. 75, 460 (1972).

13. R. A. Tobey, E. C. Anderson, and D. F. Petersen, "Properties of Mitotic Cells Prepared by Mechanically Shaking Monolayer Cultures of Chinese Hamster Cells," J. Cell. Physiol. 70, 63 (1967).

14. C. E. Hildebrand and R. A. Tobey, "Temporal Organization of DNA in Chinese Hamster Cells: Cell-Cycle Dependent Association of DNA with Membrane," Biochim. Biophys. Acta 331, 165 (1973).

15. L. R. Gurley and J. M. Hardin, "The Metabolism of Histone Fractions. I. Synthesis of Histone Fractions during the Life Cycle of Mammalian Cells," Arch. Biochem. Biophys. 128, 285 (1968).

16. L. R. Gurley, R. A. Walters, and R. A. Tobey, "Sequential Phosphorylation of Histone Subfractions in the Chinese Hamster Cell Cycle," J. Biol. Chem. (1974), in press.

17. R. A. Tobey, "Production and Characterization of Mammalian Cells Reversibly Arrested in G_1 by Growth in Isoleucine-Deficient Medium," In: Methods in Cell Biology (D. M. Prescott, ed.), Vol. 6, p. 67, Academic Press, Inc., New York (1973).

Unique Techniques for Cell-Cycle Analysis Utilizing Mithramycin and Flow Microfluorometry

(R. A. Tobey, M. S. Oka, and H. A. Crissman)

Studies of cell-cycle-specific biochemical events in synchronized cultures[1,2] or kinetic responses to drug treatment[3,4] require precise localization of the population within the cell cycle. Significant effort consequently has been expended to produce highly sophisticated techniques for cell-cycle analysis. In particular, emphasis has been placed upon the capacity for simple and rapid analysis in slowly or nontraversing populations, conditions for which standard analytical techniques are unsatisfactory. Instrumental in these newly developed protocols is the Los Alamos flow microfluorometer (FMF), developed by the Biophysics and Instrumentation Group (H-10).[5]

FMF analysis permits determination of the phase of the cell cycle in which a cell resides based upon DNA content (i.e., a cell in G_2 or M contains twice as much DNA as a G_1 cell, etc.). The principle involved stems from the binding of a fluorescent dye in direct proportion to the cellular DNA content; following excitation, the cells fluoresce, with the intensity proportional to DNA content. In Fig. 1 (lower panels), the acriflavine-Feulgen procedure was utilized to obtain population DNA distributions from exponentially growing cultures of two types of human cells, strain WI38 and line HeLa, along with

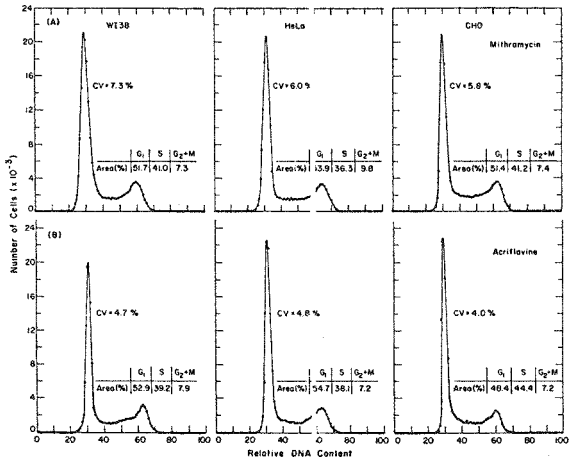

Fig. 1. DNA distributions obtained by FMF analysis of WI38, HeLa, and CHO cells stained with either (A) mithramycin[7] or by the (B) acriflavine-Feulgen procedure.[6] Coefficients of variation (CV) for the G_1 distributions and the percentage of cells in G_1, S, or G_2 plus M were obtained by computer-fit analyses of the DNA distribution curves.

line CHO Chinese hamster cells. The peak at a scale value of approximately 31 represents cells in G_1, while the second peak at a scale value of 62 represents cells in G_2 or M with twice the DNA content; cells in S phase, having replicated different fractions of their DNA, are located at intermediate positions between the two peaks. For convenience, the calculated cell-cycle distribution is presented for each culture. The principal disadvantages of the acriflavine-Feulgen procedure are (a) the complexity (large number) of operations required for dispersal, fixation, and staining,[6] and (b) the duration of the fixation period, 18 h for optimal results.

To circumvent these difficulties, a technique was devised in collaboration with Dr. H. A. Crissman of Group H-10 in which cells were stained with the drug mithramycin. The protocol involves suspension of cells in 25% aqueous ethanol containing 15 mM $MgCl_2$ and 100 µg/ml of mithramycin, with results available *within 20 min* following removal of a sample from an experimental culture.[7] Cell-cycle analyses of exponentially growing cultures of WI38, HeLa, and CHO cells obtained with mithramycin are presented in the upper panels of Fig. 1. It is readily apparent that the mithramycin-generated results are essentially identical to those obtained utilizing the acriflavine-Feulgen procedure, with the added

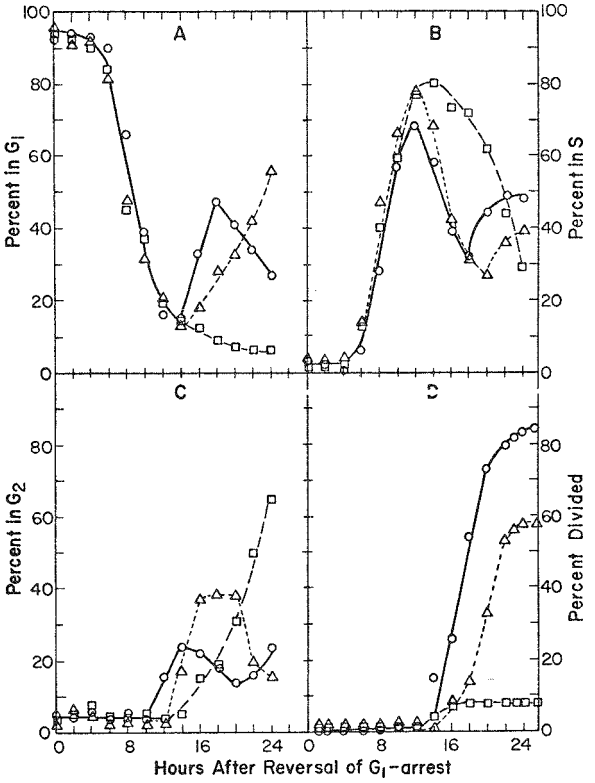

Fig. 2. Progression of synchronized CHO cells through the cell cycle following treatment with streptozotocin or chlorozotocin. Cells arrested in G_1 by cultivation in isoleucine-deficient medium for 36 h were treated for a 2-h period with either 300 µg/ml of streptozotocin (-△-) or 8 µg/ml of chlorozotocin (-□-), then returned to cycle by resuspension in fresh complete medium. An untreated culture served as control (-○-). The drug concentrations employed yielded a survival value of approximately 5%. Following return to complete F-10 medium, the samples were removed for determination of the fraction of cells in each phase of the cell cycle by means of FMF analysis. Cell number determinations were made with an electronic cell counter. The divided fraction represents $N/N_0 - 1$ so that a true population doubling would appear as an increase from 0 to 1 on the scale provided.

features of speed and simplicity of operation (i.e., one centrifugation step preceding staining and FMF analysis).

In view of the rapidity with which results are obtained utilizing the mithramycin-FMF technique, it is now possible to continuously monitor population kinetics in ongoing experiments. For example, in Fig. 2 are presented results obtained in an experiment designed to detect the kinetic response of initially G_1-arrested cells treated with the anticancer drugs streptozotocin or chlorozotocin, then

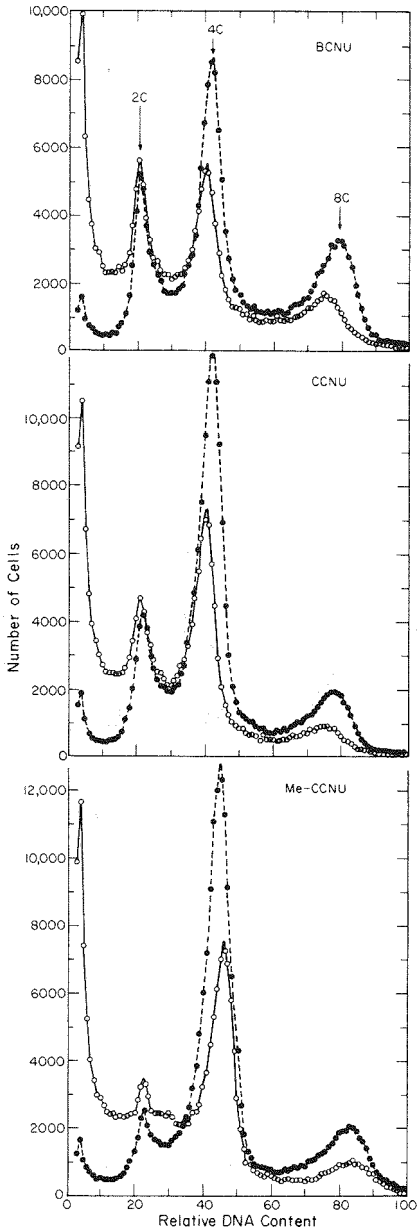

Fig. 3. Detection of DNA distributions in populations of intact cells and in populations of intact plus fragile cells in cultures treated with BCNU, CCNU, or Me-CCNU. Exponentially growing suspension cultures of CHO cells were treated for 2 h with either 10 µg/ml BCNU, 20 µg/ml CCNU, or 18 µg/ml Me-CCNU; then the cells were resuspended in drug-free complete medium. These concentrations of drug yielded 1% survival values. After 4 days, FMF analysis was performed utilizing the standard acriflavine-Feulgen procedure[6] to yield the intact cell DNA population distribution (-O-) or the mithramycin protocol[7] to yield the DNA distribution pattern for intact plus fragile cell populations (-●-). Approximately 200 000 cells were examined in each preparation.

returned to cycle in drug-free medium.[4] Experiments of this nature, which employ a simple, inexpensive cultured cell system, are utilized in an attempt to predict kinetic responses of susceptible tumor cells in man. The results in Fig. 2 indicate that streptozotocin (triangles) (a) did not affect the rate of traverse of G_1; (b) induced a slight increase in time required for progression through S phase, relative to the drug-free control (circles); (c) caused a transitory delay of approximately 4 h in progression through G_2; and (d) allowed part of the population to divide at a rate nearly equivalent to that in the control. In contrast, chlorozotocin (squares) produced a distinct elongation of S phase and caused most of the cells in the population ultimately to accumulate in the G_2 phase of the cell cycle. Note in particular that arrested populations such as those at late times after treatment with chlorozotocin are readily analyzable by FMF analysis, whereas it would be impossible to locate these cells utilizing standard cell-cycle analysis which involves the scoring of ^{3}H-thymidine-labeled cells and the mitotic fraction. Similarly, cells arrested in G_1, or in S phase under conditions where thymidine transport is inhibited, are readily analyzable by FMF analytical techniques.

A difficult but important parameter to assess in drug-treated cultures is the phase (or phases) in the cell cycle in which cells are dying. The acriflavine-Feulgen protocol involves treatment of cells with EDTA, trypsin, and acid hydrolysis,[6] procedures which destroy dying and damaged cells, selectively removing them from the population. Since the mithramycin technique eliminates the manipulations in the standard protocol that destroy fragile cells,[7] duplicate aliquots may be stained with acriflavine (Fig. 3, open circles) or with mithramycin (solid circles), and an attempt may be made to detect differences reflecting cell loss in the Feulgen procedure. In Fig. 3 are results obtained from cycling populations treated for 2 h with the anti-cancer drugs BCNU, CCNU, or Me-CCNU, followed by incubation for 96 h in drug-free medium prior to FMF analysis.[3] The results are most easily interpreted by consideration of the relative *ratios* of 2C (G_1), 4C (G_2 and M), and 8C DNA-containing cells in the cultures stained by the two procedures. For

all three agents, the 4C and 8C DNA-containing cells were reduced proportionately to the greatest extent in the Feulgen-stained cells, indicating that these cells are the most sensitive to disruption and, therefore, are among the first cells to die in treated populations.

FMF data in Fig. 3 yield additional information which is difficult to obtain by other techniques. There is a pronounced broadening of the base of the G_1 (2C) peak in drug-treated cultures which is never observed in untreated cultures. This broadening reflects nondisjunctive errors occurring during mitosis and cell division, resulting in an unequal partitioning of DNA between daughter cells.[8] The drugs also induce the formation of polyploid cells (cells with 8C DNA content). Thus, in addition to its other advantages, FMF analysis permits detection of drug-induced aberrations in progression through mitosis.

In summary, the mithramycin/FMF technique provides a valuable tool for highly detailed cell-cycle analysis, under conditions where standard analytical techniques are unsatisfactory. Among the advantages of the mithramycin/FMF procedure are the ability to (a) monitor population kinetics in ongoing experiments, with the added option of altering an experiment in progress in response to a population change; (b) analyze populations comprised of slowly progressing or arrested cells; (c) monitor populations which have been prelabeled with radiocompounds under conditions where ^{3}H-thymidine autoradiography is impossible; (d) analyze populations devoid of cells in S or M phase; (e) analyze populations containing cells unable to transport ^{3}H-thymidine; (f) detect aberrations in progression through mitosis such as nondisjunction or polyploidization; and (g) distinguish between intact and fragile (dying) cells in drug-treated or virus-infected cells.

REFERENCES

1. R. A. Tobey, L. R. Gurley, C. E. Hildebrand, R. L. Ratliff, and R. A. Walters, "Sequential Biochemical Events in Preparation for DNA Replication and Mitosis," In: Control of Proliferation in Animal Cells (B. Clarkson and R. Baserga, eds.), pp. 665-679, Cold Spring Harbor Laboratory Press, Cold Spring Harbor, New York (1974).

2. R. A. Tobey, L. R. Gurley, C. E. Hildebrand, P. M. Kraemer, R. L. Ratliff, and R. A. Walters, "Sequential Biochemical Events in the Mammalian Cell Cycle," In: Mammalian Cells: Probes and Problems, AEC Life Sciences Symposium Series, Technical Information Center, U. S. Atomic Energy Commission, Oak Ridge, Tennessee (1974), submitted.

3. R. A. Tobey and H. A. Crissman, "Comparative Effects of Three Nitrosourea Derivatives on Mammalian Cell-Cycle Progression," Cancer Res. (1974), in press.

4. R. A. Tobey, M. S. Oka, and H. A. Crissman, "Differential Effects of Two Chemotherapeutic Agents, Streptozotocin and Chlorozotocin, on the Mammalian Cell Cycle," Eur. J. Cancer (1974), in press.

5. D. M. Holm and L. S. Cram, "An Improved Flow Microfluorometer for Rapid Measurement of Cell Fluorescence," Exp. Cell Res. 80, 105 (1973).

6. R. A. Tobey, H. A. Crissman, and P. M. Kraemer, "A Method for Comparing Effects of Different Synchronizing Protocols on Mammalian Cell Cycle Traverse. The Traverse Perturbation Index," J. Cell Biol. 54, 638 (1972).

7. H. A. Crissman and R. A. Tobey, "Cell-Cycle Analysis in Twenty Minutes," Science 184, 1297 (1974).

8. P. M. Kraemer, L. L. Deaven, H. A. Crissman, and M. A. Van Dilla, "DNA Constancy Despite Variability in Chromosome Number," In: Advances in Cell and Molecular Biology (E. J. DuPraw, ed.), Vol. 2, pp. 47-108, Academic Press, Inc., New York-London (1972).

Effects of X-Irradiation on DNA Precursor Metabolism and Deoxyribonucleoside Triphosphate Pools in Chinese Hamster Cells

(R. A. Walters, L. R. Gurley, R. A. Tobey, M. D. Enger, and R. L. Ratliff)

One of the primary early effects of ionizing radiation administered to mammalian cells is the inhibition of incorporation of selected radioactive precursors (primarily thymidine) into DNA. Although such responses generally have been interpreted as a radiation-induced inhibition of DNA synthesis,[1] any effects on DNA precursor metabolism might alter precursor incorporation without actually affecting DNA synthesis. For instance, it has been shown that the degree of inhibition of precursor incorporation into DNA after irradiation was variable when a number of different precursors were used in various cell lines.[2,3] Further, it has been suggested that at least a portion of the x-ray-induced reduction of radioactive thymidine incorporation into DNA

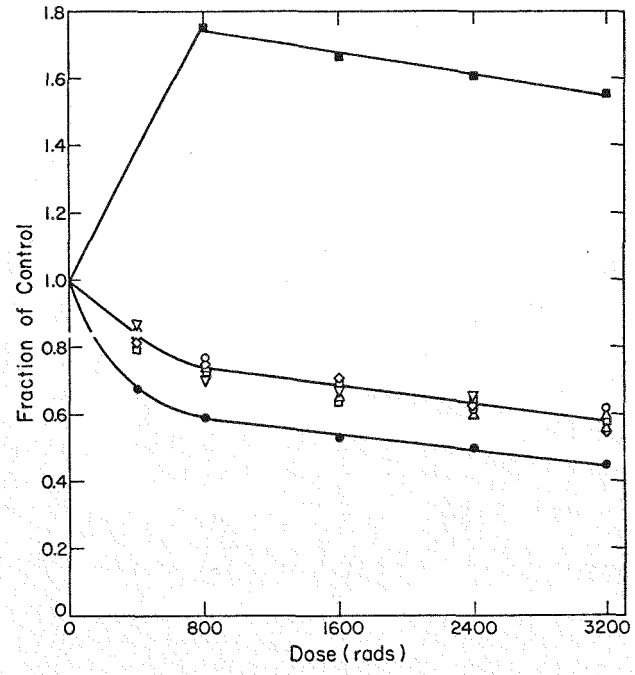

Fig. 1. Effect of increasing x-ray exposures on the incorporation of ^{3}H-labeled precursors into DNA during a 1-h pulse immediately after irradiation. Cells were growing asynchronously at the time of irradiation. Incorporation is expressed as the fraction of the control specific activity (cpm/A_{260}) of the DNA hydrolysate obtained from a modified Schmidt-Thannhauser procedure: (-O-) ^{3}H-guanosine; (-□-) ^{3}H-deoxyguanosine; (-△-) ^{3}H-adenosine; (-◇-) ^{3}H-deoxyadenosine; (-▽-) ^{3}H-thymidine; (-●-) ^{3}H-cytidine; and (-■-) ^{3}H-deoxycytidine.

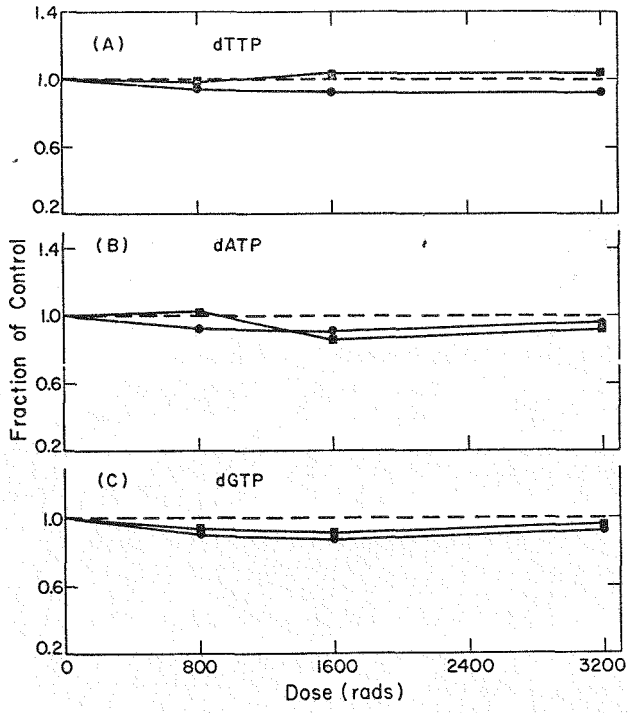

Fig. 2. Effect of increasing exposures of x-irradiation on the size and specific activity of the acid-soluble pools of (A) dTTP labeled with ^{3}H-thymidine; (B) dATP labeled with ^{3}H-deoxyadenosine; and (C) dGTP labeled with ^{3}H-deoxyguanosine. Cells were synchronized by mitotic selection and irradiated 11 h after synchronization. The cells were pulse-labeled with the appropriate precursor for 1 h immediately after irradiation. The data were normalized to the same cell number, then expressed as a fraction of control: (-●-) pool size [dNTP/sample (all panels)]; and (-■-) pool specific activity [^{3}H-dNTP/pmole dNTP (all panels)]. Control pool sizes were 136, 43.4, and 24.1 pmoles/sample of dTTP, dATP, and dGTP, respectively. Control specific activities were 374, 164, and 175 cpm ^{3}H-dNTP/pmole dNTP of dTTP, dATP, and dGTP, respectively.

resulted from an expansion of the thymidine triphosphate pool size and subsequent reduction of the pool specific activity, possibly by limited DNA degradation.[4] Before any conclusions can be drawn concerning the radiation effect(s) on DNA synthesis, it must first be established that the procedures commonly used to measure synthesis rates provide valid assays. For this reason, we have examined the effects of x-irradiation on DNA precursor metabolism and the deoxyribonucleoside triphosphate pools in Chinese hamster cells (line CHO).

Radiation effects on radioactive precursor incorporation into DNA. The data in Fig. 1 show the dose-response curves obtained for the incorporation into DNA of a variety of precursors. It can be seen that the incorporation of thymidine and the ribonucleosides and deoxyribonucleosides of guanine and adenine were experimentally indistinguishable. Cytidine incorporation was reduced to a somewhat greater extent than the others, while deoxycytidine incorporation was greatly stimulated. It can also be seen that the inhibition of precursor incorporation after irradiation followed the biphasic dose-response expected. A similar biphasic dose-response was also obtained after ^{32}P-phosphate labeling (data not shown). We could find no evidence that ^{32}P-phosphate incorporation was either less sensitive to inhibition by irradiation[3,5] or yielded a monophasic, as opposed to an apparent biphasic, dose-response curve.[5]

Radiation effects on acid-soluble deoxyribonucleoside triphosphate pools. The radiation-induced stimulation of deoxycytidine incorporation

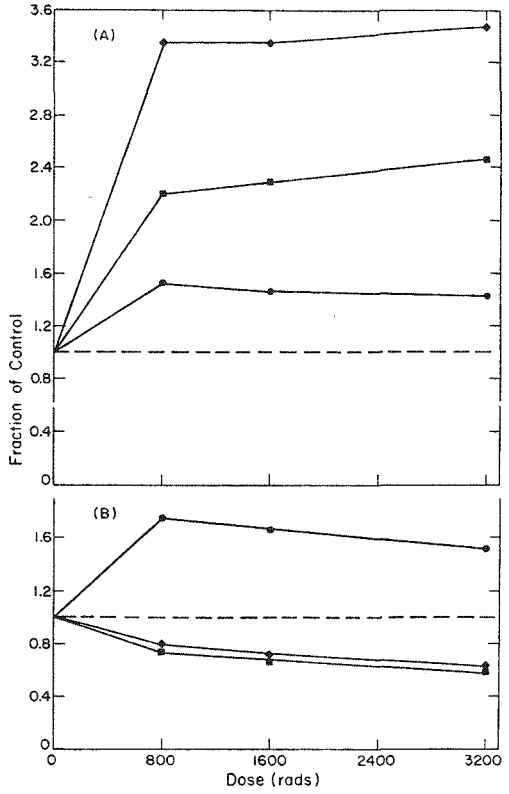

Fig. 3. Effect of increasing exposures of x-irradiation on ^{3}H-deoxycytidine incorporation into the acid-soluble deoxycytidine triphosphate pool and DNA during a 1-h pulse immediately after irradiation of asynchronously growing cells. (A) Effect of radiation on the acid-soluble dCTP pool. The data were normalized to the same cell number, then expressed as the fraction of control: (-●-) pool size (pmoles dCTP/sample); (-◆-) ^{3}H-dCTP/sample; and (-■-) pool specific activity (cpm ^{3}H-dCTP/pmole dCTP). Control values were 57.2 pmoles dCTP/sample, 17 238 cpm ^{3}H-dCTP/sample, and 301 cpm ^{3}H-dCTP/pmole dCTP. (B) Incorporation into DNA expressed as the fraction of control: (-●-) specific activity of DNA labeled with ^{3}H-deoxycytidine; (-◆-) specific activity of DNA labeled with ^{3}H-deoxycytidine after correcting for the increased specific activity of the dCTP pool from panel A; and (-■-) specific activity of DNA labeled with ^{3}H-thymidine.

suggests radiation effects on precursor metabolism unrelated to that of DNA replication. Since cells *in vivo* draw upon the acid-soluble deoxyribonucleoside triphosphate pools for DNA replication, the effect of radiation on these pools was examined. The triphosphate pools were isolated and assayed enzymatically, as previously described.[6] The data in Fig. 2 show that there was little or no effect of radiation on the size or specific activity of the dTTP, dATP, or dGTP pools. However, as shown in

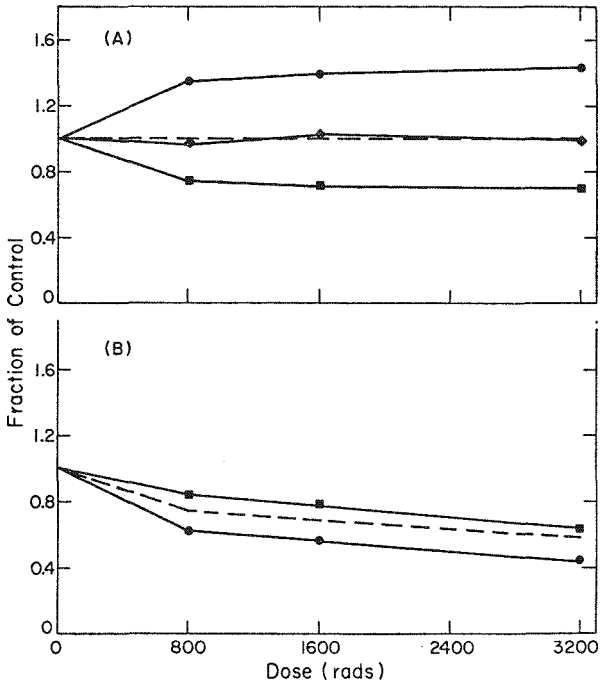

Fig. 4. Effect of increasing exposures of x-irradiation on ^{3}H-cytidine incorporation into the acid-soluble deoxycytidine triphosphate pool and DNA during a 1-h pulse immediately after irradiation of asynchronously growing cells. (A) Effect of radiation on the acid-soluble dCTP pool. The data were normalized to the same cell number, then expressed as the fraction of control: (-●-) pool size (pmoles dCTP/sample; (-◆-) ^{3}H-dCTP/sample; and (-■-) pool specific activity (cpm ^{3}H-dCTP/pmole dCTP). Control values were 59.2 pmoles dCTP/sample, 20 033 cpm ^{3}H-dCTP/sample, and 338 cpm ^{3}H-dCTP/pmole dCTP. (B) Incorporation into DNA expressed as the fraction of control: (-●-) specific activity of DNA labeled with ^{3}H-cytidine; and (-■-) specific activity of DNA labeled with ^{3}H-cytidine after correcting for the specific activity of the dCTP pool from panel A. The dashed line represents the incorporation of ^{3}H-thymidine into DNA (taken from Fig. 3B).

Fig. 3A, radiation had a very pronounced effect on the dCTP pool isolated from cells pulse-labeled with ^{3}H-deoxycytidine. Both the size and specific activity of the dCTP pool were increased after irradiation. When one corrects the incorporation of ^{3}H-deoxycytidine into DNA for the increased specific activity of the dCTP pool after irradiation, results are obtained that are not significantly different from that of ^{3}H-thymidine incorporation after irradiation (Fig. 3B).

The effect of radiation on the dCTP pool labeled with ^{3}H-cytidine was quite different from that

obtained with ^{3}H-deoxycytidine labeling. Although the size of the dCTP pool was again increased after irradiation, the specific activity was somewhat decreased (Fig. 4A). When the incorporation of ^{3}H-cytidine into DNA was corrected for the specific activity of the dCTP pool, there was reasonable agreement with that obtained by thymidine labeling (Fig. 4B).

We found that adding unlabeled thymidine to the growth medium (at concentrations up to 250 μM) was very effective in ameliorating the radiation-induced stimulation of ^{3}H-deoxycytidine incorporation into DNA (Fig. 5B). However, when the size and specific activity of the dCTP pool (labeled with ^{3}H-deoxycytidine) were examined in cells treated with 250 μM thymidine, we still observed a radiation-induced increase in both the pool size and the level of pool ^{3}H-dCTP derived from ^{3}H-deoxycytidine (see Fig. 5A). It will be noted, however, that the increase in the two parameters was approximately equal, yielding a pool specific activity very close to that of the control. It would appear then that the ameliorating effect on the radiation-induced stimulation of ^{3}H-deoxycytidine incorporation into DNA occurs, not as a result of abolishing either the radiation-induced increase in the level of ^{3}H-dCTP derived from ^{3}H-deoxycytidine or the increased pool size, but by equalizing the change in magnitude of the two parameters.

Conclusions. From the data presented above, it would appear that one cannot explain the radiation-induced reduction of precursor incorporation into DNA on the basis of pool dilution. Neither the size nor the specific activity of the dTTP, dGTP, and dATP pools was altered by x-irradiation. Deoxyribonucleoside triphosphate pool dilution after irradiation is also inconsistent with a number of additional observations. We know, for example, that Chinese hamster cells have a dTTP pool sufficient to replicate ~ 2% of the DNA or enough to support DNA synthesis for ~ 5 min.[6] However, the dATP and dGTP pools are only 25% and 20%, respectively, as large as the dTTP pool.[6] If we assume for the moment that the uptake kinetics of ^{3}H-thymidine into DNA after irradiation is due to pool dilution, then ~ 0.9% of the cell DNA would have to be degraded every 5-8 min. Since thymidine incorporation is depressed for 2-3 h after irradiation,[7] a large amount of DNA would have to be degraded, a rather unlikely event.[8,9] In addition, rather extensive DNA degradation would likely involve long stretches of DNA containing all four major DNA constituents. Since the dATP and dGTP pools are much smaller than the dTTP pool, pool dilution would be much more pronounced for dATP and dGTP than dTTP. This is not consistent with either the results from precursor incorporation (Fig. 1) or pool studies (Fig. 2).

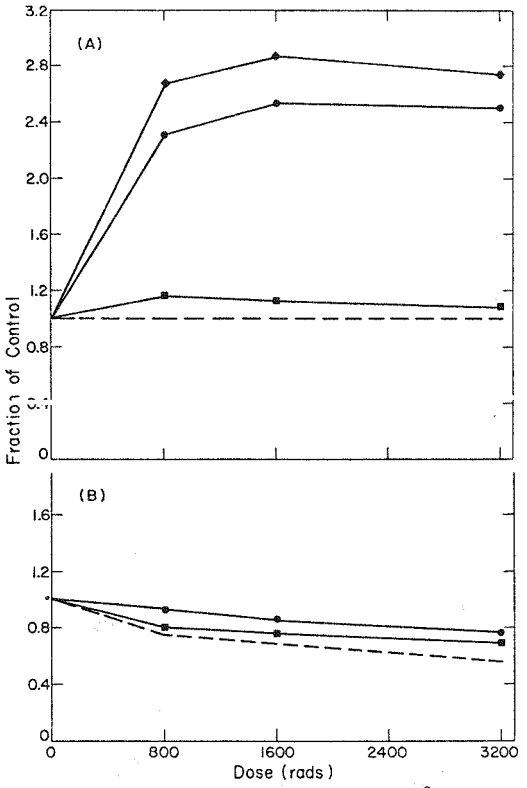

Fig. 5. Effect of 250 μM thymidine on ^{3}H-deoxycytidine incorporation into the acid-soluble dCTP pool and DNA after exposure of asynchronously growing cells to increasing doses of x-irradiation. Cells were pulsed-labeled 1 h immediately after irradiation. (A) Effect of radiation on the dCTP pool. The data were normalized to the same cell number, then expressed as a fraction of the control: (-●-) pool size (pmoles dCTP/sample); (-◆-) ^{3}H-dCTP/sample; and (-■-) pool specific activity (cpm ^{3}H-dCTP/pmole dCTP). Control values were 18.6 pmoles dCTP/sample, 20 811 cpm ^{3}H-dCTP/sample, and 1119 cpm ^{3}H-dCTP/pmole dCTP. (B) Incorporation into DNA expressed as the fraction of control: (-●-) specific activity of DNA labeled with ^{3}H-deoxycytidine; and (-■-) specific activity of DNA labeled with ^{3}H-deoxycytidine after correcting for the specific activity of the dCTP pool from panel A. The dashed line represents incorporation of ^{3}H-thymidine into DNA (taken from Fig. 3B).

The effect of radiation on the dCTP pool is quite interesting. Although the radiation-induced stimulation of ^{3}H-deoxycytidine incorporation into DNA (Figs. 1 and 3B) and the ameliorating effect of thymidine thereon (Fig. 5B), upon cursory examination, would appear to be consistent with regulatory control by dTTP on formation of dCTP via ribonucleotide reductase activity, a number of lines of evidence argue against such a mechanism. We have previously shown[7] that addition to exogenous Chinese hamster cells of increasing concentrations of unlabeled thymidine *reduced* the size of the dCTP pool, increased the pool specific activity after deoxycytidine labeling, and flooded the dTTP pool. Thus, high concentrations of intracellular dTTP resulted in a feedback inhibition of the reductive conversion of CDP to dCDP and a concomitant increase in the utilization of exogenous ^{3}H-deoxycytidine, similar to that seen in bacteria.[10] Since radiation produced an increased rather than decreased dCTP pool (Fig. 5A), failed to expand the dTTP pool (see Fig. 2), and failed to inhibit the incorporation of ^{3}H-cytidine into the dCTP pool (Fig. 4A) in a cell line known to respond to dTTP control of dCTP synthesis via nucleotide reductase, we conclude that the radiation-induced changes in the dCTP pool are not a result of radiation effects on the dTTP pool.

The ability of exogenously added thymidine to eliminate the radiation-induced stimulation of ^{3}H-deoxycytidine incorporation into DNA is quite interesting. It is clear that thymidine treatment does not eliminate either the radiation-induced increase in amount of ^{3}H-dCTP derived from exogenously added ^{3}H-deoxycytidine or the increase in pool size but simply equalizes the change in magnitude of the two parameters, thus resulting in a dCTP pool specific activity very similar to that of the control. It may be that thymidine exerts this peculiar effect on deoxycytidine metabolism in irradiated cells by forcing the cell to draw more efficiently on deoxycytidine nucleotides for dCTP synthesis, since it is known that dTTP inhibits the conversion of cytidine nucleotides to deoxycytidine nucleotides.[7] We have no information as yet concerning the mechanism(s) by which radiation exerts its effect on the dCTP pool.

REFERENCES

1. S. Okada, "Radiation Effects on Progress through the Cell Cycle," In: Radiation Biochemistry: Cells (K. I. Altman, G. B. Gerber, and S. Okada, eds.), Vol. I, p. 189, Academic Press, Inc., New York (1970).

2. J. B. Little, "Factors Influencing Exogenous Nucleoside Utilization in DNA Synthesis by Irradiated Human Cells," Exp. Cell Res. 62, 368-374 (1970).

3. S. J. Adelstein and G. B. Manasek, "X-Irradiation of Splenic Lymphocytes. II. Differential Incorporation of Pyrimidine Nucleotide Precursors into DNA," Internat. J. Radiation Biol. 12, 593-595 (1967).

4. L. A. Smets, "Discrepancies between Precursor Uptake and DNA Synthesis in Mammalian Cells," J. Cell. Physiol. 74, 63-66 (1969).

5. L. A. Smets, "The Dependency of Thymidine Incorporation on Irradiation Dose," Internat. J. Radiation Biol. 11, 197-199 (1966).

6. R. A. Walters, R. A. Tobey, and R. L. Ratliff, "Cell-Cycle Dependent Variations of Deoxyribonucleoside Triphosphate Pools in Chinese Hamster Cells," Biochim. Biophys. Acta 319, 336-347 (1973).

7. R. A. Walters, L. R. Gurley, R. A. Tobey, M. D. Enger, and R. L. Ratliff, "Effects of X-Irradiation on DNA Precursor Metabolism and Deoxyribonucleoside Triphosphate Pools in Chinese Hamster Cells," Radiation Res. 60, 173-201 (1974).

8. J. B. Little, "Radiation-Induced DNA Degradation in Human Cells. Lack of Evidence following Moderate Doses of X-Rays," Internat. J. Radiation Biol. 13, 591-595 (1968).

9. M. Hill, "The Search for X-Ray Induced DNA Degradation in Mouse L Cells," Internat. J. Radiation Biol. 15, 483-490 (1969).

10. P. Reichard, "The Biosynthesis of Deoxyribonucleotides," Eur. J. Biochem. 3, 250-266 (1968).

Cell-Cycle-Specific Changes in the Organization of Chromatin in Mammalian Nuclei

(C. E. Hildebrand and R. A. Tobey)

The organization of chromatin in nuclei of eukaryotic cells has been the subject of intensive research efforts during the past decade.[1] Interest more recently has focused on changes in chromatin organization in cells in different states of proliferation and growth arrest.[2-4] These studies are fundamental to elucidation of the mechanisms by which a cell maintains an orderly arrangement of DNA

both for duplication of the DNA and for regulation of transcription.

Several methods (including morphological and biochemical) have been used to measure changes in chromatin organization in the interphase nucleus.[2-5] The results of ultrastructural studies show an increasing dispersion of chromatin fibers as measured by the inter-fiber distance as cells progress through G_1 into S phase of the cell cycle.[2] Accessibility of DNA to ^{3}H-actinomycin D and DNase I has been found to increase in S-phase chromatin compared with G_1 chromatin in synchronized HeLa cells.[3,4] Also, an increased binding of *Escherichia coli* RNA polymerase in proliferating WI38 cells, compared with cells in noncycling confluent monolayers, has been reported.[5] All of these findings suggest a loosening of chromatin structure as cells progress through the pre-DNA synthetic phase of the proliferation cycle. With the exception of electron microscopic studies, probes (^{3}H-actinomycin D, DNase I, RNA polymerase) of chromatin structure interact directly with the DNA component of chromatin. We have investigated the usefulness of polyanions, which interact specifically with the histone component of chromatin, in observing changes in the intranuclear organization of chromatin.

Both natural (heparin) and synthetic (dextran sulfate, polyethylene sulfonate, polystyrene sulfonate, polyaspartic acid, polyribonucleotides) polyanions have been studied with respect to their interaction with isolated nuclei and chromatin.[6-16] These polyanions have been reported to produce many effects: stimulation of template efficiency of chromatin for both endogenous and exogenous RNA polymerases;[6-10] increased template availability for exogenous DNA polymerase;[11] induction of nuclear swelling;[12] release of DNA from nuclei; and enhancement of ^{3}H-actinomycin D binding by nuclei.[13] All of these effects arise from the specific interaction of polyanions with histones. This finding has been confirmed in our Laboratory.

The specificity with which polyanions bind histones[14-16] suggested that polyanions may be a useful probe for studying the relationship between histones and DNA in chromatin organization during interphase. In our studies, we have measured the efficiency with which the natural polyanion heparin disperses chromatin from nuclei. Previous reports

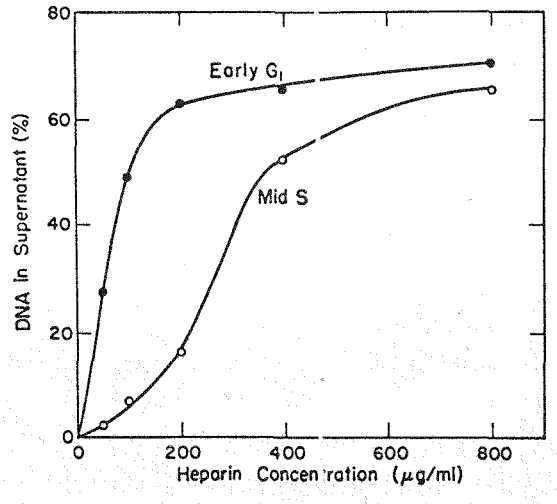

Fig. 1. Heparin-mediated release of DNA from Chinese hamster nuclei. Cells were uniformly labeled with ^{14}C-thymidine and synchronized as previously described.[18] Nuclei were prepared[18] from aliquots of cells taken at 1 h and 9.5 h post-mitosis, washed with 0.02 M Tris-Cl (pH 7.5 at 24°C) and 0.25 M sucrose, and resuspended in the same buffer at a concentration of 3×10^7 nuclei/ml. Samples (0.15 ml) containing nuclei at 1.5×10^7 nuclei/ml and the indicated concentrations of heparin were incubated at 2°C for 5 min. Fifty volumes of 0.01 M Tris (pH 7.5 at 24°C) were added to the samples. Each sample was mixed vigorously with a vortex mixer for 15 sec. Samples were centrifuged at 60 000 x g for 25 min at 4°C. Aliquots were taken before and after centrifugation for liquid scintillation counting. The percent of DNA remaining in the supernatant was then determined.

have shown that a large fraction of nuclear DNA is released from isolated rat liver nuclei in a highly dispersed state.[12,15] We have quantitated the heparin-mediated release of DNA from isolated nuclei as a measure of the extent of chromatin decondensation (dispersion) resulting from heparin treatment.

To study the heparin-mediated dispersion of nuclear DNA during interphase, we used synchronized cultures of Chinese hamster (line CHO) cells prepared by mitotic selection.[17] A comparison of the efficiency with which heparin disperses chromatin from G_1 and mid-S phase nuclei is shown in Fig. 1. The percentage of the bulk DNA which is dispersed in 5 min at 4°C by a given concentration of heparin is considerably less for nuclei from cells in mid-S phase compared with G_1 nuclei. Two additional features of these data are (1) the fraction of the bulk DNA which is resistant to dispersion by heparin is approximately the same at large heparin concentrations regardless of the position of nuclei in

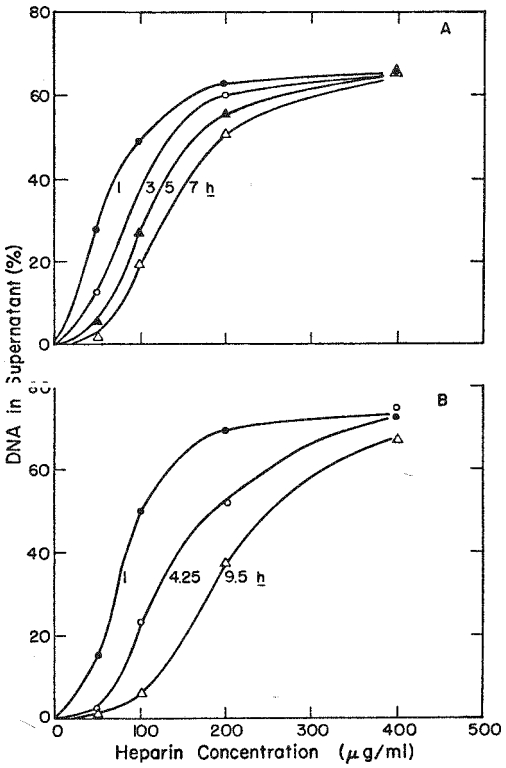

Fig. 2. Changes in heparin-mediated release decondensation of Chinese hamster nuclei during early interphase. (A) The cells synchronized by mitotic selection were sampled at various times post-mitosis, and assays were performed as described in Fig. 1. (B) The cells were synchronized by mitotic selection and treated with hydroxyurea (1 mM) beginning at 1 h post-mitosis. Assays were performed as in (A).

interphase and (2) the release of DNA from nuclei appears to occur in a cooperative fashion. The implications of these two points are presently being investigated. These results demonstrate a decreased susceptibility of chromatin to heparin-mediated dispersion as cells progress through early interphase.

The rate at which the heparin-mediated chromatin decondensation changes during interphase was determined by establishing a family of curves such as shown in Fig. 1 for various times following resumption of growth of mitotically selected cells. These results (Fig. 2A) indicate that the change in susceptibility of nuclei to dispersion by heparin begins in early interphase and continues into early S phase. It should be noted that these data also show that the fraction of chromatin resistant to dispersion remains approximately constant during early interphase. One obstacle to evaluating these results in a mitotically synchronized population is the (natural) synchrony decay which occurs as cells traverse interphase. A significant fraction of cells is detected entering S phase by 4 h post-mitosis. The synthesis of histones and increase in DNA mass concomitant with entry of cells into S phase alter the stoichiometric relationship between heparin and histone. Hence, as cells progress into S phase and the amount of chromatin per cell (nucleus) increases, one would expect to observe a decreased decondensation of chromatin for a given number of S phase nuclei compared with the same number of G_1 nuclei. To determine how much effect synchrony decay has on these observations, hydroxyurea (1 mM) was added to a mitotically selected population of cells at 1 h post-mitosis, and samples were taken at various times during traverse of G_1.[18,19] The data in Fig. 2B show that the observed decrease in dispersion of chromatin by heparin is not due to an increased (i.e., DNA plus histone) mass per nucleus, since both DNA replication and histone synthesis are inhibited in the presence of hydroxyurea.[20]

Quantitation of the heparin-mediated dispersion of chromatin was done by determining the heparin concentration at 50% of the maximum amount of dispersed chromatin (i.e., the level of dispersed chromatin at large heparin concentrations). The values were measured for the curves in Fig. 2 and are plotted in Fig. 3. The results show good agreement between the cells traversing G_1 in the presence of hydroxyurea and in the nontreated population. If the curve for heparin-mediated chromatin dispersion is extrapolated to the early G_1 level, the change in heparin-mediated chromatin dispersion can be estimated to precede the entry into S phase (extrapolation of labeled fraction data to 0) by 2 to 3 h. Thus, a significant change in organization of chromatin during early interphase is detectable by treatment of isolated nuclei with an agent which has been shown to interact specifically with histones. On this basis, we propose that an alteration of the structural relationship of histones to DNA in chromatin occurs during the G_1 phase of the cell cycle. Independent studies in our Laboratory have demonstrated a G_1-specific phosphorylation of histone f1 which precedes initiation of S phase by 2 h.[20,21] Hence, this histone modification correlates qualitatively with the observed changes in chromatin organization. The possibility that the changes in

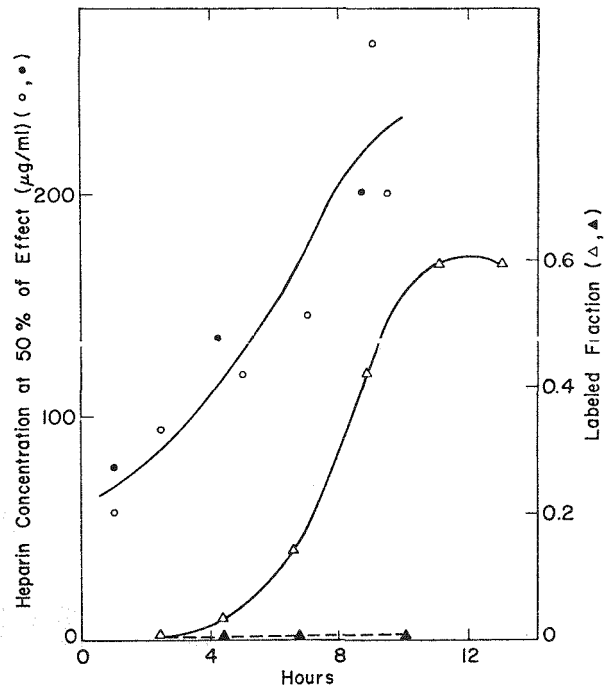

Fig. 3. Cell-cycle dependence of heparin dispersion of Chinese hamster nuclei. Heparin concentrations required to release 50% of the maximum amount of DNA from nuclei were determined from data such as shown in Fig. 2 for cells synchronized by mitotic selection and treated (-●-) or not treated (-○-) with hydroxyurea. Labeled fraction determinations were performed on unlabeled synchronized populations of cells simultaneously with the above experiments [treated with hydroxyurea (-▲-) and nontreated (-△-)].

chromatin arrangement measured by heparin-mediated chromatin dispersion is a result of the synthesis and interaction of nonhistone proteins with chromatin during G_1 must be considered.[21] Ongoing experiments are designed to evaluate these possibilities.

REFERENCES

1. *Cold Spring Harbor Symposia on Quantitative Biology*, Vol. XXXVIII, Cold Spring Harbor Laboratory Press, Cold Spring Harbor, New York (1973).

2. W. C. Dewey, J. S. Noel, and C. M. Dettor, "Changes in Radiosensitivity and Dispersion of Chromatin during the Cell Cycle of Synchronous Chinese Hamster Cells," Radiation Res. 52, 373-394 (1972).

3. T. Pederson and E. Robbins, "Chromatin Structure and the Cell Division Cycle: Actinomycin Binding in Synchronized HeLa Cells," J. Cell Biol. 55, 322-327 (1972).

4. T. Pederson, "Chromatin Structure and the Cell Cycle," Proc. Natl. Acad. Sci. USA 69, 2224-2228 (1972).

5. B. T. Hill and R. Baserga, "Changes in the Number of Binding Sites for Ribonucleic Acid Polymerase in Chromatin of WI38 Fibroblasts Stimulated to Proliferate," Biochem. J. 141, 27-34 (1974).

6. P. Chambon, M. Ramuz, P. Mandel, and J. Doly, "The Influence of Ionic Strength and a Polyanion on Transcription *in vitro*. I. Stimulation of the Aggregate RNA Polymerase from Rat Liver Nuclei," Biochim. Biophys. Acta 157, 504-519 (1968).

7. P. Chambon, H. Karon, M. Ramuz, and P. Mandel, "The Influence of Ionic Strength and a Polyanion on Transcription *in vitro*. II. Effects on the Template Efficiency of Rat Liver Chromatin for a Purified Bacterial RNA Polymerase," Biochim. Biophys. Acta 157, 520-531 (1968).

8. T. C. Spelsberg and L. S. Hnilica, "Studies on the RNA Polymerase-Histone Complexes," Biochim. Biophys. Acta 195, 55-62 (1969).

9. G. Miller, L. Berlowitz, and W. Regelson, "Chromatin and Histones in Mealy Bug Cell Explants: Activation and Decondensation of Facultative Heterochromatin by a Synthetic Polyanion," Chromosoma (Berlin) 32, 251-261 (1971).

10. D. I. dePomerai, C. J. Chesterton, and P. H. W. Butterworth, "The Effect of Heparin on Structure and Template Properties of Chromatin," FEBS Letters 42, 149-153 (1974).

11. R. J. Kraemer and D. S. Coffey, "The Interaction of Natural and Synthetic Polyanions with Mammalian Nuclei. I. DNA Synthesis," Biochim. Biophys. Acta 224, 553-567 (1970).

12. R. J. Kraemer and D. S. Coffey, "The Interaction of Natural and Synthetic Polyanions with Mammalian Nuclei. II. Nuclear Swelling," Biochim. Biophys. Acta 224, 568-578 (1970).

13. M. A. Tubbert and L. Berlowitz, "Chromatin and Histones in Mealy Bug Spermatogonia," Exp. Cell Res. 85, 205-211 (1974).

14. L. Berlowitz, R. Kitchin, and D. Palotta, "Histones and RNA Synthesis: Selective Binding of Histones by a Synthetic Polyanion in Calf Thymus Nuclei," Biochim. Biophys. Acta 262, 160-168 (1972).

15. E. A. Arnold, D. H. Yawn, D. G. Brown, R. C. Wyllie, and D. S. Coffey, "Structural Alteration in Isolated Rat Liver Nuclei after Removal of Template Restriction by Polyanions," J. Cell Biol. 53, 737-757 (1972).

16. G. J. Miller, L. Berlowitz, and W. Regelson, "Chromatin and Histones in Hen Erythrocyte Nuclei," Exp. Cell Res. 71, 409-421 (1972).

17. R. A. Tobey, E. C. Anderson, and D. F. Petersen, "Properties of Mitotic Cells Prepared by

Mechanically Shaking Monolayer Cultures of Chinese Hamster Cells," J. Cell. Physiol. 70, 63-68 (1967).

18. C. E. Hildebrand and R. A. Tobey, "Temporal Organization of DNA in Chinese Hamster Cells: Cell-Cycle Dependent Association of DNA with Membrane," Biochim. Biophys. Acta 331, 165-180 (1973).

19. L. R. Gurley, R. A. Walters, and R. A. Tobey, "Cell-Cycle-Specific Changes in Histone Phosphorylation Associated with Cell Proliferation and Chromosome Condensation," J. Cell Biol. 60, 356-364 (1974).

20. L. R. Gurley, R. A. Walters, and R. A. Tobey, "Metabolism of Histone Fractions. Phosphorylation and Synthesis of Histones in Late G_1-Arrest," Arch. Biochem. Biophys. 164, 469-477 (1974).

21. E. W. Gerner and R. M. Humphrey, "The Cell-Cycle Phase Synthesis of Non-Histone Proteins in Mammalian Cells," Biochim. Biophys. Acta 331, 117-127 (1973).

THE CELL SURFACE

Population Analysis of Arrested Human Diploid Fibroblasts by Flow Microfluorometry

(P. M. Kraemer)

The mitotic activity of human diploid fibroblasts in culture can be inhibited by reducing the serum concentration of the incubation medium from 10% to 0.1 or 0.5%.[1] Cells maintained in this manner for up to 6 months can be induced to reenter a state of rapid proliferation by subcultivation with medium containing 10% serum. This method for inhibiting division in cultured cells may offer an experimental tool for the investigation of growth regulation in intact animals. This may be true especially for those cells which *in vivo* exhibit little or no mitotic activity unless exposed to a specific stimulus (i.e., the fibroblasts of connective tissue during wound healing).[2]

Figure 1 shows the DNA distribution patterns obtained by FMF from cells taken at confluency (0 day) and after 14 and 28 days of exposure to medium containing 0.5% serum. Computer analysis of the DNA content of exponentially distributed cell populations has been used to demonstrate that the fraction of cells in each phase of the division cycle was comparable to fractions deduced by biochemical cell-cycle analysis.[3,4] The major peak represents cells that have the G_1 phase of the cell cycle. The peak at twice the mode of the G_1 DNA content represents cells in G_2 + M. Cells in S phase, with varying degrees of completion of DNA replication, are distributed between the G_1 and the G_2 + M peaks. The distribution plots for the three sample points shown in Fig. 1 are representative of the data obtained at all sample points. These results showed that exposure to low serum medium maintained the population distribution that was present when the cells attained confluency in medium containing 10% serum.

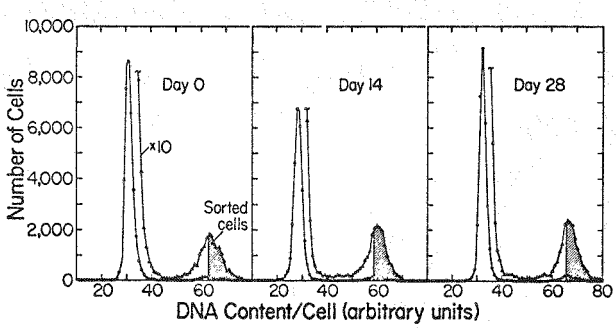

Fig. 1. DNA content distribution of CF-1 cultures maintained on medium containing 0.5% serum for 0, 14, and 28 days. The solid triangles represent the same data as the solid circles except for a 10-fold magnification of the ordinate scales. The crosshatched areas indicate the cells sorted out with a 4C DNA content.

When the FMF frequency distribution data for all time points (0, 3, 7, 14, 21, and 28 days) were submitted to computer analysis,[4] the results shown in Table I were obtained. Throughout the experiment, approximately 90% of the cells had a DNA content of G_1 cells (i.e., for the entire 28 days, approximately 10% of the cells at any time were beyond the G_1/S boundary). S-phase cells, on the basis of DNA content, ranged from 4.6 to 9.2%. The 0-day sample had very few cells with a 4C DNA content (G_2 + M fraction), but all other samples gave values ranging from 3.4 to 4.5%. This population distribution can be contrasted to cells in the log phase of growth which have 40.6% G_1, 46.9% S, and 12.5% G_2 + M cells. These results indicate that CF-1 cells incubated with medium containing 0.5% serum maintain a fairly stable distribution of cells among the different phases of the cell cycle for as long as 28 days. This population distribution is similar to that achieved at confluency and is in agreement with Tobey and Ley who found that, in stationary phase culture of CHO cells, more than 90% of the population was in the G_1 phase of the division cycle.[5]

TABLE I

CELL-CYCLE COMPOSITION OF CF-1 CELLS

MAINTAINED ON MEDIUM CONTAINING 0.5% SERUM

Day	Phase		
	G_1	S	G_2 + M
0	90.4	9.1	0.5
3	92.0	4.6	3.4
7	87.3	9.2	3.5
14	90.7	4.8	4.5
21	90.4	5.9	3.7
28	89.9	6.5	3.6

TABLE II

LABELING INDEX OF CF-1 CELLS EXPOSED TO ^{3}H-THYMIDINE FOR 72 H BEFORE HARVEST

Day	Total Population	G_2 + M Fraction
0	5.4	1.4
3	4.0	1.8
7	2.6	1.8
14	4.5	1.8
21	5.4	1.8
28	6.0	4.8

To determine if the population distributions obtained by FMF were those of static populations, we labeled the cells with ^{3}H-thymidine for 72 h before harvest. The labeling indices, as determined by autoradiography for the entire population and for a "sorted" population[6] consisting of cells with a 4C DNA content (G_2 + M fraction), are shown in Table II. Despite the FMF evidence that 10% of the cells had a DNA content of greater than 2C, the overall labeling indices after 72 h of exposure to ^{3}H-thymidine were only 2.6 to 6.0%. This suggests that S phase was prolonged and that DNA synthesis occurred at a very slow rate. This conclusion is supported by the fact that almost all labeled cells had a sparse grain density after 1 wk of exposure. With respect to the sorted population of cells with a 4C DNA content, it was determined that less than 1% of these cells were in mitosis; therefore, the sorted fraction was composed of essentially all G_2 phase cells. The labeling indices from this fraction ranged from 1.4 to 4.8% during the 28-day experimental period. These data show that a minimum of 95% of the cells in G_2 at the time of harvest crossed the S/G_2 boundary 72 h before harvest. Again, as with the S phase, there was an enormously prolonged G_2 phase of the division cycle in cells exposed to medium containing 0.5% serum.

The results from the experiments described herein show that human diploid fibroblasts maintained with medium containing 0.5% serum achieve a stable population distribution for as long as 28 days in culture. This distribution is similar to that occurring when a population reaches confluency under stationary culture conditions; however, this is not a static population. The arrested populations continued to show evidence of slow cell-cycle traverse during the entire experimental period. The low labeling indices, especially those of the G_2 sorted cells, the sparse grain density of the cells that were labeled, and the presence of some mitotic cells indicated that a very limited amount of cell-cycle traverse did occur but that both the S and the G_2 phases were enormously prolonged. In addition to this, it seems likely that the length of time the cells spend in the G_1 phase is increased also because of the number of cells detected in this fraction. These experiments do not distinguish between the possibilities of a subpopulation moving through the division cycle with the majority blocked in one phase (G_1) or the entire population traversing. However, what is clear is that the cells involved in traverse are proceeding through G_1, S, and G_2 at a much reduced rate.

The cells of many tissues *in vivo* are described as being expanding populations. Scattered mitotic cells can be detected in these tissues which have an average daily mitotic rate of less than 0.5%.[7] It has been postulated that the majority of cells in these tissues are inhibited from cell-cycle traverse at particular phases of the division cycle. These arrested cells have been considered to be in abnormally long G_1 or G_2 periods, which can be shortened dramatically by the stimulus to proliferate.[8] They have also been envisioned to be in a G_0 phase which, while distinct from G_1, has certain properties such as DNA content in common with cells in G_1.[9] In a like manner, cells in culture achieving confluency and in a stationary culture condition have been shown to be inhibited from cell-cycle traverse to the same extent and at the same stages of the division cycle. The system employed in the study described herein

allows for the long-term maintenance of the population distribution found at confluency in human diploid fibroblast cultures. Since this distribution can be related to that found in certain tissues *in situ*, it may offer an *in vitro* model system for the study of the regulatory processes occurring in these tissues.

REFERENCES

1. R. T. Dell'Orco, "Maintenance of Human Diploid Fibroblasts as Arrested Populations," Federation Proc. 33, 1969 (1974).

2. W. S. Bullough and E. B. Laurance, "The Control of Mitotic Activity in Mouse Skin," Exp. Cell Res. 21, 394 (1960).

3. P. M. Kraemer, L. L. Deaven, H. A. Crissman, J. A. Steinkamp, and D. F. Petersen, "On the Nature of Heteroploidy," in: Cold Spring Harbor Symposia on Quantitative Biology, Vol. 38 (1974), pp. 133-144.

4. P. N. Dean and J. H. Jett, "Mathematical Analysis of DNA Distributions Derived from Flow Microfluorometry," J. Cell Biol. 60, 523 (1974).

5. R. A. Tobey and K. D. Ley, "Regulation of Initiation of DNA Synthesis in Chinese Hamster Cells," J. Cell Biol. 46, 151 (1970).

6. J. A. Steinkamp, M. J. Fulwyler, J. R. Coulter, R. D. Hiebert, J. L. Horney, and P. F. Mullaney, "A New Multiparameter Separator for Microscopic Particles and Biological Cells," Rev. Sci. Instr. 44, 1301 (1973).

7. C. P. LeBlond, "Classification of Cell Populations on the Basis of Their Proliferative Behavior," Natl. Cancer Inst. Monograph 14, 119 (1964).

8. S. Gelfant, "Patterns of Cell Division: The Demonstration of Discrete Cell Populations," Methods Cell Physiol. 2, 359 (1966).

9. H. M. Pott and H. Quastler, "Radiation Effects on Cell Renewal and Related Systems," Physiol. Rev. 43, 357 (1963).

CYTOGENETICS

The Nature of Chromosome Instability in Heteroploid Cell Populations

(L. L. Deaven, P. C. Sanders, P. Jose, and D. F. Petersen)

Variability in chromosome number and structure is a characteristic of heteroploid cell lines. Previous studies in this Laboratory have shown that, although the DNA content of heteroploid cells is usually higher than that of the diploid parent, there is virtually no increase in variability of cell-to-cell DNA content. At present, it is impossible to distinguish differences between karyologic alterations arising *in vivo* and transformations arising either spontaneously or as a result of treatment with a transforming agent *in vitro*. However, the phenomenon of heteroploidy, regardless of origin, appears to offer the opportunity to study karyotype control particularly in those instances where prolonged cultivation in the laboratory permitted documentation of persistent instability and where transitions from stability to instability could be observed to occur over fairly brief intervals. Because phenomena other than those recognized may occur in tumors, the further restriction to evolved cell lines *in vitro* is provisionally applied here and may be extended on the basis of additional evidence.

The most succinct description of the paradox related to stability of DNA content and variability of chromosome number within a heteroploid cell population is that of Kraemer *et al.*[1] The present studies were initiated to establish the DNA content and chromosomal composition of several stem lines within a heteroploid population of Chinese hamster cells (line CHO) with a modal chromosome number of 35 and a perimodal dispersion of 10 chromosomes. A large number of clones was derived from this population, and a series from the collection of clones was selected on the basis of chromosome number for more intensive study.

Populations derived from the selected clones were examined to determine the stability of chromosome number, DNA content by flow microfluorometric techniques,[2-4] and chromosome structure by Giemsa banding.[4] Some clones had relatively narrow chromosome number distributions (i.e., perimodal dispersions of 2 or 3 chromosomes), while other clones appeared to revert rapidly to dispersions as great as the 10-chromosome dispersion of the parent line. Although the modal chromosome number of the clones varies from a high of 38 to a low of 29, the DNA analyses and chromosome counts summarized in Fig. 1 indicate that all of them contained amounts of DNA almost identical to that of the parental line. In each case, the DNA content was approximately 1.5 times the DNA content of diploid Chinese hamster cells, with a coefficient of variation within the clonal populations of 6%.

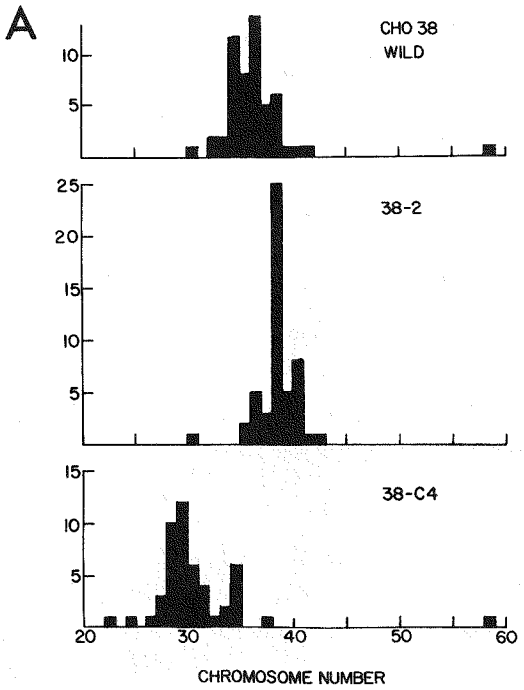

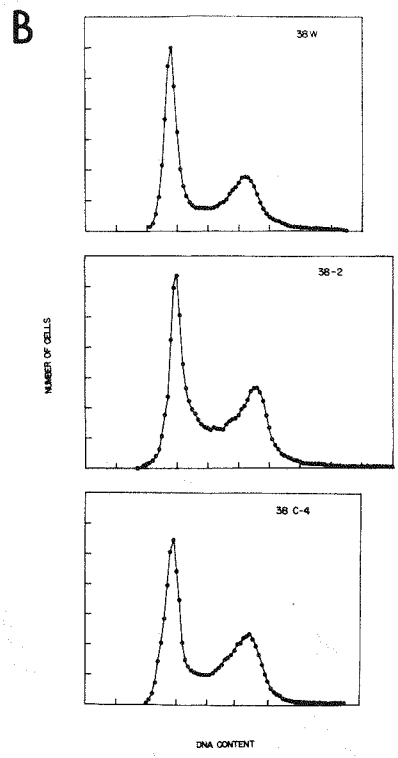

Fig. 1. (A) Chromosome number counts of metaphase cells from CHO 38 "wild type" (parental line) and clones CHO 38-2 and CHO 38C-4. (B) Acriflavine-Feulgen-DNA distributions of CHO 38W, 38-2, and 38C-4. Each of the high heteroploid lines contains almost identical amounts of DNA (1.5 times the diploid Chinese hamster).

Karyologic analysis of the individual clones represented by Figs. 2, 3, and 4 supports the observation of DNA content stability to the extent that the clones and the parent line, regardless of chromosome number, contained the same complement of large chromosomes (i.e., chromosome numbers 1 and 2). Similar complements of medium-sized chromosomes, numbers 4 through 8 and X, can also be demonstrated. However, these clones exhibited greater variability in their complements of small chomosomes (i.e., numbers 9 to 11) as well as minutes.

Several features of evolving cell populations appear to be consistent with these results. Most important of these is the strong pressure to regulate the amount of DNA present. Regardless of the chromosome number, a constant albeit elevated DNA content appears to be a requirement for indefinite survival of the heteroploid line and, when present in

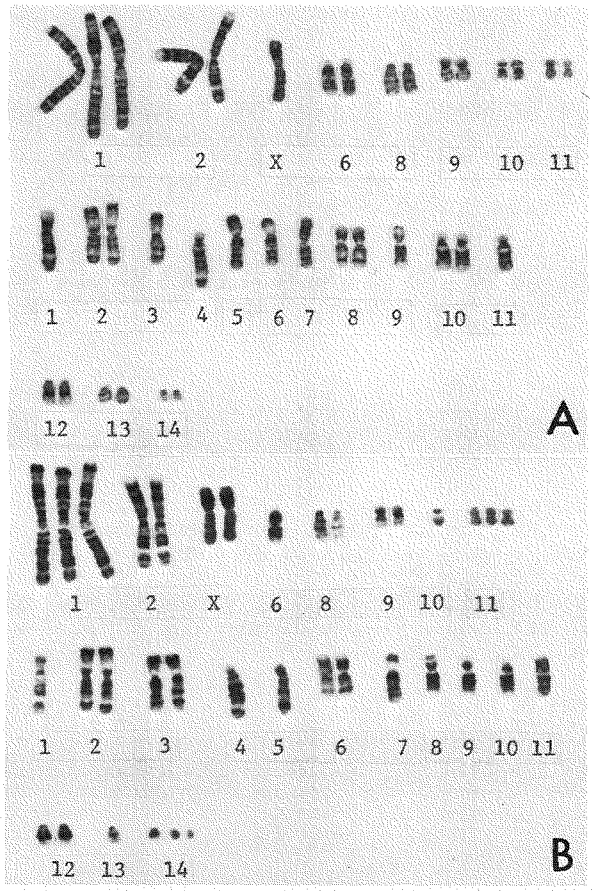

Fig. 2. Trypsin-induced Giemsa bands in two CHO 38 "wild type" cells. Unaltered Chinese hamster chromosomes are on the top line, and the rearranged chromosomes are on the bottom lines. The chromosome number for each cell is 36; however, there are compensatory substitutions in several classes of chromosomes which make each karyotype unique.

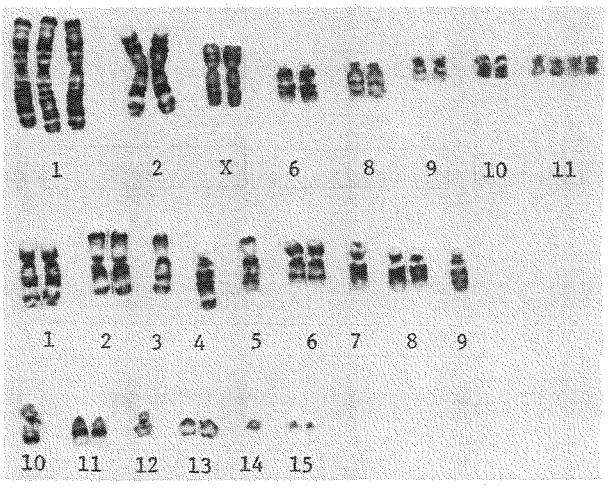

Fig. 3. Trypsin-induced Giemsa bands in a cell from clone 38-2. Unaltered Chinese hamster chromosomes are on the top line, and the rearranged chromosomes are on the bottom lines. Chromosome number = 41.

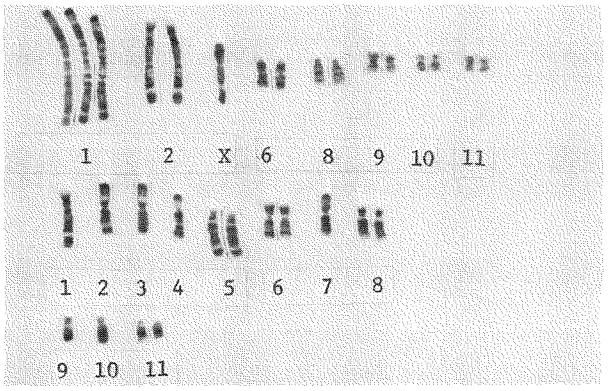

Fig. 4. Trypsin-induced Giemsa bands in a cell from clone 38C-4. Unaltered Chinese hamster chromosomes are on the top line, and the rearranged chromosomes are on the bottom lines. Chromosome number = 32.

amounts in excess of the DNA content of the parent diploid cell, appears in multiples of the haploid amount rather than at random. We have remarked before about the clustering of heteroploid lines in the region of 1.5C and 2C G_1 DNA contents.[4] The other feature of cellular evolution deserving comment is the mechanism by which a relatively stable amount of DNA can be segregated into a variable number of chromosomes. The explanation remains ambiguous in that data from a large number of human heteroploid (tumor) cells appear to reflect no bias related to size of the chromosomes involved in karyotypic abnormality,[5] while the data presented here show a clear trend toward excessive number variability in the smaller chromosomes. Other studies which also bear on the problem[6,7] tend to support the tentative conclusion of this report. Finally, based on the assumption that Giemsa banding is related to the identity of specific areas of organized chromatin, the patterns exhibited by the clones examined suggest three sets of material rather than random acquisition of excess DNA.

REFERENCES

1. P. M. Kraemer, L. L. Deaven, H. A. Crissman, and M. A. Van Dilla, "DNA Constancy Despite Variability in Chromosome Number," in: Advances in Cell and Molecular Biology, Vol. 2 (E. J. DuPraw, ed.), Academic Press, Inc., New York-London (1972), pp. 47-108.

2. D. M. Holm and L. S. Cram, "An Improved Flow Microfluorometer for Rapid Measurements of Cell Fluorescence," Exp. Cell Res. 80, 105 (1973).

3. P. M. Kraemer, D. F. Petersen, and M. A. Van Dilla, "On DNA Constancy in Heteroploidy and the Stem-Line Theory of Tumors," Science 174, 714 (1971).

4. L. L. Deaven and D. F. Petersen, "Measurements of Mammalian Cellular DNA and Its Localization in Chromosomes," in: Methods in Cell Biology, Vol. 8 (D. M. Prescott, ed.), Academic Press, Inc., New York (1974), pp. 179-204.

5. J. L. Minkler, J. W. Gofman, and R. K. Tandy, "A Specific Common Chromosomal Pathway for the Origin of Human Malignancy. II. Evaluation of Long-Term Human Hazards of Potential Environmental Carcinogens," Adv. Biol. Med. Phys. 13, 107 (1970).

6. L. L. Deaven and D. F. Petersen, "The Chromosomes of CHO, An Aneuploid Chinese Hamster Cell Line: G-Band, C-Band and Autoradiographic Analyses," Chromosoma 41, 129 (1973).

7. L. L. Deaven, P. C. Sanders, J. L. Grilly, P. M. Kraemer, and D. F. Petersen, "Chromosome G-Banding and DNA Constancy in Aneuploid Cell Populations," in: Mammalian Cells: Probes and Problems, AEC Symposium Series CONF-731007, Technical Information Center, Oak Ridge, Tennessee (1974), submitted.

MICROBIAL STUDIES

Increased Frequencies of Lysogeny in Heavily Ultraviolet Irradiated Populations of Temperate Bacteriophage

(B. J. Barnhart and S. H. Cox)

When temperate phage infect permissive bacteria, the phage may exhibit either a lytic response with phage replication and lysis of the host cell or a lysogenic response in which the phage genome becomes integrated into the host chromosome where it is

repressed from replicating except as a gene on the bacterial DNA.[1] This repressed phage genome or prophage may be derepressed by exposure of the lysogenic cell to physical or chemical agents.

The work we are reporting here describes the effect of ultraviolet radiation (uv) on the frequencies of observed lysogenic responses when populations of temperate *Haemophilus* phages HP1c1 and S2 are exposed to increasing doses of radiation. We have calculated the frequencies of lysogeny by assuming that PFU titers on agar with 0.02 µg of mitomycin C (MC) per ml (a level which induces prophage to enter the lytic cycle) represent phage titers in the absence of significant frequencies of lysogeny. The ratio of the difference in titers between plates with and without MC to the titer on MC plates gives a number less than 1.0, which represents the fraction of phage entering the lysogenic rather than the lytic cycle, i.e.:

$$\text{Frequency of lysogeny} = \frac{PFU_{+MC} - PFU_{-MC}}{PFU_{+MC}}$$

In Figs. 1a and 1b it can be seen that the frequencies of lysogeny calculated using the above equation display a dose-dependence, with the highest frequencies occurring in heavly irradiated phage populations. The greatest increases in lysogenic responses on uvr^+ hosts occur over a range of uv doses which result in the less sensitive component of the phage inactivation curves (Figs. 2a and 2b). The PFU survival curves in Fig. 2 for phage assayed on strains Rd and BC200 display characteristic breaks at about 300 to 400 ergs/mm^2.[2] The frequencies of lysogeny for both phages HP1c1 and S2 are highest at uv doses above 400 to 600 ergs/mm^2 on these uvr^+ host strains (Fig. 1). However, the frequencies of lysogeny for uv-irradiated HP1c1 (Fig. 1a) on strain BC100 uvr^- do not increase below doses of 100 ergs/mm^2, a dose at which this PFU survival curve breaks. At variance with this, the frequencies of lysogeny for uv-irradiated temperate phage S2 (Fig. 1b) assayed on this uvr^- host increase at lower doses as when assayed on uvr^+ hosts, but again the lysogenic responses are greatest at those uv

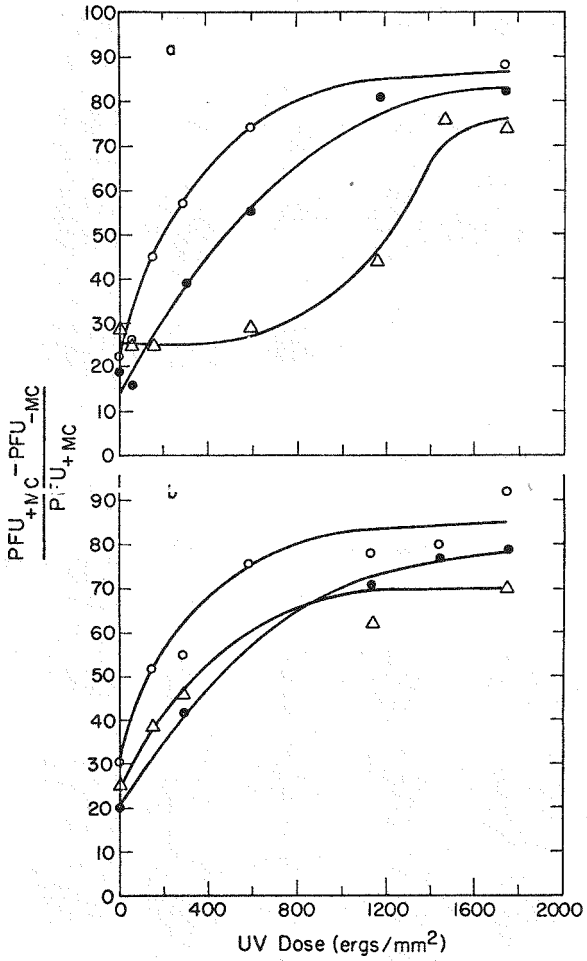

Fig. 1. The frequencies of lysogeny of uv-irradiated phages: (a) phage HP1c1 was irradiated at the indicated doses and assayed on strains of *H. influenzae* plated on CaBH-agar ± 0.02 µg mitomycin C (MC) per ml; and (b) phage S2 irradiated and assayed as for HP1c1. Phage host strains: Rd uvr^+ (-●-), BC200 uvr^+ (-○-), and BC100 uvr^- (-△-).

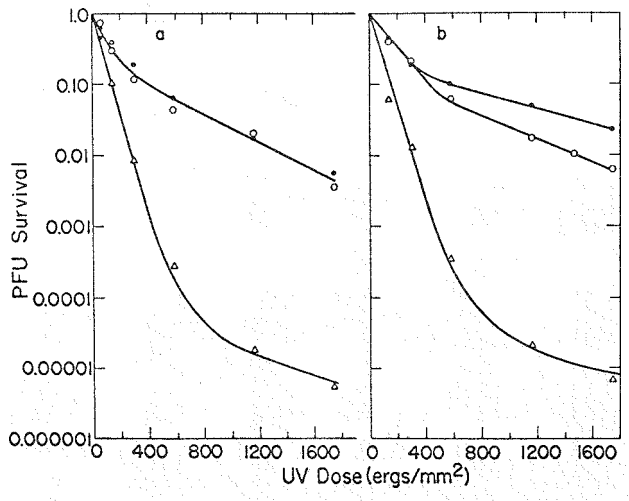

Fig. 2. Survival of phage plaque-forming units (PFUs) as a function of uv dose: (a) phage HP1c1 was irradiated at the indicated doses and assayed at a MOI less than 1.0 on strains of *H. influenzae* and (b) phage S2 irradiated and assayed as for HP1c1. Phage host strains: Rd uvr^+ (-●-), BC200 uvr^+ (-○-), and BC100 uvr^- (-△-).

doses resulting in a less sensitive PFU inactivation component (Fig. 2b).

The results we have presented show that uv-irradiated temperate *Haemophilus* phages HP1c1 and S2 display a PFU-survival curve which reflects two effects of uv irradiation on the phage genome: (1) the plaque-forming ability is reduced (i.e., transcription of phage genes essential to phage replication and development is inactivated or at least sufficiently damaged so as to give a competitive disadvantage to entry into the lytic pathway and (2) the probability of entering the lysogenic rather than the lytic pathway is enhanced among phage particles still possessing plaque-forming ability (as measured on agar containing MC). In addition, our results indicate that, at relatively high uv doses where inactivation of PFUs is less efficient per unit dose, the lysogenic response occurs in the majority of infections by biologically active phages. In less heavily irradiated populations, the phages predominantly enter the lytic pathway. We cannot offer an explanation for the difference in dose-dependencies of phage HP1c1 and S2, but these results apparently describe a measurable difference in the abilities of irradiated populations of these phages to lysogenize the *uvr*$^-$ host used in this study.

REFERENCES

1. M. E. Gottesman and R. A. Weisberg, "Prophage Insertion and Excision," in: The Bacteriophage Lambda (A. D. Hershey, ed.), Cold Spring Harbor Laboratory Press, Cold Spring Harbor, New York (1971), pp. 113-138.

2. J. K. Setlow and M. E. Boling, "Bacteriophage of *Haemophilus influenzae*. II. Repair of Ultraviolet-Irradiated Phage DNA and the Capacity of Irradiated Cells to Make Phage," J. Mol. Biol. 63, 349-362 (1972).

The Development of Bacterial Virus HP1c1 after Ultraviolet Induction of Temperature-Sensitive Mutants of Phage HP1c1

(B. J. Barnhart, R. T. Okinaka, and S. H. Cox)

Four temperature-sensitive (ts) mutants of bacteriophage HP1c1 have been isolated from mutagenized cultures of an ultraviolet-induced lysogen, BC200 (HP1c1). This report describes the isolation techniques and also provides a partial characterization of one of these mutants.

An exponentially growing culture of the lysogen was uv-irradiated to induce the prophage. After 35 min, a time when phage DNA is replicating, 300 μg of N-methyl-N'-nitro-N-nitrosoguanidine (MNNG) per ml was added for 6 min. Isolated plaques obtained from these mutagenized cultures were used to inoculate replicate plates of the indicator strain for incubation at the permissive (34.5°) and the non-permissive (40.5°) temperatures. Cultures of lysogenic bacteria were grown from stabs of lysis areas from 34.5° plates which had no corresponding lysis at 40.5°. Isolated colonies from the cultures were grown up in broth and were then looped onto lawns of the indicator strain. These plates were incubated at 34.5° and 40.5° to determine which clones were both lysogenic and temperature-sensitive with respect to spontaneous phage production.

Four phage mutants were isolated which failed either to lyse the host bacterium or to produce plaque-forming units (PFU) when lysogenic derivatives were incubated at 40.5°. Phage ts 51 lyses its host at 40.5°, but the burst size of PFUs is 0.005 that of the yield at 34.5°. Both phages ts 114 and ts 217 do not lyse their hosts at 40.5°. The respective burst sizes for ts 114 and ts 217 at 40.5° are 0.001 and 0.05 of the 34.5° burst.

The mutant ts 217 also displays an unusual phenotype at the permissive temperature. When grown at 34.5°, the ts 217 lysogen has a delayed lysis time and a 3- to 4-fold increase in its burst size when compared to the wild type HP1c1 phage. This is illustrated in Fig. 1 which depicts the intracellular development of phage in wild type HP1c1 and ts 217 lysogens grown at 34.5°. The data indicate that the mutant begins phage production nearly 20 min after the wild type and produces a much larger yield of phages. It is evident that ts 217 is much more efficient at phage production than the wild type HP1c1.

Earlier studies have suggested that wild type HP1c1 may have an inefficient timing mechanism between its lysis function and its maturation processes and hence produces many incomplete phage particles and a relatively small burst of viable phage.[1,2] The growth data above suggest that the timing mechanism of the ts 217 mutant may have been partially corrected, which would lead to larger burst sizes.

This mutant has been characterized further by electron microscopic analysis of the phage components

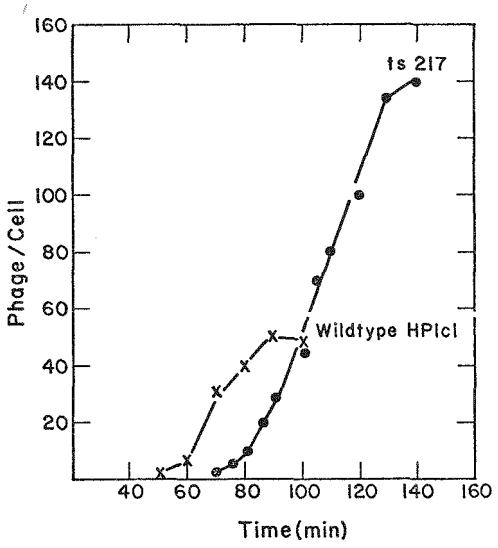

Fig. 1. Growth of HP1cl and ts 217 bacteriophages in *H. influenzae* BC200 by intracellular phage development or premature lysis. At the times indicated on the abscissa, aliquots were removed and blown into dilution buffer saturated with $CHCl_3$. After proper dilutions were made, these samples were plated for plaque-forming units on non-lysogenic BC200 cultures.

present in induced cultures grown at 40.5° and 34.5°. Lysogens of ts 217 were fixed and embedded at appropriate times after uv-induction. These were later sectioned, as described elsewhere.[2] Thus far the 40.5° cultures have revealed no significant phage or phage-like components in the sections. This may indicate that the temperature-sensitive lesion is an early function (including lysis or DNA synthesis).

Figure 2A represents a portion of an *Haemophilus influenzae* cell which was grown at 34.5° and fixed at 110 min after induction, a time when the average phage-containing cell has 80 phages. It can be seen that this cell contains complete (dense-staining) DNA-filled phage particles. This is noteworthy because complete phage are seldom seen in control (wild type) cultures.[2] In Fig. 2B is shown a cell which contains both complete and incomplete (diffuse-staining) particles. These two cell types are representative of the entire culture and provide some evidence that ts 217 lysogens are more stable during the lytic cycle than its wild type parent.

It is clear that ts 217 grown at the permissive temperature is much more suited to developmental studies than the wild type HP1cl. Further characterization of this and other mutants is currently in progress.

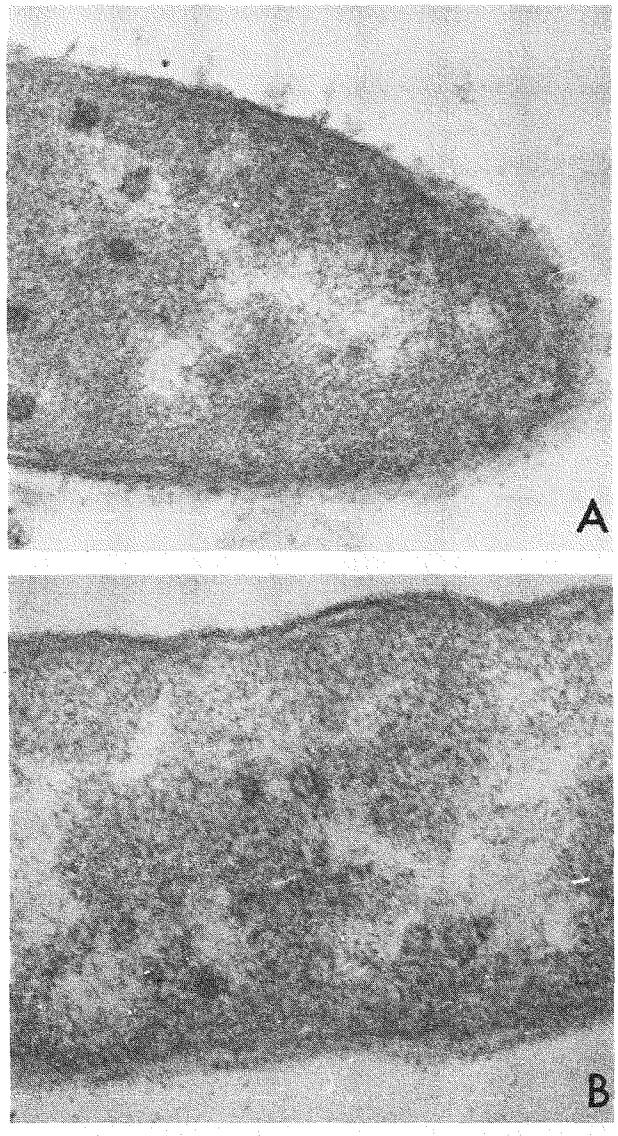

Fig. 2. Thin-sections of *H. influenzae* lysogenic for ts 217 at 110 min after uv-treatment (A). Cells were fixed in 1% OsO_4 and then embedded in Epon 812, sectioned, stained, and examined in a Phillips 200 electron microscope (B).

REFERENCES

1. B. J. Barnhart, R. T. Okinaka, and S. H. Cox, "The Development of Bacterial Virus HP1cl after Ultraviolet Induction," in: Annual Report of the Biomedical and Environmental Research Program of the LASL Health Division, January through December 1973, Los Alamos Scientific Laboratory report LA-5633-PR (May 1973), pp. 53-55.

2. R. T. Okinaka and B. J. Barnhart, "The Accumulation of Incomplete Particles following UV-Light Induction of *Haemophilus influenzae* Lysogenic for Bacteriophage HP1cl," J. Virol. 14, 1604-1606 (1974).

BIOPHYSICS AND INSTRUMENTATION GROUP (H-10)

P. F. Mullaney, Ph.D., Group Leader
H. L. Barrington, Secretary

Staff Members

M. T. Butler, B.S.
L. S. Cram, Ph.D.
H. A. Crissman, Ph.D.
J. M. Crowell, Ph.D.
P. N. Dean, M.S.
J. C. Forslund, B.S.
C. A. Goad, B.S.
K. M. Hansen, B.A.
P. K. Horan, Ph.D.
J. H. Jett, Ph.D.
J. H. Larkins, B.S.[a]
J. C. Martin, B.A.
J. D. Perrings
M. R. Raju, D.Sc.
C. Richman, Ph.D.
A. Romero, B.S.
G. C. Salzman, Ph.D.
J. A. Steinkamp, Ph.D.
T. T. Trujillo, B.S.

Biology Technicians

E. Bain
P. L. Wanek

Electronics Technicians

J. M. Blossom
L. J. Carr
J. L. Horney
W. T. West

Visiting Staff Member (Long-Term)

P. W. Todd, Ph.D.
Pennsylvania State University
University Park, Pennsylvania

Visiting Staff Members (Short-Term)

J. Lehman, Ph.D.
University of Colorado Medical Center
Denver, Colorado

J. J. Reidy, Ph.D.
University of Mississippi
University, Mississippi

R. Wilenzick, Ph.D.
Tulane University
New Orleans, Louisiana

Consultants

R. E. Anderson, M.D.
University of New Mexico
School of Medicine
Albuquerque, New Mexico

A. Armstrong, Ph.D.
San Diego, California

S. S. Friedland, Ph.D.
University of Tel Aviv
Tel Aviv, Israel

M. Makino, Ph.D.
University of California
Santa Barbara, California

R. A. Malmgren, M.D.
George Washington University
Washington, D. C.

T. T. Puck, Ph.D.
University of Colorado Medical Center
Denver, Colorado

STEP Program

M. S. Oka

[a]Half-time.

INTRODUCTION

During calendar year 1974, there have been several changes in the personnel roster for the Biophysics and Instrumentation Group (H-10). Karen Hansen, an experienced board-certified cytotechnologist, has joined our staff. Additional technical help to aid the biological effort has been obtained by the addition of E. Bain and P. Wanek, both of whom come to us with considerable prior experience. The demands on our 3 cell analysis and sorting instruments have increased considerably during the last year due to the increased level of biological experimentation. To obtain more efficient use of these machines, an instrument operator will be added to the staff late this year. His responsibilities are the operation and maintenance of these several instruments.

Another staff member addition includes J. M. Crowell, Ph.D., who was previously a postdoctoral appointee within the group. C. A. Goad also joined us and has responsibilities for the software aspects of our PDP-11 systems.

Also during the past year, two of our staff members have left the LASL: P. N. Dean has joined the staff of the Lawrence Livermore Laboratory, and P. K. Horan has taken a position with the University of Rochester of Rochester, New York. In addition, E. H. Clinard and M. L. Bartlett, who are working exclusively on USDA-related projects, were transferred to Group H-6 (Agriculture Biosciences).

The activities of the group fall into several categories: (1) development of flow-systems instrumentation for rapid cell analysis and sorting; (2) development of cell staining and preparational

techniques suitable for use with flow-systems instruments; (3) biological and medical applications of these instruments; (4) physical dosimetry and radiobiology studies at the biomedical channel at LAMPF; and (5) electronic and computer support for many of the activities in the LASL biomedical program. Specific information on each of these areas is given below.

One of the major advances made in the last year has been the implementation of the drug mithramycin as a DNA stain. This chemical has been shown to be as specific for DNA as the dyes acriflavine, ethidium bromide, and propidium iodide. It has the additional advantage that the staining protocol is simple and rapid. Within 20 to 30 min after obtaining a cell sample, DNA measurements can be made using the flow microfluorometry (FMF) technique.

Our instrumentation development efforts have centered on improvements to the cell sorter, investigation of light scattering as a suitable marker, and further incorporation of computer capabilities in the cell analysis and sorting instruments. A comparison of the light scattered at two angles, one within the forward scattering lobe and one outside this lobe, has permitted us to differentiate several white blood cell types in humans and animals. This particular area of research shows great promise as a non-destructive method for cell identification.

During 1974, one of the more interesting immunofluorescent investigations involved using the cell sorter to isolate IgM-producing lymphocytes from a mouse. These lymphocytes were then injected into a histocompatible but allotypically distinct mouse where a switch in immunoglobulin expression from IgM to IgG was observed using a sensitive radio-immune assay.

This last research was conducted in cooperation with investigators from the University of New Mexico in Albuquerque. Our personnel continue to be available for collaboration with scientists from other institutions. Cooperative experiments have been performed with the Division of Cancer Treatment and Division of Cancer Biology and Diagnosis of the National Cancer Institute; the U. S. Department of Agriculture in Ames, Iowa; University of Colorado; Lawrence Livermore Laboratory; University of Virginia Medical School; SUNY Downstate Medical Center in Brooklyn, New York; and Department of Radiation Medicine of the University of Kentucky, among others. Our cooperative efforts through interagency agreements with the USDA and NCI have continued at a slightly increased level from last year.

Our pioneering work in cell analysis continues to draw national and international attention. We were represented at the International Workshop and Symposium in Impulse Cytophotometry at Nijmegen, The Netherlands, in September. Our personnel have also been invited to speak on the state-of-the-art in the flow-systems field at several National Cancer Institute symposia including An Overview of the National Cancer Diagnosis Program, National Cancer Program June 1974, and the Annual Symposium on Recent Developments in Research Methods and Instrumentation (October 1974). Several Group H-10 personnel have also prepared, on invitation, a chapter for the next volume of Methods in Cell Biology (edited by D. M. Prescott). Also, a course in the fundamentals of the FMF techniques, sponsored by the LASL and the Tissue Culture Association, was held in July 1974. Most of the senior staff in our group were instructors in this course.

Several of our instrumentation projects have resulted in patent disclosures: (1) dual logarithmic amplifiers (Docket No. 5544-777); (2) multiangle light-scattering photometer (Docket No. 545-325); (3) potential sensing; and (4) ellipsoidal flow chamber (Docket No. 5544-776).

DEVELOPMENT OF FLOW-SYSTEMS INSTRUMENTATION FOR RAPID CELL ANALYSIS AND SORTING

(G. C. Salzman, J. M. Crowell, J. C. Martin, J. A. Steinkamp, P. F. Mullaney, M. T. Butler, J. H. Jett, and C. A. Goad)

Multiangle Laser Light Scattering from Biological Cells in Fast Flow Systems

Early in the calendar year, a photodiode array was obtained, which consists of 32 concentric rings of photodiode material, for the purpose of examining the possibilities of using multiangle light scattering in fast flow systems for cell investigations. The experimental setup shown in Fig. 1 was used for this work. A 5-mW helium-neon laser was used as the light source. The laser light, collected with a 16-cm focal length lens, illuminates cells as they traverse a flow chamber of the FMF type.

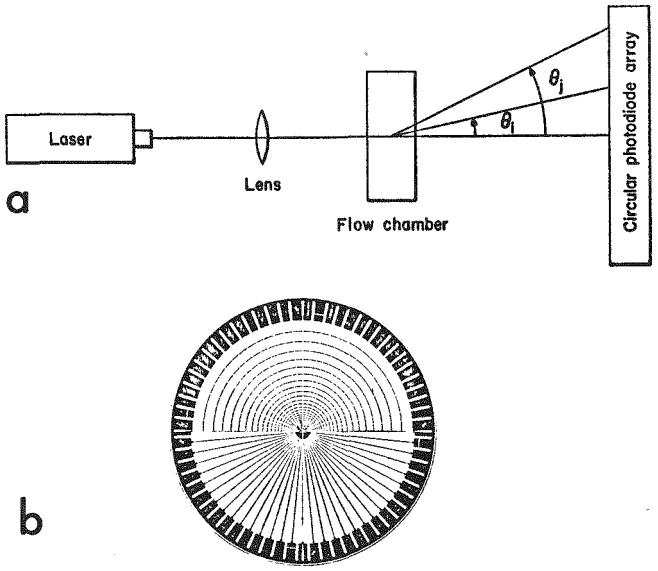

Fig. 1. (a) Top view of the experimental arrangement used to measure simultaneously the intensity of light scattered by a cell in a flow system at two angles. The photomultiplier tube at 90° with respect to the laser beam is not shown. (b) Face of the 32-ring photodiode array. The wedges were not used.

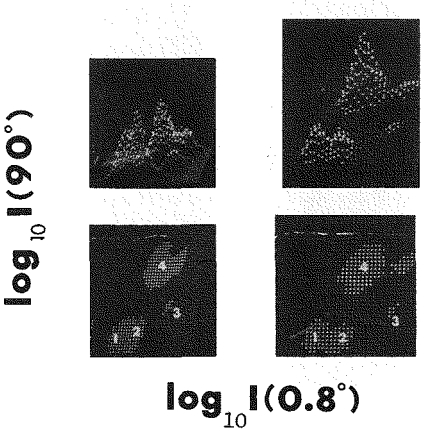

Fig. 2. Two-parameter light-scatter distributions from the buffy coats of two individuals. Both contour (lower half) and isometric (upper half) displays are shown for each individual. Based on standard leukocyte differentials, the groups were tentatively identified as (1) small lymphocytes; (2) large lymphocytes; (3) monocytes; and (4) granulocytes.

Light-scattering measurements are made using both a multiplier phototube placed at 90° to the optical axis of the system and a 32-element photodiode array centered on the optical axis of the system. Because of the large dynamic range of the light-scattering signals, special 3-decade logarithmic amplifiers were designed with a unique DC-coupled feedback system to allow measurement of small light pulses in the presence of a high DC background.

Only two angles of light scattering were implemented initially so that the data could be displayed on a two-parameter pulse-height analyzer. The two light-scatter signals were chosen from any two rings on the photodiode array or one signal from the array and one from the 90° detector. This system was first applied to the analysis of unfixed, unstained human leukocytes obtained from buffy coats which were prepared by centrifugation and lysis of the erythrocytes. The results are shown in Fig. 2. The three major peaks were identified as shown in Table I. The peaks correspond to lymphocytes, monocytes, and neutrophils. More recent work with blood from irradiated monkeys with high eosinophil counts shows the presence of a fourth peak which was shown to be eosinophils based on sorting and cytological

TABLE I

LEUKOCYTE DIFFERENTIAL FOR EACH OF THE SORTED GROUPS

Leukocyte Type	Composition of Sorted Group (%) Group 1	Group 2	Group 3
Neutrophil (segmented)	85.9	4.3	1.6
Neutrophil (band)	7.4	0.8	0.3
Monocyte	2.1	79.8	2.3
Lymphocyte	4.2	15.1	95.8
Eosinophil	0.4	0.0	0.0

examination. This work is significant because it was done with viable, unfixed, unstained cells. An automated leukocyte differential analysis method could be based on this approach. The main advantages of the method are its non-destructive nature and rapidity of the test.

Encouraged by these results with two angles, the computer-based system shown in Fig. 3 is being fabricated. With this instrument, 32 angles of light-scatter information can be collected for each cell in a fast flow system at a rate of about 1000 cells/sec and saved on a disk storage device. The light-scatter signal from each element of the photodiode array is logarithmically amplified and momentarily stored in a peak sense-and-hold circuit. A master control unit then multiplexes each of the

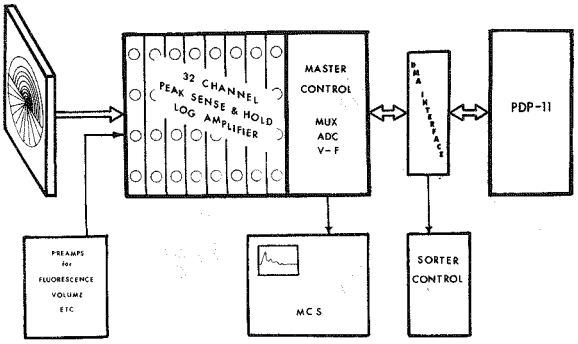

Fig. 3. Block diagram showing flow of information in the computer-based multiangle light-scattering system.

signals into an analog-to-digital converter (ADC) and then into the PDP-11/20 computer memory via a direct memory access interface. The pulse-height distributions for a given light-scatter angle are formed by reading the raw events from the disk, unpacking them, and generating a histogram in computer memory. Alternatively, the light-scatter intensity vs angle may be obtained directly by using a multichannel scaler. The resulting light-scatter angular distribution can represent that for a single cell or an averaged distribution for many cells.

After the light-scatter signatures are collected for several thousand cells, pattern recognition and feature extraction algorithms are applied to the data to determine the number of distinct classes into which the light-scatter signatures may be divided and to determine the minimum number of scattering angles needed to achieve these classifications. Data acquisition is then continued with the smaller set of scattering angles. Each class of cells can then be sorted physically based on software pulse-height windows and placed on slides for cytopathological examination.

A module has also been designed and constructed which will enable one of the existing cell sorters to be tied into the computer through this same master control unit and interface, thus allowing computer-controlled, simultaneous acquisition of Coulter volume, light scatter, green and red fluorescence signals, and software-controlled sorting. The computer-based light-scattering system described above is currently undergoing systems checkout and testing.

Advanced Flow Cell Development

The flow cell currently employed in our multiparameter cell analysis and sorting instrument has several drawbacks. Its construction is quite complicated; maintenance of the chamber can become cumbersome. The output windows were designed for use with approximately f/1.0 collection lenses; hence, a large fraction of the fluorescence signal is not collected. To overcome these shortcomings, several new flow cell designs are under consideration. These fall into two categories: (1) 4π chambers and (2) flat flow cells with simplified interior plumbing.

The flat flow cell is shown schematically in Fig. 1. The frame for the cell consists of brass and is shaped like a window frame. The two windows, optical flats of Supersil quartz, are cemented to this frame. The input and output ports for the sheath and sample fluids are small subunits which are inserted in the top and bottom of the chamber. Stability of flow and droplet formation have been achieved with this design. The large flat windows permit light-scattering measurements to be made at

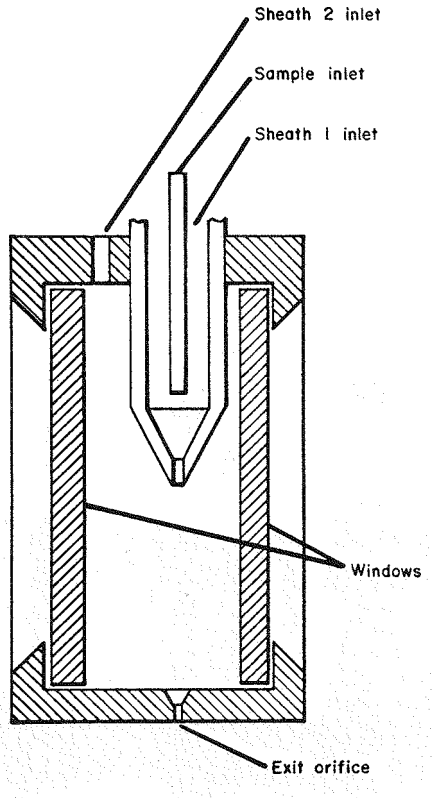

Fig. 1. Cross-sectional drawing of the flat flow chamber used in the multiangle light-scattering measurements. The square windows are about 17 mm on a side.

angles as large as 60° from the optical axis. Fluorescence detection will be accomplished in the manner described earlier by the Gottingen group under Dr. Jovin.[1]

The 4π chamber developed at LASL has an ellipsoidal interior[2] with the cell stream-light beam intersection centered at one focus and the optical detector centered at the second focus. The chamber is shown schematically in Fig. 2. Fluorescent light emitted by a cell at the primary focus is collected with a tapered light guide at the secondary focus. The interior of the chamber is gold plated and has given a 10-fold increase in signal over the current FMF arrangement. This increased sensitivity, for example, will be useful in immunofluorescent work where the signal levels are often quite low. In addition, use of this chamber will make several of the weaker argon lines useful. A demonstration of the increased sensitivity offered is given in Fig. 3

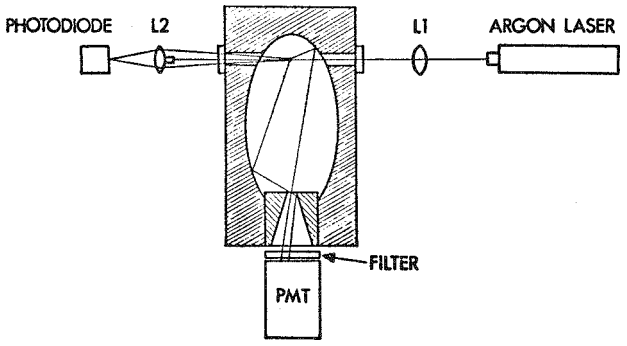

Fig. 2. Schematic drawing of the ellipsoidal flow chamber fluorescence detector (patent pending, AEC Docket No. S44-776).

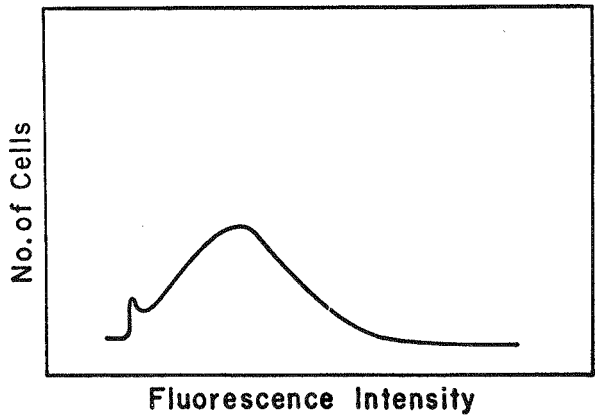

Fig. 3. Fluorescence intensity distribution of *E. coli* bacteria stained with 10^{-5} M acridine orange and excited at 488 nm.

where the fluorescence of acridine orange-stained *Escherichia coli* is shown. These same *E. coli* are not detectable with the standard FMF instrument.

REFERENCES

1. D. J. Arndt-Jovin and T. M. Jovin, J. Histochem. Cytochem. 22, 622-625 (1974).

2. G. C. Salzman, J. M. Crowell, H. A. Crissman, and P. F. Mullaney (1974), manuscript in preparation.

Sorter Improvements

Several improvements have been made on the LASL cell sorters and the associated electronics and computer systems. Both instruments are now equipped with an improved, hard-wired, data-processing system. The second sorter is interfaced to the PDP-11/20 through a four-parameter interface designed and fabricated at LASL. This interface can be expanded to handle as many as 32 parameters in four-parameter increments. A Tektronics 4010 terminal and 4610 hard-copy unit have replaced the teletype as the main method of communicating with the computer. An additional 16K of core storage and a 2.4×10^6 word dual disk storage system have also been added. This system, using the DEC RT-11 software, is now operational. A graphics capability for routine analysis of FMF data through the 4010 terminal is under development which will permit "on-line" life-cycle analysis and computer-controlled cell sorting.

Other improvements to the system are designed to provide ease of operation and include changes in the fluid control system, pressurization and regulation of the sheath supplies, ceramic orifices to replace plastic ones on the machine, a strobe employing light-emitting diodes rather than the General Radio Strobatac, and a combined oscillator driver to operate both the piezoelectric transducer and the strobe. A very important improvement involves the development of circuitry which analyzes the waveform produced as a cell crosses the light beam and measures the duration of the light signal. The duration of the signal (fluorescence or light scattering) is converted to a voltage pulse and processed in the usual manner. The time-to-amplitude conversion (TAC) method has proven useful in determining cellular dimensions as well as DNA and protein content and nuclear-to-cytoplasmic ratios. Details on the method and some

typical applications are given elsewhere in this report. The main advantage of the method is that DNA, protein, nuclear size, and cell size measurements can be made simultaneously on each cell.

Potential Sensing Technique

The potential sensing technique,[1] an improvement over the usual Coulter counting technique, was reported in the 1973 annual report. Improvements in the fabrication of the composite orifice assembly and the shape and size of the electrodes have been made during the current year.[2] Several of these new orifice-electrode assemblies have been made and are incorporated into a personnel testing apparatus. Testing of the device is currently underway.

A computer program has been developed to describe electrically the orifice assembly and the response of the system when a cell of given impedance passes through the orifice in the presence of a constant DC current. This model describes well the response of the system, including the expected shape of the pulses. The model is now being expanded to the AC case where impedance rather than simple resistance is measured. Cell capacitance can be obtained from the impedance measurement.[3] Capacitance may provide a method of determining membrane properties. Development of this computer model is well underway.

REFERENCES

1. G. C. Salzman, P. F. Mullaney, and J. R. Coulter, in Biophysical Society Abstracts, 17th Annual Meeting, Columbus, Ohio (February 27-March 2, 1974), Abstract No. FPM-F11.

2. G. C. Salzman, J. M. Crowell, R. D. Hiebert, and P. F. Mullaney (1974), manuscript in preparation.

3. E. C. Gregg and K. D. Steidley, Biophys. J. 5, 393 (1969).

DEVELOPMENT OF CELL STAINING AND PREPARATIONAL TECHNIQUES SUITABLE FOR USE WITH FLOW-SYSTEMS INSTRUMENTS

(H. A. Crissman, P. K. Horan, and A. Romero)

The successful application of flow systems for rapid, single-cell analysis is critically dependent upon the preparative techniques which maintain the cells in a monodispersed state during fixation, staining, and subsequent measurement. In instances where fluorescent staining techniques are employed, the quality and specificity of cellular staining must also be evaluated to ascertain the reliability of the analytical results. Automated analytical systems which are designed to perform rapid and precise measurements on individual cells cannot be totally relied on to distinguish cellular debris or cell clumps from properly stained single cells. Therefore, sample preparation involving both disaggregation of tissues into single cells and cell staining continues to play an extremely important role in flow-systems methodology.

Cell Dispersal

In most of our earlier studies, cellular analysis was performed on cells grown in tissue culture since these cells were relatively easy to disperse and the amount of cellular debris resulting from the preparative process was negligible. However, increased interest in analysis of specific tissues from *in vivo* systems has caused us to focus greater attention on adapting our present protocols and on seeking new methods for dispersal. We have found that modification of our conventional methods for cell dispersal, including the use of trypsin, EDTA, and DNase, is quite adequate for obtaining quality single-cell suspensions. Both C3H mouse mammary carcinomas and the EMT mouse carcinoma can be treated in this manner. In addition, collagenase is being used routinely for dispersal of human cervical and vaginal material since this enzyme produces a higher yield of single cells, compared to the trypsin protocol which tends to disrupt a large number of the cells. Collagenase may also be useful for dispersal of other tissues which prove to be quite sensitive to trypsin. At present, we are evaluating the use of trypsin, collagenase, and other enzymes including elastase and hyaluronidase on tumors such as mouse melanomas, sarcomas, and lung carcinomas as well as human tumor material when available.

Staining Methods Specific for Cellular DNA and Protein

Following a suggestion of Dr. E. Reich of the Rockefeller Institute, a study was undertaken in collaboration with R. A. Tobey (Group H-9) to determine the feasibility of using the antibiotic

mithramycin to stain cellular DNA for analysis by the FMF technique. The results of these studies led to an extremely rapid method requiring only 20 min staining time.[1] Mithramycin is highly selective for DNA and does not interact significantly with RNA.[2] With the exception of the requirement of magnesium, the mechanism of mithramycin-DNA binding is believed similar to that for actinomycin. No hydrolysis or RNase treatment is required in the staining protocol. Cells unfixed prior to staining or ethanol-fixed cells treated for 20 min with the staining solution (100 µg/ml mithramycin in 25% ethanol and 15 mM $MgCl_2$) yield DNA distributions comparable to those obtained with Feulgen-stained cells (see Fig. 1). Prior DNase treatment negates staining, while RNase has no effect on cellular staining.

Mithramycin has a maximum excitation peak at about 395 nm and an emission peak at 530 nm. Since excitation of mithramycin-stained cells in Fig. 1 was made suboptimally at 457 nm, the lowest efficient wavelength available in the argon-ion laser, the coefficient of variation (CV = 100 x standard deviation divided by the mean) for the cell population was somewhat higher than that of the acriflavine stained cells. However, the fraction of cells in G_1, S, and G_2 + M obtained by computer-fit analysis[3] compared well. Mithramycin appears to be superior to our standard acriflavine-Feulgen procedure for staining human vaginal and cervical material since the latter protocol tends to result in considerable non-specific cytoplasmic staining. It is now being used on human material here at LASL, as well as at the Laboratory of Pathology at the National Cancer Institute.

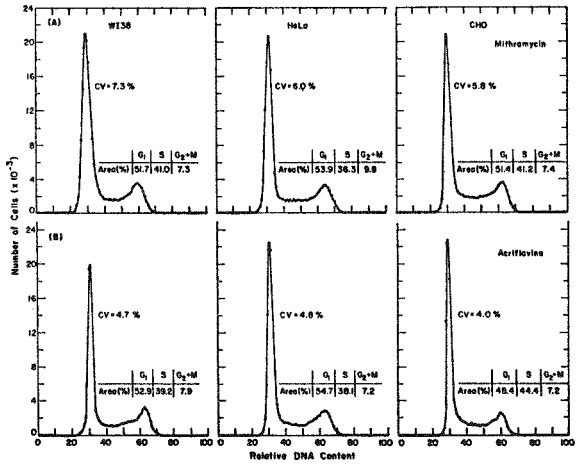

Fig. 1. Comparison of DNA distributions of WI38, HeLa, and CHO cells stained with mithramycin (A) or by the acriflavine-Feulgen procedure (B). The percentage of cells in the various phases of the cell cycle, as well as the coefficients of variation (CV) for the G_1 peaks, were obtained by computer-fit analysis.

Use of propidium iodide and fluorescein isothiocyanate for staining DNA and cytoplasmic protein, respectively,[4] has also been extremely advantageous for determining the nuclear-to-cytoplasmic ratio of single cells in flow systems.[5] Details of this application are given elsewhere in this report. This analytical technique employs bicolor staining which assigns one fluorochrome (red) specific for the nucleus and another fluorochrome (green) for the cytoplasm.

A number of red fluorescent protein dyes are being examined for use in combination with mithramycin as a more rapid method for DNA and protein analysis in single cells. These dyes include tetramethylrhodamine, rose bengal, and rosalic acid. The dyes of choice possess an emission spectrum at wavelengths longer than mithramycin so that adequate color resolution can be achieved.

REFERENCES

1. H. A. Crissman and R. A. Tobey, "Cell Cycle Analysis in Twenty Minutes," Science 184, 1297-1298 (1974).

2. D. C. Ward, E. Reich, and I. H. Goldberg, "Base Specificity in the Interaction of Polynucleotides with Antibiotic Drugs," Science 149, 1259-1263 (1965).

3. P. N. Dean and J. H. Jett, "Mathematical Analysis of DNA Distributions Derived from Flow Microfluorometry," J. Cell Biol. 60, 523-527 (1974).

4. H. A. Crissman and J. A. Steinkamp, "Rapid Simultaneous Measurement of DNA, Protein, and Cell Volume in Single Cells from Large Mammalian Cell Populations," J. Cell Biol. 59, 766-771 (1973).

5. J. A. Steinkamp and H. A. Crissman, "Automated Analysis of Deoxyribonucleic Acid, Protein, and Nuclear-to-Cytoplasmic Relationships in Tumor Cells and Gynecologic Specimens," J. Histochem. Cytochem. 22, 616-621 (1974).

BIOLOGICAL AND MEDICAL APPLICATIONS OF FLOW-SYSTEMS

CELL ANALYSIS AND SORTING INSTRUMENTATION

(L. S. Cram, H. A. Crissman, J. A. Steinkamp, M. S. Oka, P. K. Horan, A. Romero, and J. C. Forslund)

Newcastle Disease Virus (NDV)

The major difficulty encountered by the U. S. Department of Agriculture in the control of exotic Newcastle disease virus (NDV) strains has been the unavailability of a rapid test for differentiating the many strains of NDV. Immunological assays have not been developed because of the lack of immunological specificity. We are measuring the effect of NDV infection on cellular systems using the LASL flow microfluorometer (FMF). A detailed protocol for infecting mammalian cells, their dispersal, fluorescent DNA staining, and measuring the degree of cell fusion has been reported.[1] While several virulent strains of the virus have been shown to produce more fusion than do less virulent strains, the generality of this conclusion is still under investigation. Several cell lines have been used for cell fusion measurements in the hope of finding a cell type that is highly susceptible to NDV-induced fusion. Human embryonic lung (HEL), porcine kidney (PK-15), beef turbinate (BT), and baby hamster kidney (BHK/21) cells all proved to be less susceptible to cell fusion than either chick embryo fibroblasts (CEF) or human amnion (FL) cells.

Because cell loss is a problem with particular NDV strains, the number of fused cells in suspension vs those attached to the culture flask was measured after 16 h of incubation. In at least one case, the ratio of single cells in suspension to fused cells in suspension was not the same as the equivalent ratio for cells remaining attached. In such circumstances, it is necessary to count the total number of fused cells in suspension plus attached to avoid under- or overestimating the amount of fusion. Classical methods of determining the fusion index rely on counting the number of fused cells remaining attached to a microscope slide. Thus, any cells that have fused and detached from the monolayer are not counted. With the flow-analysis system we are employing at LASL, the total amount of fusion is determined.

Cell loss is a serious problem that can greatly alter the determination of the amount of cell fusion. Several of the virulent strains produce fused cells that are extremely fragile. Processing fragile cell suspensions is difficult and does not always result in a sample representative of the original material. The amount of cell fusion for some virulent strains is smaller than one would expect and shows too much variability between repeat experiments.

Fifteen NDV strains have been received from Dr. Robert Hanson of the University of Wisconsin and are presently being characterized for their ability to cause cell fusion. Strain virulence is also being determined by alternative techniques. The outcome of this study will answer the central question of what relationship exists between the ability of NDV to induce cell fusion and its virulence *in vivo*.

REFERENCE

1. L. S. Cram, "Rapid Differential Diagnosis of Newcastle Disease Virus," Annual Report from July 1, 1972-June 30, 1973, Los Alamos Scientific Laboratory report LA-5421-PR (June 30, 1973).

Lymphocyte Stimulation with Specific Mitogens

The objective of this project was the application of FMF to the detection and diagnosis of tuberculosis in cattle. The flow microfluorometer was used to study the specificity of bovine peripheral lymphocyte response to two purified protein derivatives [avium (PPD-A) and bovis (PPD-B)] and to phytohemagglutinin (PHA). The instrument was used to measure the degree of lymphocyte stimulation according to cellular DNA content. Three weeks following the infection of an animal with *Mycobacterium avium* or *Mycobacterium bovis*, the peripheral lymphocytes were found to be sensitized to the corresponding PPD as evidenced by their entry into a DNA synthetic period.

The FMF techniques developed at LASL were able to detect 11 out of 11 infected animals and to correctly differentiate the two strains of *Mycobacterium*. Analysis of lymphocyte stimulation by the FMF has several very important advantages over current tritiated thymidine analysis: sample preparation requires only 20 min, non-specific uptake of thymidine is not a problem, and the hazards of using large amounts of radioactive tracer for large-scale routine animal screening are eliminated.

Immunological Investigations

A modest experimental immunobiology program was initiated during the summer of 1974 and is being designed to take maximum advantage of the LASL rapid cell analysis and sorting capability. Several preliminary experiments have been performed, one of which, although incomplete, is described here.

The potential immunoglobulin expression of restricted populations of murine lymphoid cells was investigated in a cooperative project with Drs. Arthur Bankhurst and Robert Anderson of the University of New Mexico School of Medicine. The functional assessment of immunoglobulin expression was done *in vivo* using histocompatible but allotypic distinct congenic lines of mice. The LASL cell sorter was used to isolate splenic-derived B cells bearing a single immunoglobulin class (IgM) from BE6 mice. These lymphocytes were then placed in irradiated C57B1/6 mice by tail vein injection. The production of donor immunoglobulin is being assessed by radioimmunoassay using sera taken from recipients at various times after cell transfer. The initial results indicate that the donor IgM-producing cells are switching over to produce IgG in the recipient mouse.

A New Method for Measurement of Nuclear and Cytoplasmic Size in Individual Mammalian Cells

A new technique for rapid measurement of nuclear and cytoplasmic sizes and their relationship has been developed recently[1] and is currently under evaluation using both tissue culture cells and human gynecological material. The method is based on quantitative fluorescent staining of nuclear DNA with one dye and total cellular protein with a second dye. The early steps in the development of the two-color staining technique were reported in the 1973 LASL annual report.

Cells can be stained with a single fluorescent dye such as acriflavine[2] or mithramycin[3] which is DNA-specific or with two different dyes, propidium di-iodide (PI) (red fluorescence) and fluorescein isothiocyanate (FITC) (green fluorescence) which stain DNA and protein, respectively.[4] Depending on which of the two staining procedures is used, two methods of analysis are possible. For example, if a cell population is stained using the two-color technique, then DNA, protein, and nuclear and cytoplasmic dimensions can be determined from the fluorescence measurements. However, if a single nuclear stain is used, the DNA content and nuclear dimension can be obtained from the fluorescence measurement and the whole cell dimension from a simultaneous light-scattering measurement.[5]

The way cells are measured is illustrated in Fig. 1. Cells stained with a fluorescent dye(s) enter the flow chamber and flow at a constant velocity across the shaped beam of exciting light from the argon laser.[6] As each cell crosses the laser beam, the light-scattering and fluorescent signals generated are collected. From these analog signal waveforms, two types of information can be obtained. Electronic integration of the red PI (DNA) and green FITC (protein) signals gives the total DNA and protein content of each cell. Similar integration of the DNA content and light-scatter signals yields total DNA and whole cell size (cytoplasm) on each cell. Since the cells are moving at a constant velocity in laminar flow, the time duration of the two signals (T_c for the cytoplasm, T_n for the nuclear signal) can be converted to a dimension by the

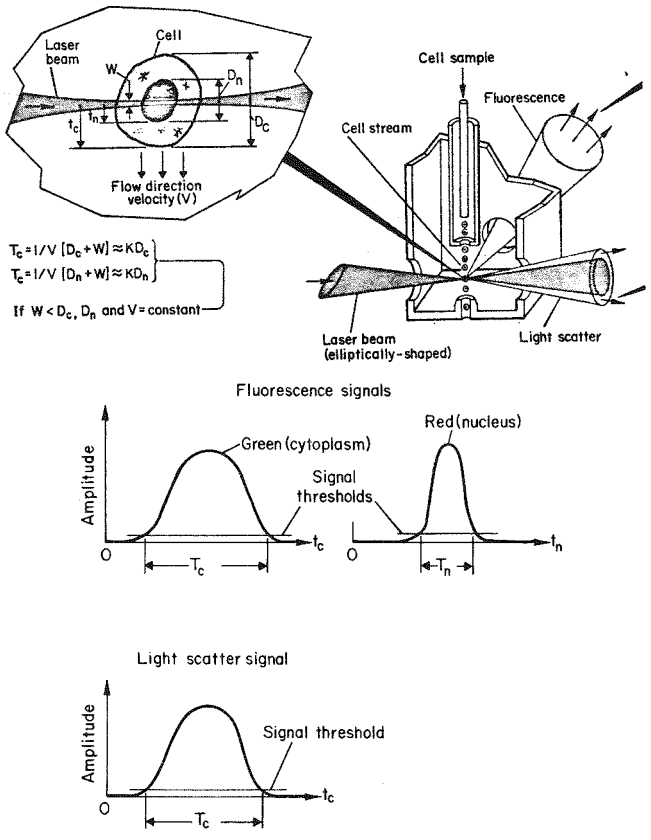

Fig. 1. Diagram illustrating a sectional view of the flow chamber, expanded view of a typical cell traversing across the laser beam, and typical signal waveforms.

use of time-to-amplitude conversion circuits. A nuclear-to-cytoplasmic ratio can also be constructed by taking the ratio of these two signals. The capability of processing these signals either individually or as ratios or other combinations has been developed previously at LASL.[6] These data are usually displayed as frequency distribution histograms using a multichannel pulse-height analyzer in either the single or dual parameter mode. Cells can also be sorted[6] based on various parameters. Our technique differs from the computerized slit-scan method of Wheeless and Patten[7] in that the Wheeless system records fluorescence contours from acridine orange-stained cells, and nuclear and cytoplasmic size relationships are computed from these contours.

The DNA and protein content distributions for EMT-6 cells cultured *in vitro* and stained with the double stain protocol PI/FITC[4] are shown in Fig. 2. Also shown are the nuclear (N) and cytoplasmic (C)

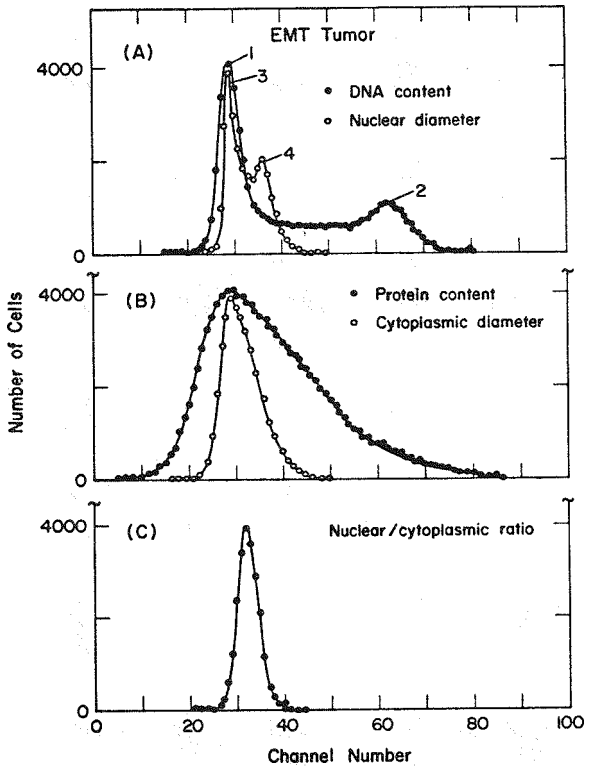

Fig. 2. Frequency distribution histograms of EMT-6 tumor cells cultured *in vitro* and stained with propidium di-iodide (DNA content) and fluorescein isothiocyanate (total protein): (A) DNA content and nuclear diameter distributions; (B) total protein and cytoplasmic diameter distributions; and (C) the nuclear-to-cytoplasmic diameter ratio distribution.

dimensions and the N/C ratio distribution. Peaks 1 and 2 of Fig. 2A represent the relative DNA content of cells in G_1 and $(G_2 + M)$, with the S phase cells distributed between the two peaks. Peaks 3 and 4 represent the relative nuclear dimension of G_1 and $(G_2 + M)$ cells, respectively. The ratio of the modal channels of peak 2/peak 1 (DNA content) and peak 4/peak 3 (nuclear dimension) are 2.14 and 1.26, respectively. Since it has been shown previously that the DNA content and nuclear volume are proportional,[8] then the cube root of the $(G_2 + M)/G_1$ DNA ratio should be approximately equal to the same nuclear dimension ratio if the cells are reasonably spherical. The value calculated from the DNA ratio is 1.29 and is in good agreement with the experimental value.

Figure 2B shows both the total protein and cytoplasmic dimension distributions. The N/C ratio was obtained by a simultaneous measurement of the time duration of the nuclear and cytoplasmic fluorescence signals and analog division for each cell in the population.

Figure 3 shows the DNA content, light scattering, nuclear and cytoplasmic dimensions, and the N/C ratio distributions for EMT-6 cells stained using the acriflavine-Feulgen[2] protocol. Peaks 1 and 2 correspond to the G_1 and $(G_2 + M)$ DNA content, and peaks 3 and 4 are the distributions of nuclear diameters for G_1 and $(G_2 + M)$ cells. The ratios of peak 2 to 1 modal channel (DNA content) and peak 4 to peak 3 modal channel (nuclear diameter) are 2.07 and 1.18, respectively. Again the experimental diameter ratio 1.18 is in good agreement with the calculated value of 1.27. The small-angle light-scattering distributions are shown in Fig. 3B.

The cytoplasmic diameter distribution was obtained by measurement of the time duration of the scatter signal. The N/C ratio is shown in Fig. 3C and was constructed by the simultaneous analysis of the duration of the light-scattering signal and the DNA fluorescence signal.

Figure 4A and 4B show the nuclear and cytoplasmic dimension distribution for human vaginal cells obtained from a normal individual. The cells were stained with the two-stain protocol. The nuclear dimension distribution is unimodal, whereas the cytoplasmic dimension distribution is bimodal, indicating that two size classes of cells are

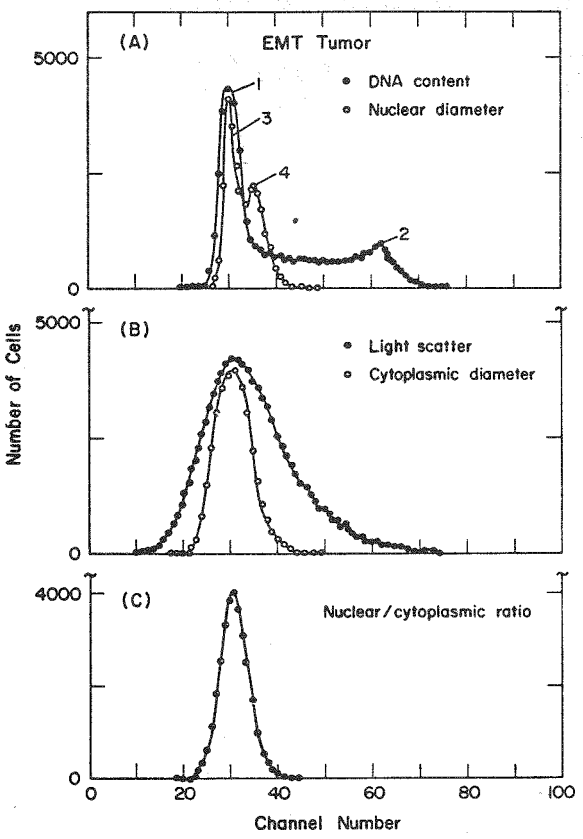

Fig. 3. Frequency distribution histograms of EMT-6 tumor cells cultured *in vitro* and stained with acriflavine (DNA content): (A) DNA content and nuclear diameter distributions; (B) light-scatter and cytoplasmic diameter distributions; and (C) nuclear-to-cytoplasmic diameter ratio distribution.

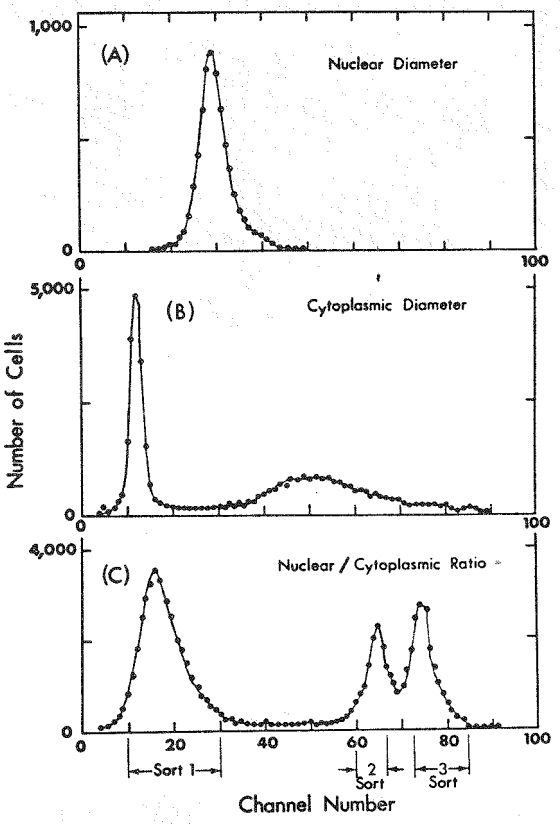

Fig. 4. Frequency distribution histograms of normal human vaginal cells stained with propidium di-iodide (DNA) and fluorescein isothiocyanate (protein): (A) nuclear diameter distribution; (B) cytoplasmic diameter distribution; and (C) nuclear-to-cytoplasmic diameter ratio distribution.

present. The N/C ratio is shown in Fig. 4C and indicates the presence of three different cell classes. The cells were sorted on the basis of the N/C ratio designated by regions 1, 2, and 3. Photomicrographs of the original mixture and the sorted cells are shown in Fig. 5. Figure 5A shows the sample prior to sorting. Cells with the low (region 1) N/C ratio were separated and identified as normal squamous cells and are shown in Fig. 5B. Cells with higher (regions 2 and 3) N/C ratios were sorted and identified as trichomonads, as shown in Fig. 5C.

These results demonstrate a new capability for studying and establishing relationships between cellular DNA and protein content and between nuclear and cytoplasmic size for both normal and abnormal human and cultured cells.

REFERENCES

1. J. A. Steinkamp and H. A. Crissman, J. Histochem. Cytochem 22, 616 (1974).

2. R. A. Tobey, H. A. Crissman, and P. M. Kraemer, J. Cell Biol. 54, 638 (1972).

3. H. A. Crissman and R. A. Tobey, Science 184, 1297 (1974).

4. H. A. Crissman and J. A. Steinkamp, J. Cell Biol. 59, 766 (1973).

5. P. F. Mullaney and P. N. Dean, Biophys. J. 10, 764 (1970).

6. J. A. Steinkamp, A. Romero, P. K. Horan, and H. A. Crissman, Exp. Cell Res. 84, 15 (1974).

7. L. L. Wheeless and S. F. Patten, Acta Cytol. 17, 333 (1973).

8. K. P. Baetcke, A. H. Sparrow, C. H. Nauman, and S. S. Schwemmer, Proc. Natl. Acad. Sci. USA 58, 533 (1967).

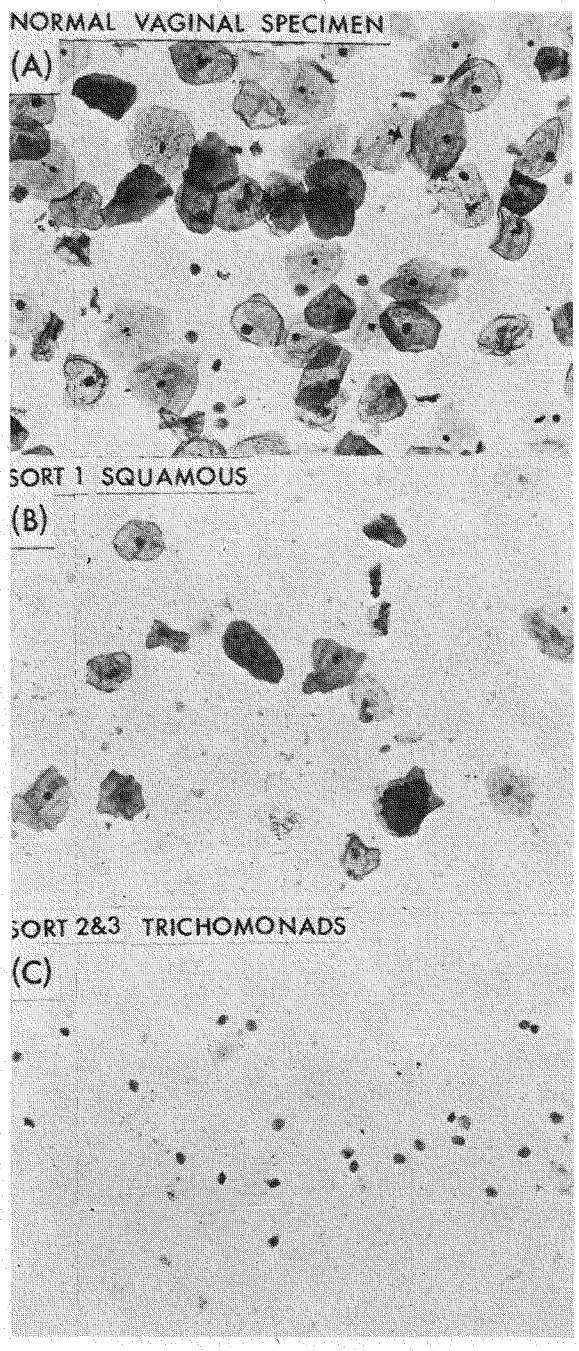

Fig. 5. Photomicrographs of cells sorted from a normal human vaginal specimen and counterstained with the Papanicolaou technique: (A) the specimen prior to sorting; (B) sorted normal squamous cells; and (C) sorted trichomonads.

Analysis of Chlorophyll Fluorescence in Algae by Flow Microfluorometry

Preliminary studies at LASL have demonstrated the feasibility of flow-system single-cell analysis of various algae genera, including blue-green (*Anacystis*) and green (*Chlorella* and *Chlamydamonas*), forms on the basis of laser-excited chlorophyll fluorescence. In these studies, total fluorescence, Coulter volume, and light-scattering (size) analysis were performed on unstained and unfixed cultured samples. Distributions obtained by flow analysis showed the blue-green algae to be smaller in size and, therefore, of much lower fluorescence compared to the green algae. Although complete spectral analysis of these three algal genera on a cell-to-cell basis were not performed, these capabilities are becoming available at LASL in the near future. Since it is known that the various algae do contain distinguishing pigmentation, complete spectral flow-system analysis can provide for even better general characterization of phytoplankton when coupled with sizing and total fluorescence analysis. One general indication of water quality degradation is the increase in blue-green algae populations with a concomitant decrease in the green forms. In thermally polluted water, thermophilic forms of the blue-green algae also become prominent. Cell sorting, a capability now available, can permit the segregation of various viable populations for visual inspection or for cultivation of the organisms for other biochemical and metabolic studies.

Effects of Culture Conditions on Chinese Hamster DNA Content and Cell-Cycle Traverse

Previous studies of x-irradiation-induced cycle delay in Chinese hamster cells have indicated that the cause of the delay is independent of the culturing conditions.[1] It was felt that, in these previous studies, insufficient consideration was given to culture conditions which might significantly alter cell-cycle traverse. The present experiments were conducted using the LASL FMF which provides a unique method for detecting changes in the distribution of cells throughout the cell cycle.[2-4] Chinese hamster cells were maintained in both monolayer and spinner culture in (1) complete F-10 medium; (2) thymidine-free F-10 medium; (3) McCoy's 5A medium; and

(4) McCoy's 5A medium with thymidine. All media were supplemented with 10% calf and 5% fetal calf sera. The amount of thymidine added to the McCoy's medium was equal to that found in the F-10 medium (0.7 mg/liter). Monolayer and spinner cultures were grown for at least 2 wk to ensure acclimation of the cells to each growth medium. Cell volume was measured with a Coulter volume spectrometer. Growth rates were followed for all cultures, and FMF studies for DNA content were also conducted on each culture.

Differences in volume of cells cultured under different conditions were not significant. Morphological characteristics, as measured with the light microscope, also were not significantly different. The growth rates of Chinese hamster cells under various culture conditions are shown in Table I. The cells appear to grow optimally in complete F-10 medium. Addition of thymidine to McCoy's 5A medium did not have any remarkable effect on the growth rate; however, the method of culture very definitely affects the growth rate in the case of McCoy's 5A medium, as shown in Table I. This expansion of the cell-cycle time is exhibited to a lesser extent in the cells cultured in thymidine-free F-10 medium. The expansion of the cell-cycle time is exhibited to a lesser extent in cells cultured in F-10 medium without thymidine. This medium significantly decreases the growth rate in spinner as compared to the rate for cells in complete F-10 medium. This effect is not as great in the monolayer cultures. A comparison of the growth rate of the cells grown in complete F-10 and McCoy's 5A media shows a sizable difference in generation time, especially in the case of the spinner cultures.

The cell-cycle distributions are shown in Table II. There is no significant redistribution of

TABLE I

GROWTH RATES FOR CHINESE HAMSTER CELLS GROWN IN VARIOUS MEDIA

Medium	Growth Rate (h) Monolayer	Spinner
F-10	13.7	13.0
F-10 less Thymidine	14.3	17.7
McCoy's 5A	15.8	20.8
McCoy's 5A plus Thymidine	14.3	20.7

TABLE II

PERCENTAGE OF CELLS IN VARIOUS PHASES OF THE CELL CYCLE FOR SEVERAL GROWTH MEDIA

Culture Medium	G_1	S	(G_2 + M)
Monolayer			
F-10	45.90	46.12	7.99
F-10 without Thymidine	26.77	62.69	10.55
McCoy's 5A	42.09	48.43	9.48
McCoy's 5A plus Thymidine	37.18	49.84	10.99
Spinner			
F-10	54.14	40.87	4.99
F-10 without Thymidine	34.30	59.10	6.60
McCoy's 5A	44.52	49.82	5.67
McCoy's 5A plus Thymidine	37.48	51.60	10.92

the various populations except for the cells grown in thymidine-free F-10 medium. Under these conditions, more cells are present in S phase of the cycle in both monolayer and spinner culture.

Studies are currently underway with R. A. Walters and R. L. Ratliff (Group H-9) to investigate the change in precursor pool sizes associated with Chinese hamster cells cultivated in thymidine-free F-10 medium.

REFERENCES

1. D. B. Leeper, M. H. Schneiderman, and W. L. Dewey, "Effect of Culturing Conditions on Radiation-Induced Cycle Delay in Synchronized CHO CEIls X-Irradiated in G_1," Internat. J. Radiation Biol. 21, 191-196 (1972).

2. P. F. Mullaney, J. A. Steinkamp, H. A. Crissman, L. S. Cram, and D. M. Holm, "Laser Flow Microphotometers for Rapid Analysis and Sorting of Individual Mammalian Cells," in Laser Applications in Medicine and Biology, Vol. 2 (M. L. Wolbarsht, ed.), Academic Press, Inc., New York (1974), pp. 151-204.

3. M. A. Van Dilla, T. T. Trujillo, P. F. Mullaney, and J. R. Coulter, "Cell Microfluorometry: A Method for Rapid Fluorescence Measurement," Science 163, 1213-1214 (1969).

4. D. M. Holm and L. S. Cram, "An Improved Flow Microfluorometer for Rapid Measurements of Cell Fluorescence," Exp. Cell Res. 80, 105-110 (1973).

Simultaneous Analysis of DNA Content and Cell Volume in Cells Treated with a Chemotherapeutic Agent

The determination of the effects of chemotherapeutic agents on cell-cycle progression is a difficult and tedious task. Cell enumeration and autoradiographic data can reveal cell division and DNA synthetic activity but do not indicate readily the presence of non-progressing or arrested cells. Autoradiography may not reflect the percentage of the cell population in the S phase if cellular thymidine pools or cell membranes are seriously affected by the drug. However, use of flow-systems analysis, which is independent of progression capacity, in conjunction with autoradiography and cell enumeration can be extremely valuable for providing the clinician with information which could be useful for the design of regimens for drug administration.

Simultaneous analysis of the DNA content and volume of cells provides a powerful method for studying the effects of drugs. DNA distributions, as indicated above, reveal capability for cell-cycle traverse, while cell volume analysis yields information relating to the gross biosynthetic capacity of cell populations. Figure 1 shows both separate and simultaneous DNA and cell volume analyses for CHO cells treated continuously with 1-(2-chloroethyl)-3-(4-methylcyclohexyl)-1-nitrosourea (MeCCNU) for 24 h immediately following release from G_1-arrest.[1] Similar DNA and cell volume data are also shown for cultures of asynchronous, G_1-arrested, and control CHO cell populations at 24 h following synchrony release. At 24 h, control cells had undergone

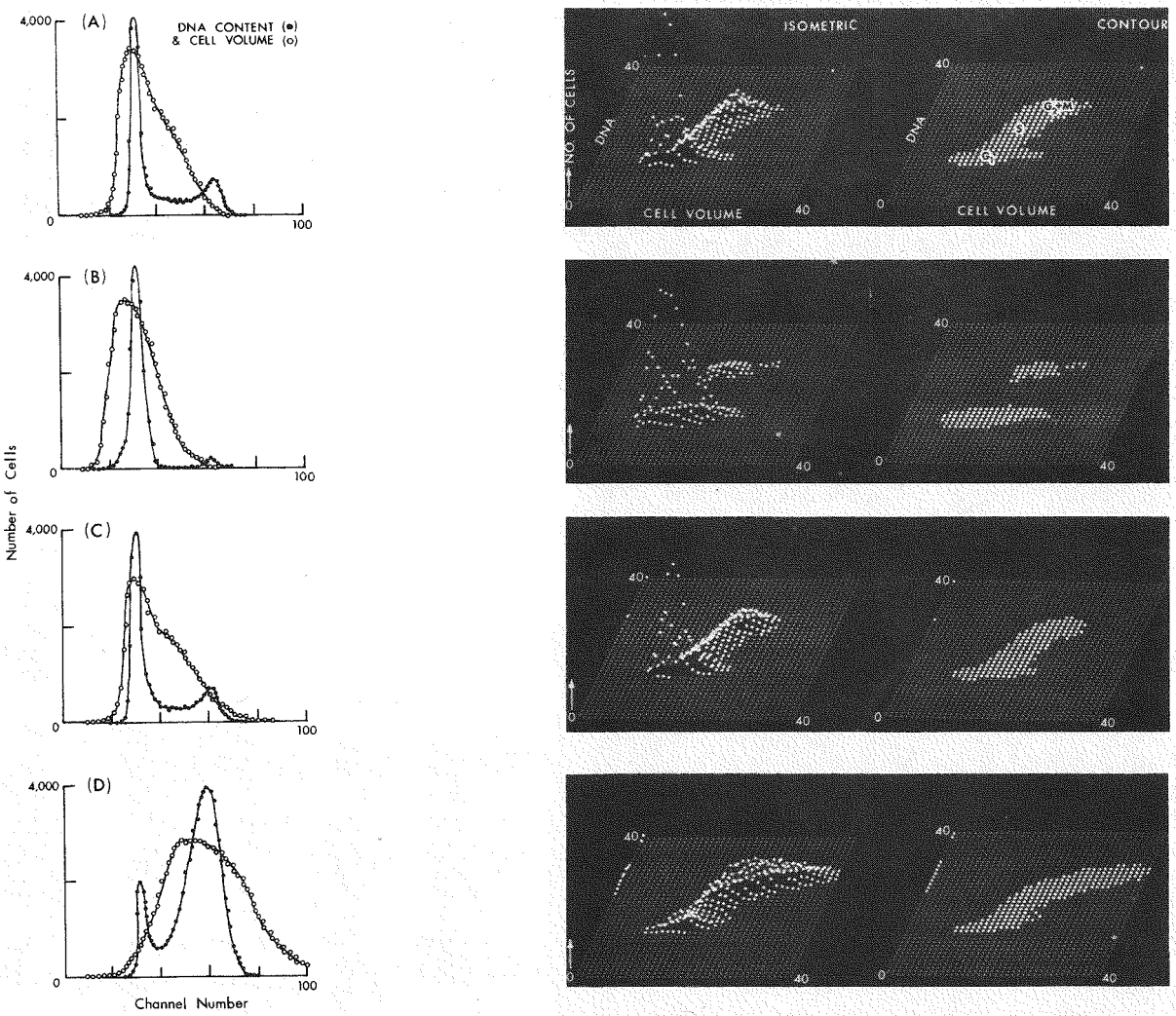

Fig. 1. Separate and simultaneous analyses of DNA and cell volume of control and MeCCNU-treated CHO cells. Untreated asynchronous (A), G_1-arrested (t = 0 h) (B), and control cell population (C) at 24 h following release from G_1 were fixed and stained by the acriflavine-Feulgen procedure. Cells synchronized in G_1 and released in the presence of MeCCNU (10 µg/ml) were collected at 24 h (D) and analyzed similarly.

synchrony decay and were quite similar in both DNA content and cell volume to the asynchronous population. However, the MeCCNU-treated cells had accumulated in late interphase and likewise showed a significant increase in cell volume. Simultaneous analysis indicates vividly that it is only those cells in late S and G_2 that continue to increase in size, while the volumes for cells in G_1 and early S remain near control values. It is clear from the simultaneous analyses that drug-treated cells arrested in late interphase had lost cell division capacity but were not grossly inhibited for synthesis of other cellular macromolecules. However, these unbalanced growth conditions (e.g., excessively high cell volume-to-DNA ratio) will result eventually in cell death.

REFERENCE

1. R. A. Tobey and H. A. Crissman, "Comparative Effects of Three Nitrosourea Derivatives on Mammalian Cell-Cycle Progression," Cancer Res. (1974), in press.

Sorting and Autoradiographic Analysis of ^{3}H-Thymidine Labeled Cells

The DNA content distribution of CHO cells pulse-labeled with ^{3}H-thymidine is shown in Fig. 1. Equal numbers of cells were sorted on the basis of G_1, S, and (G_2 + M) content and were examined using conventional autoradiographic techniques. The percentage of labeled cells obtained from each sorted region is shown in Fig. 1. The small percentage of labeled cells in the sorted G_1 fraction is due to early S cells, while the labeled cells in the (G_2 + M) sorted fraction are predominantly late S cells and cells which had moved from S into G_2 during the pulse-labeling period. The cell population had a total labeling index of 33%. Using similar techniques, the assessment of non-traversing cells can be obtained by sorting cells which have been continuously labeled with ^{3}H-thymidine for appropriate time periods. The occurrence and number of unlabeled G_1, S, and (G_2 + M) cells can reflect the extent of any phase-specific arrest of cells in the population. Similar methods have been used in the study of the nature of cell-cycle kinetics for populations of human diploid cells maintained in low serum-containing medium.[1]

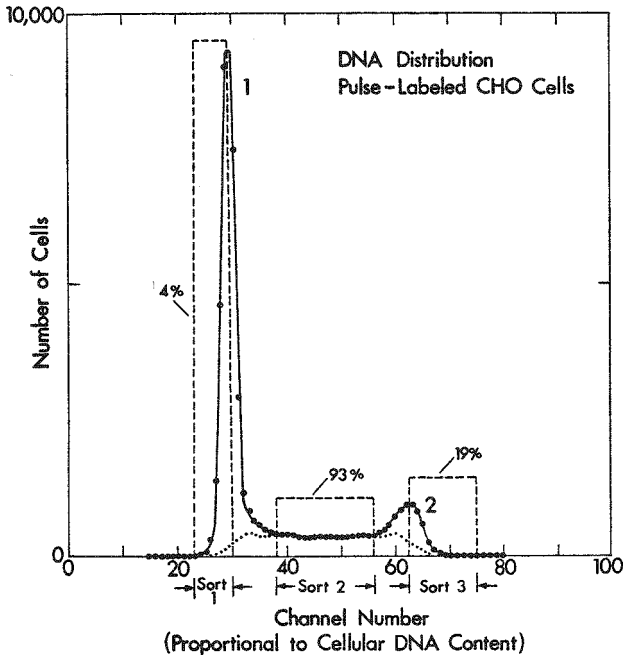

Fig. 1. DNA content frequency distribution histogram of CHO cells pulse-labeled 15 min with 5 μCi/ml of ^{3}H-thymidine, stained with propidium iodide, and sorted on the basis of DNA content. The dotted line is a second-degree polynomial computer curve fit representing cells in S phase. The percentage of ^{3}H-thymidine-labeled cells from each sorted region is indicated.

REFERENCE

1. R. T. Dell'Orco, H. A. Crissman, J. A. Steinkamp, and P. M. Kraemer, "Population Analysis of Arrested Human Diploid Fibroblasts by Flow Microfluorometry," Exp. Cell Res. (1974), in press.

PHYSICAL DOSIMETRY AND RADIOBIOLOGY STUDIES AT LAMPF

[M. R. Raju, C. Richman, T. T. Trujillo, and J. H. Jett, in conjunction with R. A. Walters and R. A. Tobey (H-9)]

Age-Response of Line CHO Cells to X-Irradiation and Alpha Particles from Plutonium

Age-response studies of mammalian cells are of interest in studying the mechanisms of cell killing by ionizing radiations since there are large variations in radiosensitivity of cells across the cell cycle. With some exceptions, cells are sensitive when in the mitotic (M) phase and resistant when in the late DNA synthetic (S) phase. The differences in radiosensitivity between these two stages for x-irradiation are nearly the same as those of oxygenated and hypoxic cells. Hence, stage sensitivity

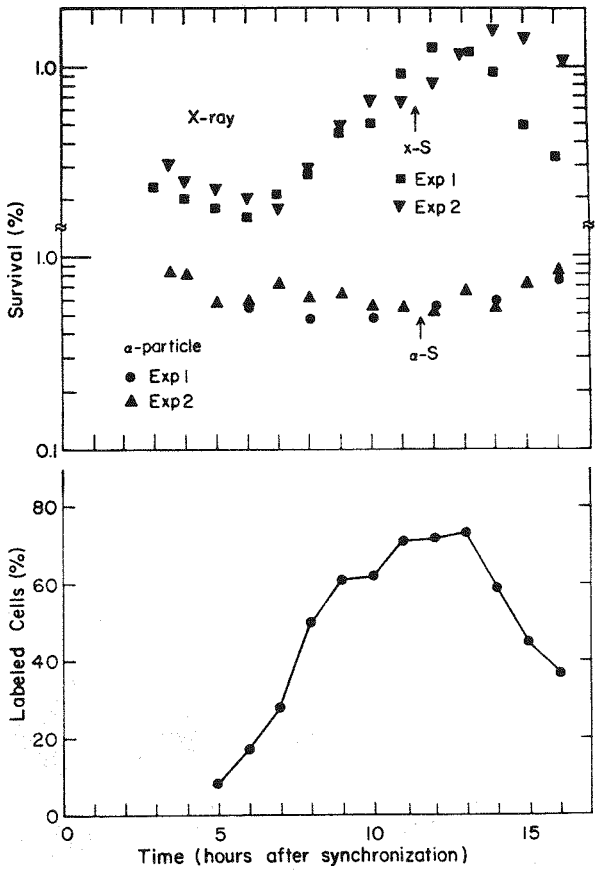

Fig. 1. (Top) Percent cell survival after exposure to 900 rad of x-rays and after exposure to 250 rad of alpha particles at different times after mitotic selection. (Bottom) Percent labeled cells as a function of time after mitotic selection.

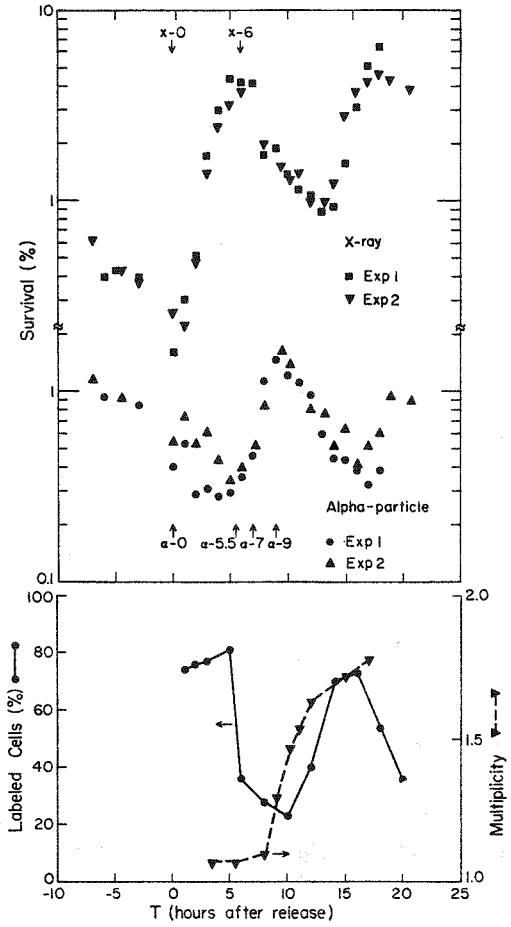

Fig. 2. (Top) Percent cell survival after exposure to 900 rad of x-rays and after exposure to 250 rad of alpha particles as a function of time after release from hydroxyurea. (Bottom) Percent labeled cells and cell multiplicity as a function of time after release from hydroxyurea.

variations, in a practical sense, could be just as important as the oxygen effect in radiotherapy.

High-LET radiations are being actively considered in radiotherapy for the treatment of resistant tumor types. It is known that, for high-LET radiations, the shape of the mammalian cell-survival curves approaches an exponential and that environmental factors such as the presence or absence of oxygen have minimal effect on radiosensitivity. It is felt that agedistribution of cells in different tissues can be different and that variation of radiosensitivity with the cell cycle is an important factor in therapy. Although the stage sensitivity of synchronized cells has been studied extensively, there is no clear consensus as to its variation (or lack thereof) using high-LET radiations.

The age-response of Chinese hamster cells (line CHO) synchronized by mitotic selection and by mitotic selection with hydroxyurea resynchronization was studied for x-rays and alpha particles from plutonium of 4.4-MeV residual energy. The age-response for alpha particles when mitotically synchronized cells were used indicated that cells in S phase are slightly more sensitive but that the magnitude of variation is quite small (Fig. 1). When cells were synchronized first by mitotic selection and then resynchronized by hydroxyurea, the variation of radiosensitivity as a function of the cell cycle for x-rays was found to be enhanced because of a higher degree of synchrony (Fig. 2). In the case of alpha particles, it was found that cells in the late S phase were more sensitive and that there was a clear peak of resistance corresponding to cells in G_2-early G_1.

Cell Survival Curves

[M. R. Raju, T. T. Trujillo, and E. Bain, in conjunction with J. Dicello (MP-3)]

Measurement of cell survival curves at points of interest for negative pions under oxygenated and hypoxic conditions is of primary value. Because of possible uncertainties in getting the beam at the expected time and limited dose rate, in the initial stages the biological system should be adopted to suit these conditions. The technique of using capsules of 1-ml plastic pipettes, as described by Hall *et al.*,[1] is very practical. Hypoxic conditions were obtained by using a large concentration of cells (3×10^6/ml) in a sealed pipette capsule. Cells in a concentration of 3×10^4/ml remained under oxygenated conditions. Pipette pieces 7 mm long were sealed with 0.3 ml of cell suspension by using a modified soldering iron, and the sealed ends were immersed in a molten wax to ensure a good seal. Chinese hamster ovary cells (CHO) were used in these studies because they are continuously maintained in suspension culture at LASL. The number of cells needed for these investigations is very small when compared to their normal use by the Cellular and Molecular Radiobiology Group (H-9).

About a 5-h storage was found to be adequate to deplete the oxygen in capsules containing 0.3 ml at a cell concentration of 3×10^6/ml. Figure 1 shows the survival curves for 250-KVP x-rays at a dose

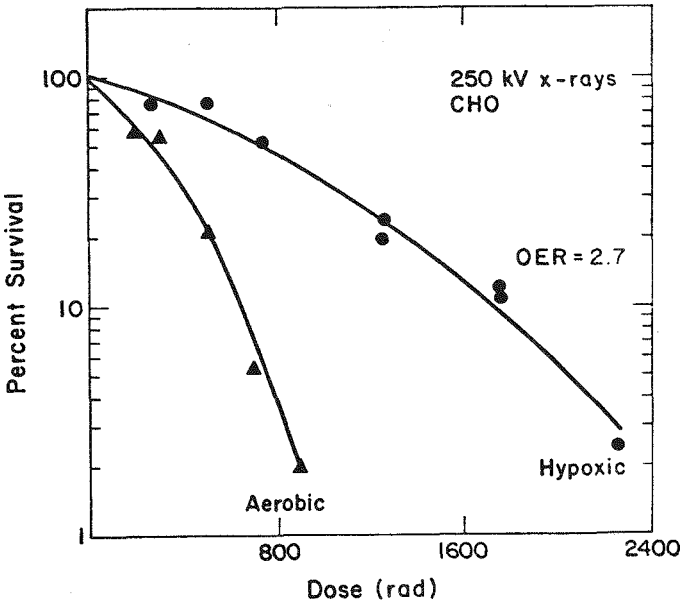

Fig. 1. Cell survival curves for x-rays under oxygenated and hypoxic conditions.

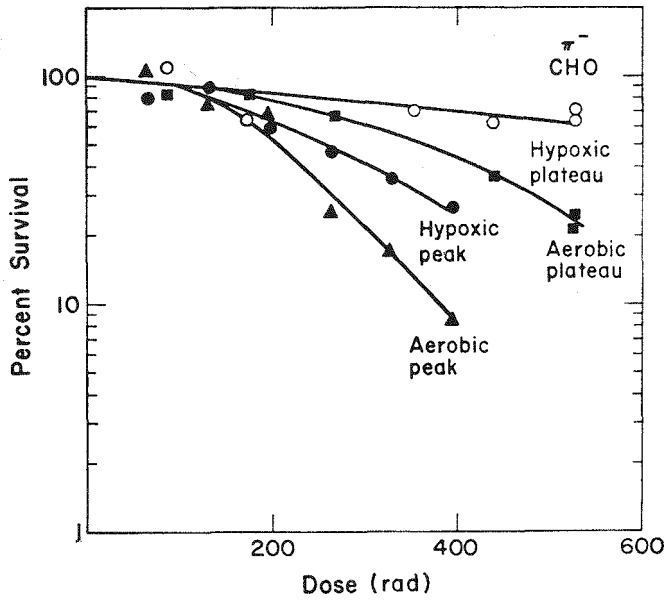

Fig. 2. Cell survival curves at the plateau and peak for negative pions under oxygenated and hypoxic conditions.

rate of 200 rad/min. The oxygen enhancement ratio (OER) at 1% survival was 2.7. Figure 2 shows the survival curves at the middle of the plateau and peak for negative pions. The dose rate of negative pions at the middle plateau is about 3 rad/min and is 5 rad/min at the peak. The biological effectiveness at the peak, compared to the middle plateau at 50% survival, is about 2.0. The OER at the peak is found to be lower than at the plateau. Because of the low dose rate of the pion beam, the experimental points at lower survival could not be obtained.

Survival curves at the peak and at 0.5 cm on either side of the peak, under aerobic and hypoxic conditions, were also measured to see if there were significant variations in the biological effects. Figure 3 shows the results. Within the experimental errors, no significant differences were found. The OER at 10% survival was found to be 1.5.

REFERENCE

1. E. J. Hall, L. A. Rozin-Towle, and R. D. Colvett, "RBE and OER Determinations for Radium and Californium-252," Radiology 110, 699-704 (1974).

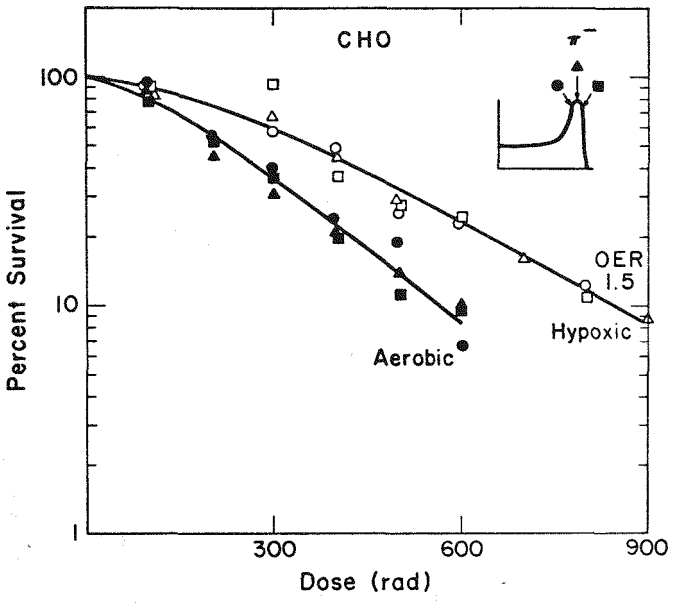

Fig. 3. Cell survival curves for negative pions at the peak and 7 mm on either side of the peak for negative pions under oxygenated and hypoxic conditions.

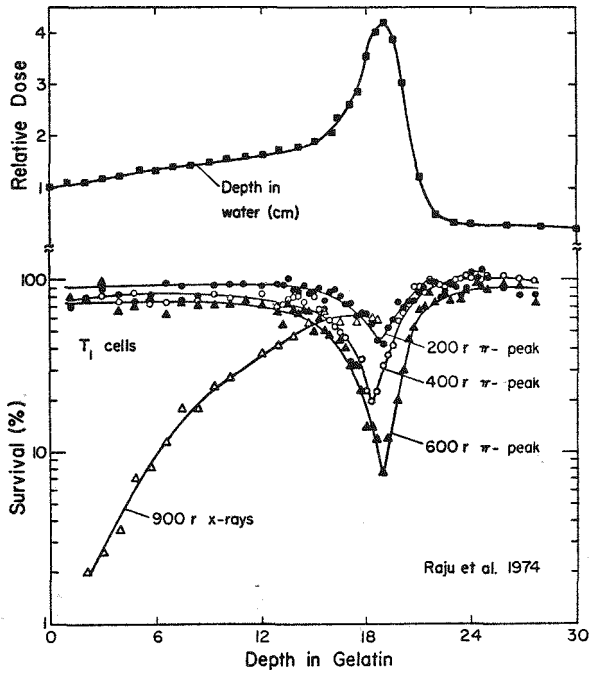

Fig. 1. Cell survival as a function of depth for negative pions at 200, 400, and 600 rad at the peak and for 900 rad of x-rays on the top side of the tube.

Cell Survival as a Function of Depth

[M. R. Raju, T. T. Trujillo, and E. Bain, in conjunction with J. Dicello (MP-3)]

Because of changes in radiation quality as negative pions pass through the medium, measurement of cell survival as a function of depth is important before using such a beam for therapy. A practical technique using gelatin to do such measurements was described in the previous annual report, and these measurements were made with negative pions at a dose rate of about 5 rad/min.

Figure 1 shows cell survival as a function of depth for different doses. Cell survival at a depth for 250-KVP x-rays is also shown for comparison. It can be seen that, with increasing dose, the effect is much more pronounced at the peak position because of sharp dose localization characteristics of the negative pions.

Figure 2 shows the data for 250-KVP x-rays and negative pions when the dose is delivered in two opposite ports. As one would expect, the differences between single- and two-port irradiations are very large for x-rays, whereas the differences are very small because of good dose localization characteristics of the negative pions.

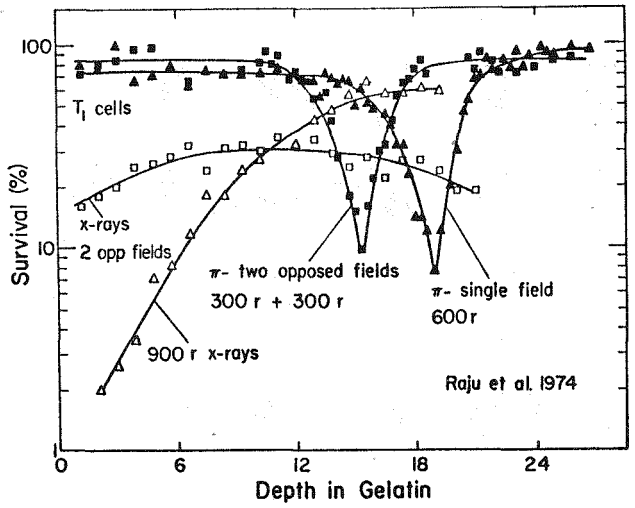

Fig. 2. Cell survival as a function of depth for single and two opposed fields for x-rays (900 rad and 450 plus 450 rad) and for negative pions (600 rad and 300 plus 300 rad).

Response of Normal Skin (Mouse Foot) to Fractionated Doses of X-Irradiation

[M. R. Raju, in conjunction with S. G. Carpenter, J. Farr, L. M. Holland, O. S. Johnson, C. Kasunic, and P. Larragoite (H-4)]

The mouse foot system is a good and practical experimental model for renewing normal tissues for

RBE studies of negative pions. This system permits a study of both acute and late reactions. The dose rate of negative pions is still not adequate to use this system; however, adequate dose rates are expected by July 1975.

Single dose-response data for x-rays were reported in the 1972 annual report. The fractionated experiments are done with x-rays for different fractionation schedules (1F, 2F/2d, 3F/4d, 4F/4d, 5F/4d, 6F/11d, 10F/11d, 9F/18d, and 15F/18d) to obtain base-line data for x-rays and as a preparation for the pion exposures in July 1975. Figure 1 shows the average skin reaction as a function of time after exposure for different doses with fractionation schedules of 1F, 5F/4d, 1F/11d, and 15F/18d.

Figure 2 shows the average reaction as a function of dose for the above fractionation schedules. As expected, there is more recovery with increasing numbers of fractions. It will be another 4 months before late effects can be observed.

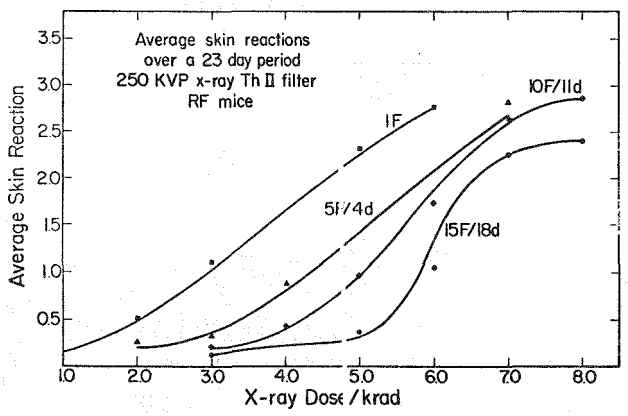

Fig. 1. Average skin reaction (23 days) as a function of dose.

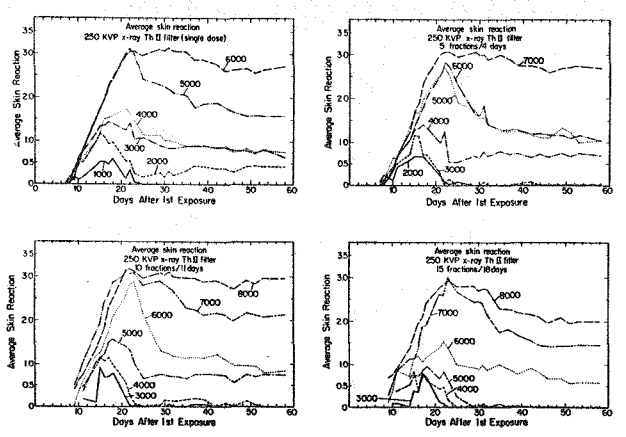

Fig. 2. Average skin reaction (6 mice) as a function of time after exposure for different doses.

ELECTRONIC COMPUTER AND OTHER SUPPORT FOR THE LASL BIOMEDICAL PROGRAM

(J. H. Jett, C. A. Goad, J. H. Larkins, J. D. Perrings, and P. N. Dean)

A Clustering Algorithm for Multiparameter Data Reduction

Several algorithms for processing 32-angle light-scattering data have been developed and implemented on the PDP-11/40. The first is a clustering algorithm. Given a set of points in a space of up to 32 dimensions, the algorithm partitions the points into a small number of clusters. In the case of the scattering data, each scattering pattern observed can be considered as a point in (up to) 32 dimensional spaces. A population of cells containing several cell types will generate a set of scattering points. This set should fall into several clusters, each cluster corresponding to one cell type within the population. Hence, by applying the clustering algorithm to such a set of scattering patterns, we hope to divide the patterns into clusters with the property that all patterns within a cluster are generated by cells of the same type. The algorithm has been tested extensively with artificially generated data in high dimensional spaces and has been tried on real 2-angle scattering data. The results have been very promising in both cases, and it is expected that the performance of the algorithm on real scattering data will improve as more angles of scatter become available for processing. The algorithm itself is a hybrid of peak finding and nearest-neighbor approaches to the clustering problem. A paper on the algorithm is presently in preparation.

The second algorithm which has been implemented is what is classically called a pattern recognition algorithm. Given a set of points (in a space of arbitrary dimension) partitioned into several classes, it finds a piecewise linear boundary which separates the points of a specified class from the points in the other classes. That is, the algorithm divides the pattern space into two regions, the first of which contains a specified class and the other region of which contains the points of all other classes. In the case of scattering data, the procedure is to run the clustering algorithm first. One of the clusters generated is then selected, and the pattern recognition program is run. The output

is a description of a boundary which optimally separates the selected cluster from all the other clusters. Then one runs the cell sorter in the sorting mode: for each cell that comes through the machine, it is determined (in real time) which side of the separating boundary the cell lies on, and the cell is sorted accordingly. One can sort out all cells from a population whose scattering patterns lie in the region of a given cluster in this way. If successful, the cluster will correspond to a cell type, and one will thus have arrived at the capability of sorting cells of one type from a mixed population. The pattern recognition algorithm uses standard linear separation methods.

The method has been tested on light-scattering data obtained at two angles for both human and monkey white blood cells. In both cases, the algorithm was able to distinguish the several blood cell types correctly. The clustering results agreed with the experimental evidence based on cell sorting.

Finally, a feature selection algorithm has been developed which will select from, say, 32 dimensions of data actually needed to separate one cluster of patterns from another. It is likely that, in most cases, only 4 or 5 of the 32 dimensions of scattering data will actually be needed to distinguish one cell type from another; this algorithm is designed to find which dimensions these are. The algorithm has been tested on artificial data in high dimensions with success; as the dimension reduction problem in two dimensions is trivial, there is nothing to be gained in testing the algorithm on the 2-dimensional real data now available.

ORGANIC AND BIOCHEMICAL SYNTHESIS GROUP (H-11)

D. G. Ott, Ph.D., Group Leader
E. M. Sullivan, Secretary

Staff Members

C. T. Gregg, Ph.D.[a]
J. Y. Hutson, Ph.D.[b]
V. N. Kerr, M.A.
V. H. Kollman, M.S.
T. W. Whaley, Ph.D.

Chemistry Technician

T. G. Sanchez

AWU Graduate Student

A. W. Harmon

Undergraduate Co-Op Students

E. G. Adame
J. E. Angel
M. Gonzales
E. H. Lucero
D. W. Montoya
M. A. Nevarez

Visiting Staff Members (Short Term)

G. H. Daub, Ph.D.
University of New Mexico
Albuquerque, New Mexico

E. S. Olson, Ph.D.
South Dakota State University
Brookings, South Dakota

W. W. Shreeve, M.D., Ph.D.
Veterans Administration Hospital
Northport, Long Island, New York

[a]Professional Research and Teaching Leave (through August 1974).

[b]Casual.

INTRODUCTION

Stable isotopes, because of their unique properties and nonradioactive nature, have great potential for many fields of science and technology. In particular, isotopes of carbon, nitrogen, oxygen, and sulfur (the basic building blocks of all biological molecules) would be widely used in biomedical and environmental research if they were economically available in sufficient quantities and in the required chemical forms. The major objective of our program continues to be stimulation of the widespread utilization of stable isotopes and the commercial involvement through development and demonstration of applications which have potential requirements for large quantities of isotopes. Thus, demand will be created which is necessary for large-scale production of stable isotopes and labeled compounds and concomitant low unit costs. The program continues to produce a variety of labeled materials needed for clinical, biomedical, chemical, and environmental applications which serve as effective demonstrations of unique and advantageous utilization of stable isotopes. Future commercial involvement should benefit, and is a consideration in our research and development, from the technology transfer that can readily be made as a result of our organic and biochemical syntheses and also of various techniques involved in applications.

Many of our projects involving development of applications, as well as those in more fundamental research, are carried out through collaboration with investigators in other laboratories, institutions, and industries. A number of mutual interest, cooperative investigations are shared with the LASL Inorganic Chemistry Group (CNC-4), particularly those involving carbon-13 nuclear magnetic resonance spectroscopy. This LASL group also carries out production of the enriched isotopes which are, of course, absolutely essential to the entire program. Particular acknowledgment for direct contributions to several projects discussed later in this report is made to the following Group CNC-4 personnel: N. A. Matwiyoff, biochemical and biomedical nmr investigations; R. E. London, nmr characterization of labeled cells and biosynthesized molecules; B. B. McInteer and T. Mills, mass spectrometric isotope ratio determinations for clinical breath samples and other products; and S. Pike (LASL STEP Program participant), isolation and purification of biosynthetic labeled protein and nucleic acid derivatives.

An interagency agreement with the Food and Drug Administration has been initiated in which

certain specifically labeled carcinogens and pesticides are to be prepared for investigations being conducted at the National Center for Toxicological Research in Jefferson, Arkansas. In addition to supplying essential components to the FDA projects, this effort (at the 1.1 man-year level) will also contribute to our objective of encouraging new and unique applications of stable isotopes.

A proposal has been submitted to the Division of Research Resources, National Institutes of Health, for a "National, Stable Isotopes Resource at Los Alamos" (N. A. Matwiyoff, CNC-4, principal investigator). If approved, in addition to contributing to NIH objectives, it would also increase and broaden our capabilities and thus be beneficial to presently established goals as well.

In the coming year, it is anticipated that increased attention will be given to Group H-11's existing and potential capabilities for contributing to solutions of environmental problems and other aspects of developing energy programs (e.g., solar energy utilization through photosynthesis and bioconversion).

No changes have occurred in personnel this year except for those occasioned by the rotational nature of the Undergraduate Co-Op Program which continues to be regarded as most worthwhile -- both to the group and to the students. Dr. C. T. Gregg has returned from LASL Professional Research and Teaching Leave at the Pharmakologisches Institut (Embryonal-Pharmakologie) der Freien Universitat, West Berlin, where he was a Visiting Professor and conducting research of mutual interest.

This report summarizes the methods and results of the past year's activities and is a continuation of similar reports in this series for the previous three years[1-3] which contain additional information concerning the group's interests and capabilities.

REFERENCES

1. C. R. Richmond and G. L. Voelz, eds., "Annual Report of the Biological and Medical Research Group (H-4) of the LASL Health Division, January through December 1971," Los Alamos Scientific Laboratory report LA-4923-PR (April 1972), pp. 119-130.

2. C. R. Richmond and G. L. Voelz, eds., "Annual Report of the Biological and Medical Research Group (H-4) of the LASL Health Division, January through December 1972," Los Alamos Scientific Laboratory report LA-5227-PR (March 1973), pp. 102-124.

3. C. R. Richmond and E. M. Sullivan, eds., "Annual Report of the Biomedical and Environmental Research Program of the LASL Health Division, January through December 1973," Los Alamos Scientific Laboratory report LA-5633-PR (May 1973), pp. 117-136.

PREPARATION OF LABELED COMPOUNDS

The necessity to convert the basic starting materials from the isotope enrichment process into a wide variety of labeled compounds required for various applications has resulted in a unique synthesis capability which effectively utilizes and combines the many techniques of both organic and biochemical synthesis. As the stable isotopes program progresses, so do the complexity and difficulty of the syntheses. The reportoire of developed methods for efficient production of labeled compounds increases continuously. Particularly valuable are proven procedures for producing basic compounds and key synthetic intermediates which can then be used to introduce labels into a wide variety of more complex molecules. Each new synthesis has the additional benefit of simplification of future problems. This report primarily aims to indicate additions and improvements to our synthesis capabilities developed during the past year; previous annual reports in this series contain much additional information. Particular acknowledgment is made to Professors Daub and Olson (Visiting Staff Members) for their continuing contributions to development and application of organic syntheses. The essential starting materials are obtained, for the most part, from the isotope separation facility of Group CNC-4 (i.e., carbon-^{13}C monoxide and carbon-^{13}C dioxide at ca. 90 mol % ^{13}C and ammonium-^{15}N sulfate at ca. 99 mol % ^{15}N). Certain applications (e.g., the $^{13}C_6$-2,4,5-T, -TCDD, -ENS, -2-AAF, other isotope-dilution analysis applications, and biological effects studies) require ca. 99 mol % ^{13}C which is purchased through the AEC's Mound Laboratory at Miamisburg, Ohio.

The preparations of certain materials are made on a repetitive basis. There are several reasons why procedures must be repeated rather than prepare enough originally for all future needs (e.g., a practical maximum limit to the scale of preparation, development of unanticipated requirements, and

TABLE I

REPETITIVE SYNTHESES

Compound	Method of Preparation	Isotope Isomer and Quantities Prepared
Acetic acid	Carbonylation of methanol in presence of rhodium trichloride and hydriodic acid	-$^{13}C_2$, 6.5 mol -2-^{13}C, 1.4 mol
Acetylene	Hydrolysis of lithium carbide produced from carbon dioxide and lithium	-$^{13}C_2$, 0.9 mol
Algae	Photosynthesis	^{13}C-*Chlorella pyrenoidosa* 400 g (90 mol % ^{13}C) 200 g (20 mol % ^{13}C) ^{13}C-*Anacystis nidulans* 200 g (90 mol % ^{13}C) 200 g (20 mol % ^{13}C)
Benzene	Trimerization of acetylene in presence of vanadium oxide on alumina	-$^{13}C_6$, 0.2 mol
Bromoacetic acid	Bromination of acetic acid in presence of phosphorus	-2-^{13}C, 0.6 mol
Ethanol	Hydrogenation of acetic acid, rhenium heptoxide catalyst	-$^{13}C_2$, 0.7 mol -2-^{13}C, 0.4 mol
Fructose	Photosynthesis -- tobacco	-$^{12}C_6$, 0.08 mol
Galactose	Photosynthesis -- kelp	-$^{13}C_6$, 0.05 mol
Glucose	Photosynthesis -- tobacco	-$^{13}C_6$, 0.6 mol -$^{12}C_6$, 0.5 mol
Glycerol	Photosynthesis -- kelp	-$^{13}C_3$, 0.05 mol
Isopropyl formate	Carbon monoxide and isopropyl alcohol in presence of sodium isopropoxide	-^{13}C, 1.1 mol
Methane	Hydrogenation of carbon dioxide in presence of ruthenium catalyst	-^{13}C, 1.8 mol -^{13}C-d_4, 3.4 mol
Methanol	Hydrogenation of carbon dioxide in presence of copper-zinc-chromium catalyst	-^{13}C, 9.1 mol
Methy iodide	Iodination of methanol in presence of phosphorus	-^{13}C, 0.7 mol

availability of starting materials). Preparations previously developed and used which have been repeated this year are listed in Table I. These are carried out frequently with incorporation of beneficial modifications which were conceived since the time of the previous preparation. Following Table I are summaries of syntheses which have been developed this year or for which significant improvements have been made.

2-Acetylaminofluorene-5,5a,6,7,8,8a-$^{13}C_6$ (2-AAF). The series of reactions which are being used to prepare this compound with one of the aromatic rings containing all carbon-13 is shown in Scheme 1. The Friedel-Crafts reaction of m-nitrobenzoyl chloride in carbon disulfide[1] using limited amounts of benzene gives 3-nitrobenzophenone in yields of 92 to 97%. Reduction of both the nitro group and the ketone function in a Paar hydrogenation apparatus using a palladium on charcoal catalyst gives m-benzylaniline which is not isolated but directly acetylated to give m-benzylacetanilide. The overall yield is essentially quantitative. Preliminary experiments have shown that conversion of m-benzylacetanilide to N-chloro-m-benzylacetanilide by the action of potassium hypochlorite and subsequent treatment of the N-chloroamide with aluminum

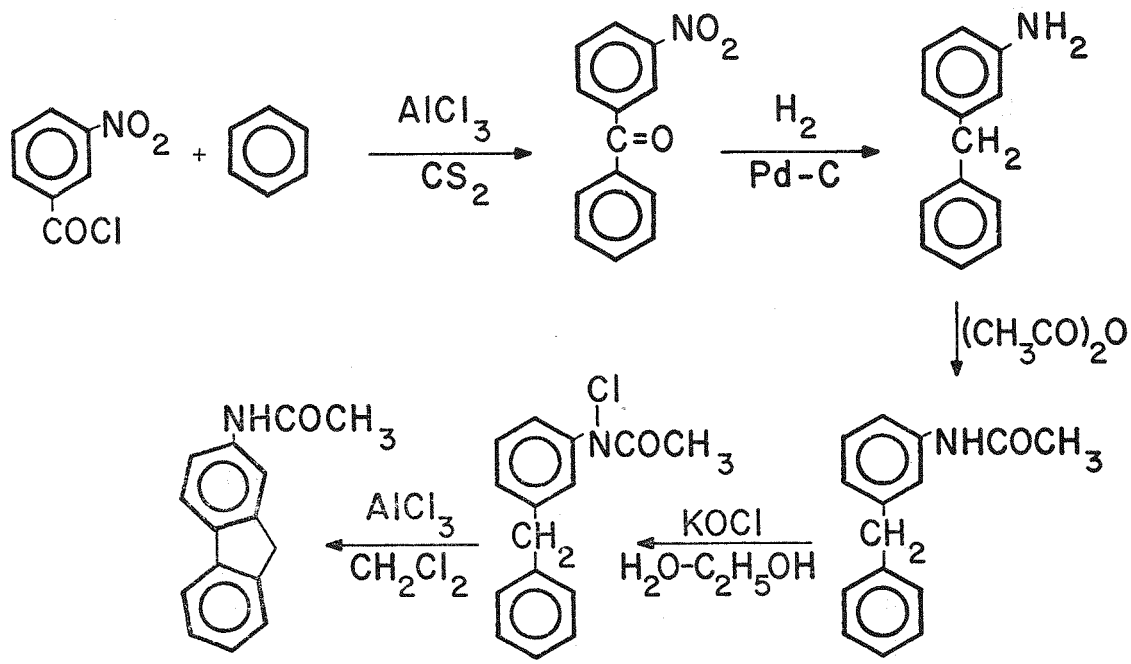

Scheme I

chloride in methylene chloride gives a mixture of products containing the desired 2-acetylaminofluorene. Additional refinement of the experimental techniques of the last two steps will be necessary, but the sequence appears to be an acceptable route for preparing the isotopic 2-acetylaminofluorene.

Amino Acids, Carbon-13 Labeled. Subsequent to lipid removal (as described in another section), carbon-13 enriched algae (*Anacystis nidulans*) were lyophilized to remove volatile solvents. The cells were disrupted by sonication using 50-g batches of material dissolved in 1.5 liters of distilled water. The insoluble cell residue was removed by centrifuging the mixture at 10 000 x g for 15 min. The cell residue was resuspended in 1.5 liters of water, and the extraction procedure was repeated two more times. The combined supernatant solutions were lyophilized, yielding 20 g of crude protein. The crude protein was suspended in enough 0.25 N trifluoroacetic acid (TFA) to make a concentration of 20 mg/cm^3, and the mixture was refluxed in a nitrogen atmosphere at 95°C for 12 h. The hydrolysis mixture was cooled, and the insoluble material was removed by centrifugation. The supernatant solution was set aside for later recovery of carbohydrates. The protein residue was washed in cold 0.25 N TFA and lyophilized. The dry material weighed 7.5 g. Hydrolysis of the crude protein was carried out in 6 N HCl for 12 h under reflux conditions in an inert atmosphere. The hydrolysis mixture was cooled and filtered, and the insoluble residue was washed several times. Hydrochloric acid was removed by repeated concentration *in vacuo* to a syrup. The last traces of hydrochloric acid were removed by drying *in vacuo* for 24 h.

The dried crude amino acids were treated with Dowex 50, and the ion exchange resin was washed thoroughly. Amino acids were washed from the resin with 6 N ammonium hydroxide, concentrated, and lyophilized. The product was dissolved in water and decolorized using activated charcoal; the charcoal was then washed with 0.1 N ammonium hydroxide. The final yield was about 6 g of a white powder (12% yield).

Preliminary investigations have been made toward separation of amino acid mixtures by column chromatography using a 9-mm x 200-cm column of Dowex 50 X8 (-400 mesh) maintained at 37°C. The column was loaded with about 100 mg of amino acids which were eluted in the order shown in Table II. The 0.05 M pyridinium formate (pH 3.1) buffer was fed to the column at a rate of 18.6 cm^3 h^{-1}, and 3.1-cm

TABLE II

CHROMATOGRAPHIC SEPARATION OF LABELED AMINO ACIDS

Amino Acid	Fraction (cut)	Volume (ml)	Elution Buffer
Aspartic acid	15 - 35	65.1	0.05 M pyridinium formate (pH 3.1)
Proline	76 - 79	12.4	
Threonine	90 - 111	68.2	
Serine	128 - 160	102.3	
Glutamic acid	190 - 216	83.7	
Alanine	260 - 299	124.0	0.1 M pyridinium formate (pH 3.1)
Valine	440 - 478	120.9	
Isoleucine	732 - 738	21.7	0.2 M pyridinium acetate (pH 4.4)
Leucine	749 - 759	31.0	
Phenylalanine	812 - 835	74.4	
Tyrosine	910 - 925	49.6	
Lysine	1051 - 1069	58.9	
Arginine	1115 - 1140	80.6	

fractions were collected. After fraction 240, 0.1 M pyridinium formate (pH 3.1) was substituted, and at fractions 545 and 689, 0.2 M pyridinium formate (pH 3.1) and 0.2 M pyridinium acetate (pH 4.4) were substituted, respectively (Table II). Purity can be determined by ^{13}C nmr or gas-liquid chromatography of the N-trifluoroacetyl butyl esters.[2]

The 12% yield from cells of *A. nidulans* is about half that described by Putter[3] for *Scenedesmus obliquus*. The described chromatographic separation requires less elution time, with increased amino acid resolution and fewer gradients than previously reported.[4] Various extraction procedures are being considered to remove the more tightly bound protein in *A. nidulans*.

Ammonia-d. A mixture statistically equivalent to ammonia-d is obtained by equilibrating ammonia (2.33 mol) with sodium hydroxide (1 mol) and deuterium oxide (2 mol). After equilibration, water is removed cryogenically to give ammonia-d in > 90% recovery.

Benzidine-$^{15}N_2$ and N-Acetylbenzidine-$^{15}N_2$. These two compounds have been prepared by the sequence of reactions shown in Scheme 2. An improved synthesis of 4,4'-biphenyldicarbonyl chloride from 4,4'-biphenyldicarboxylic acid which gives yields of 70 to 80% has been found using Bosshard's thionyl chloride-dimethyl formamide reagent in chlorobenzene.[5] A common modification of this method employs dimethylformamide as a solvent instead of using catalytic amounts. In the biphenyldicarboxylic acid system, this modification results in the formation of N,N,N',N'-tetramethyl 4,4'-biphenyldicarboxamide as the only isolable product. The diacid chloride reacts smoothly with ammonia-^{15}N, which is generated *in situ* by the action of triethylamine on ammonium-^{15}N sulfate, to give 4,4'-biphenyldicarboxamide-$^{15}N_2$ in 75 to 85% yield. When subjected to basic hypochlorite using Magnien and Baltzly's modification of the Hofmann reaction,[6] the diamide undergoes a double rearrangement in 40 to 50% yield to give benzidine-$^{15}N_2$. Attempts to monoacetylate benzidine according to published procedures[7,8] have not given satisfactory results owing to the statistical nature of the monoacetylation of the diamine in solution. We have found that monoacetylation of benzidine can be accomplished in 85 to 90% yield by employing small volumes of ether so that the monoacetyl compound separates from the reaction slurry as it is formed. It is hoped that N-acetylbenzidine-$^{15}N_2$ will also serve as a precursor to N-hydroxybenzidine-$^{15}N_2$ through a series of functional group modifications.

Butyl Lactate-$^{13}C_3$, Butyl Pyruvate-$^{13}C_3$, and Sodium Pyruvate-$^{13}C_3$. Butyl lactate is prepared from zinc lactate which can be obtained from chemical synthesis or biosynthesis. A one-step procedure in which Dowex 50 (H^+) cation exchange resin is used to convert zinc lactate to lactic acid and also to serve as a hydrogen ion source for esterification

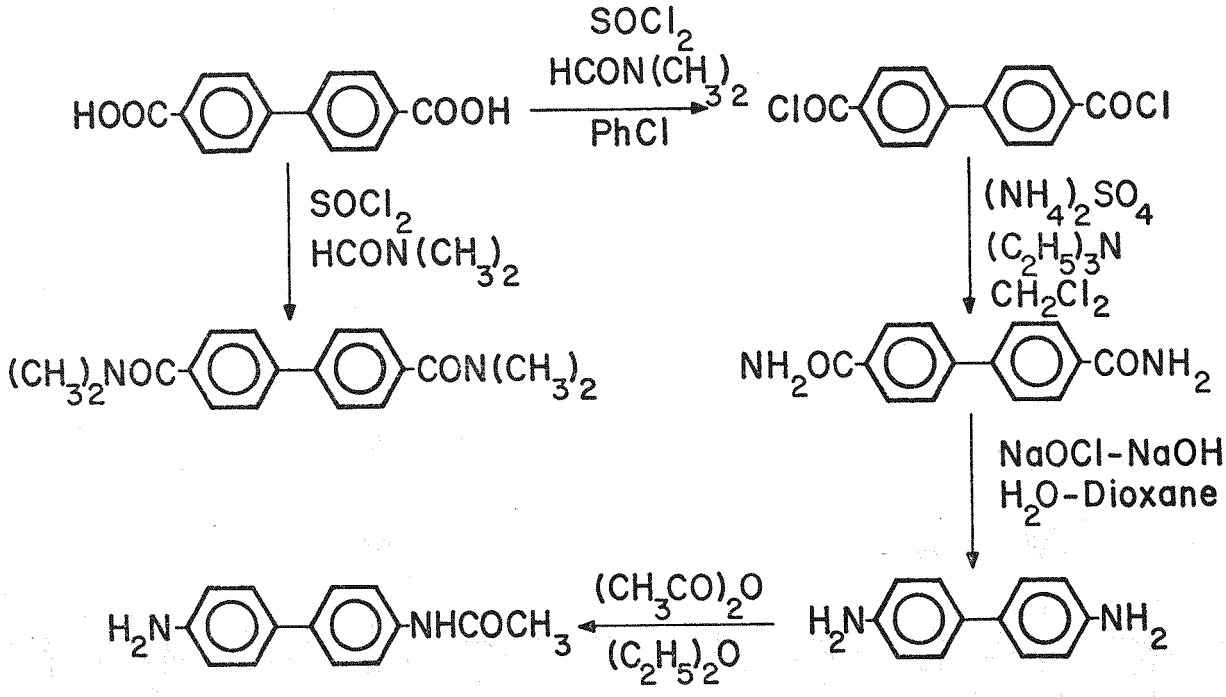

Scheme 2

was investigated but found not to be useful because of erratic yields. Treatment of zinc lactate-$^{13}C_3$ with Dowex 50 (H^+), followed by esterification with 1-butanol and sulfuric acid, gives butyl lactate-$^{13}C_3$ in an overall yield of better than 90%. The oxidation of butyl lactate to butyl pyruvate with aqueous potassium permanganate does not give satisfactory yields, presumably due to continued oxidation of the ketoester. The two-phase oxidation using ether and chromic acid, as described by Brown *et al.*,[9] results in the smooth oxidation of butyl lactate-$^{13}C_3$ to butyl pyruvate-$^{13}C_3$ in approximately 80% yield. Facile hydrolysis of the ketoester occurs by adjusting the pH of a solution of the ester to 10 with sodium hydroxide to give sodium pyruvate in 80% isolated yield.

Carbon-^{13}C Disulfide. The reaction between methane-^{13}C and hydrogen sulfide[10,11] in a quartz tube at 975°C with relative flow rates of 1:6 and using helium as a carrier gas gives carbon-^{13}C disulfide. The product is cryogenically trapped as the gas mixture exits the tube and distilled to give an 85% yield of carbon-^{13}C disulfide.

Carbonyl-^{13}C Sulfide. This compound is prepared by the reaction of carbon-^{13}C monoxide and sulfur in methanol in the presence of sodium methoxide.[12] The reaction is conveniently carried out in a stainless steel gas sampling cylinder. Fractional distillation of the reaction mixture through Lithasorb (to remove traces of carbon dioxide by-product) gives carbonyl-^{13}C sulfide in 90% yield.

Di-2,5-(1-naphthyl)-1,3,4-oxadiazole and Di-2,5-(naphthyl)-1,3,4-oxadiazole. The condensation of 1-naphthoyl chloride with hydrazine in pyridine solution produces the dinaphthoyl hydrazine shown in Scheme 3. Cyclization of this intermediate with phosphorus oxychloride gives di-2,5-(1-naphthyl)-1,3,4-oxadiazole.[13] Repetition of the sequence

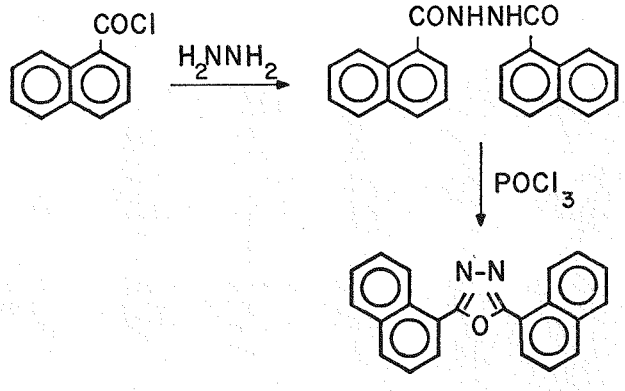

Scheme 3

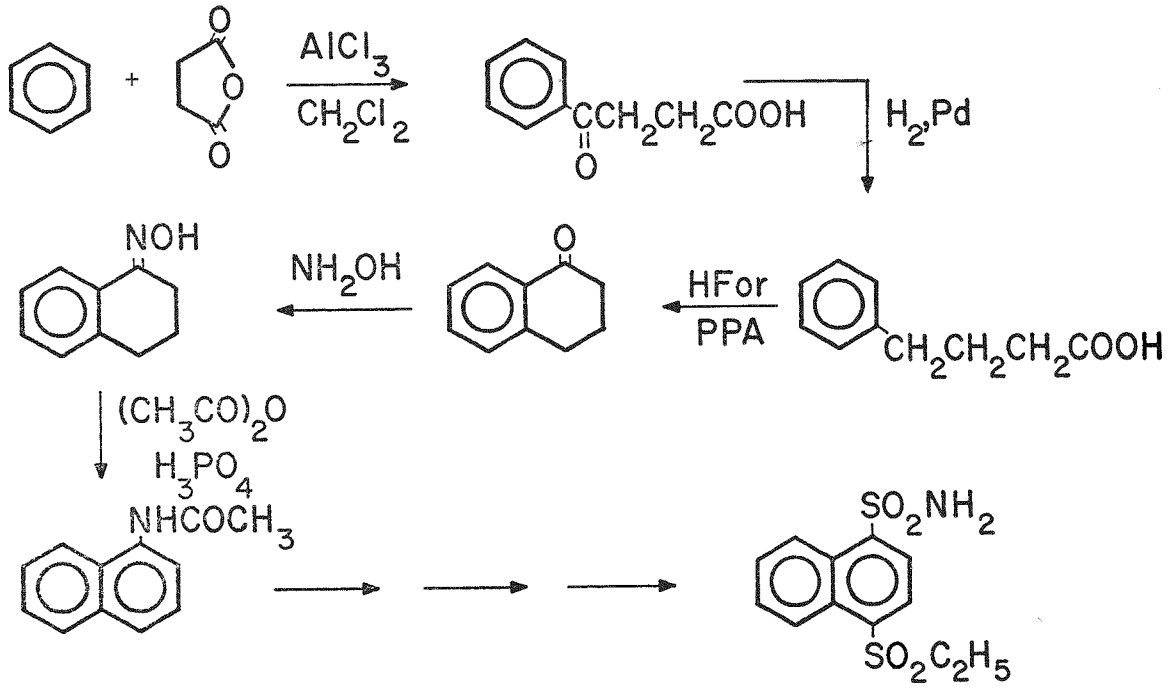

Scheme 4

using 2-naphthoyl chloride yields di-2,5-(2-naphthyl)-1,3,4-oxadiazole.

4-(Ethylsulfonyl)1-naphthalenesulfonamide-4a,5,6,7,8,8a-$^{13}C_6$ (ENS). The synthetic pathway to this compound which is currently being studied is shown, in part, in Scheme 4. The Friedel-Crafts succinoylation of benzene using a limited quantity of benzene gives a 98% yield of β-benzoylpropionic acid when methylene chloride is used as a solvent. The same reaction gives a 70% yield of the product in carbon disulfide but does not take place in 1,1,2,2-tetrachloroethane. The reduction of β-benzoylpropionic acid to γ-phenylbutyric acid by catalytic hydrogenation with palladium on charcoal and the cyclization of γ-phenylbutyric acid to α-tetralone using either polyphosphoric acid or anhydrous hydrogen fluoride are both well characterized reactions which give yields of 96% and 80 to 85%, respectively.[14] An alternative method of preparing α-tetralone in one step from benzene and γ-butyrolactone is a well known reaction,[15] but attempts to carry out this reaction using *limited* amounts of benzene and γ-butyrolactone using aluminum chloride in 1,1,2,2-tetrachloroethane, aluminum chloride in methylene chloride, polyphosphoric acid, anhydrous hydrogen fluoride, anhydrous hydrogen fluoride and trifluoroacetic acid, and anhydrous hydrogen fluoride and sulfuric acid failed to produce α-tetralone. Using Newman's procedure,[16] α-tetralone is converted into its oxime by treatment with hydroxylamine in 95 to 98% yield, and the oxime is aromatized to N-(1-naphthyl)acetamide in 82% yield by the action of acetic anhydride and phosphoric acid. From N-(1-naphthyl)acetamide there are several possible pathways to 4-(ethylsulfonyl)-naphthalenesulfonamide which all begin with the introduction of functionalized sulfur at position four of the activated naphthalene ring.

Formamide-^{13}C-^{15}N and Sodium Cyanide-^{13}C-^{15}N. The ammonolysis of isopropyl formate-^{13}C with ammonia-^{15}N using 10% excess over the stoichiometric quantity of isopropyl formate-^{13}C affords, after fractionation, formamide-^{13}C-^{15}N in 88% yield based on ammonia-^{15}N. Dehydration of the formamide-^{13}C-^{15}N using the triphenylphosphine-carbon tetrachloride reagent described in previous annual reports gives sodium cyanide-^{13}C-^{15}N.

Galactose-$^{13}C_6$ and Glycerol-$^{13}C_3$. The carbohydrate 2-hydroxyl-1-(hydroxymethyl)ethyl-α-D-galactopyranoside (galactosylglycerol) was prepared

from the photosynthetic incubation of the marine red algae *Gigartina* in the presence of carbon-^{13}C dioxide enriched to the 91.5 atom % level. The ^{13}C-enriched galactoside was extracted from the incubated thalli and acid-hydrolyzed to galactose and glycerol. Pure compounds were obtained by column chromatographic separation.

The three species of algae used were *Gigartina corymbifera*, *Gigartina harveyana*, and *Gigartina californica*. The algae were obtained fresh in 5-kg quantities within 36 h of harvest. During shipment, the algae were kept in the dark at 18 to 20°C. The photosynthetic incubation of about 4.5 kg of thalli was carried out in three sealed polycarbonate chambers joined together on a common oscillating mechanism and illuminated from the upper and lower surfaces.[17] Carbon-^{13}C dioxide was added to the chambers until the desired concentration was reached (Fig. 1). As needed, carbon dioxide was added during the incubation period. Photosynthesis was continued for varying time intervals to 40 h. The decline in carbon dioxide uptake after 30 h was accompanied by a noticeable bleaching of the thalli with a consequent decrease in photosynthetic activity.

At the conclusion of the illumination period, the thalli were removed from the chambers, washed free of salts, and extracted with 80% ethanol. The ethanolic extract was concentrated to a thick syrup, and the crude galactoside was isolated by acetylation, followed by deacetylation and crystallization

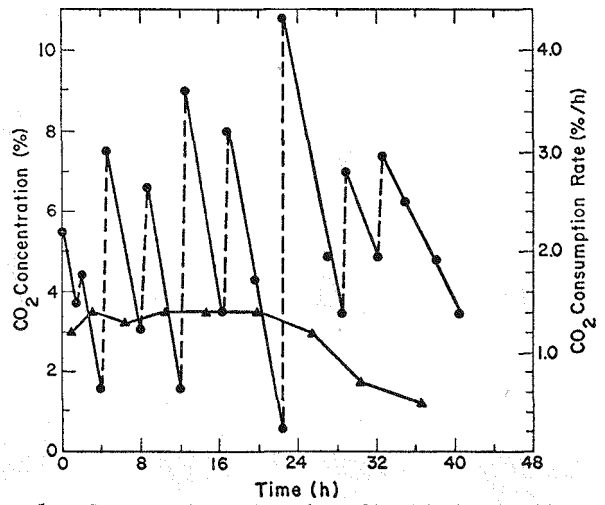

Fig. 1. Consumption of carbon dioxide by thalli: (—●—) carbon dioxide concentration in chamber; (--●--) carbon dioxide added to chamber; and (—▲—) rate of carbon dioxide consumption.

from absolute ethanol. Purity of the crystalline galactosylglycerol-$^{13}C_9$ was determined by melting point (128 to 129°C) and by its optical rotation in water $(\ )_D$ = +161°C.

Galactosylglycerol-$^{13}C_9$ was hydrolyzed to a mixture of galactose-$^{13}C_6$ and glycerol-$^{13}C_3$ using 0.1 N trifluoroacetic acid. Acid removal was by anion exchange, followed by concentration of the sugar mixture under reduced pressure to a thick syrup. The sugars were separated on a 5 x 100-cm column of Dowex 50W X8 (200 to 400 mesh, Ba^{++}) resin.[18] Solid galactose-$^{13}C_6$ was obtained by crystallization from aqueous alcohol; the glycerol-$^{13}C_3$ was concentrated and stored at -20°C. Purity of the galactose was determined by optical rotation measurements, melting point, and enzymatic assay. Glycerol purity was established by enzymatic assay using Calbiochem's glycerol Stat-Pack and by ^{13}C nmr spectroscopy (see later section of this report). Average carbon-13 enrichment was determined by oxidation to carbon dioxide, followed by mass spectrometric analysis.

Glycine-$^{13}C_2$-^{15}N, Glycine-2-^{13}C-^{15}N, and Glycine-$^{13}C_2$. The Gabriel synthesis of glycine which has been described in previous annual reports has been used to prepare glycine-$^{13}C_2$-^{15}N and -2-^{13}C-^{15}N from ethyl bromoacetate-$^{13}C_2$ and -2-^{13}C, respectively, and potassium phthalimide-^{15}N. For isotopic glycine not containing ^{15}N, it has now been determined that it is preferable to utilize the reaction between bromoacetic acid and aqueous ammonia. The formation of iminodiacetic acid (IDA) and nitrilotriacetic acid (NTA) as side products can be circumvented by experimental manipulations. Thus, the introduction of dilute aqueous bromoacetic-$^{13}C_2$ acid into a large excess of cold ammonium hydroxide with vigorous stirring gives glycine-$^{13}C_2$ in approximately 90% yield with negligible amounts of side products. Traces of IDA and NTA, if present, are removed by the recrystallization process.

(2-Hydroxyethyl)trimethyl-$^{13}C_3$-ammonium Chloride (Choline-$^{13}C_3$ Chloride). The parent choline structure is prepared from the reaction of 2-aminoethanol and methyl-^{13}C iodide and isolated as the air-stable Reineckate salt in 87% yield. A solution of choline Reineckate is treated with silver sulfate and filtered to remove silver

Reineckate. Precipitation of sulfate by the addition of barium chloride and filtration of barium sulfate give a solution of choline chloride. Evaporation and crystallization from alcohol-ether give (2-hydroxyethyl)trimethyl-$^{13}C_3$-ammonium chloride (choline-$^{13}C_3$ chloride) as hygroscopic white crystals in about 50% recovery from the Reineckate salt.

L-Lactic-$^{13}C_3$ Acid. Glucose-$^{13}C_6$, fructose-$^{13}C_6$, and sucrose-$^{13}C_{12}$ were fermented singly and in various combinations to L-lactic-$^{13}C_3$ acid by *Lactobacillus delbrueckii* (ATCC No. 11443). Lactic acid was removed from the concentrated acidified fermentation medium by extraction with ether and isolated as crystalline zinc lactate which could be converted subsequently to sodium lactate solution by ion exchange methods. This technique is a large-scale modification of that previously described.[19]

The fermentation medium was prepared by dissolving trypton (5 g), yeast extract (5 g), Tween-80 (2 cm^3), L-(+)-cysteine hydrochloride (100 mg), sodium thioglycolate (50 mg), vitamin B_{12} (10 μg), sodium acetate (10 g), Brin's inorganic salts solution (5 cm^3), and the sugars in about 800 cm^3 of water. After the pH of the fermentation medium was adjusted to 6.8, the volume was increased to 1 liter with water, and the solution was autoclaved. The inoculum of *L. delbrueckii* was from 10 cm^3 of inoculated medium which had been kept at 37°C for 16 h. The large-scale fermentation was done in an automatic Micro Ferm Laboratory fermentor (New Brunswick Scientific Company) and was continued until production of lactic acid ceased (Fig. 2) as indicated by stable pH and sugar depletion.

After fermentation, the mixture was cooled to 10°C and acidified with cold 4 N sulfuric acid. The cells were then removed by centrifugation, and the cell-free medium was concentrated to a semi-solid mass by evaporation at 5°C under reduced pressure. This material was subsequently extracted with diethyl ether, and the combined extracts were concentrated to an oil and taken up in water. The aqueous lactic acid solution was shaken several times with ether, and the combined ether layers were back-washed with water. Solid zinc carbonate was added to the combined aqueous phases until a constant pH of 6.5 was obtained. This suspension was treated with decolorizing carbon and filtered, and the resulting

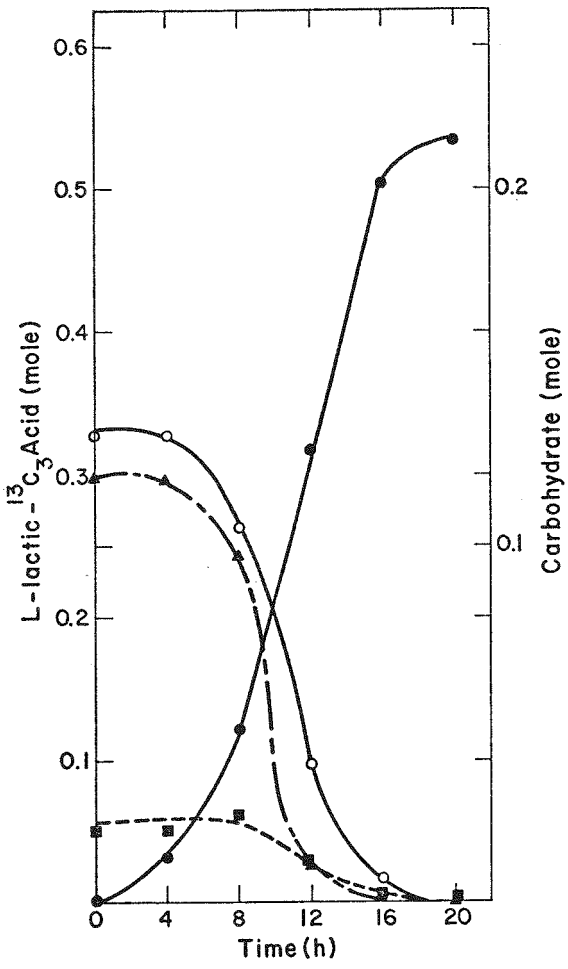

Fig. 2. Lactic-$^{13}C_3$ acid production (-●-) during fermentation of a mixture of glucose-$^{13}C_6$ (-○-), fructose-$^{13}C_6$ (-▲-), and sucrose-$^{13}C_{12}$ (-■-).

clear solution was concentrated and diluted with alcohol to afford crystalline zinc lactate dihydrate which was filtered and washed. Anhydrous material was obtained by heating at 110°C in a vacuum desiccator for 24 h. Product purity was determined by optical rotation and enzymatic assay using Calbiochem's Rapid Lactate Stat-Pack. The carbon-13 enrichment of the lactic acid was determined by oxidation to carbon dioxide, followed by mass spectrometric analysis. The carbon-13 enrichment of the product was essentially that of the sugar substrate used. Based upon enzymatic analysis of the fermentation mixture, yields greater than 90% were obtained. However, actual recovery of product as zinc lactate was somewhat less.

The carbon-13 enriched sugars were obtained from the photosynthetic incubation of mature excised

tobacco leaves in the presence of carbon-^{13}C dioxide using published procedures.[20]

Lipids, Carbon-13 Labeled. *Chlorella pyrenoidosa* and *Anacystis nidulans* were grown as previously described[21-23] on carbon-^{13}C dioxide enriched to the 91 mol % or 20 mol % levels. The future use of the extracted material determined the desired level of enrichment (e.g., lipids labeled to the 20% level are preferred for use in certain nmr experiments to avoid complications of ^{13}C-^{13}C multiplets).[24]

The lipids and pigments were removed from dry intact whole cells in a dry-nitrogen atmosphere by washing the cells three times with oxygen-free absolute ethanol and twice each with oxygen-free absolute ethanol-chloroform (9:1 v/v) and benzene. Each solvent wash was continued for 30 min, after which the cells were removed from the solvent by vacuum filtration. The extracts were pooled and concentrated to dryness under reduced pressure. The crude lipid extract was taken up in a minimum amount of oxygen-free ether and centrifuged to remove ether-insoluble material, and the soluble lipids were decanted. The lipid extract was concentrated to dryness and allowed to remain under vacuum for 12 h to ensure complete solvent removal. Both species of algae have been used in 40- to 50-g quantities per lipid extraction. Based on dry weight, the lipid fraction is about 12%.

Lipids were chromatographically separated into pure components, in 300-mg amounts, on a 2.5 x 22-cm column of DEAE-acetate. Shown in Fig. 3 is a chromatogram of *A. nidulans* lipids. The order of elution and weight percent of each lipid are shown in Table III. The four major lipids separated were

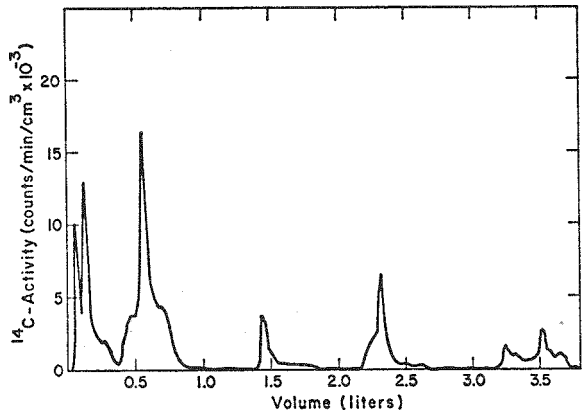

Fig. 3. Separation of 300 mg of crude lipid extract using a 2.5 x 22-cm column of DEAE-acetate resin. Carbon-13 material was spiked with tracer quantities of carbon-14 labeled crude lipid for easy location in the eluant.

mono- and digalactosyl diglycerides, sulphoquinovosyl diglyceride, and phosphatidyl glycerol. Quantities of crude lipid extracts to 3 g have been separated with a 5 x 50-cm column of DEAE-acetate. Resolution with this column was comparable to that shown in Fig. 3.

The four major lipids obtained from *A. nidulans* have been shown to be the predominant lipids in the chloroplasts of green algae (*C. pyrenoidosa*) and higher plants.[25] Within these four groups occur a large number of compounds distinguished by the different fatty acids attached to carbons 1 and 2 of the glycerides. The fatty acid composition of *C. pyrenoidosa* and *A. nidulans* is shown in Table IV. The degree of fatty acid unsaturation for *C. pyrenoidosa* is about 1.7 times greater than for *A. nidulans*. The four groups of major lipids have been characterized by ^{13}C nmr, and their possible

TABLE III

DEAE-ACETATE COLUMN CHROMATOGRAPHY OF CRUDE ALGAL LIPID EXTRACT

Solvents[a]	Volume (ml)	Compounds Identified	*Anacystis nidulans*[b] (whole cells)
C	360	Pigments, nonpolar lipids	32
C/M (49:1)	408	Monogalactosyl diglyceride	37
C/M (19:1)	355	--	--
C/M (9:1)	429	Digalactosyl diglyceride	13
C/M (2:1)	450	Phosphatidyl glycerol	9
C/M (2:1), 0.8% AA	534	Sulfolipid	8

[a]Abbreviations: C, chloroform; M, methanol; AA, ammonium acetate.

[b]The values are given in weight % of lipids eluted from the column.

TABLE IV

FATTY-ACID COMPOSITION

Fatty Acid	*C. pyrenoidosa* (relative %)	*A. nidulans* (relative %)
Myristic (14:0)	--	1
Myristoleic (14:1)	--	3
Palmitic (16:0)	22	55
Palmitoleic (16:1)	3	35
Palmitolinoleic (16:2)	19	--
Palmitolinolenic (16:3)	5	--
Stearic (18:0)	--	1
Oleic (18:1)	2	6
Linoleic (18:2)	37	--
Linolenic (18:3)	7	--
Saturated	22	55
Unsaturated	73	44

involvement with the photosynthetic apparatus[26] is being investigated.

Octanoic-1-^{13}C acid and Methyl Octanoate-1-^{13}C. The carbonation of heptylmagnesiumbromide with carbon-^{13}C dioxide affords, after acidification and distillation, octanoic-1-^{13}C acid in 88% yield. Esterification of the acid using dimethylformamide dimethylacetal in carbon tetrachloride gives methyl octanoate-1-^{13}C in approximately 70% yield. Future preparations will use less exotic esterification procedures.

Nucleotides, Carbon-13 Labeled. Ribo- and deoxyribonucleic acids were extracted from the blue-green algal cell residue (remaining after lipid extraction) by a modification of the method described by Marmur.[27] The residue was treated with sodium dodecyl sulfate to release the intracellular material and successively deproteinized by centrifuging and decanting an emulsion formed after shaking the residue with a chloroform-isoamyl alcohol solution. The water-soluble nucleic acids present in the decanted liquid were then precipitated with two volumes of 95% ethanol and isolated by centrifugation. The DNA and RNA were dissolved in dilute saline citrate, and the DNA was selectively precipitated with 0.54 volume of isopropanol alcohol added to the rapidly stirred solution. The DNA was collected as threads wrapped tightly around a glass stirring rod, washed in progressively increasing concentrations of cold ethanol (75 to 95%), and lyophilized. The RNA remaining in solution was precipitated with two volumes of cold ethanol and collected by centrifugation. It was likewise washed with progressively increasing concentrations of ethanol and lyophilized. The DNA was then treated with ribonuclease to remove any traces of RNA, and the RNA was treated with deoxyribonuclease I to remove traces of DNA. The DNA and RNA were again precipitated and collected, as described above, and lyophilized after washing with ethanol.

The 5'-deoxyribonucleotides were obtained by treating the lyophilized DNA with deoxyribonuclease I and snake venom phosphodiesterase. The nucleotides were then desalted by passage through a Bio-Gel P-2 column (9 mm x 140 cm) and separated on a column of Dowex 50W X4 (-400 mesh, H^+, 9 mm x 75 cm) resin. Elution with 0.05 M ammonium formate,[28] pH 3.2, separates the nucleotides in the following order: TMP, GMP, CMP, and AMP (Fig. 4). The column has been used to separate mixtures of nucleotides in 80-mg quantities.

Hydrolysis of RNA with snake venom phosphodiesterase has been unsuccessful. When the concentrated, desalted hydrolysate was eluted through the Dowex 50W X4 column, only one peak was observed -- eluting with the void volume. This is characteristic of unhydrolyzed DNA and RNA. The lack of hydrolysis is probably due to the secondary and perhaps tertiary structure of RNA.[29] Efforts are being focused on a procedure to alleviate this problem by

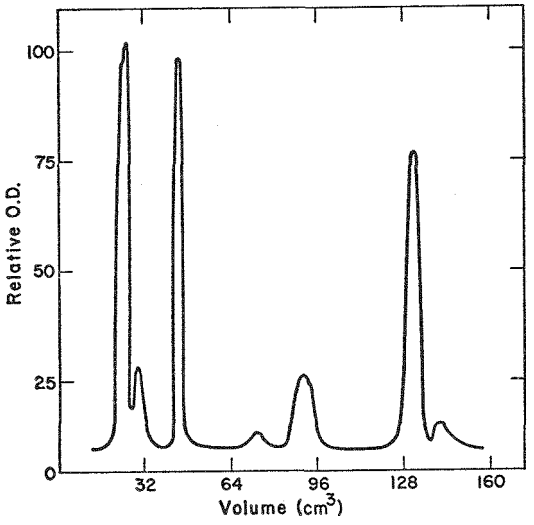

Fig. 4. Separation of deoxy-5'-nucleotides in their order of elution: thymidine-5'-monophosphate; deoxyguanosine-5'-monophosphate; deoxycytidine-5'-monophosphate; and deoxyadenosine-5'-monophosphate.

preceding the hydrolysis with a denaturation of the RNA.

Approximately 1.3% of the dry weight of blue-green algae was extracted as DNA, while 0.33% was extracted as RNA. These values compare well with recent estimates of the total amount of DNA and RNA present in blue-green algae (0.43 to 1.7% of the dry weight as DNA; 0.37 to 0.50% of the dry weight as RNA).[30] Purity of the DNA was determined by comparing the optical density at 260 nm to that at 230 and 280 nm. For commercially prepared DNA ("A" grade, California Corporation for Biochemical Research), the 230:260 ratio was 0.41 and the 280:260 ratio 0.57. The 230:260 ratio for the extracted DNA was 0.43 and the 280:260 ratio 0.56. Problems have been encountered with the DNA tending to hydrolyze to nucleosides and with enzyme inhibition by metal ions bonded to the double helix.[31]

2,4,5-Trichlorophenoxy-$^{13}C_6$-acetic Acid (2,4,5-T), N-(2,4,5-trichlorophenoxy-$^{13}C_6$-acetyl)glycine, and 2,3,7,8-tetrachlorodibenzo-p-dioxin-$^{13}C_{12}$ (TCDD). The synthesis of these three compounds from the common intermediate 2,4,5-trichlorophenol-$^{13}C_6$ is shown in Scheme 5. Benzene-$^{13}C_6$, which is readily obtained from the trimerization of acetylene-$^{13}C_2$, can be chlorinated using an iron catalyst as described by Holleman[32] to give 1,2,4,5-tetrachlorobenzene-$^{13}C_6$. Nucleophilic aromatic substitution of one of the four equivalent chlorines on tetrachlorobenzene by hydroxide to give 2,4,5-trichlorophenol is accomplished by heating to 220°C with sodium hydroxide, methanol, and water in a closed vessel. The reaction yields a mixture of 2,4,5-trichlorophenol (ca. 90%) and 2,4,5-trichloroanisole (ca. 10%), with the latter product being converted to the phenol upon a second treatment with base. O-Alkylation of the 2,4,5-trichlorophenol-$^{13}C_6$ with ethyl chloroacetate, followed by saponification of the ester, yields 2,4,5-trichlorophenoxy-$^{13}C_6$-acetic acid in good yield. The O-alkylation-saponification sequence has been found to give better yields than direct reaction between chloroacetic acid and sodium trichlorophenoxide. Conversion of 2,4,5-trichlorophenoxy-$^{13}C_6$-acetic acid to the acid chloride and condensation with glycine gives N-(2,4,5-trichlorophenoxy-$^{13}C_6$-acetyl)glycine. Attempts to prepare this compound from N-(chloroacetyl)-glycine and sodium phenoxide were unsuccessful. Buo-Hoi's method[33] for preparing 2,3,7,8-tetrachlorodibenzo-p-dioxin by self-condensation of 2,4,5-trichlorophenol in the presence of potassium carbonate and copper powder will be used to prepare 2,3,7,8-tetrachlorodibenzo-p-dioxin-$^{13}C_{12}$.

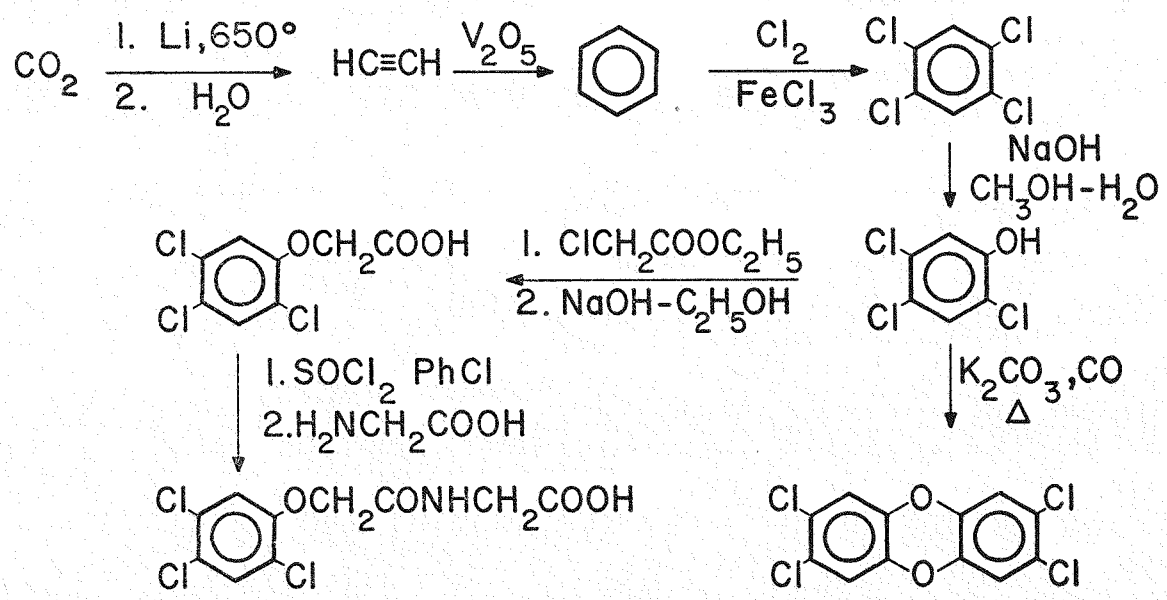

Scheme 5

REFERENCES

1. P. J. Montagne, "The Action of an Alcoholic Solution of Potassium Hydroxide on Ketones. IV," Rec. trav. chim. 36, 258 (1916); Chem. Abstr. 11, 3032 (1917).

2. B. Thom and J. W. Parsons, "Gas-Liquid Chromatography of N-trifluoracetyl n-Butyl Esters of Amino Acids: A Comparison of High-Performance and Acid-Washed Chromosorb-W as the Support Material," J. Chromatog. 90, 370 (1974).

3. I. Putter, A. Barreto, J. L. Markley, and O. Jardetzky, "Nuclear Magnetic Resonance Studies of the Structure and Binding Sites of Enzymes. X. Preparation of the Selectively Deuterated Analogs of Staphylococcal Nuclease," Proc. Natl. Acad. Sci. USA 64, 1396 (1969).

4. J. S. Cohen and I. Putter, "The Isolation of Deuterated Amino Acids," Biochim. Biophys. Acta 222, 515 (1970).

5. H. H. Bosshard, R. Mory, M. Schmid, and Hch. Zollinger, "Eine Methode zur Katalysierten Herstellung von Carbonsäure-und sulfosäure-chloriden mit Thionylchlorid," Helv. Chim. Acta 42, 1653 (1959).

6. E. Magnien and R. Baltzly, "A Re-Examination of the Limitations of the Hofmann Reaction," J. Org. Chem. 23, 2029 (1958).

7. G. Matzdorf, "Monoacetylbenzidine," Germ. Pat. 523,519 (1927), Chem. Abstr. 25, 3671 (1931).

8. J. C. Cain, "Nitrosoacetylamino Derivatives of the Benzene and Diphenyl Series," J. Chem. Soc. Trans. 95, 714 (1909).

9. H. C. Brown, C. P. Garg, and K.-T. Liu, "The Oxidation of Secondary Alcohols in Diethyl Ether with Aqueous Chromic Acid. A Convenient Procedure for the Preparation of Ketones in High Epimeric Purity," J. Org. Chem. 36, 387 (1971).

10. H. I. Waterman and C. van Vlodrop, "The Preparation of Carbon Disulfide from Methane and Hydrogen Sulfide," J. Soc. Chem. Ind., London 58, 109 (1939).

11. P. Feiler, "Carbon Disulfide," Germ. Pat. 803,114 (March 1, 1951), Chem. Abstr. 45, 6810 (1951).

12. E. Swakon and E. Field, "Preparation of Carbonyl Sulfide," U. S. Pat. 3,235,333 (Feb. 15, 1966).

13. F. N. Hayes, B. S. Rogers, and D. G. Ott, "2,5-Diaryloxazoles and 2,5-Diaryl-1,3,4-oxadiazoles," J. Amer. Chem. Soc. 77, 1850 (1955).

14. H. R. Snyder and F. X. Werber, "α-Tetralone," in Organic Synthesis, Coll. Vol. III (E. C. Horning, ed.), John Wiley and Sons, Inc., New York (1955), p. 798.

15. C. E. Olson and A. R. Bander, "α-Tetralone," in Organic Synthesis, Coll. Vol. IV (N. Rabjohn, ed.), John Wiley and Sons, Inc., New York (1963), p. 898.

16. M. S. Newman and W. M. Hung, "An Improved Aromatization of α-Tetralone Oximes to N-(1-Naphthyl)acetamides," J. Org. Chem. 38, 4073 (1973).

17. V. H. Kollman, C. T. Gregg, J. L. Hanners, T. W. Whaley, and D. G. Ott, "Large-Scale Photosynthetic Production of Carbon-13 Labeled Sugars," in Proceedings of the First International Conference on Stable Isotopes in Chemistry, Biology and Medicine, Argonne National Laboratory, Argonne, Illinois, May 9-11, 1973 (P. D. Klein and S. V. Peterson, eds.), U. S. Atomic Energy Commission report CONF-730525 (1973), pp. 30-40 (National Technical Information Service, Department of Commerce, Springfield, Va.).

18. J. K. N. Jones and R. A. Wall, "The Separation of Sugars on Ion-Exchange Resins," Can. J. Chem. 38, 2290 (1960).

19. M. Brin, "L(+) and D(-) Lactic Acids," in Biochemical Preparations, Vol. 3 (E. E. Snell, ed.), John Wiley and Sons, Inc., New York (1953), p. 61.

20. V. H. Kollman, J. L. Hanners, J. Y. Hutson, T. W. Whaley, D. G. Ott, and C. T. Gregg, "Large-Scale Photosynthetic Production of Carbon-13 Labeled Sugars: The Tobacco Leaf System," Biochem. Biophys. Res. Commun. 50, 826 (1973).

21. E. B. Fowler, W. H. Adams, C. W. Christenson, V. H. Kollman, and J. R. Buchholz, "Kinetic Studies of *C. pyrenoidosa* Using 94% $^{13}CO_2$," Biotechnol. Bioeng. XIV, 819 (1972).

22. J. R. Buchholz, W. H. Adams, C. W. Christenson, C. W. Johnson, V. H. Kollman, and E. B. Fowler, "Apparatus for the Mass Production of *Chlorella pyrenoidosa* with 94% $^{13}CO_2$ and 6% $^{12}CO_2$ as a Carbon Source," Los Alamos Scientific Laboratory report LA-4902 (April 1972).

23. W. A. Kratz and J. Myers, "Nutrition and Growth of Several Blue-Green Algae," Amer. J. Bot. 42, 282 (1955).

24. R. E. London, V. H. Kollman, and N. A. Matwiyoff, "The Quantitative Analysis of Carbon-Carbon Coupling in the ^{13}C NMR Spectra of Molecules Biosynthesized from ^{13}C Enriched Precursors," Biochim. Biophys. Acta (1974), in press.

25. B. W. Nichols, "Comparative Lipid Biochemistry of Photosynthetic Organisms," in Phytochemical Phylogeny (J. B. Harbourne, ed.), Academic Press, Inc., London (1970), pp. 105-118.

26. C. N. Kenyon and R. Y. Stanier, "Possible Evolutionary Significance of Polyunsaturated Fatty Acids in Blue-Green Algae," Nature 227, 1164 (1970).

27. J. Marmur, "A Procedure for the Isolation of Deoxyribonucleic Acid from Micro-Organisms," J. Mol. Biol. 3, 208 (1961).

28. V. H. Doctor, A. Burrs, P. Bailey, and S. Bryant, "Separation of Nucleotides, Nucleosides, and Bases of DNA with Cation Exchange Columns," Prep. Biochem. 3(2), 113 (1973).

29. J. P. Miller, M. E. Hirst-Bruns, and G. R. Philipps, "Action of Venom Phosphodiesterase on Transfer RNA from *Escherichia coli*," Biochim. Biophys. Acta 217, 176 (1970).

30. C. P. Wolk, "Physiology and Cytological Chemistry of Blue-Green Algae," Bacteriol. Rev. 37, 32 (1973).

31. M. Pieber, P. A. Kroon, J. H. Prestegard, and S. I. Chan, "Erratum. Tautomerism of Nucleic Acid Bases," J. Amer. Chem. Soc. 95, 3408 (1973).

32. A. F. Holleman, "The Three Tetrachlorobenzenes, Pentachlorobenzene and Hexachlorobenzene; Their Reaction with Sodium Methylate," Rec. trav. Chim. 39, 736 (1920), Chem. Abstr. 15, 1705 (1921).

33. N. P. Buo-Hoi, G. Saint-Ruf, P. Bigot, and M. Mangane, "Preparation, proprietes et identification de la 'dioxine' (tetrachloro-2,3,7,8 dibenzo-p-dioxine) dans les pyrolysats de defoliants a base d'acide trichloro-2,4,5 phenoxyacetique et de ses esters et des vegetaux contamines," C. R. Acad. Sc. Paris, Serie D, 273, 708 (1971).

BIOMEDICAL APPLICATIONS OF STABLE ISOTOPES

Stable isotope techniques are expected to have great impact in clinical medicine. There are two main reasons. The first is the ability to do metabolic tracer studies, especially in children and pregnant women, without consideration of the health hazards and inconvenience which can be attributed to radioactive isotopes. The inconvenience arises principally from the many regulations that must be followed in human studies with radioactive compounds. The second reason for the impact of stable isotopes on clinical studies is sensitivity. Current mass spectrometric methods make it possible to measure stable isotope-labeled compounds at concentrations far less than are practical with radioactive isotopes. This point is discussed in more detail elsewhere.[1,2]

Clinical applications of stable isotopes are of two general types. In the first type, applications suitable for mass screening are sought; examples are the ^{13}C-tolerance tests for glucose, galactose, or lactose. These tests are alike in requiring relatively large amounts of stable isotope administration to the patients (i.e., of the order of 0.1 g or more) and depend upon the simple and non-invasive measurement of breath carbon-^{13}C dioxide for evaluation. Adoption of such tests for mass screening would lead to very large requirements, both for production of stable isotopes and for preparation of suitable labeled compounds. The second approach is to apply stable isotope techniques to the widest possible variety of unsolved clinical problems. The isotope usage of individual studies is not high, but they may stimulate an increasing number of other investigations. Such diversified isotope usage could ultimately be even larger than the proposed "mass screening" tests. Examples of both types of clinical approaches are given below.

The central dogma underlying the use of stable isotopes for clinical investigations, especially those in pregnant women or children, is that the biological effects of stable isotope-labeled compounds are insignificant, in contrast to the considerations with ionizing radiation. That stable isotopes in the amounts used are completely safe is widely assumed on theoretical grounds and on the basis of what limited experimental studies have been made. However, more and better studies of biological effects of stable isotopes, especially in mammalian systems, are essential. Some of these studies are described in the following paragraphs. Finally, applications of stable isotopes to a number of basic research areas are being made at the LASL, and those which are in the general category of biomedical studies are also discussed in this section.

Clinical Studies

The most highly developed ^{13}C-clinical test is one using ^{13}C-galactose as a test for liver dysfunction. Under loading conditions, the liver is the primary site of galactose metabolism. The extent to which galactose is converted to glucose in the liver (and is thus made available for oxidation to carbon dioxide) depends on the redox state (effectively the NADH/NAD ratio) in that tissue. The reducing potential of the liver is increased by cirrhosis, hepatitis, and neoplasia, and this increase is expected to reduce the excretion of carbon-^{13}C

dioxide from galactose in patients with any of these conditions, as compared with normal controls.

As pointed out in the previous report,[3] early studies with both ^{13}C- and ^{14}C-galactose showed promise. This has been confirmed by subsequent tests.[4] At present, some 9 normal patients and 6 patients with cirrhosis have been tested with ^{13}C-galactose by Dr. Jon Shoop and his colleagues at the University of New Mexico, School of Medicine, in Albuquerque, and 9 normal and 21 cirrhotic patients have been given ^{14}C-galactose by Dr. Walton Shreeve of the Veterans Administration Hospital in Northport, New York. In cirrhosis, the rate of appearance of labeled carbon dioxide in the breath is one-fourth to one-half that of controls. Most importantly, there is no overlap of rates between controls and cirrhotics for at least the first 3 h after oral administration of the sugar. This has two important consequences. The first is that even a single breath sample may be adequate for analysis, once sufficient data are available. The second consequence is that the breath test is much more definitive for liver dysfunction than are assays of alkaline phosphatase, serum glutamic-pyruvic transaminase, or serum albumin levels, all of which overlap badly between normal and cirrhotic values. The breath test is also significantly better than the measurement of total bilirubin for diagnostic purposes. The results of the breath test for cirrhosis and the measurement of serum albumin levels correlate well.

Since hypothyroidism also reduces the rate of excretion of carbon dioxide from galactose, the ^{13}C-galactose tolerance test may be useful in diagnosis of thyroid function in those cases where differential diagnosis has excluded liver malfunction. The inability of the ^{13}C-glucose tolerance test to identify "borderline" diabetics was discussed in the previous annual report.[3] Other studies with the same end in view (that is, screening for adult-onset diabetes) are also planned by Dr. Shreeve using ^{13}C-lactate as the loading substance, probably in the presence of unlabeled glucose.

Another aspect of carbohydrate metabolism in humans is being investigated by Dr. Dennis Bier, Department of Pediatrics, University of California Medical School, San Francisco. It is known from animal studies that the liver maintains blood glucose within acceptable limits primarily by gluconeogenesis from alanine. Data on the importance of this pathway in man, and especially in children, are lacking. Dr. Bier is studying both ^{13}C-glucose and ^{13}C-alanine turnover in children, and the conversion of labeled alanine to labeled glucose. Investigations are being made both in children with chronic hypoglycemia (possibly due to the failure of alanine to act as a gluconeogenic substrate) and in normal patients.

In another study, Dr. John Watkins of Boston University is investigating the metabolism of ^{13}C-trioctanoin in children with cystic fibrosis. Breath samples are taken in Boston, and their ^{13}C contents are measured by Dr. Peter Klein at the Argonne National Laboratory. Tests of carbon-^{13}C dioxide excretion in these children show that the triglyceride is metabolized abnormally slowly. The metabolic rate, which is increased by pancreatic enzyme therapy but is still below that of normal children, can be readily followed.

Preliminary studies using breath analysis, after oral administration of ^{13}C-glucose, are being carried out on children with Leigh's syndrome (and controls) in an effort to understand the metabolic lesion in this usually fatal disease. This work is being done in collaboration with Professor Dr. Hans Helge of the Department of Pediatrics, the Free University, Berlin. Since suitable analytical facilities were not available in Berlin before August 1974 and the shipment of samples to Los Alamos seemed impractical, no results on the first tests are yet available.

The possible *in utero* feeding of the malnourished human infant is also being investigated (initially using ^{13}C-glucose) in cooperation with Professor Dr. Eric Saling of the Department of Gynecology, the Free University, Berlin. Since suitable patients are comparatively infrequent and because of analytical problems, no definite statements can yet be made on the results of this study. Some unsolved technical difficulties still exist in the acquisition and measurement of breath samples on infants in the first few minutes of extra-uterine life.

Pharmacological Studies

These investigations seek detectable biological effects of stable isotopes by incorporation of

high levels of label (compared to those used in clinical testing) into mammalian embryonic material at various stages of development. They are not designed to "prove" that stable-isotope enrichment does or does not have significant biological effects but, rather, to set upper limits on such effects if they occur. The results of such studies will be a statement that, in a particular test system, no discernible biological effect (lethal, mutagenic, teratogenic, or carcinogenic) occurs below a certain level of enrichment. The levels of enrichment tested will be the maximum that can be achieved in practice in the various systems. When mass screening tests with stable-isotope labeled compounds become a reality, much more extensive testing will be required, but this scale of operation is inappropriate for LASL under the present circumstances. What are sought in these studies are indications of biological effects, or their absence, for the guidance of those considering clinical applications.

These studies are part of a continuing collaboration between Group H-11 and the Embryonal Pharmacology Group of the Free University, Berlin. All of these studies have begun; none are to the point where definite conclusions can be drawn. For some of the investigations, no final analysis will be possible for several years. Two *in vitro* systems are in use. The limb bud system[5-7] is created by placing the excised limb bud of an 8-day-old mouse embryo on filter paper in a suitable medium. This amorphous blob of tissue is completely programmed to develop into a fully formed limb, and surprisingly this process can be simulated *in vitro* in two dimensions. The limb develops over a period of some 6 days, increasing in length and depositing collagen in those locations where, *in vivo*, calcification of the cartilage would produce the bones of, for example, the shoulder, upper and lower arms, wrist, hand, and fingers. Cartilage deposition can be clearly followed by suitable staining. However, neither nerve nor muscle is formed.

The limb-bud medium contains a very high (and essential) level of glucose. Replacement of this glucose with glucose-$^{13}C_6$ is the basis of this experiment. The developing limb bud *in vitro* is extremely sensitive to the presence of teratogenic drugs which lead, *in vitro* as *in vivo*, for example, to definite shortening of the long bones (phocomelia) and/or fusion of the digits (syndactylia).[7] In addition to morphological studies at both the light- and electron-microscopic levels, biochemical measurements of the formation of DNA, RNA, protein, and collagen (hydroxyproline) have been made.[6] Similar studies are in progress on limb buds incubated with ^{13}C-glucose, and both ^{13}C and ^{14}C studies are being carried out to measure the amount of ^{13}C actually incorporated during the period of incubation. Preliminary experiments indicate that about 10% of the carbon of the limb bud is replaced during the incubation. Direct measurement of incorporation of ^{13}C by combustion of the limbs is practical.

The second *in vitro* system involves the washing out, from the Fallopian tubes, of fertilized mouse embryos of known gestational age and the transfer of these to *in vitro* culture. Culture from the 4-cell stage to blastocyst has been successful routinely; culture from the 2-cell stage is much less so. Although such early embryos will not grow with glucose as the sole carbon source, nevertheless, they incorporate carbon primarily from glucose and, subsequent to the 8-cell stage, will grow on this substrate alone.[8] The ^{14}C studies indicate that we can expect incorporation of ^{13}C as high as 30 to 50% of the total embryo carbon. There is no direct way at present to measure the ^{13}C incorporation because the mass of the pre-implantation embryo is only of the order of 50 ng (dry weight).

The second state of the experiment is to reimplant the blastocysts into pseudopregnant females (i.e., those mated with sterile males at the same time the experimental mice were mated with fertile males), then to examine the embryos at various stages for abnormalities, either biochemical or morphological. The most striking abnormalities would be failure of the pre-implantation embryo to grow *in vitro* in a ^{13}C-containing medium, failure of the transferred embryos to implant, or early death of the embryos following implantation, leading to resorption. Some offspring from these foster mothers ultimately will be allowed to grow to adulthood and mated to check for possible mutagenic effects of stable isotope incorporation.

At present, the losses of pre-implantation embryos on implanting in foster mothers, either with or without ^{13}C treatment, are high enough so that evaluation of the results is difficult. These

difficulties can hopefully be overcome. The experiment is obviously a pulse-labeling one. Incorporated ^{13}C is rapidly diluted out as the embryo implants and grows in the foster mother. Experiments of this type assess the effects of high levels of ^{13}C enrichment on the growth of pre-implantation embryos, on the process of implantation itself, and on early development *in utero*.

A second type of pulse-labeling experiment is conducted on intact pregnant mice *in vivo*. Carbon-13 labeled glucose is administered for a total of 8 h, during the interval of day 8 to 9 of pregnancy. During this time, embryo weight increases over 100-fold in a period of some 30 h (an overall generation time of about 5 h, or substantially less than even the most rapidly growing mammalian tumor cells either *in vivo* or *in vitro*).[9] Most of the organs of the adult animal are also formed in this interval, and this period is extremely susceptible to embryotoxic agents. Chemical fractionation[10] of embryos following such administration of ^{13}C-glucose indicates that the range of ^{13}C enrichment of various fractions is 2 to 18%.[11] In the experiments presently underway, embryos so treated will be examined for morphological or biochemical changes by established methods. Some of the treated embryos are allowed to go to term and subsequently mated to search for mutagenic effects.

The experiments described thus far require very small amounts of labeled material. The final experiment planned in this series requires much more. In this case, timed pregnancies are produced, and then the pregnant mice are immediately placed on a ^{13}C-enriched diet. The diet will consist of ^{13}C-starch and yeast mixed with normal laboratory chow to give a dietary intake of 20 to 30 mol % ^{13}C. This diet will be continued throughout pregnancy and a few days into the postnatal period, some 23 to 24 days in all. Mice will be sacrificed at intervals and embryos examined morphologically and biochemically; other embryos will go to term and some to adulthood for subsequent mating.

Some preliminary ^{14}C experiments are being done in support of these longer term studies. These consist of creating timed pregnancies, then administering ^{14}C-labeled compounds in the same way in which ^{13}C will be given and measuring the amount of incorporation achieved and the rate at which isotopic equilibrium in the feces, urine, fetuses, and other tissues is approached. Previous experiments[1] showed that brief periods of isotope administration were much more effective in raising tissue incorporation levels than more protracted administration at lower levels. The "wash-out" of isotope label will also be studied in the ^{14}C experiments, since this bears on the interpretation of data from the two pulse-labeling experiments on pre-implantation embryos and the day 8-9 experiment.

Biochemical Studies

One of the oldest applications of stable-isotope labeling is that of isopycnic separation of enriched from unenriched material. We showed earlier that DNA from mouse embryos, following administration to the mothers of comparatively small amounts of ^{13}C-glucose, could be separated from unlabeled material in the analytical ultracentrifuge.[11] A more sophisticated application of this method is also in progress. Ribonucleic acid was isolated from ^{13}C-labeled yeast by standard methods, purified by density gradient centrifugation, and hydrolyzed enzymatically, and the mononucleotides were isolated by column chromatography. The AMP will be enzymatically phosphorylated to ATP, and this reaction mixture will be used immediately (with the addition of other unlabeled nucleotide triphosphates) in an RNA polymerase system in which the enzyme activity is furnished by isolated nuclei. Nuclear systems contain all the required initiation factors so that true RNA copies of the DNA template can be synthesized, but they have the great disadvantage of containing large amounts of exogenous RNA as well. By using the stable isotope label, the newly formed RNA may be separated from the endogenous RNAs by either analytical or density gradient ultracentrifugation.

A number of cmr studies were carried out in collaboration with Group CNC-4 in which a variety of ^{13}C-labeled compounds were used. Most of these studies are published and will only be mentioned here. Two types of studies were carried out on hemoglobin. One dealt with carbon-^{13}C monoxide binding to hemoglobins, both crude and purified, from a number of animal species. The result of this investigation showed that two distinct carbon monoxide binding sites could be distinguished by cmr in the

hemoglobin from a number of animal species, as shown earlier.[12] These two sites result from slight differences in the alpha and beta chains of hemoglobin. However, in hemoglobin from some rabbits, a third binding site was found which apparently results from hemoglobin heterogeneity in commercial rabbit strains. No electrophoretic differences could be shown between the hemoglobins of "two-site" and "three-site" rabbits. The same differences were found when carbon-^{13}C monoxide binding was examined by infrared spectroscopy.[13]

A second type of experiment was one first done in 1971[14] before Fourier transform cmr spectroscopy was available at LASL. More recent experiments using the Fourier transform technique showed that histidine-2-^{13}C incorporated into the alpha and beta chains of mouse hemoglobin was rigidly locked into the hemoglobin structure and that those histidines bound to iron, or those which were part of the alpha-beta interchain contact regions, could not be distinguished in the cmr spectrum even in the presence of carbon-^{13}C monoxide, which would be expected to shift the resonances of the iron-bound histidines.[15] It was clear from measurement of the spin-lattice relaxation times for ^{13}C-histidine labeled hemoglobin, both intra- and extracellularly, tnat the viscosity of the intracellular milieu was little different from that of hemolysates, a point on which there has been considerable discussion.

In addition to the cmr studies, several types of gas chromatography-mass spectroscopy experiments have been carried out with multiply ^{13}C-labeled compounds. As part of his doctoral thesis research for Oklahoma State University, Anthony Harmon has made the methyl esters of fatty acids from lipid extracts of ^{13}C-labeled algae. These were then separated by high pressure liquid chromatography and characterized by gas chromatography. Preliminary GC/MS experiments carried out at Oklahoma State University suggest that ^{13}C enrichment is lower in the more highly unsaturated fatty acids. There are also indications of isotope fractionation during gas chromatography. Since this would seriously affect the interpretation of results (in both this experiment and others using multiply labeled stable-isotope compounds), these observations are being further investigated.

Studies were also made on the mass spectroscopy of glucose-$^{13}C_6$ (by direct inlet) both using a field desorption instrument at Varian MAT in Bremen and the quadrupole instruments in the Finnigan applications laboratory in Munich. The field desorption studies, while extremely easy to carry out, gave nearly uninterpretable spectra, suggesting the formation of covalent dimers and trimers of glucose under field desorption conditions. Much of the chemistry of the field desorption process unfortunately is still poorly understood. The biochemical applications of this technique seem to be most impressive in the spectroscopy of high molecular weight compounds. The studies in Munich were also made by direct inlet, since no suitable derivatives of glucose had yet been made. Under chemical ionization conditions with ammonia as the reagent gas, glucose gave a molecular ion (glucose-NH_4^+) as the base peak (dominant species) and only two peaks of much lower intensity than the base peak, corresponding to loss of ammonium ion and/or water. Suitable derivatives of ^{13}C-glucose and ^{13}C-galactose were subsequently prepared,[16] characterized by gas chromatography, and will be analyzed by GC/MS using the Finnigan system. The goal is to establish detection limits for these multiply labeled compounds and to investigate the suitability of the GC/MS approach as an adjunct to the cmr procedures for establishing the degree of non-uniform labeling in multiply labeled compounds.

A similar investigation was carried out in collaboration with the Finnigan applications laboratory in Sunnyvale, California. Protein from ^{13}C-labeled yeast (a by-product of the nucleic acid isolation previously described) was hydrolyzed and converted to the N-acetyl, propyl ester derivatives of the amino acids, then the mixture was run through the Finnigan GC/MS under electron impact conditions. Excellent separation of all amino acids present (the sulfur amino acids were missing) was obtained. A further experiment of this sort is intended using algal amino acids to look for isotope effects in the biosynthesis of the aromatic amino acids (those with the largest number of carbons) compared to the simple aliphatic amino acids. Such isotope effects were reported previously,[17] but the effects were small and the degree of enrichment and the instrumental

methods then available cast some doubt on the significance of the results.

REFERENCES

1. M. Anbar and W. H. Aberth, "Field Ionization Mass Spectroscopy: A New Tool for the Analytical Chemist," Anal. Chem. 46, 59A-64A (1974).

2. C. T. Gregg, "Some Applications of Stable Isotopes in Clinical Pharmacology," Eur. J. Clin. Pharmacol. 7, 315-319 (1974).

3. C. R. Richmond and E. M. Sullivan, eds., "Annual Report of the Biomedical and Environmental Research Program of the LASL Health Division, January through December 1973," Los Alamos Scientific Laboratory report LA-5633-PR (May 1974), pp. 131-133.

4. W. W. Shreeve, J. D. Shoop, D. G. Ott, and B. B. McInteer, "Evaluation of Liver Function by Oxidation of Galactose-^{14}C or -^{13}C *in vivo*," J. Nuclear Med. 15, 532 (1974).

5. M. B. Aydelotte and D. M. Kochhar, "Development of Mouse Limb Buds in Organ Culture: Chondrogenesis in the Presence of a Proline Analog, L-Azetidine-2-carboxylic Acid," Develop. Biol. 28, 191-201 (1972).

6. D. Neubert, H.-J. Merker, and S. Tapken, "Comparative Studies on the Prenatal Development of Mouse Extremities *in vivo* and in Organ Cultures," Naunyn-Schmiedeberg's Arch. Pharmacol. (1974), in press.

7. D. Neubert, S. Tapken, and H.-J. Merker, "Induction of Skeletal Malformations in Organ Cultures of Mammalian Embryonic Tissue," Naunyn-Schmiedeberg's Arch. Pharmacol. (1974), in press.

8. R. L. Brinster, "Incorporation of Carbon from Glucose and Pyruvate into the Preimplantation Mouse Embryo," Exp. Cell Res. 58, 153-158 (1969).

9. C. T. Gregg, "Some Aspects of the Energy Metabolism of Mammalian Cells," in Growth, Nutrition and Metabolism of Cells in Culture (G. H. Rothblat and V. J. Cristofalo, eds.), Academic Press, Inc., New York (1972), pp. 83-136.

10. R. Krowke, K. Pielsticker, and G. Siebert, "A Simple Fractionation Procedure for Studying Incorporation of Radioactively Labeled Precursors into Mammalian Main Cell Components," Naunyn-Schmiedeberg's Arch. Pharmacol. 271, 121-124 (1971).

11. C. T. Gregg, D. Smith, D. G. Ott, J. Malanify, B. B. McInteer, N. A. Matwiyoff, and D. Neubert, "Incorporation of Carbon-13 into Fetal and Maternal Protein and Nucleic Acid during Various Intervals of Pregnancy in Mice," in Abstracts, Ninth International Congress of Biochemistry, Stockholm, Sweden (July 1973).

12. R. B. Moon and J. H. Richards, "Nuclear Magnetic Resonance Studies of ^{13}CO Binding to Various Heme Globins," J. Amer. Chem. Soc. 94, 5093-5095 (1972).

13. N. A. Matwiyoff, P. J. Vergamini, T. E. Needham, C. T. Gregg, J. A. Volpe, and W. S. Caughey, "Carbon-13 Nuclear Magnetic Resonance and Infrared Spectroscopic Studies of ^{13}CO Bind-in to Rabbit Hemoglobin," J. Amer. Chem. Soc. 95, 4429-4431 (1973).

14. C. T. Gregg, "Biological Applications of Carbon-13," in Proceedings of the First National Symposium on Carbon-13, Los Alamos, New Mexico, June 1971 (D. G. Ott, ed.), Los Alamos Scientific Laboratory report (1974), in press.

15. R. E. London, C. T. Gregg, and N. A. Matwiyoff, "Carbon-13 Nuclear Magnetic Resonance Study of the Rotational Mobility of Intra- and Extra-Cellular Mouse Hemoglobin Labeled with ^{13}C Enriched Histidine," Science (1974), submitted.

16. J. Szafranek, C. D. Pfaffenberger, and E. C. Horning, "Separation of Aldoses and Alditols Using Thermostable Open Tubular Glass Capillary Columns," Anal. Letters 6, 479-493 (1973).

17. W. A. Vanden Heuvel and J. S. Cohen, "Gas-Liquid Chromatography-Mass Spectroscopy of Carbon-13 Enriched Amino Acids as Trimethylsilyl Derivatives," Biochim. Biophys. Acta 208, 251-259 (1970).

BIOSYNTHESIS AND CARBON-13 NUCLEAR MAGNETIC RESONANCE CHARACTERIZATION OF LABELED CELLS

Carbon-13 nmr spectroscopy has been used as an investigatory probe for studying both synthetic liposome membranes[1,2] and, in several cases, naturally occurring membrane systems.[3,4] Line-width, spin-lattice relaxation times, and chemical shift data provide detailed information about the structure and dynamics of unperturbed membrane lipids.[5] However, recent investigations with naturally occurring membranes have been somewhat less successful than studies of synthetic liposomes due to the low carbon-13 concentrations and the more complex nature of natural systems. The technique of specific enrichment of growing cells with carbon-13 enriched membrane components has been used as one method for dealing with these problems.[6] In our studies, non-specific enrichment of *Candida utilis* by growth on 20 mol % carbon-13 enriched acetate and growth of *Anacystis nidulans* on 20 mol % carbon-^{13}C dioxide was used to obtain adequate signal-to-noise levels for cell spectra (Figs. 1 and 2). Growth at the 20 mol % enrichment level avoided the complications of ^{13}C-^{13}C multiplets which are more significant at

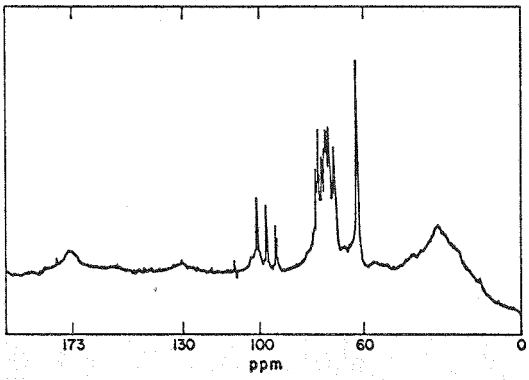

Fig. 1. Whole-cell FT ^{13}C nmr spectrum of the blue-green alga *A. nidulans* taken at 25°C and representing 43 729 scans. Chemical shifts are in ppm relative to TMS.

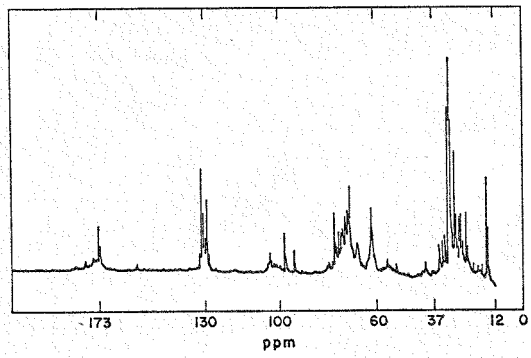

Fig. 2. Whole cell FT ^{13}C nmr spectrum of *C. utilis* taken at 26°C and representing 3320 scans. Chemical shifts are given in ppm relative to TMS.

higher levels of carbon-13 enrichment. We obtained a substantial simplification of the ^{13}C nmr spectrum by removing water-soluble constituents by a combination of freeze-thaw cycling and osmotic shock. The cell sample remaining consisted of lipid-protein complex as well as the peptidoglycan cell wall, the latter being physically separated from the former as observed by microscopic examination (Fig. 3). The resulting cell-wall membrane system proved to be amenable to nmr study, the resolution of the fatty acid resonances being superior to that of any previously described carbon-13 membrane spectrum, synthetic or natural.[7]

The cell disruption techniques used were sufficiently gentle so that most of the proteins associated with the lipid were not significantly denatured, a conclusion supported by the nmr spectrum. We believe that studies of such systems are important

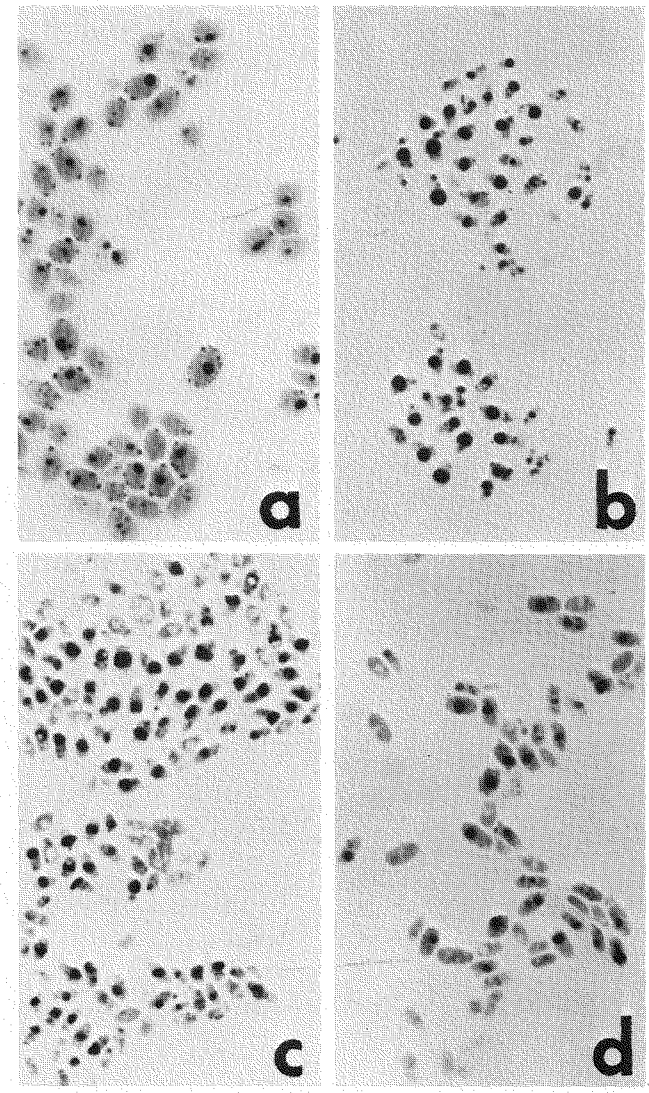

Fig. 3. *Candida utilis* stained with Oil Red O prior to osmotic shock (a), subsequent to osmotic shock (b and c), and after a mild lipid extraction (d).

for determining how closely the synthetic membrane systems which have been more extensively studied compare with the less characterized natural systems in which protein-lipid interactions may be significant. The high resolution character of the carbon-13 spectra of the yeast system, for fatty acid resonances particularly, has permitted precise measurements of spin-lattice relaxation times (T_1) and chemical shifts as a function of temperature.[8] From the data, we conclude that the "fractionated" yeast system exhibits mobility gradients for the fatty acid chains similar to those determined in other synthetic and natural liposome systems. In these studies, a chemical shift gradient has also

been measured. If such shifts arise from a steric interaction between γ carbons, as postulated previously by Batchelor *et al.*,[9] the data reflect a gradient in ΔE (the energy difference between gauche and anti conformations) along the fatty acid chain. Also, the effect of intermolecular lipid interactions on the magnitude of ΔE was estimated.

Initial membrane labeling studies are in progress using glucose-$^{13}C_6$ (81.5 mol %) and (2-hydroxyethyl)trimethyl-$^{13}C_3$-ammonium chloride (choline-C_3 chloride) to label Chinese hamster ovary (CHO) cells. These initial experiments are concerned with the determination of the most effective membrane labeling techniques and assignment of membrane resonances using nmr spectroscopy. Effects of added paramagnetic ions and lanthanide shift reagents on the systems are under investigation.

REFERENCES

1. P. E. Godici and F. R. Landsberger, "Dynamic Structure of Lipid Membranes. Carbon-13 Nuclear Magnetic Resonance Study Using Spin Labels," Biochemistry 13, 362 (1974).

2. J. H. Prestegard, "Fusion of Dimyristollecithin Vesicles as Studied by Proton Magnetic Resonance Spectroscopy," Biochemistry 13, 1122 (1974).

3. A. G. Lee, N. J. M. Birdsall, and J. C. Metcalfe, "^{13}C Fourier NMR Relaxation Studies of Biological Molecules," Chem. Brit. 9(3), 116 (1973).

4. K. M. Keough, E. Oldfield, D. Chapman, and P. Beynon, "Carbon-13 and Proton Nuclear Magnetic Resonance of Unsonicated Model and Mitochondrial Membranes," Chem. Phys. Lipids 10, 37 (1973).

5. J. Seelig and W. Niederberger, "Deuterium Labeled Lipids as Structural Probes in Liquid Crystalline Bilayers. Deuterium Magnetic Resonance Study," J. Amer. Chem. Soc. 96, 2069 (1974).

6. J. C. Metcalfe, N. J. M. Birdsall, and A. G. Lee, "Carbon-13 NMR Spectra of Acholeplasma Membranes Containing Carbon-13 Phospholipids," FEBS Lett. 21, 335 (1972).

7. R. E. London, V. H. Kollman, and N. A. Matwiyoff, "^{13}C FT NMR Studies of Fractionated *Candida utilis* Membranes," Biochemistry (1974), submitted.

8. R. E. London, V. H. Kollman, and N. A. Matwiyoff, "The Quantitative Analysis of Carbon-Carbon Coupling in the ^{13}C NMR Spectra of Molecules Biosynthesized from ^{13}C Enriched Precursors," Biochim. Biophys. Acta (1974), in press.

9. J. G. Batchelor, J. H. Prestegard, R. J. Cushley, and S. R. Lipsky, "Conformational Analysis of Lecithin in Vesicles by Carbon-13," Biochem. Biophys. Res. Commun. 48(1), 70 (1972).

CARBON-13 NUCLEAR MAGNETIC RESONANCE ANALYSIS OF BIOSYNTHESIZED MOLECULES

The Formation of Lactate by Glycolysis

The technique of using correlated enrichment to study a biosynthetic pathway is illustrated by the fermentation of a mixture of ^{13}C enriched and natural abundance sugars to lactate by *Lactobacillus delbrueckii*. Using an equimolar mixture of glucose uniformly labeled with carbon-13 to the 71.1 mol % level and natural abundance glucose for the fermentive substrate, lactate was isolated and examined by mass spectrometry and nmr. As expected, mass spectrometry indicated that 36.2% of the carbon atoms are carbon-13 and that the nmr spectrum (Fig. 1) can be fit well by assuming that the lactate-$^{13}C_3$ is uniformly enriched to 73 mol % ^{13}C. This is consistent with the glycolysis pathway in which lactate is

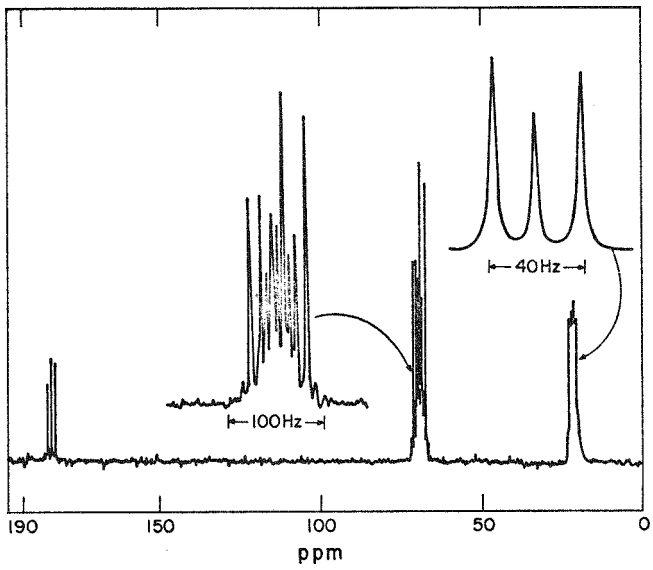

Fig. 1. Proton noise decoupled ^{13}C nmr spectrum of zinc lactate. The methyl (20.9 ppm) and carboxyl (182.6 ppm) resonances are combinations of a singlet, corresponding to species in which C-2 (68.5 ppm) is unlabeled, and a doublet, corresponding to species in which C-2 is labeled. The C-2 resonance is a combination of a singlet, two pairs of doublets, and a quartet for a total of 9 peaks. Due to the differences between $J_{1,2}$ = 37.6 Hz and $J_{2,3}$ = 55.8 Hz, the doublets arising from the labeling of C-2 and either the carboxyl or the methyl carbon can be distinguished.

formed by the direct breakdown of 6-carbon sugar into two 3-carbon units without scrambling of the carbons which would have given an entirely different nmr spectrum.

Photosynthetic Incorporation of Carbon Dioxide into Galactosylglycerol by Red Algae

The use of red algae for obtaining galactosylglycerol-$^{14}C_9$ was first studied by Bean *et al.*[1] and by Bean and Hassid.[2] They found that galactosylglycerol becomes radioactive very early in the photosynthetic process and that, after 4 min of photosynthesis, the galactose/glycerol activity ratio is approximately 2. Although, as was pointed out by Bean and Hassid, this result is consistent with the equivalent labeling of all carbons, a number of inequivalent labeling schemes can lead to the same ratio. Adjunct to our preparation of galactosylglycerol-$^{13}C_9$ by this biosynthetic method, we have used ^{13}C nmr as a probe for investigating the biosynthetic pathway.

The biosynthesized galactosylglyercol-$^{13}C_9$ was extracted at 1, 2, and 40 h as described in the preparations section. Nmr spectra of the acetylated species are shown in Fig. 2. In addition, glycerol-$^{13}C_3$ samples obtained from different runs after 12 and 24 h of photosynthetic activity were also analyzed (Fig. 2). The fact that the glycerol C-1 and C-3 resonances appear as distinct peaks reflects nonequivalence of these carbon atoms due to the asymmetry of the galactosyl moiety at C-2. In pure glycerol (Fig. 3), only a single resonance is observed for carbons C-1 and C-3. In addition to the singlet peaks, the multiplets arising from ^{13}C-^{13}C coupling in multiply labeled compounds are also present. A complete analysis of the galactose spectrum cannot be performed due to the overlapping of the C-2 and C-5 resonances; however, the multiplet structure of the glycerol spectrum can be considered quantitatively. The C-1/C-3 resonance is a singlet if C-2 is unlabeled (neglecting the small long-range splitting in galactosylglycerol) or a doublet if C-2 is labeled. The C-2 resonance can be either a singlet, doublet, or quartet, as is characteristic of an AB_2 spectrum. The two center lines of the quartet, which are separated by ~ 6.8 Hz, overlap the singlet. Using values of $J = 41.1$ Hz and $\Delta\nu = 242$ Hz for the glycerol carbon coupling constant and

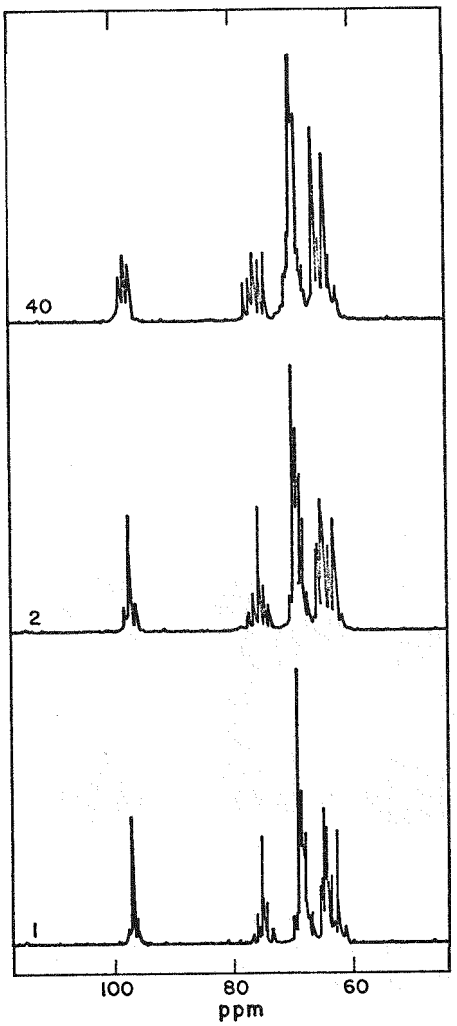

Fig. 2. Proton noise decoupled spectra of acetylated galactosylglycerol-$^{13}C_9$ dissolved in $CDCl_3$ (the acetyl resonances are not shown). The singlet resonances correspond to galactose C-1 (96.6 ppm), galactose C-2/C-5 (67.2 to 68.7 ppm), and alactose C-6 (62.3 ppm) and to glycerol C-2 (74.8 ppm) and glycerol C-1 and C-3 (64.0 and 64.2 ppm, respectively) (peak positions are relative to TMS). The spectra are for samples taken after 1, 2, and 40 h of photosynthetic activity. A noticeable change is apparent in the singlet-to-doublet ratio of the C-1 and C-3 resonances between 1 and 2 h.

peak separation between C-2 and C-1/C-3, the relative intensities of the quartet lines can be calculated. The intensity of the center two lines is 0.917 of the intensity of the outer two lines. Thus, the intensity of the center two lines of the quartet can be calculated and subtracted from the intensity of the observed center resonances to obtain the singlet intensity. An additional problem in the galactosylglycerol spectrum is the overlapping of the upfield sidebands of the glycerol C-1/C-3 and

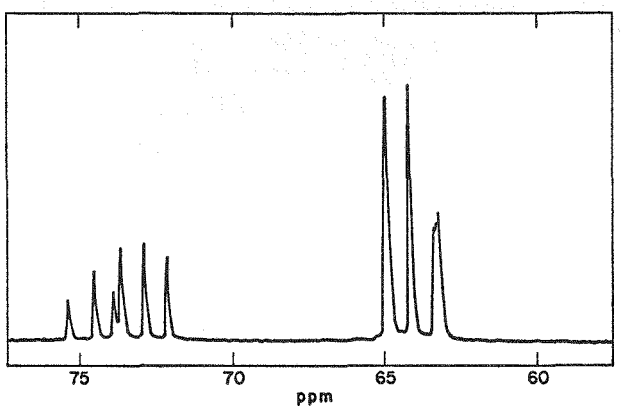

Fig. 3. Proton noise decoupled spectrum of glycerol prepared from galactosylglycerol extracted after 12 h of photosynthesis. The C-2 resonance (73.7 ppm) consists of a combination of a singlet, doublet, and quartet, where the quartet structure is that calculated for an AB_2 spectrum. The central quartet peaks overlap the singlet resonance, but the relative intensities can be determined. The C-1 and C-3 resonances (64.3 ppm) also consist of a combination of singlet, doublet, and quartet peaks. However, the quartet structure is not resolvable from the doublet structure, with the two downfield quartet lines overlapping the downfield doublet and the two upfield quartet lines overlapping the upfield doublet. The intensity ratio of the downfield doublet to the upfield doublet is approximately equal to the ratio of the two downfield quartet lines to the two upfield quartet lines.[3]

the downfield sideband of the galactose C-6. Using parameters measured in the galactosylglycerol spectrum, J = 43.5 Hz and $\Delta\nu$ = 268.3 Hz; the intensity of the upfield sideband is calculated to be 0.724 times the intensity of the downfield glycerol C-1/C-3 sideband. Three independent ratios can be measured for the glycerol spectrum. These have been arbitrarily chosen as the doublet/singlet ratio (d/s) for C-2 and C-1, C-3 and the quartet/doublet ratio (q/d) for C-2. Measured values, along with some values obtained for C-1 and C-6 for galactose, are summarized in Table I. In addition, the average enrichment of the various samples, as determined by mass spectrometric analysis of samples combusted to carbon dioxide, is also shown.

A comparison of the average enrichment with the observed multiplet splitting indicates that the galactosylglycerol is not uniformly enriched. The data can most readily be explained by assuming that a large concentration of natural abundance galactosylglycerol is present initially and that, to this pool, newly synthesized and highly labeled material is added as photosynthesis progresses. Thus, the gradual increase in the doublet/singlet ratios indicated in Table II corresponds to a decreasing fraction of natural abundance galactosylglycerol which

TABLE I

MULTIPLET INTENSITY RATIOS FOR GLYCEROL-$^{13}C_3$ AND ACETYLATED GALACTOSYLGLYCEROL-$^{13}C_9$ SAMPLES

Sample	Photosynthetic Period (h)	C-1 d/s	C-6 d/s	C-2 d/s	C-2 q/d	C-1/C-3 d/s	Mol % ^{13}C
Galactosylglycerol	1	0.469	0.478	0.883	0.650	0.652	5.0
Galactosylglycerol	2	0.640	0.615	1.101	0.938	1.090	5.1
Glycerol	12	--	--	3.909	1.366	2.436	24.1
Glycerol	24	--	--	3.320	1.248	2.301	28.0
Galactosylglycerol	40	1.408	1.652	6.035	1.859	3.810	43.8

TABLE II

RESULTS OF UNIFORM LABELING MODEL

Sample	Photosynthetic Period (h)	Fraction Labeled (%)	Enrichment of Labeled Material (%)	Calculated Ratios C-2 d/s	C-2 q/d	C-1/C-3 d/s
Galactosylglycerol	1	4.9	56	0.881	0.647	0.660
Galactosylglycerol	2	5.4	66	1.098	0.945	1.081
Glycerol	12	34.5	73	3.908	1.352	2.448
Glycerol	24	26.0	72	3.313	1.253	2.328
Galactosylglycerol	40	51.0	80	6.047	2.000	3.755

contributes, to a good approximation, only to the observed singlet. Bean and Hassid have characterized the galactosylglycerol of red algae as the main reserve carbohydrate, analogous to sucrose in the higher plants.[2] The presence of a large pool, even after 36 h in the dark, indicates that it is not rapidly converted into energy and carbon dioxide, consistent with the fact that galactose, unlike glucose, is not immediately fermentable. Therefore, the function of the galactosylglycerol in the red algae may be primarily as a reserve for structural material, particularly since a galactose polymer is known to be a main structural component of the organism.[2]

Another interesting feature of the spin splitting ratios is the gradual increase in the ratio of the C-2 quartet/doublet. Since the natural abundance galactosylglycerol does not contribute appreciably to these multiplets, this increase indicates a slow change which is occurring in the labeling probabilities of the newly synthesized material. There are several possible causes for this: (1) at the time when the labeling begins, all of the photosynthetic metabolites (e.g., ribulose diphosphate, seduheptulose 7-phosphate, etc.) are not labeled. Therefore, the metabolic products of the photosynthetic process will not be labeled to the extent of the input carbon dioxide until all of the intermediates have been labeled to this level. (2) The respiration process will produce unlabeled carbon dioxide, thus decreasing the enrichment of the carbon dioxide which is being fixed relative to that supplied externally. As time progresses, newly synthesized metabolites will contribute increasingly to the respired carbon dioxide, and the dilution effect will decrease. (3) As a result of the long period in the dark, the algae activate catabolic enzymes which continue to function for varying lengths of time after the light is turned on. Therefore, catabolic processes are producing unlabeled carbon dioxide at the beginning of the experiment.

The carbon-carbon coupling data alone are insufficient to completely determine the enrichment of the individual carbon atoms in galactosylglycerol. However, information can be obtained by considering various reasonable models and fitting the observed data. The simplest model is that the sample is a mixture of natural abundance and newly synthesized, uniformly labeled galactosylglycerol. The results obtained with this model, summarized in Table II, indicate that a very good fit to the observed splitting ratios can be obtained, most of the errors being less than 5%. Of the three possibilities suggested above for the gradual increase in the labeling of the newly synthesized material, only the first would be expected to result in substantial differences in the enrichment of the different carbons. Since a uniform labeling model provides such a good fit to the data, it is unlikely that this effect is important. Nevertheless, the enrichment calculated for the 1- and 2-h samples probably represents an average of gradually increasing enrichment. For example, for the C-1 and C-3 carbons of the glycerol portions of the galactosylglycerol, the same splitting ratios for the 1-h sample would be obtained if the enrichment of C-2 increased linearly to 3/2 (56%) = 84%. In fact, the entire 1-h period cannot be approximated reasonably by a linear increase, since the enrichment appears to level off at approximately 73%. The model also gives rough agreement with the average labeling data, as determined by mass spectrometry, although the nmr values obtained, assuming that the galactose and glycerol are labeled equivalently, are somewhat lower. Nmr determinations of the fraction of natural abundance product become more inaccurate as the fraction of highly labeled product increases; thus, estimations of the average labeling based on these fractions are less accurate for the later samples.

The labeling of the galactosylglycerol appears to follow three stages: (1) the labeling percentages of the glycerol carbons increase initially, eventually leveling off at about 73%. (2) Between 12 and 24 h, there is relatively little change in the net carbon-13 content and ^{13}C nmr spectrum of the galactosylglycerol pool. During this period, the organism may be drawing on the pool to some extent but not synthesizing much highly labeled new material, thus leaving the labeling levels relatively stable. (3) Between 24 and 40 h, there is a further apparent increase in enrichment of newly synthesized material (i.e., not considering the natural abundance pool) to 80%. It is interesting to note that this increase occurs despite a marked decrease in the uptake of carbon dioxide after 24 h (see preparation section above). The decrease in carbon dioxide

uptake is accompanied by a bleaching of the cells, indicating a decline in photosynthetic activity which may reflect a loss in viability of the cells. The quantity of galactosylglycerol extractable per unit cell mass also drops from about 3.8 to 2.7 g/kg between 24 and 40 h, indicating that the organism may be drawing on its galactosylglycerol reserve, perhaps for the synthesis of structural polymer. Since any output from the galactosylglycerol pool reflects the average labeling of the pool while the input is of highly labeled material, these effects will increase the labeling percentages as observed, but at the expense of galactosylglycerol.

REFERENCES

1. R. C. Bean, E. W. Putman, R. E. Trucco, and W. Z. Hassid, "Preparation of ^{14}C-Labeled D-Galactose and Glycerol," J. Biol. Chem. 204, 169 (1953).

2. R. C. Bean and W. Z. Hassid, "Assimilation of $^{14}CO_2$ by a Photosynthesizing Red Algae, *Iridophycus flaccidum*," J. Biol. Chem. 212, 411 (1955).

3. R. E. London, V. H. Kollman, and N. A. Matwiyoff, "The Quantitative Analysis of Carbon-Carbon Coupling in the ^{13}C NMR Spectra of Molecules Biosynthesized from ^{13}C Enriched Precursors," Biochim. Biophys. Acta (1974), in press.

ENVIRONMENTAL, CHEMICAL, AND OTHER APPLICATIONS

The initial trial of mass-21 methane (i.e., methane-^{13}C-d_4) as an atmospheric tracer has produced encouraging results following its release in Idaho and subsequent detection in Minnesota (and other locations).[1] Additional quantities of methane of mass-20 and -21 (CD_4 and $^{13}CD_4$) are being synthesized for further studies.

Isolation, purification, and high resolution mass spectrometric techniques involved in using carbon-13 labeled fatty acids in a multidisciplinary, large-scale ecological study at Oklahoma State University are being developed by Mr. A. W. Harmon. He is a graduate student in the Department of Chemistry (Professor L. Varga, advisor) at Oklahoma State University and is performing part of his thesis research at Los Alamos under an Associated Western Universities, Inc., appointment. The algae systems described elsewhere in this report serve as sources of the required materials.

As time permits, compounds labeled with stable isotopes are prepared for various LASL chemistry and physics research projects. These include materials such as sodium cyanide-^{13}C-^{15}N and formic-^{13}C acid for vibrational spectroscopy studies in Group CNC-4 and carbonyl-^{13}C sulfide, carbon-^{13}C disulfide, and ammonia-d for the Laser Research and Technology (L) Division. Some non-isotopic compounds (not commercially available) have also been prepared for L-Division needs (e.g., the naphthyloxadiazoles, mentioned in the preparation section of this report).

It is anticipated that Group H-11's capabilities can be of increasing usefulness as Laboratory and national programs develop in the energy and environmental fields. Stable isotope-labeled compounds as tracers in environmental, atmospheric, metabolic, and toxicological studies are expected to become very useful in these areas of increasing emphasis and concern.

REFERENCE

1. G. A. Cowan, D. G. Ott, A. Turkevich, L. Machta, and N. R. Daly, "Heavy Methanes as Atmospheric Tracers," Science (1974), submitted.

APPENDIX

1974 BIBLIOGRAPHY FOR BIOMEDICAL AND ENVIRONMENTAL RESEARCH PROGRAM

MAMMALIAN RADIOBIOLOGY GROUP (H-4)

Publications

E. O. Goodrich, Jr., J. R. Prine, and J. S. Wilson, "Iodized Starch Granules as a Cause of Starch Peritonitis," Surgical Forum, Vol. XXV, 372-374 (1974).

W. T. Ham, Jr., H. A. Mueller, A. I. Goldman, B. E. Newnam, L. M. Holland, and T. Kuwabara, "Ocular Hazard from Picosecond Pulses of Nd:YAG Laser Radiation," Science 185(4148), 362-363 (1974).

J. W. Healy, C. R. Richmond, and E. C. Anderson, "A Review of the Natural Resources Defense Council Petition Concerning Limits for Insoluble Alpha Emitters," Los Alamos Scientific Laboratory report LA-5810-MS (November 1974).

L. H. Hempelmann, W. H. Langham, G. L. Voelz, and C. R. Richmond, "Biomedical Follow-Up of the Manhattan Project Plutonium Workers," in: Proceedings of the Third International Congress of the International Radiation Protection Association, Vol. I (W. S. Snyder, ed.), National Technical Information Service report CONF-730907-P1, Springfield, Virginia (1974), pp. 713-718.

L. M. Holland, J. F. Spalding, J. R. Prine, and O. S. Johnson, "Comparative Immediate and Long-Term Effects of Gamma-Ray Dose Protraction by Fractionation and Continuous Low-Dose-Rate Exposure in Dogs and Monkeys," in: Abstracts of the 5th International Congress of Radiation Research, Seattle, Washington (July 14-20, 1974), Abstract No. B-37-1, p. 144.

C. R. Richmond, L. M. Holland, G. A. Drake, and J. S. Wilson, "Biological Response to Small Discrete Radioactive Sources. III. Effects of Surgically Implanted $^{238}PuO_2$ and $^{239}PuO_2$ Microspheres in Beagles," in: Abstracts of Papers Presented at the 19th Annual Meeting of the Health Physics Society, Houston, Texas (July 7-11, 1974), Abstract No. P/127, p. 33.

C. R. Richmond, "Current Status of Information Obtained from Plutonium Contaminated People," in: Abstracts of the 5th International Congress of Radiation Research, Seattle, Washington (July 14-20, 1974), Abstract No. C-9-3, p. 161.

C. R. Richmond, "Human Experience as Related to Plutonium," in: Plutonium Information Meeting of an Ad Hoc Subcommittee of the Advisory Committee on Reactor Safeguards, USAEC Technical Information Center, Oak Ridge, Tennessee, report CONF-740115 (December 1974).

J. F. Spalding, L. M. Holland, O. S. Johnson, J. R. Prine, J. E. London, and P. M. LaBauve, "Recovery and Residual Injury in Monkeys Exposed to Large Doses of Radiation by Fractionation," Los Alamos Scientific Laboratory report LA-5724-MS (September 1974).

J. F. Spalding, O. S. Johnson, and R. F. Archuleta, "Life-Shortening in Mice Exposed to Discrete Doses of Gamma Rays at Low Dose Rates," in: Abstracts of the 5th International Congress of Radiation Research, Seattle, Washington (July 14-20, 1974), Abstract No. B-37-2, p. 144.

J. F. Spalding, O. S. Johnson, R. F. Archuleta, and G. L. Tietjen, "Dose-Rate Effect on Life-Shortening in Mice," Los Alamos Scientific Laboratory report LA-5722-MS (September 1974).

Manuscripts Submitted

E. C. Anderson, L. M. Holland, J. R. Prine, and C. R. Richmond, "Lung Irradiation with Static Plutonium Microspheres," in: Experimental Lung Cancer, Carcinogenesis and Bioassays, Battelle Seattle Research Center, Seattle, Washington (June 23-26, 1974), Springer-Verlag, Heidelberg, CONF-740648-1 (in press).

J. E. Furchner, J. E. London, and J. S. Wilson, "Comparative Metabolism of Radionuclides in Mammals. IX. Retention of Selenium-75 in the Mouse, Rat, Monkey, and Dog," Health Phys. (1974), submitted.

C. R. Richmond, "The Importance of Nonuniform Dose-Distribution in an Organ," in: Second Annual Life Sciences Symposium on Plutonium -- Health Implications for Man, Los Alamos, New Mexico (May 22-24, 1974), submitted.

C. R. Richmond, "Current Status of Information Obtained from Plutonium Contaminated People," in: Proceedings of the Symposium on Transuranium Element Toxicity -- Dose-Response Relationships at Low Exposure Levels, 5th International Congress of Radiation Research, Seattle, Washington (July 14-20, 1974), in press.

C. R. Richmond and R. L. Thomas, "Plutonium and Other Actinide Elements in Gonadal Tissue of Man and Animals," Health Phys. (1974), in press.

J. F. Spalding, L. M. Holland, O. S. Johnson, and J. R. Prine, "Recovery Rate and Residual Injury in Monkeys Exposed to Large Doses of Radiation by Fractionation," Radiation Res. (1974), submitted.

R. G. Thomas, "Uptake Kinetics of Relatively Insoluble Particles by Tracheobronchial Lymph Nodes," in: Proceedings of the Conference on Radiation and the Lymphatic System, Battelle-Northwest Laboratories, Richland, Washington (September 30-October 4, 1974), submitted.

INDUSTRIAL HYGIENE GROUP (H-5)

Publications

J. C. Elder, M. Gonzales, and H. J. Ettinger, "Plutonium Aerosol Size Characteristics," Health Phys. 27, 45 (1974).

L. W. Ortiz and B. L. Isom, "Transfer Techniques for Electron Microscopy of Membrane Filter Samples," Amer. Ind. Hyg. Assoc. J. 35, 423 (1974).

M. I. Tillery, "A Concentric Aerosol Spectrometer," Amer. Ind. Hyg. Assoc. J. 35, 62 (1974).

Manuscript Submitted

J. F. McInroy, M. W. Stewart, and W. D. Moss, "Studies of Plutonium in Human Tracheobronchial Lymph Nodes," in: Proceedings of the Conference on Radiation and the Lymphatic System, Battelle-Northwest Laboratories, Richland, Washington (September 30-October 4, 1974), submitted.

ENVIRONMENTAL STUDIES GROUP (H-8)

Publications

S. Barr, "Environmental Surveillance at Los Alamos during 1973," Los Alamos Scientific Laboratory report LA-5586 (May 1974), p. 57.

S. Barr, "On the National β-Activity of the Air in the Atmospheric Surface Layer - Discussion," Atmospheric Environment 8, 867 (1974).

S. Barr and C. W. Kreitzberg, "Horizontal Variability and Boundary Layer Modeling, 1975," Boundary-Layer Meteorology 5, 91-100 (1974).

T. E. Hakonson and L. J. Johnson, "Distribution of Environmental Plutonium in the Trinity Site Environs after 27 Years," in: Proceedings of the Third International Congress of the International Radiation Protection Association, Vol. I (W. S. Snyder, ed.), National Technical Information Service report CONF-730907-P1, Springfield, Virginia (1974), pp. 242-247.

T. E. Hakonson and L. J. Johnson, "The Distribution of Plutonium in Liquid Waste Disposal Areas at Los Alamos," in: Proceedings of the Third International Congress of the International Radiation Protection Association, Vol. I (W. S. Snyder, ed.), National Technical Information Service report CONF-730907-P1, Springfield, Virginia (1974), pp. 248-253.

T. E. Hakonson and K. V. Bostick, "The Use of Honeybee Colonies as Bio-Indicators of Cesium-137, Tritium and Plutonium in the Los Alamos Environs," in: Abstracts of Papers Presented at the 19th Annual Meeting of the Health Physics Society, Houston, Texas (July 7-11, 1974), Abstract No. P/83, p. 22.

W. C. Hanson, "Ecological Considerations of Depleted Uranium Munitions," Los Alamos Scientific Laboratory report LA-5559 (1974).

W. C. Hanson, J. C. Elder, H. J. Ettinger, L. W. Hantel, and J. W. Owens, "Particle Size Distribution of Fragments from Depleted Uranium Penetrators Fired against Armor Plate Targets," Los Alamos Scientific Laboratory report LA-5654 (October 1974).

W. D. Purtymun, F. C. Koopman, S. Barr, and W. E. Clements, "Air Volume and Energy Transfer through Test Holes and Atmospheric Pressure Effects

on the Main Aquifer," Los Alamos Scientific Laboratory report LA-5725-MS (1974).

Manuscripts Submitted

W. E. Clements and M. H. Wilkening, "Atmospheric Pressure Effects on Radon-222 Transport across the Earth-Air Interface," J. Geophys. Res. (1974), in press.

T. E. Hakonson and F. W. Whicker, "Cesium Kinetics in a Montana Lake Ecosystem," Health Phys. (1974), in press.

T. E. Hakonson, "Environmental Pathways of Plutonium into Terrestrial Plants and Animals," Health Phys. (1974), submitted.

T. E. Hakonson and K. V. Bostick, "The Use of Honeybee Colonies as Bio-Indicators of Cesium-137, Tritium and Plutonium in the Los Alamos Environs," Health Phys. (1974), submitted.

T. E. Hakonson and F. W. Whicker, "The Use of Cesium Kinetics Data for Estimating Food Consumption Rates of Trout," Health Phys. (1974), submitted.

W. C. Hanson, "Behavior of Plutonium in the Environment," in: USAEC report CONF-740115 (1974), in press.

W. C. Hanson, "Ecological Considerations of the Behavior of Plutonium in the Environment," Health Phys. (1974), in press.

J. W. Nyhan, "Sampling Mixtures of Soil and Carbon-14 Labeled Plant Materials," Proc. Soil Sci. Amer. (1974), in press.

J. W. Nyhan, "Decomposition of Carbon-14 Labeled Plant Materials in a Grassland Soil under Field Conditions," Proc. Soil Sci. Soc. Amer. (1974), in press.

CELLULAR AND MOLECULAR RADIOBIOLOGY GROUP (H-9)

Publications

B. J. Barnhart and S. H. Cox, "Inactivation by Ultraviolet Radiation of Induced Prophage Replication and Maturation," Bacteriological Proceedings, Abstracts 1974, Abstract No. V19, p. 203.

L. L. Deaven, P. C. Sanders, M. M. Kligerman, and D. F. Petersen, "Chromosome Banding Analysis of *In Vitro* Cell Populations," in: Abstracts of the 5th International Congress of Radiation Research, Seattle, Washington (July 14-20, 1974), Abstract No. E-23-5, p. 283.

L. L. Deaven, P. C. Sanders, and D. F. Petersen, "The Nature of Chromosome Instability in Heteroploid Cell Populations," in: Abstracts of Papers Presented at the 14th Annual Meeting of the American Society for Cell Biology, San Diego, California (November 21-23, 1974), Abstract No. 157, p. 79a.

C. DeLisi and D. F. Petersen, "Absolute Determinations of Antibody Affinity and Secretion Rate Distributions from Hemolytic Plaque Experiments," Federation Proc. 33(5), 1239 (1974), Abstract No. 81.

M. D. Enger and E. W. Campbell, "Synthesis of Heterogeneous Nuclear, Informosomal Messenger-Like, and Polysomal Messenger RNA in Synchronized Chinese Hamster Cells," Federation Proc. 33(5), 1418 (1974), Abstract No. 1098.

M. D. Enger, R. A. Walters, and E. W. Campbell, "Effects of Ionizing Radiation on RNA Metabolism in Cultured Mammalian Cells. II. Patterns of Precursor Incorporation into Messenger-Related RNAs of Exponentially Growing and Synchronized Populations," Biochim. Biophys. Acta 353, 227-237 (1974).

M. D. Enger, R. A. Walters, A. E. Hampel, E. W. Campbell, and J. L. Hanners, "Sub-Ribosomal Particles of Cultured Chinese Hamster Cells: Relationship between RNA and Protein Components," Eur. J. Biochem. 43, 17-28 (1974).

D. Enlander, T. Scott, and R. A. Tobey, "The Four Faces of CHO," in: Proceedings of the 32nd Annual Meeting of the Electron Microscopy Society of America, St. Louis, Missouri (August 13-15, 1974), Claitor's Publishing Division, Baton Rouge (1974), pp. 268-279.

D. Enlander, T. Scott, and R. A. Tobey, "Observations of the Surface of Synchronized Chinese Hamster Ovary Cells in Suspension Culture," in: Proceedings of Scanning Electron Microscopy, Part III (O. M. Johari, ed.), Illinois Institute of Technology Press, Chicago, Illinois (1974), pp. 573-579.

D. M. Gray, C. W. Gray, R. L. Ratliff, and D. A. Smith, "Buoyant Densities of Natural and Synthetic DNAs in CsCl and Cs_2SO_4 Considered as Sequence-Dependent Properties," Biopolymers 13, 2265-2272 (1974).

L. R. Gurley, R. A. Tobey, C. E. Hildebrand, and R. A. Walters, "Sequential Histone Phosphorylation Events in the Cell Cycle," in: Abstracts of Papers Presented at the Fourteenth Annual Meeting of the American Society for Cell Biology, San Diego,

California (November 21-23, 1974), Abstract No. 251, p. 126a.

L. R. Gurley, R. A. Walters, and R. A. Tobey, "The Metabolism of Histone Fractions. Phosphorylation and Synthesis of Histones in Late G_1 Arrest," Arch. Biochem. Biophys. 164, 469-477 (1974).

C. E. Hildebrand and R. T. Okinaka, "Preparation of Nuclear Membranes from Cultured Chinese Hamster Cells by Heparin Treatment," Federation Proc. 33(5), 1328 (1974), Abstract No. 591.

C. E. Hildebrand and R. A. Tobey, "Cell Cycle Dependent Changes in Organization of Mammalian Nuclei," in: Abstracts of Papers Presented at the Fourteenth Annual Meeting of the American Society for Cell Biology, San Diego, California (November 21-23, 1974), Abstract No. 273, p. 137a.

D. E. Hoard, F. N. Hayes, and W. B. Goad, "Mathematical Analysis of the Destruction of the Base Moieties of Thymidine 5'-Monophosphate and Polydeoxythymidylate in Solution by X Irradiation," in: Abstracts of the 5th International Congress of Radiation Research, Seattle, Washington (July 14-20, 1974), Abstract No. E-17-1, p. 270.

D. E. Hoard, F. N. Hayes, and W. B. Goad, "Degradation of Nucleic Acid in Aqueous Solution by Ionizing Radiation. I. Loss of Ultraviolet Absorption of Solutions of Thymine or Thymine Derivatives upon X-Irradiation," Internat. J. Radiation Biol. 25, 603-609 (1974).

P. M. Kraemer, "Isolation of Native Cell Surface Heparan Sulfate from Cultured Cells," in: Abstracts of Papers Presented at the Fourteenth Annual Meeting of the American Society for Cell Biology, San Diego, California (November 21-23, 1974), Abstract No. 348, p. 174a.

P. M. Kraemer and D. A. Smith, "High Molecular-Weight Heparan Sulfate from the Cell Surface," Biochem. Biophys. Res. Commun. 56, 423-430 (1974).

P. M. Kraemer and P. Todd, "Macromolecules Secreted by Cultured Human Cells and Their Effects on Cell Growth and Adhesion," in: Abstracts of Papers Presented at the Fourteenth Annual Meeting of the American Society for Cell Biology, San Diego, California (November 21-23, 1974), Abstract No. 349, p. 175a.

P. M. Kraemer, L. L. Deaven, H. A. Crissman, J. A. Steinkamp, and D. F. Petersen, "On the Nature of Heteroploidy," in: The Organization of Genetic Material in Eukaryotes, Vol. 38, Cold Spring Harbor Laboratory, Cold Spring Harbor, New York (1974), pp. 133-144.

P. M. Kraemer, Chairman, P. L. Flynn, G. M. Talley, R. A. Tobey, and L. M. Holland, LASL Health Division Biohazards Committee, "Biohazards Manual," Los Alamos Scientific Laboratory report LA-5267-M (January 1974).

H. Nagasawa, J. T. Lett, and D. F. Petersen, "Radiation Effects on Synchronized Radiosensitive Mutant L5178Y Cells; Cell Killing Division Delay. Chromosome Aberration," in: Abstracts of the 5th International Congress of Radiation Research, Seattle, Washington (July 14-20, 1974), Abstract No. B-6-6, p. 80.

B. J. Noland, R. A. Walters, R. A. Tobey, J. M. Hardin, and G. R. Shepherd, "Effects of Ionizing Radiation upon Intracellular Levels of Microtubule Protein in Cultured Mammalian Cells," Exp. Cell Res. 85, 234-238 (1974).

R. T. Okinaka and B. J. Barnhart, "Accumulation of Incomplete Particles following UV-Light Induction of *Haemophilus influenzae* Lysogenic for Bacteriophage HP1c1," J. Virol. 14, 1604-1606 (1974).

R. T. Okinaka, B. J. Barnhart, and S. H. Cox, "The Development of Prophage HP1c1 after Ultraviolet Induction: Accumulation of Incomplete Particles," Bacteriological Proceedings, Abstracts 1974, Abstract No. V18, p. 203.

D. F. Petersen and L. L. Deaven, "Genome Preservation in Aneuploid Cell Lines," Federation Proc. 33(5), 1519 (1974), Abstract No. 1671.

D. F. Petersen, L. L. Deaven, and M. M. Kligerman, "Cell-Cycle Analyses of Candidate Lines for RBE Studies with Negative Pions," in: Abstracts of the 5th International Congress of Radiation Research, Seattle, Washington (July 14-20, 1974), Abstract No. D-13-5, p. 188.

R. L. Ratliff, D. A. Smith, F. N. Hayes, and D. E. Hoard, "Preparation and Properties of the Polymers $d(AIC)_n \cdot d(ICT)_n$ and $d(AGC)_n \cdot d(GCT)_n$," Federation Proc. 33(5), 1424 (1974), Abstract No. 1134.

A. G. Saponara, M. D. Enger, and J. L. Hanners, "The Isolation from Ribonucleic Acid of Substituted Uridines Containing α-Aminobutyrate Moieties Derived from Methionine," Biochim. Biophys. Acta 349, 61-77 (1974).

D. A. Smith and A. M. Martinez, "Initiation of *in vitro* RNA Synthesis by Covalent Attachment to X-Irradiated DNA," Federation Proc. 33(5), 1417 (1974), Abstract No. 1090.

D. A. Smith and A. M. Martinez, "Initiation of *In Vitro* RNA Synthesis with Deoxyribosyl Oligomers," Biochim. Biophys. Acta 353, 475-486 (1974).

G. F. Strniste and D. A. Smith, "Induction of Stable Linkage between the Deoxyribonucleic Acid-Dependent Ribonucleic Acid Polymerase and $d(A-T)_n \cdot d-(A-T)_n$ by Ultraviolet Light," Biochemistry 13, 485-493 (1974).

R. A. Tobey and H. A. Crissman, "Use of Flow Microfluorometry in Detailed Analysis of Effects of Chemical Agents on Cell-Cycle Progression," in: Year Book of Cancer (R. L. Clark and R. W. Crumley, eds.), Year Book Medical Publishers, Chicago, Illinois (1974), pp. 481-482.

P. Todd, B. S. Allen, and J. M. Hardin, "A Search for a Nucleoprotein Photoproduct in Mammalian Cells Exposed to Ultraviolet Light," in: American Society for Photobiology Book of Abstracts, Second Annual Meeting, Vancouver, British Columbia, Canada (July 23-26, 1974), p. 66.

R. A. Walters, L. R. Gurley, R. A. Tobey, and R. L. Ratliff, "Effects of X Irradiation on DNA Precursor Metabolism and Deoxyribonucleoside Triphosphate Pools in Chinese Hamster Cells," Federation Proc. 33(5), 1539 (1974), Abstract No. 1783.

R. A. Walters, L. R. Gurley, R. A. Tobey, M. D. Enger, and R. L. Ratliff, "Effects of X-Irradiation on DNA Precursor Metabolism and Deoxyribonucleoside Triphosphate Pools in Chinese Hamster Cells," Radiation Res. 60, 173-201 (1974).

R. A. Walters, L. R. Gurley, and R. A. Tobey, "Effects of Caffeine on Radiation-Induced Phenomena Associated with Cell-Cycle Traverse of Mammalian Cells," Biophys. J. 14, 99-118 (1974).

Manuscripts Submitted

B. J. Barnhart, S. H. Cox, and J. H. Jett, "Prophage Induction and Inactivation by Ultraviolet Light," Photochem. Photobiol. (1974), submitted.

B. J. Barnhart and S. H. Cox, "Increased Frequencies in the Lysogenic Response of Ultraviolet-Irradiated *Haemophilus* Phages," J. Virol. (1974), submitted.

L. L. Deaven, P. C. Sanders, J. L. Grilly, P. M. Kraemer, and D. F. Petersen, "Chromosome G-Banding and DNA Constancy in Aneuploid Cell Populations," in: First Annual Life Sciences Symposium on Mammalian Cells: Probes and Problems, Los Alamos, New Mexico (October 17-19, 1973), AEC Symposium Series, Technical Information Center, Oak Ridge, Tennessee (1974), submitted.

R. T. Dell'Orco, H. A. Crissman, J. A. Steinkamp, and P. M. Kraemer, "Population Analysis of Arrested Human Diploid Fibroblasts by Flow Microfluorometry," Exp. Cell Res. (1974), in press.

M. D. Enger, E. W. Campbell, and J. L. Hanners, "RNA Synthesis in Chinese Hamster Cells. III. Non-Coordinate Increases during Interphase in Synthesis Rates for Informosomal, Polysomal, and Heterogeneous Nuclear RNAs," Biochem. Biophys. Acta (1974), submitted.

D. M. Gray and R. L. Ratliff, "Circular Dichroism Spectra Show that the Conformations of poly d(A-C)·poly d(G-T), poly r(A-C)·poly r(G-U), and Hybrids poly d(A-C)·poly r(G-U) and poly r(A-C)·poly d(G-T) are Similar in the Presence of Ethanol," Biopolymers (1974), in press.

L. R. Gurley, R. A. Walters, and R. A. Tobey, "Sequential Phosphorylation of Histone Subfractions in the Chinese Hamster Cell Cycle," J. Biol. Chem. (1974), in press.

F. N. Hayes, D. E. Hoard, P. N. Dean, and W. B. Goad, "Degradation of Nucleic Acid in Aqueous Solution by Ionizing Radiation. II. Analysis of the Contribution of Various Water Radicals to the Loss of Ultraviolet Absorption by Thymidylate Solutions during X-Irradiation," Internat. J. Radiation Biol. (1974), in press.

C. E. Hildebrand and R. A. Tobey, "Cell-Cycle-Specific Changes in Chromatin Organization," Biochem. Biophys. Res. Commun. (1974), in press.

P. Hohmann, R. A. Tobey, and L. R. Gurley, "Cell-Cycle-Dependent Phosphorylation of Serine and Threonine in Chinese Hamster Cell F1 Histones," Biochem. Biophys. Res. Commun. (1974), in press.

M. M. Kligerman, E. A. Knapp, and D. F. Petersen, "Biomedical Program Leading to Therapeutic Trials of Pion Radiation Therapy at Los Alamos," Cancer (1974), in press.

M. M. Kligerman, J. F. Dicello, H. T. Davis, R. G. Thomas, C. J. Sternhagen, L. Gomez, and D. F. Petersen, "Initial Comparative Response of Experimental Tumors to Peak Pions and X-Rays," Radiology (1974), submitted.

P. M. Kraemer, "Chairman's Remarks -- Section V: The Cell Surface," in: First Annual Life Sciences Symposium on Mammalian Cells: Probes and Problems, Los Alamos, New Mexico (October 17-19, 1973), AEC Symposium Series, Technical Information Center, Oak Ridge, Tennessee (1974), submitted.

P. M. Kraemer, "Chairman's Closing Remarks -- Session V: The Cell Surface," in: First Annual Life Sciences Symposium on Mammalian Cells: Probes and Problems, Los Alamos, New Mexico (October 17-19, 1973), AEC Symposium Series, Technical Information Center, Oak Ridge, Tennessee (1974), submitted.

D. F. Petersen, E. C. Anderson, and R. A. Tobey, "Biochemical Events during the Mammalian Cell Cycle," in: Proceedings of the Symposium on Radiation Survival and the Cell Cycle, Fourth International Congress of Radiation Research, Evian, France (June 29-July 4, 1970), Gordon and Breach, New York (1974), in press.

R. A. Tobey, "Different Drugs Arrest Cells at a Number of Distinct Stages in G_2," Nature (1974), submitted.

R. A. Tobey and H. A. Crissman, "Comparative Effects of Three Nitrosourea Derivatives on Mammalian Cell-Cycle Progression," Cancer Res. (1974), in press.

R. A. Tobey and H. A. Crissman, "Unique Techniques for Cell-Cycle Analysis Utilizing Mithramycin and Flow Microfluorometry," Exp. Cell Res. (1974), submitted.

R. A. Tobey, M. S. Oka, and H. A. Crissman, "Differential Effects of Two Chemotherapeutic Agents, Streptozotocin and Chlorozotocin, on the Mammalian Cell Cycle," Eur. J. Cancer (1974), submitted.

R. A. Tobey, L. R. Gurley, C. E. Hildebrand, P. M. Kraemer, R. L. Ratliff, and R. A. Walters, "Sequential Biochemical Events in the Cell Cycle," in: First Annual Life Sciences Symposium on Mammalian Cells: Probes and Problems, Los Alamos, New Mexico (October 17-19, 1973), AEC Symposium Series, Technical Information Center, Oak Ridge, Tennessee (1974), submitted.

P. W. Todd, "Heavy Ion Irradiation of Human and Chinese Hamster Cells *In Vitro*," Radiation Res. (1974), in press.

R. A. Walters and M. D. Enger, "Effects of Ionizing Radiation on Nucleic Acid Synthesis in Mammalian Cells," in: Advances in Radiation Biology (J. T. Lett, ed.), Academic Press, Inc., New York (1974), submitted.

BIOPHYSICS AND INSTRUMENTATION GROUP (H-10)

Publications

A. Brunsting and P. F. Mullaney, "Differential Light Scattering from Spherical Mammalian Cells," Biophys. J. 14, 439-453 (1974).

L. S. Cram, "Application of Cell Analysis and Sorting Techniques to Disease Detection (Rapid Differential Diagnosis of Newcastle Disease Virus," Los Alamos Scientific Laboratory report LA-5565-MS (April 1974).

L. S. Cram, "Application of Cell Analysis and Sorting Techniques to Disease Detection (July 1, 1973-June 30, 1974)," Los Alamos Scientific Laboratory report LA-5719-PR (September 1974).

L. S. Cram and J. C. Forslund, "A Quantitative Method for Evaluating Fluorescent Antibodies and the Conjugation Process," Immunochemistry 11, 667-672 (1974).

L. S. Cram and G. F. Strniste, "Flow Microfluorometric Studies on the Cell Fusion Capabilities of Newcastle Disease Virus," Bacteriological Proceedings, Abstracts 1974, Abstract No. V361, p. 260.

L. S. Cram, J. C. Forslund, P. K. Horan, and J. A. Steinkamp, "Application of Flow Microfluorometry (FMF) and Cell Sorting Techniques to the Control of Animal Diseases," in: Automation in Microbiology and Immunology, Chapter 4 (C.-G. Heden and T. Illeni, eds.), John Wiley and Sons, Inc., New York (1964), pp. 49-66.

H. A. Crissman and R. A. Tobey, "Cell-Cycle Analysis in Twenty Minutes," Science 184, 1297-1298 (1974).

P. N. Dean, "*In Vivo* Detection of Transuranic Elements in the Human Lung," Trans. Amer. Nucl. Soc. 18, 384 (1974).

P. N. Dean and J. H. Jett, "Mathematical Analysis of DNA Distributions Derived from Flow Microfluorometry," J. Cell Biol. 60, 523-527 (1974).

R. Fiel and P. F. Mullaney, "Experimental and Theoretical Light-Scattering Studies on Suspensions of Red Blood Cell Ghosts," in: Abstracts of Papers Presented at the American Chemical Society Light Scattering Symposium, Los Angeles, California (March 31-April 5, 1974), Abstract No. COLL19.

P. K. Horan, J. H. Jett, A. Romero, and J. M. Lehman, "Flow Microfluorometry Analysis of DNA Content in Chinese Hamster Cells following Infection with Simian Virus 40," Internat. J. Cancer 14, 514-521 (1974).

P. K. Horan, A. Romero, M. R. Raju, and J. C. Martin, "Flow-System Analysis of DNA Content as an Indicator of Malignancy," in: Abstracts of the 5th International Congress of Cytology, Bal Harbour, Miami Beach, Florida (May 29-June 1, 1974), Abstract No. 68.

P. K. Horan, A. Romero, J. A. Steinkamp, and D. F. Petersen, "Detection of Heteroploid Tumor Cells," J. Natl. Cancer Inst. 52, 843-848 (1974).

M. Horan, P. K. Horan, and C. A. Williams, "Quantitative Immunofluorescence Measurements of SV40 T-Antigen Production," Bacteriological Proceedings, Abstracts 1974, Abstract No. V256, p. 243.

P. F. Mullaney and G. C. Salzman, "Light-Scattering Studies on Individual Mammalian Cells," in: Abstracts of Papers Presented at the American Chemical Society Light Scattering Symposium, Los Angeles, California (March 31-April 5, 1974), Abstract No. COLL18.

P. F. Mullaney, J. A. Steinkamp, H. A. Crissman, L. S. Cram, and D. M. Holm, "Laser Flow Microphotometers for Rapid Analysis and Sorting of Individual Mammalian Cells," in: Laser Applications in Medicine and Biology, Vol. 2, Chapter 5 (M. L. Wolbarsht, ed.), Plenum Press, New York-London (1974), pp. 151-204.

P. F. Mullaney, J. A. Steinkamp, H. A. Crissman, P. K. Horan, J. C. Martin, and A. Romero, "Multiparameter Cell Sorting and Analysis as Applied to Tumor Cell Identification," in: Overview of Diagnosis Program, Division of Cancer Biology and Diagnosis, National Cancer Institute, Williamsburg, Virginia (June 10-12, 1974), Book B, p. 265.

M. R. Raju, "Some Applications of Particle Accelerators and Particle Counting Techniques in Biology and Radiation Therapy," in: Proceedings of the Symposium on Advanced Technology Arising from Particle Physics Research, Argonne National Laboratory, Argonne, Illinois (May 17, 1973), ANL-8080 (1974), pp. 2.1-2.19.

M. R. Raju, "Negative Pions in Radiotherapy: A Brief Review," Eur. J. Cancer 10, 211-215 (1974).

M. R. Raju, "Physical and Radiobiological Characteristics of Negative Pions and Heavy Ions," in: Abstracts of Papers Presented at the XIth International Cancer Congress, Florence, Italy (October 20-26, 1974), Part 1, pp. 82-83.

M. R. Raju and J. H. Jett, "RBE and OER Variations of Mixtures of Plutonium Alpha Particles and X-Rays for Damage to Human Kidney Cells (T-1)," Radiation Res. 60, 473-481 (1974).

M. R. Raju, T. T. Trujillo, P. F. Mullaney, A. Romero, J. A. Steinkamp, and R. A. Walters, "The Distribution in the Cell Cycle of Normal Cells and of Irradiated Tumor Cells in Mice," Brit. J. Radiol. 47, 405-410 (1974).

G. C. Salzman and P. F. Mullaney, "An Ellipsoidal Cavity Flow Cell and Fluorescence Detector for Flow Microfluorometry," Federation Proc. 33(5), 1303 (1974), Abstract No. 451.

G. C. Saunders, E. H. Clinard, J. C. Forslund, M. L. Bartlett, and D. M. Holm, "Semiannual Report, Serologic Test Systems Development, July through December 1973," Los Alamos Scientific Laboratory report LA-5556-PR (April 1974).

J. A. Steinkamp and H. A. Crissman, "Automated Analysis of Deoxyribonucleic Acid, Protein, and Nuclear-to-Cytoplasmic Relationships in Tumor Cells and Gynecologic Specimens," J. Histochem. Cytochem. 22, 616-621 (1974).

J. A. Steinkamp and P. M. Kraemer, "Flow Microfluorometric Studies of Lectin Binding to Mammalian Cells. II. Estimation of the Surface Density of Receptor Sites by Multiparameter Analysis," J. Cell. Physiol. 84, 197-204 (1974).

J. A. Steinkamp and A. Romero, "Identification of Discrete Classes of Normal Human Peripheral Lymphocytes by Multiparameter Flow Analysis," Proc. Soc. Exp. Biol. Med. 146, 1061-1066 (1974).

J. A. Steinkamp, H. A. Crissman, and A. Romero, "Automated Cytology: Two-Color Fluorescence Analysis and Sorting of Gynecological Specimens," in: Abstracts of the 5th International Congress of Cytology, Bal Harbour, Miami Beach, Florida (May 29-June 1, 1974), Abstract No. 151.

J. A. Steinkamp, P. K. Horan, J. C. Martin, G. C. Salzman, and H. A. Crissman, "Automated Cancer Cell Sorting and Analysis (Progress Report April 1-September 30, 1974)," Los Alamos Scientific Laboratory report LA-5796-PR (December 1974).

J. A. Steinkamp, A. Romero, P. K. Horan, and H. A. Crissman, "Multiparameter Analysis and Sorting of Mammalian Cells," Exp. Cell Res. 84, 15-23 (1974).

Manuscripts Submitted

H. A. Crissman, "Cell Preparation and Staining for Flow Systems," in: First Annual Life Sciences Symposium on Mammalian Cells: Probes and Problems, Los Alamos, New Mexico (October 17-19, 1973), AEC Symposium Series, Technical Information Center, Oak Ridge, Tennessee (1974), submitted.

H. A. Crissman and J. A. Steinkamp, "Preparative Methods for Analysis of DNA, Protein, and Nuclear-to-Cytoplasmic Ratios in Normal and Tumor Cell Populations," in: Proceedings of the Pulse-Cytophotometry International Symposium and Workshop on Automated Cytofluorometry, with Special Reference to Methodology, Cancer-Screening and Leukemia, University Hospital, Nijmegen, The Netherlands (September 18-21, 1974), submitted.

H. A. Crissman, P. F. Mullaney, and J. A. Steinkamp, "Methods and Applications of Flow Systems for Analysis and Sorting of Mammalian Cells," in: Methods in Cell Biology (D. M. Prescott, ed.), Academic Press, Inc., New York (1974), in press.

J. M. Crowell, G. C. Salzman, P. F. Mullaney, and J. C. Martin, "High-Speed Optical Analysis of Microscopic Particles," in: Proceedings of the Technical Sessions at Electro-Optics '74 West and the International Laser Exposition, San Francisco, California (November 5-7, 1974), submitted.

P. K. Horan and H. S. Smith, "Single-Cell Measurement of DNA Content in Human Tumor Lines," J. Natl. Cancer Inst. (1974), submitted.

M. Horan, P. K. Horan, and C. A. Williams, "Quantitative Measurement of SV40 T-Antigen Production," Exp. Cell Res. (1974), in press.

P. F. Mullaney, J. A. Steinkamp, M. R. Raju, and P. K. Horan, "Tumor Cell Identification and Separation Using High-Speed Multiparameter Cell-Sensing Techniques," in: Proceedings of the Second International Symposium on Cancer Detection and Prevention, Bologna, Italy (April 9-13, 1973), submitted.

M. R. Raju, "The Biological Effects of Negative Pions," in: Proceedings of the XIIIth International Congress of Radiology, Madrid, Spain (October 15, 1973), in press (1974).

M. R. Raju, "Pions and Heavy Ions in Radiotherapy: A Brief Review," in: Proceedings of the XIth International Cancer Congress, Florence, Italy (October 20-26, 1974), in press.

M. R. Raju, P. K. Horan, A. Romero, J. C. Martin, and C. J. Sternhagen, "Application of Flow Microfluorometry to Problems in Radiotherapy," Brit. J. Radiol. (1974), in press.

M. R. Raju, R. A. Tobey, J. H. Jett, and R. A. Walters, "Age Response for Line CHO Chinese Hamster Cells Exposed to X-Irradiation and Alpha Particles from Plutonium," Radiation Res. (1974), submitted.

C. Richman, "Characteristics of a Negative Pion Beam in a Therapeutic Application," Radiology (1974), submitted.

G. C. Salzman, J. M. Crowell, J. C. Martin, T. T. Trujillo, A. Romero, P. F. Mullaney, and P. M. LaBauve, "Cell Classification by Laser Light Scattering: Identification and Separation of Unstained Leukocytes," Acta Cytol. (1974), submitted.

J. A. Steinkamp, "Multiparameter Cell Sorting and Analysis," in: First Annual Life Sciences Symposium on Mammalian Cells: Probes and Problems, Los Alamos, New Mexico (October 17-19, 1973), AEC Symposium Series, Technical Information Center, Oak Ridge, Tennessee (1974), submitted.

ORGANIC AND BIOCHEMICAL SYNTHESIS GROUP (H-11)

Publications

C. T. Gregg, "Some Applications of Stable Isotopes in Clinical Pharmacology," Eur. J. Clin. Pharmacol. 7, 315-319 (1974).

M. Oka, A. Fry, J. Hinton, and T. W. Whaley, "Carbon-13 Tracer Study of the Acid-Catalyzed Rearrangement of 2,2,4-Trimethyl-3-Pentanone-3-^{13}C," in: Abstracts of Papers Presented at the Second Rocky Mountain Regional Meeting, American Chemical Society, Albuquerque, New Mexico (July 8-9, 1974).

D. G. Ott, V. N. Kerr, T. W. Whaley, T. Benziger, and R. K. Rohwer, "Syntheses with Stable Isotopes: Methanol-^{13}C, Methanol-^{13}C-d_4 and Methanol-^{12}C," J. Labelled Compds. 10, 315-324 (1974).

W. W. Shreeve, J. D. Shoop, D. G. Ott, and B. B. McInteer, "Evaluation of Liver Function by Oxidation of ^{14}C- or ^{13}C-Labeled Galactose *In Vivo*," in: Proceedings of the First World Congress of Nuclear Medicine, Tokyo-Kyoto, Japan (September 30-October 5, 1974), p. 26, abstract.

W. W. Shreeve, J. D. Shoop, D. G. Ott, and B. B. McInteer, "Evaluation of Liver Function by Oxidation of Galactose-^{14}C or -^{13}C *In Vivo*," J. Nucl. Med. 15, 532 (1974), abstract.

T. W. Whaley and D. G. Ott, "Syntheses with Stable Isotopes: Pyridine-^{15}N," J. Labelled Compds. 10, 283-286 (1974).

T. W. Whaley and D. G. Ott, "Syntheses with Stable Isotopes: Acetylene-$^{13}C_2$ and Lithium Acetylide-$^{13}C_2$ Ethylenediamine Complex," J. Labelled Compds. 10, 461-468 (1974).

Manuscripts Submitted

A. J. Campillo, R. C. Hyer, V. H. Kollman, S. L. Shapiro, and H. D. Sutphin, "Fluorescence Lifetimes of α- and β-Carotenes," Biochem. Biophys. Acta (1974), submitted.

R. E. London, C. T. Gregg, and N. A. Matwiyoff, "Carbon-13 Nuclear Magnetic Resonance Study of the Rotational Mobility of Intra- and Extracellular Mouse Hemoglobin Labeled with ^{13}C Enriched Histidine," Science (1974), in press.

R. E. London, V. H. Kollman, and N. A. Matwiyoff, "The Quantitative Analysis of Carbon-Carbon Coupling in the ^{13}C NMR Spectra of Molecules Biosynthesized from ^{13}C Enriched Precursors," Biochim. Biophys. Acta (1974), in press.

R. E. London, V. H. Kollman, and N. A. Matwiyoff, "^{13}C FT NMR Studies of Fractionated *Candida utilis* Membranes," Biochemistry (1974), submitted.

N. A. Matwiyoff, G. A. Cowan, D. G. Ott, and B. B. McInteer, "Problems and Potentialities of Stable Isotopes as Tracers for Studying Pollutant Behavior under Field Conditions," in: Proceedings of the Symposium on Isotope Ratios as Pollutant Source and Behavior Indicators, Vienna, Austria (November 18-2, 1974), Food and Agriculture Organization of the United States and International Atomic Energy Agency (1974), submitted.

D. G. Ott, "Organic Synthesis of Carbon-13 Compounds," in: Proceedings of the First National Symposium on Carbon-13, Los Alamos, New Mexico (June 8-11, 1971), Los Alamos Scientific Laboratory report (1974), in press.

D. G. Ott, "Carbon-13 Labelled Compounds," in: Book on Stable Isotopes, Vol. I (Committee of Stable Isotopes, Japan, eds.), submitted (1974).

T. W. Whaley and D. G. Ott, "Syntheses with Stable Isotopes: Urea-^{13}C, Urea-^{12}C, and Urea-^{13}C-$^{15}N_2$," J. Labelled Compds. (1974), in press.

T. W. Whaley and D. G. Ott, "Syntheses with Stable Isotopes: Sodium Cyanide-^{13}C," J. Labelled Compds. (1974), in press.

SPECIAL ACTIVITIES

SECOND ANNUAL LIFE SCIENCES SYMPOSIUM, PLUTONIUM -- HEALTH IMPLICATIONS FOR MAN (May 22-24, 1974)

The Los Alamos Scientific Laboratory's Second Annual Life Sciences Symposium on "Plutonium -- Health Implications for Man," sponsored by the Los Alamos Scientific Laboratory and the U. S. Atomic Energy Commission, was held on May 22-24, 1974. Individuals from various agencies of the federal government, selected state governments, industry, universities, and other organizations interested in deriving or applying standards intended to protect the worker or the public were invited. Thus, the audience was composed largely of individuals engaged in applying the information rather than to persons involved in research.

Each of the five general sessions was opened by the appointed chairman, followed by presentations by individuals recognized in their specialized fields. A short question and answer period followed each presentation, and a general discussion and summary of all five sessions were presented by the chairman of the sixth session, followed by a general discussion by the attendees and speakers. An outline of the program follows:

May 22, 1974

SESSION I: THE POTENTIAL PROBLEM

Chairman's Remarks

C. Walske, Atomic Industrial Forum, Inc.
New York City, New York

"The Future of Plutonium -- An Overview"

C. E. Larson, U. S. Atomic Energy Commission
Washington, D. C.

"The Plutonium Fuel Cycle"

T. H. Pigford, University of California
Berkeley, California

"Confinement Facilities for the Handling of Plutonium"

W. J. Maraman, Los Alamos Scientific Laboratory
Los Alamos, New Mexico

"Waste Management"

H. F. Soule, U. S. Atomic Energy Commission
Washington, D. C.

SESSION II: PLUTONIUM AND MAN. I.

Chairman's Remarks

R. O. McClellan, Lovelace Foundation for Medical Education and Research, Albuquerque, New Mexico

"The Origin of Current Standards"

J. W. Healy, Los Alamos Scientific Laboratory
Los Alamos, New Mexico

"Body Distribution vs Route of Administration"

P. W. Durbin, Lawrence Berkeley Laboratory
Berkeley, California

"Animal Data on Plutonium Toxicity"

R. C. Thompson, Battelle Northwest Laboratories
Richland, Washington

"The Use of Animal Data in Derivation of Standards"

A. M. Brues, Argonne National Laboratory
Argonne, Illinois

May 23, 1974

SESSION III: PLUTONIUM AND MAN. II.

Chairman's Remarks

N. F. Barr, U. S. Atomic Energy Commission
Washington, D. C.

"The Importance of Nonuniform Dose Distribution in an Organ"

C. R. Richmond, Los Alamos Scientific Laboratory, Los Alamos, New Mexico

"The Concepts of Critical Organ and Radiation Dose as Applied to Plutonium"

J. N. Stannard, University of Rochester
Rochester, New York

"What We Have Learned from Humans"

G. L. Voelz, M.D., Los Alamos Scientific Laboratory, Los Alamos, New Mexico

"Other Considerations in Establishing Standards"

C. C. Gamertsfelder, U. S. Atomic Energy Commission, Washington, D. C.

SESSION IV: PLUTONIUM IN THE ENVIRONMENT

Chairman's Remarks

W. A. Mills, Environmental Protection Agency
Washington, D. C.

"Resuspension and Redistribution of Plutonium in Soils"

P. L. Phelps, Lawrence Livermore Laboratory
Livermore, California

"Environmental Pathways of Transuranics to Terrestrial Animals"

T. E. Hakonson, Los Alamos Scientific Laboratory, Los Alamos, New Mexico

"Plutonium in Aquatic Systems"

W. R. Schell, University of Washington
Seattle, Washington

"Experiences with Plutonium in the Environment"

D. W. Wilson, Lawrence Livermore Laboratory
Livermore, California

May 24, 1974

SESSION V: MEASUREMENT OF PLUTONIUM

Chairman's Remarks

H. D. Bruner, M.D., U. S. Atomic Energy Commission, Washington, D. C.

"Assessment of the Occupational Environment"

H. F. Schulte, Los Alamos Scientific Laboratory
Los Alamos, New Mexico

"Measurement Problems in the Environs"

C. W. Sill, U. S. Atomic Energy Commission
Washington, D. C.

SESSION VI: GENERAL DISCUSSION AND SUMMARY

Chairman's Remarks

H. M. Parker, HMP Associates
Richland, Washington

General Discussion by Attendees and Speakers

Concluding Remarks

H. M. Parker

SYMPOSIUM ATTENDEES

R. F. Abbey, Jr.
Division of Reactor Research and Development
U. S. Atomic Energy Commission
Washington, D. C.

E. L. Albenesius
Savannah River Plant
E. I. Du Pont de Nemours and Company
Aiken, South Carolina

R. E. Alexander
Regulatory Standards
U. S. Atomic Energy Commission
Washington, D. C.

E. C. Anderson
Los Alamos Scientific Laboratory
University of California
Los Alamos, New Mexico

K. E. Apt
Los Alamos Scientific Laboratory
University of California
Los Alamos, New Mexico

J. A. Auxier
Health Physics Division
Oak Ridge National Laboratory
Oak Ridge, Tennessee

R. E. Baker
Office of Regulation
U. S. Atomic Energy Commission
Washington, D. C.

N. F. Barr
Division of Biomedical and Environmental Research
U. S. Atomic Energy Commission
Washington, D. C.

B. G. Bennett
Health and Safety Laboratory
U. S. Atomic Energy Commission
New York City, New York

R. W. Bistline
Rocky Flats Division
Dow Chemical Company
Rocky Flats, Colorado

B. B. Boecker
Lovelace Foundation for Medical Education and Research
Albuquerque, New Mexico

J. A. Bonnell
Medical Branch
Nuclear Health and Safety Department
Central Electricity Generating Board
London, England

S. E. Bronisz
Los Alamos Scientific Laboratory
University of California
Los Alamos, New Mexico

A. M. Brues
Division of Radiological and Environmental Research
Argonne National Laboratory
Argonne, Illinois

H. D. Bruner, M.D.
Office of the Commissioners
U. S. Atomic Energy Commission
Washington, D. C.

G. Burley
Exposure Criteria Branch
Office of Radiation Programs
Environmental Protection Agency
Washington, D. C.

R. L. Butenhoff
Division of Biomedical and Environmental Research
U. S. Atomic Energy Commission
Washington, D. C.

C. S. Caldwell
Babcock and Wilcox Company
New York City, New York

E. E. Campbell
Los Alamos Scientific Laboratory
University of California
Los Alamos, New Mexico

S. Carpenter
Los Alamos Scientific Laboratory
University of California
Los Alamos, New Mexico

C. E. Carter
Division of Biomedical and Environmental Research
U. S. Atomic Energy Commission
Washington, D. C.

E. L. Christensen
Los Alamos Scientific Laboratory
University of California
Los Alamos, New Mexico

S. H. Cohn
Medical Research Center
Brookhaven National Laboratory
Upton, Long Island, New York

T. Cook
Los Alamos Scientific Laboratory
University of California
Los Alamos, New Mexico

G. Cowper
Nuclear Laboratories, Health Physics Branch
Atomic Energy of Canada, Ltd.
Chalk River, Ontario, Canada

D. H. Craig
Pacific Northwest Laboratory
Battelle Memorial Institute
Richland, Washington

G. E. Dagle
Biology Department
Pacific Northwest Laboratory
Battelle Memorial Institute
Richland, Washington

R. Dahlman
Environmental Sciences Division
Oak Ridge National Laboratory
Oak Ridge, Tennessee

S. Davies, Director
Bureau of Radiological Health
State Department of Health
Albany, New York

G. P. Dix
Division of Space Nuclear Systems
U. S. Atomic Energy Commission
Washington, D. C.

G. A. Drake
Los Alamos Scientific Laboratory
University of California
Los Alamos, New Mexico

R. W. Drake
Los Alamos Scientific Laboratory
University of California
Los Alamos, New Mexico

P. B. Dunaway
Nevada Operations Office
U. S. Atomic Energy Commission
Las Vegas, Nevada

P. W. Durbin
Lawrence Berkeley Laboratory
University of California
Berkeley, California

G. W. Earle
Savannah River Plant
E. I. Du Pont de Nemours and Company
Aiken, South Carolina

L. A. Emility
Los Alamos Scientific Laboratory
University of California
Los Alamos, New Mexico

H. P. Estey
Exxon Nuclear Company
Richland, Washington

H. J. Ettinger
Los Alamos Scientific Laboratory
University of California
Los Alamos, New Mexico

R. D. Evans
Scottsdale, Arizona

G. C. Facer
Division of Military Application
U. S. Atomic Energy Commission
Washington, D. C.

L. Faust
Pacific Northwest Laboratory
Battelle Memorial Institute
Richland, Washington

A. J. Finkel
Division of Scientific Activities
American Medical Association
Chicago, Illinois

M. P. Finkel
Experimental Radiation Pathology
Argonne National Laboratory
Argonne, Illinois

T. R. Folsom
Scripps Institute of Oceanography
University of California, San Diego
La Jolla, California

H. Foreman
Center for Population Studies
Mayo Hospital
University of Minnesota
Minneapolis, Minnesota

E. B. Fowler
Los Alamos Scientific Laboratory
University of California
Los Alamos, New Mexico

C. C. Gamertsfelder
Directorate of Regulatory Standards
U. S. Atomic Energy Commission
Washington, D. C.

A. Gallegos
Los Alamos Area Office
U. S. Atomic Energy Commission
Los Alamos, New Mexico

J. C. Gallimore
Los Alamos Scientific Laboratory
University of California
Los Alamos, New Mexico

I. Goldberg
Radiologic Health Section
California Department of Health
Sacramento, California

L. S. Gomez
Los Alamos Scientific Laboratory
University of California
Los Alamos, New Mexico

D. Grahn
Division of Biomedical and Environmental Research
U. S. Atomic Energy Commission
Washington, D. C.

R. S. Grier, M.D.
Los Alamos Scientific Laboratory
University of California
Los Alamos, New Mexico

J. A. Griffin, Special Assistant
Office of the Commissioners
U. S. Atomic Energy Commission
Washington, D. C.

W. E. Grummitt
Biology and Health Physics Division
Atomic Energy of Canada, Ltd.
Chalk River, Ontario, Canada

G. Gyorey
Nuclear Energy Division
General Electric Company
San Jose, California

W. Hagis
Division of International Security Affairs
U. S. Atomic Energy Commission
Washington, D. C.

T. E. Hakonson
Los Alamos Scientific Laboratory
University of California
Los Alamos, New Mexico

H. Hamester
Office of Energy Research and Development Policy
National Science Foundation
Washington, D. C.

W. R. Hansen
Advanced Technology and Studies Branch
Office of Radiation Programs
Environmental Protection Agency
Washington, D. C.

A. J. Hazle
Colorado Department of Health
Denver, Colorado

J. W. Healy
Los Alamos Scientific Laboratory
University of California
Los Alamos, New Mexico

L. H. Hempelmann, M.D.
University of Rochester
School of Medicine and Dentistry
Rochester, New York

D. W. Hendricks, Assistant Director for Radiation Operations
Environmental Protection Agency
Las Vegas, Nevada

C. H. Hobbs
Lovelace Foundation for Medical Education and Research
Albuquerque, New Mexico

L. M. Holland, D.V.M.
Los Alamos Scientific Laboratory
University of California
Los Alamos, New Mexico

H. Hollister
Division of Biomedical and Environmental Research
U. S. Atomic Energy Commission
Washington, D. C.

R. E. Ireland
LMFBR Branch, Directorate of Licensing
Office of Regulation
U. S. Atomic Energy Commission
Washington, D. C.

W. S. S. Jee
Department of Anatomy
University of Utah
Salt Lake City, Utah

J. H. Jett
Los Alamos Scientific Laboratory
University of California
Los Alamos, New Mexico

L. J. Johnson
Los Alamos Scientific Laboratory
University of California
Los Alamos, New Mexico

H. S. Jordan
Los Alamos Scientific Laboratory
University of California
Los Alamos, New Mexico

E. C. Kauffman
Radiation Protection Section
Environmental Improvement Agency
Santa Fe, New Mexico

P. M. Kraemer
Los Alamos Scientific Laboratory
University of California
Los Alamos, New Mexico

C. R. Lagerquist
Rocky Flats Division
Dow Chemical Company
Rocky Flats, Colorado

C. E. Larson
Office of the Commissioners
U. S. Atomic Energy Commission
Washington, D. C.

H. J. Larson
Allied-General Nuclear Services
Barnwell, South Carolina

J. N. P. Lawrence
Los Alamos Scientific Laboratory
University of California
Los Alamos, New Mexico

T. A. Lincoln, Medical Director
Oak Ridge National Laboratory
Oak Ridge, Tennessee

A. Lindenbaum
Division of Biology and Mèdical Research
Argonne National Laboratory
Argonne, Illinois

R. K. Lohrding
Los Alamos Scientific Laboratory
University of California
Los Alamos, New Mexico

J. E. London
Los Alamos Scientific Laboratory
University of California
Los Alamos, New Mexico

A. B. Long
Argonne National Laboratory
Argonne, Illinois

W. D. Ludemann
Lawrence Livermore Laboratory
University of California
Livermore, California

C. C. Lushbaugh, M.D.
Oak Ridge Associated Universities, Inc.
Oak Ridge, Tennessee

W. J. Maraman
Los Alamos Scientific Laboratory
University of California
Los Alamos, New Mexico

G. M. Matlack
Los Alamos Scientific Laboratory
University of California
Los Alamos, New Mexico

N. A. Matwiyoff
Los Alamos Scientific Laboratory
University of California
Los Alamos, New Mexico

C. W. Mays
Radiobiology Division
University of Utah
Salt Lake City, Utah

R. O. McClellan, D.V.M.
Lovelace Foundation for Medical Education and Research
Albuquerque, New Mexico

D. E. McCurdy
Los Alamos Scientific Laboratory
University of California
Los Alamos, New Mexico

J. F. McInroy
Los Alamos Scientific Laboratory
University of California
Los Alamos, New Mexico

M. E. McLain
Los Alamos Scientific Laboratory
University of California
Los Alamos, New Mexico

J. A. Mewhinney
Lovelace Foundation for Medical Education and Research
Albuquerque, New Mexico

D. D. Meyer
Espanola, New Mexico

J. F. Meyer
LMFBR Branch, Directorate of Licensing
Office of Regulation
U. S. Atomic Energy Commission
Washington, D. C.

R. L. Miller
Operational Safety Division
Albuquerque Operations Office
U. S. Atomic Energy Commission
Albuquerque, New Mexico

J. C. Milligan
Los Alamos Scientific Laboratory
University of California
Los Alamos, New Mexico

M. F. Milligan
Office of Regulation
U. S. Atomic Energy Commission
Washington, D. C.

W. A. Mills, Director
Criteria and Standards Division
Office of Radiation Programs
Environmental Protection Agency
Washington, D. C.

K. Z. Morgan
School of Nuclear Engineering
Georgia Institute of Technology
Atlanta, Georgia

P. E. Morrow
Department of Radiation Biology and Biophysics
University of Rochester
School of Medicine and Dentistry
Rochester, New York

W. D. Moss
Los Alamos Scientific Laboratory
University of California
Los Alamos, New Mexico

R. N. R. Mulford
Los Alamos Scientific Laboratory
University of California
Los Alamos, New Mexico

R. Mulkin
Los Alamos Scientific Laboratory
University of California
Los Alamos, New Mexico

I. C. Nelson
Pacific Northwest Laboratory
Battelle Memorial Institute
Richland, Washington

T. W. Newton
Los Alamos Scientific Laboratory
University of California
Los Alamos, New Mexico

W. D. Norwood, M.D.
U. S. Transuranium Registry
Hanford Environmental Health Foundation
Richland, Washington

D. T. Oakley, Deputy Director
Field Operations Division
Office of Radiation Programs
U. S. Environmental Protection Agency
Washington, D. C.

R. E. Olson
Westinghouse Electric Corporation
Pittsburgh, Pennsylvania

H. M. Parker
HMP Associates, Inc.
Richland, Washington

W. W. Parkinson
Health Physics Division
Oak Ridge National Laboratory
Oak Ridge, Tennessee

J. H. Patterson
Los Alamos Scientific Laboratory
University of California
Los Alamos, New Mexico

R. A. Pettitt
Los Alamos Scientific Laboratory
University of California
Los Alamos, New Mexico

P. L. Phelps
Biomedical Division
Lawrence Livermore Laboratory
University of California
Livermore, California

T. H. Pigford
Nuclear Engineering
University of California
Berkeley, California

J. W. Poston
Health Physics Division
Oak Ridge National Laboratory
Oak Ridge, Tennessee

J. R. Prine, D.V.M.
Los Alamos Scientific Laboratory
University of California
Los Alamos, New Mexico

E. A. Putzier
Research and Ecology
Rocky Flats Division
Dow Chemical Company
Rocky Flats, Colorado

O. G. Raabe
Lovelace Foundation for Medical Education and Research
Albuquerque, New Mexico

W. H. Ray
Office of Regulation
U. S. Atomic Energy Commission
Washington, D. C.

W. C. Reinig
Savannah River Plant
E. I. Du Pont de Nemours and Company
Aiken, South Carolina

B. L. Rich
Allied Chemical Corporation
Idaho Falls, Idaho

C. R. Richmond
Los Alamos Scientific Laboratory
University of California
Los Alamos, New Mexico

E. M. Romney
Laboratory of Nuclear Medicine and Radiation Biology
University of California
Los Angeles, California

D. M. Ross, Chief
Health Protection Branch
Division of Operational Safety
U. S. Atomic Energy Commission
Washington, D. C.

L. C. Rouse
Fuels and Materials, Directorate of Licensing
Office of Regulation
U. S. Atomic Energy Commission
Washington, D. C.

J. H. Rust
Chicago, Illinois

C. L. Sanders
Biology Department
Pacific Northwest Laboratory
Battelle Memorial Institute
Richland, Washington

W. Schell
Laboratory of Radiation Ecology
College of Fisheries
University of Washington
Seattle, Washington

H. F. Schulte
Los Alamos Scientific Laboratory
University of California
Los Alamos, New Mexico

H. C. Shealy
South Carolina Department of Health and
Environmental Control
Columbia, South Carolina

J. Shreve
Cimarron Facility
Kerr-McGee Nuclear Corporation
Crescent, Oklahoma

S. Shwiller, Chief
Nuclear Materials and Waste Management Branch
Weapons Production Division
Albuquerque Operations Office
U. S. Atomic Energy Commission
Albuquerque, New Mexico

C. W. Sill
Health Services Laboratory
Idaho Operations Office
U. S. Atomic Energy Commission
Idaho Falls, Idaho

G. J. Sinke
Cimarron Facility
Kerr-McGee Nuclear Corporation
Crescent, Oklahoma

D. K. Sly
Office of Regulation
U. S. Atomic Energy Commission
Washington, D. C.

D. Smith
Office of Regulation
U. S. Atomic Energy Commission
Washington, D. C.

D. R. Smith
Los Alamos Scientific Laboratory
University of California
Los Alamos, New Mexico

P. B. Smith
U. S. Environmental Protection Agency
Denver, Colorado

W. J. Smith
Los Alamos Scientific Laboratory
University of California
Los Alamos, New Mexico

H. F. Soule
Division of Waste Management and Transportation
U. S. Atomic Energy Commission
Washington, D. C.

R. G. Stafford
Los Alamos Scientific Laboratory
University of California
Los Alamos, New Mexico

J. N. Stannard
Department of Radiation Biology and Biophysics
University of Rochester
School of Medicine and Dentistry
Rochester, New York

J. H. Sterner
University of Texas
School of Public Health
Houston, Texas

W. L. Thayer
Lawrence Livermore Laboratory
University of California
Livermore, California

R. G. Thomas
Los Alamos Scientific Laboratory
University of California
Los Alamos, New Mexico

R. L. Thomas
Los Alamos Scientific Laboratory
University of California
Los Alamos, New Mexico

R. C. Thompson
Biology Department
Pacific Northwest Laboratory
Battelle Memorial Institute
Richland, Washington

G. L. Tietjen
Los Alamos Scientific Laboratory
University of California
Los Alamos, New Mexico

C. J. Umbarger
Los Alamos Scientific Laboratory
University of California
Los Alamos, New Mexico

A. M. Valentine
Los Alamos Scientific Laboratory
University of California
Los Alamos, New Mexico

G. L. Voelz, M.D.
Los Alamos Scientific Laboratory
University of California
Los Alamos, New Mexico

P. G. Voilleque
Health Services Laboratory
Idaho Operations Office
U. S. Atomic Energy Commission
Idaho Falls, Idaho

B. W. Wachholz
Division of Biomedical and Environmental Research
U. S. Atomic Energy Commission
Washington, D. C.

N. Wald
Department of Radiological Health
University of Pittsburgh
Pittsburgh, Pennsylvania

C. Walske
Atomic Industrial Forum, Inc.
New York City, New York

R. B. Walton
Los Alamos Scientific Laboratory
University of California
Los Alamos, New Mexico

G. J. Werkema
Rocky Flats Division
Dow Chemical Company
Rocky Flats, Colorado

C. S. White, President and Director
Lovelace Foundation for Medical Education
and Research
Albuquerque, New Mexico

D. Willenberg
Los Alamos Scientific Laboratory
University of California
Los Alamos, New Mexico

D. W. Wilson
Biomedical Division
Lawrence Livermore Laboratory
University of California
Livermore, California

J. S. Wilson
Los Alamos Scientific Laboratory
University of California
Los Alamos, New Mexico

A. H. Wolff
School of Public Health
University of Illinois
Chicago, Illinois

K. Y. Wong
Pickering Generating Station, Ontario Hydro
Pickering, Ontario, Canada

McD. Wrenn
Division of Biomedical and Environmental Research
U. S. Atomic Energy Commission
Washington, D. C.

G. Wright
Illinois Department of Public Health
Springfield, Illinois

THE APPLICATIONS OF MICROFLUOROMETRY TO TISSUE CULTURE (July 8-12, 1974)

The Tissue Culture Association and the Los Alamos Scientific Laboratory jointly sponsored a workshop on "The Applications of Microfluorometry to Tissue Culture" for postdoctoral and established investigators. The tutorial consisted of a lecture series and appropriate laboratory experiments to demonstrate theory practice and current biological applications of this important new analytical tool.

LECTURE TOPICS

Flow-Systems Analysis of Individual Cells
Introduction to Flow-Systems Analysis
Cell Preparation for Flow Analysis
DNA Distributions
Computer Analysis of FMF Data
Drug Effects on the Cell Cycle
Radiation Effects on the Cell Cycle
Cell Surface Studies
Light Scattering from Cells: Theory and Experiment
Quantitative Immunofluorescence

PARTICIPANTS

Dr. John Burkey
National Center for Toxicological Research
Jefferson, Arkansas

Ms. Marilyn J. Campbell
Particle Technology, Inc.
Los Alamos, New Mexico

Dr. Holger Hoene
Department of Pathology
University of Washington
Seattle, Washington

Dr. Andrew C. Huang
Borger Hospital
Kalamazoo, Michigan

Dr. Robert Moldonado
Bioquest
Cockeyesville, Maryland

Dr. Leonard Murrell
Department of Anatomy
University of Tennessee Medical School
Memphis, Tennessee

Dr. W. R. Smith
Searle, Inc.
Skokie, Illinois

SUPPORTING LASL STAFF

D. F. Petersen, Director

E. Bain	P. M. Kraemer
E. W. Campbell	P. F. Mullaney
L. S. Cram	M. R. Raju
H. A. Crissman	A. Romero
P. N. Dean	P. C. Sanders
P. K. Horan	G. C. Salzman
J. L. Horney	J. A. Steinkamp
J. H. Jett	R. A. Tobey
P. Jose	W. T. West

AMERICAN SOCIETY OF TEACHERS OF RADIOTHERAPY CONVENTION (October 30-November 2, 1974, Key Biscayne, Florida)

The following personnel were listed as contributors to the University of New Mexico Cancer Research and Treatment Center's display on "The Pi Meson Project, Los Alamos," presented by Dr. C. J. Sternhagen:

LASL

H. I. Amols (MP-3)
T. W. Armstrong (H-10)
J. E. Barnes (MP-3)
J. N. Bradbury (MP-3)
J. F. Dicello (MP-3)
F. B. Dobrowolski (MP-3)
J. A. Helland (MP-3)
R. L. Hutson (MP-3)
E. A. Knapp (MP-3)
H. B. Knowles (MP-3)
T. F. Lane (MP-3)
A. S. Lundy (MP-3)
D. F. Petersen (H-9)
M. R. Raju (H-10)
C. Richman (H-10)
L. Rosen (MP-DO)
S. D. Shlaer (MP-1)
R. G. Thomas (H-4)
P. W. Todd (H-10)
T. T. Trujillo (H-10)
G. L. Voelz (H-DO)

UNM

H. T. Davis
M. M. Kligerman, M.D.
C. Shonk
C. J. Sternhagen, M.D.
G. Tfeuffer
G. West, M.D.

☆US GOVERNMENT PRINTING OFFICE 1975—677-178/37